

The information contained in this document is protected from release to the public pursuant to FOIA Exemptions 4 (5 U.S.C. § 552(b)(4)), 7(F) (5 U.S.C. § 552(b)(7)(F)), and 6 (5 U.S.C. § 552(b)(6)). It is confidential, commercial information. Release of this information could create a competitive disadvantage. Release of certain information could also reasonably be expected to endanger the life or physical safety of any individual. Finally, release of certain information in this document could constitute an unwarranted invasion of personal privacy.

027-2203



TC Oil

RCFA for the Keystone Milepost 14 Release

Stephanie Flamberg, Bill Amend, Peter Martin, Michael
Rosenfeld, Adam Steiner, and Benjamin Zand

April 21, 2023

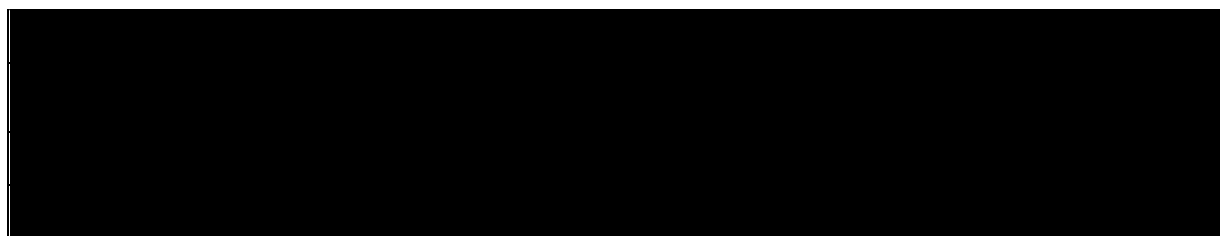
Page Intentionally Left Blank

Final Report

For

TC Oil

RCFA for the Keystone Milepost 14 Release

RSI Pipeline Solutions, LLC
102 W. Main Street, #578
New Albany, OH 43054

Disclaimer

The report provides the results of consultancy services performed by employees of RSI Pipeline Solutions, LLC. The findings of this report were performed using information provided by Client and standards of practice that is commonly accepted within the industry.

This report (including any attachments) has been prepared for the exclusive use and benefit of the Client. Unless RSI Pipeline Solutions provide express prior written consent, no part of this report should be used for the benefit of any party other than the contracting party to RSI Pipeline Solutions. We do not accept any liability if this report is used for an alternative purpose from which it is intended, nor to any third party in respect of this report. Additionally, any assumptions, facts, or information not described in this report may affect the analysis and conclusions presented in this report. No warranties, either express or implied, are intended or made.

Background and Scope of Confidential RCFA

This report examines the causal and contributing factors associated with the December 7, 2022, incident near Milepost 14 (MP 14) of the Keystone Pipeline, Cushing Extension (MP 14 Incident).

[REDACTED] TC Oil's purpose in requesting RSI's engagement in this RCFA was [REDACTED] to serve as an independent third-party pursuant to Action Item 5 of the Corrective Action Order (CPF 3-2022-074-CAO) issued on December 8, 2022, by the Pipeline and Hazardous Materials Safety Administration (PHMSA) [REDACTED]. The scope of the confidential RCFA is limited to the facts and circumstances of the MP 14 Incident.

Executive Summary

At approximately 20:01, Mountain Standard Time (MST), on December 7, 2022, the 36-inch diameter Keystone Pipeline ruptured just south of Mill Creek near MP 14 in Washington County, Kansas. At approximately 20:07 MST, the Controller initiated an emergency shutdown of the pipeline and isolation valves were commanded closed. Isolation of the affected segment¹ between the Steele City and Hope Pump Stations (PS) was achieved by 20:20 MST. TC Oil Technicians were dispatched to locate the release. When they arrived north of US Highway 36 at mainline valve STLCTB-01A they detected a hydrocarbon odor in the area and later confirmed the release location to be approximately two miles north of the highway crossing. Once the pipe was excavated, the failure was determined to have occurred at a girth weld (GWD 13530) in a fabricated bend assembly (TAG 98). The MP 14 Incident did not result in any injuries, ignition, or evacuations of the public, and no high consequence areas (HCA) were impacted. An estimated release of 14,000 barrels (588,000 gallons) of crude oil was reported initially to the National Response Center (NRC).

Corrective Action Order

PHMSA issued CAO CPF No. 3-2022-074-CAO on December 8, 2022, finding that continued operation of the affected segment is or would be hazardous to life, property, or the environment without corrective measures. The CAO outlined specific corrective actions to be taken by TC Oil to protect the public, property, and the environment. Item 5 of the CAO specified that within 90 days following receipt of the CAO, TC Oil must complete an RCFA and submit a final report of the RCFA to the PHMSA Central Region Director. The RCFA must be supplemented or facilitated by an independent, third-party vendor acceptable to the Director. The RCFA must document the decision-making process and all factors contributing to the failure. In addition, the final report must include findings and any lessons learned and whether the findings and lessons learned are applicable to other locations within TC Oil's pipeline system. RSI was selected to be the independent third-party vendor and approved by the Director.

¹ PHMSA defines "affected segment" as the approximately 96 miles of TC Oil's Keystone Pipeline that contains 36-inch diameter pipe from Steele City PS (MP 0.0) to Hope PS (MP 95.7). The "affected segment" traverses Jefferson County Nebraska, Washington County Kansas, Clay County Kansas, and Dickinson County Kansas.

An Amended Corrective Action Order (CAO) CPF No. 3-2022-074-CAO was issued on March 7, 2023, outlining additional corrective actions that TC Oil must take. As part of this amendment, new requirements were added to the RCFA portion (amended Item 4) that “the RCFA must be comprehensive, including but not limited to: consideration of pipe and fitting design, specification and manufacture of materials, material acquisition, material quality assurance & quality control, fabrication and construction history, girth weld joint design, welding procedures and qualification, previous non-destructive examinations and testing, inline inspection history, operating parameters and pressure cycling, external loading, previous evaluation of land movement, and any prior remediation or repairs.”

System Details

The Keystone Phase 2 pipeline system, referred to as the Cushing Extension, was built between April 2010 and November 2010 by TransCanada Keystone Pipeline, LP (now TC Oil). The Cushing Extension consists of approximately 298 miles of 36-inch diameter by 0.465-inch nominal wall thickness line pipe, four pump stations throughout Nebraska, Kansas, and Oklahoma, and a tank terminal facility in Cushing, Oklahoma. At Steele City, Nebraska, the Keystone pipeline splits with one branch running east for deliveries into Wood River and Patoka, Illinois and the other branch running south into Keystone Phase 2 for deliveries into Cushing, Oklahoma. The current capacity of the Keystone system is approximately 104,400 cubic meters day (m³/day) or 656,000 barrels per day (BPD).

A Special Permit containing 51 conditions was issued by PHMSA on April 30, 2007, to allow the pipeline to operate at a stress level up to 80% of the steel pipe’s specified minimum yield strength (SMYS). The conditions within the Special Permit required Keystone to implement more rigorous design, inspection, testing, and oversight processes for pipe manufacturing and pipeline construction as well as implement state-of-the art supervisory control and data acquisition (SCADA) and leak detection systems. The Special Permit also requires TC Oil to more closely inspect and monitor the Keystone Pipeline over its operational life than similar pipelines operated at a lower percent of SMYS that do not require a Special Permit.

The temperature and pressure limitations for the materials selected for the Cushing Extension were established in the design basis memorandum (DBM) in accordance with 49 CFR 195, ASME B31.4, MSS SP-75, and Special Permit requirements. Key design parameters for the US portion of the Keystone pipeline include a maximum operating pressure (MOP) of 1,440 psig (9,930 kPag), maximum operating temperature of [REDACTED], and flow capacity of 104,400 m³/day (656,000 BPD). The maximum temperature differential for the buried pipeline portion is [REDACTED]². A stress analysis for the construction spread containing the affected segment (Spread 9C) was completed in May 2010. The analysis evaluated stresses during construction, commissioning, and operating phases in support of using alternative acceptance criteria in Appendix A of API 1104 for mechanized welding.

² The maximum oil flowing temperature of [REDACTED] minus the below grade temperature of 1.7°C [REDACTED].

Fabricated Bend Assembly

During commissioning hydrostatic testing for the Cushing Extension in the fall of 2010, a fitting (elbow) manufactured by Canadoil Asia was noted as having experienced coating disbondment during the final visual inspection. The fitting was removed and tested to determine the cause. The mechanical testing showed that the actual yield strength of the fitting was [REDACTED], 20 ksi less than the minimum design yield strength of [REDACTED]. TC Oil initiated an investigation and uncovered significant quality issues at the fitting manufacturer's facility. Based on the investigation results, TC Oil determined that the strength of the [REDACTED] fittings supplied under the same purchase order (PO) could not be guaranteed to meet the project's design specification. Therefore, TC Oil decided to replace all [REDACTED] fittings supplied by Canadoil Asia.

The fabricated bend assembly TAG 98 (BND 350) was manufactured by Canadoil in Becancour, Quebec and assembled in late-2010 to replace a Canadoil Asia fitting. The assembly components consist of two 36-inch nominal diameter, 0.515-inch nominal wall thickness, API 5L Grade X70 pups³ manufactured by [REDACTED] and a 36-inch nominal diameter, Grade WPHY 70, 3D, 30° forged elbow manufactured by [REDACTED]. The pups were specified to meet API 5L⁴ Grade X70 PSL2, and supplemental specification TES-PIPE-SAW-US⁵ for double submerged arc welded longitudinal (SAWL) seam welded pipe. The elbow was specified to meet MSS SP-75-2008⁶ and supplemental specification TES-FITG-LD-US⁷ for high yield carbon steel butt welding fittings. The welding process used to join the pups to the elbow was in accordance with specification TES-WELD-AS-US⁸. The bend assembly was fabricated, radiographed, and pressure tested at [REDACTED] in Stafford, Texas and shipped to [REDACTED] in Conroe, Texas for coating application.

The TAG 98 bend assembly was installed downstream of Mill Creek in December 2010. The construction contractor performing the work was [REDACTED]. The maximum operating pressure (MOP) of 1,440 psig (9,930 kPag) was established by a hydrostatic test performed on December 11, 2010, as it pertains to the release location.

Operational History

The Steele City to Hope pipeline segment has operated below its temperature and pressure design limits since operations commenced in February 2011. The Steele City discharge pressure just before the rupture was about [REDACTED] and 1,153 psig (58% SMYS) at the failure location. Pressures were increasing at the time of the incident due to pressure transients that occurred when the Hope PS was bypassed to allow passage of an inline inspection (ILI) tool. The pressure increase was normal for this type of inspection and never exceeded the MOP or maximum allowable discharge pressure (MADP) of the line

³ A pup is a short length of pipe generally used to fill a gap between fittings and/or pipe joints.

⁴ API 5L, 44th Edition, Specification for Line Pipe, October 1, 2008.

⁵ TES-PIPE-SAW-US, Specification for SAW Pipe, Rev 1, June 24, 2009.

⁶ MSS SP-75-2008, Specification for High-Test, Wrought, Butt-Welding Fittings, 2008.

⁷ TES-FITG-LD-US, Specification for High Yield Carbon Steel Butt welding Fittings, February 9, 2007.

⁸ TES-WELD-AS-US, Welding of Assemblies and Station Piping, Rev 01, November 25, 2009.

downstream of Steele City [REDACTED]. Note, since operations began in February 2011, the affected segment has never operated above 72% SMYS.

TC Oil has regularly inspected the affected segment with ILI technologies since operations began. A profile caliper tool run was completed in December 2012 followed by high-resolution caliper, high-resolution magnetic flux leakage (MFL), and inertial mapping unit (IMU) tool runs in 2013 and 2018. An ultrasonic axial crack detection (UTCD) inspection was conducted in September 2020. The 2018 ILI tool (MFL4) was configured to detect certain types of girth weld anomalies; however, no anomalous features were detected by this tool at the failure location. The affected segment is also inspected yearly with inline leak detection tools. On the day of the incident, a P2D leak detection tool was being run in the affected segment and had recently passed the failure location. No leaks were found.

The 2012 profile caliper ILI tool identified a [REDACTED] ID restriction (due to ovality) in the TAG 98 bend assembly that had damaged the cleaner and gauge tools run prior to the caliper tool. An excavation was performed in March 2013 to evaluate the restriction. A [REDACTED] ovality was measured in the field and ultrasonic wall thickness measurements were taken. The ovality was determined not to be an integrity concern at the time as it pertained to future ILI runs and the bend assembly was backfilled without any further interventions. While the excavation was still open, discussions occurred between the Pipe Integrity team and ILI vendor about how best to proceed. Several possible options were evaluated including (1) having the ILI vendor modify their tool so that it would pass through the elbow, (2) using a multi-diameter tool, or (3) cutting out the ID restriction. The option to cut out the feature was determined not to be the most favorable option at the time. Instead, the vendor agreed that they could navigate the feature with a tool redesign. Subsequent ILI runs have successfully navigated the ID restriction without any significant issues.

Capacity Increase Projects

In 2016, TC Oil initiated a capacity increase project for the Keystone Pipeline to increase the flowrate from approximately [REDACTED] to [REDACTED] on the portion running from [REDACTED] to [REDACTED] ([REDACTED] and [REDACTED]). Activities to support this project spanned from 2016 to 2021 and included stress analyses and engineering assessments (EA) to understand the impact of the proposed operational change on the pipeline bending stresses, particularly related to the increased operating temperatures associated with the increased flowrate.

In 2020, another capacity increase project was initiated to evaluate a capacity increase to [REDACTED] on the [REDACTED] to [REDACTED] of Keystone. Another stress analysis was performed to assess bending stresses induced by internal pressure, temperature differentials, and soil restraint at bends. Temperature limits at [REDACTED], [REDACTED], [REDACTED], and [REDACTED] pump stations were set based on the results of these analyses. At the time of the MP 14 Incident, the affected segment was operating below the temperature limit set at [REDACTED] of [REDACTED].

Ramp up testing to [REDACTED] was initiated in December 2022, only a few days prior to the MP 14 Incident. The goal of the ramp test was to collect data on pressures, temperatures, pipe vibration, noise levels, power draw, etc. as well as how the increased flowrate impacted daily operations in the Control Room. Because of the incident, the ramp up test was not completed.

Investigation Details

Excavation at the failure feature revealed a circumferentially oriented crack at girth weld GWD 13530 (G59B) spanning the top of the pipe from 333° to 54°. A metallurgical failure investigation was performed by Anderson & Associates (Anderson)⁹ of Houston, Texas. The below details were reported or derived from information presented in Anderson's report. Three prominent elliptically shaped crack features were identified within GWD 13530. Crack 1 was the largest, measuring approximately 0.5-inch deep (97% of nominal wall thickness, NWT) by 8.7-inch long, centered approximately 4.5-inch (14.3°) clockwise from top dead center (TDC). The second largest crack, Crack 2, measured approximately 0.38-inch deep (74% NWT) by 4-inch long, with the deepest portion approximately 4.25-inch (13.5°) counterclockwise from TDC. Crack 3 was the smallest, measuring approximately 0.18-inch deep (35% NWT) by 4.0-inch long, with the deepest portion located approximately 13-inch (41.4°) clockwise from TDC. All three cracks appeared to be located entirely on the pup side of the girth weld. Separating each crack were two shear regions coincident with weld repairs. A wrinkle was also found in the pup upstream of GWD 13520. The wrinkle was centered at the bottom dead center of the pipe and spanned approximately 180°.

The three crack features were identified as originating at or near the inner diameter (ID) toe of the GWD 13530 and had multiple, radially oriented crack initiation features (ratchet marks). Each crack showed evidence of progressive cracking in the form of multiple crack arrest features. Crack 1 and Crack 2 exhibited 10 to 15 distinct "beach marks" or macroscopic features marking the position of the crack front over time, characteristic of a progressive or fatigue cracking mechanism from the ID surface.

The rupture was caused by a fatigue (progressive) cracking mechanism along the inner toe of GWD 13530 on the thin wall side (pup side) of the weld. The multiple fatigue crack initiation sites were coincident with lack of fusion (LOF) features with a maximum depth of 0.008-inch (200 µm) and found at the toe of the girth weld. The LOF regions were lined with a tightly adhered, high-temperature oxide scale (magnetite) that formed during the welding process. The fatigue cracks propagated linearly from the ID toward the outer diameter (OD), consistent with cyclical application of tensile stresses. The girth weld failed when the remaining ligament of the largest crack (Crack 1) could no longer support the applied load.

Finite element analyses (FEA) performed by RSI of various loading scenarios showed loads introduced during construction most likely overstressed the TAG 98 bend assembly causing it to ovalize. The effects from these local bending loads combined with the design of the bend

⁹ Anderson & Associates, 220439 TC Energy – Metallurgical Analysis of NPS-36 KS10 MP-14 Pipeline, February 7, 2023.

assembly (3D elbow with taper transition joint) had a significant stress concentrating effect at GWD 13530 (G59B). The stresses were sufficiently large to initiate cracking at the shallow LOF region which then grew by pressure- and temperature-cycle fatigue over the operational life of the bend assembly.

The microstructure, chemical composition, tensile properties, and impact toughness of the pups, elbow, and girth welds were satisfactory and complied with applicable requirements. The material properties of each component did not contribute to this incident.

Causal Factors, Contributing Factors, and Root Causes

Causal factors are gaps in equipment or personnel performance that cause an incident or allow it to become worse whereas contributing factors are underlying reasons why a causal factor occurred but not sufficiently fundamental to be a direct cause. Root causes are deficiencies in management or controls, such as procedures, training, communications, or oversight that allow a causal factor to occur.

Failure of GWD 13530 (G59B) was caused by stresses acting on a shallow LOF region at the ID toe of the weld that were sufficiently high to initiate a crack. The stresses imparted to the 3D elbow assembly concentrated at the girth welds (GWD 13530 and GWD 13520) where the wall thickness transitioned from approximately 0.890-inch in the elbow to approximately 0.540-inch in the pups. The application of a large bending load to the TAG 98 (BND 350) bend assembly during its replacement in December 2010 contributed to the stress in the weld. The bending load was large enough to ovalize the bend assembly and to eventually cause plastic deformation (wrinkle) in the upstream pup. FEA modeling showed that the most likely scenarios to have caused such a large bending stress were loads applied during construction. Postulated scenarios include loads introduced during the hydrostatic test on December 11, 2010, during final tie-in of the replacement section on December 13, 2010, or during backfill and restoration activities where pipeline support may have been inadequate during soil compaction activities. Once a crack initiated, subsequent pressure and thermal cycles were large enough to cause the progressive crack growth until the remaining ligament was no longer able to withstand the applied loads and ruptured.

Causal factors were identified for events related to (1) the design of the TAG 98 bend assembly that used a 3D elbow joined to pups with a taper transition joint that enhanced stress concentrations in GWD 13530; (2) installation of the TAG 98 elbow assembly in a manner that introduced a large bending stress; (3) the lack of a post-construction caliper tool re-run to identify construction-related damage that may have occurred during the replacement project; and (4) post-analysis of integrity assessment results that underestimated the potential risks of the identified ovality and hypothetical girth weld imperfections. Contributing factors were identified for events related to (1) a taper transition length shorter than the minimum requirements in MSS SP-75-2008; (2) introduction of a shallow LOF imperfection during fabrication of TAG 98 that served as a crack initiation site; (3) underestimation of pressure- and thermal-cycle fatigue risks from daily operations; (4) integrity assessments that did not

adequately identify the girth weld cracking threat subsequent to the use of the MFL4 technology; and (5) procedures for stress analyses and EAs that did not effectively address uncertainty related to the potential for girth weld imperfections. Event sequences related to the control room response were also investigated but determined not to be causal factors in this incident.

RSI determined that the root causes of the December 7, 2022 rupture near Washington, Kansas were (1) gaps in company standards, policies, and administrative controls (SPAC) for design of bend assemblies that did not effectively address the impacts of added stress at the girth weld from the use of 3D elbows and taper transition joints under real-world conditions; (2) lapses in construction oversight and quality control during the fitting replacement project allowed for construction techniques that introduced a large bending stress in the TAG 98 bend assembly; (3) SPAC that did not address the need to re-run a construction caliper tool after significant pipeline modifications; and (4) weaknesses in evaluation and repair criteria for ovalities in high stress bend locations.

In consideration of the above factors, RSI concludes that the most probable chain of events for the MP 14 Incident are that:

- The primary cause of the rupture was a progressive (fatigue) crack that originated from a shallow LOF at the ID toe of GWD 13530.
- The LOF occurred because of:
 - Weld workmanship that, although it was code compliant, was not sufficient for the higher stress TAG 98 elbow assembly; and
 - NDE that was unable to detect such conditions.
- The ovality in the TAG 98 bend assembly most likely occurred when excessive bending loads were applied during its installation in December 2010.
- The LOF initiated a crack when localized stresses from ovalization and the girth weld geometry (3D elbow and taper transition joint) acted as stress concentrators on the LOF flaw.
- The ovality was discovered during the September 2012 caliper survey; however, upon its discovery the ovality was not addressed because:
 - It was not deemed an integrity concern except for the fact that it might prevent passage of subsequent ILI tools;
 - Ovalities are generally not viewed as an integrity threat by the industry; and
 - Further investigations and analyses were not performed to understand the cause and integrity implications of the ovality.
- Fatigue cracking occurred during operation with contributions from both pressure and thermal cycling.
- The fatigue crack was not detected during the 2018 MFL4 ILI targeting girth weld anomalies because:

- The elbow geometry may have reduced the tool's probability of detection (POD), probability of identification (POI), and sizing accuracy;
- The crack opening may have been below detection thresholds; and
- The high-temperature oxide (magnetite) lining the crack surface may have impeded flux leakage.
- The risk of progressive girth weld cracking was underestimated during the capacity increase projects because:
 - Stress analyses and EA relied on the results of the MFL4 tool run without consideration of POD, POI, or sizing accuracy limitations in bends;
 - Sensitivity analyses were not performed to understand the impact of imperfections in transition welds, such as high-low, acceptable flaws per API 1104, or flaw sizes just below the MFL4 detection threshold under cyclic operational loads.
- The fatigue crack failed when the remaining ligament could no longer support the applied loads.

The causal factors and root causes are summarized in Table E-1 and the contributing factors are summarized in Table E-2.

Table E-1. Summary of Causal Factors and Root Causes

Effect	Causal Factors	Root Causes
Elbow Assembly Design Enhanced SCFs at GWD 13530	CF1: The selection of a 3D elbow with a taper transition (in compliance with ASME B31.4) for the TAG 98 elbow-pup joint led to high stress concentrations in the girth weld.	RC1: Gaps in SPAC for design of bend assemblies did not effectively address the impacts of added stress at the girth weld from the use of 3D elbows and taper transition joints under real-world conditions like the joint's susceptibility to accidental construction loads, weld imperfections, or cyclic operational loads.
Large Bending Stress Introduced in TAG 98 (BND 350)	CF2: Construction practices (e.g., during hydrostatic testing, fit-up, backfilling, and compaction) during the replacement of the TAG 98 (BND 350) elbow assembly led to the introduction of a large bending moment at the overbend.	RC2: Lapses in construction oversight and quality control during the fitting replacement project led to bending stresses going unnoticed.
Construction Caliper Run Not Repeated	CF3: Construction caliper re-run was not required for the fitting replacement project.	RC3: SPAC did not address the issue of re-running a construction caliper ILI after significant pipeline modifications were made along the Cushing Extension to identify construction-related damage.

Effect	Causal Factors	Root Causes
Post-Analysis of Caliper ILI Results Insufficient	CF4: Further investigations or assessments as to the cause and implications of the ovality were not performed as part of the March 2013 integrity dig. Focus was on future ILI runs for integrity management rather than cause of the ovality and the risk of increased stress at the transition weld.	RC4: Evaluation and repair criteria for ovalities within bends needs improvement, especially where stresses are known to be high and the risk of girth weld failure is elevated (weld transitions).

Table E-2. Summary of Contributing Factors

Effect	Contributing Factors
Taper Transition Length	CTF1: The taper transition length on the TAG 98 (BND 350) elbow was less than the 1.00-inch minimum requirement in Figure 3 of MSS SP-75-2008 which can enhance stress concentration in the girth weld.
LOF Flaw in GWD 13530 (59B)	CTF2: The selected welding process and NDE methods required at the fabrication shop did not consider the higher stress girth welds associated with the TAG 98 elbow assembly design. Therefore, additional precautions beyond API 1104 minimum requirements were not instituted to ensure that the weld workmanship and flaw detection sensitivity were acceptable for the service in which it was placed.
Thermal and Pressure Cycling Led to Crack Growth	CTF3: Thermal and pressure cycles led to crack growth until the critical flaw size was reached.
Stress Analyses and EAs did not Analyze Effects of Girth Weld Imperfections	CTF4: SPAC for stress analyses and EAs for capacity increase projects need improvement to address when girth weld imperfections should be considered or applying more stringent safety factors to account for the uncertainty of these real-world conditions.
Over-reliance on MFL4 Inspection Results	CTF5: EAs used the results of the MFL4 ILI to determine that the girth weld threat did not degrade the maximum stress criterion, but the analysis overlooked the potential for missed flaws or flaws below detection and reporting thresholds.
Crack in GWD 13530 (G59B) Not Detected by MFL4 ILI	CTF6: Though the MFL4 ILI was used as a tool to find certain types of girth weld anomalies, the vendor notes that the POD, POI, and sizing accuracies are affected within a bend. Moreover, girth weld anomalies need to have an opening of at least 0.01-inch (0.25 mm) to achieve a high POD. These factors likely limited the ability of the MFL4 tool in detecting the flaw indications within GWD 13530 (G59B).

Applicability of Findings and Lessons Learned to Other Locations within TC Oil's Liquid Pipeline Operations

The findings and lessons learned from this incident are potentially applicable to other locations along Keystone where ovalities or ID restrictions have been identified in tight radius (3D) fabricated bend assemblies that contain a taper transition weld between the elbow and pups. In addition, all fabricated 3D bend assemblies that were replaced in 2010 could have similar

shallow LOF imperfections as identified for the TAG 98 bend assembly. Therefore, the girth welds for these bend assemblies should be examined with appropriate ILI or NDE techniques based on risk priority to identify any potential girth weld cracking concerns.

Recommendations

Several recommendations are proposed for TC Oil's consideration based on the causal factors (CF) and root causes (RC) identified for the MP 14 Incident.

- R1. Perform ILI with a validated circumferential crack detection tool or NDE of the girth welds for the 3D bend assemblies replaced in 2010 based on risk priority to determine if any flaws exist that could compromise pipeline integrity (RC1).**

Lessons Learned: Although the welding performed for TAG 98 complied with API 1104 code requirements for workmanship, a shallow LOF region was found in GWD 13530 (G59B) that was undetectable using conventional radiographic inspection techniques. The design of the TAG 98 bend assembly combined with the external bending load applied during construction was such that the stresses imparted to the weld were sufficiently high to initiate a crack at the shallow LOF. Other 3D elbows with taper transition joints are inherently higher stress and may also be susceptible to crack initiation at undetectable, shallow LOF regions. Therefore, the intent of R1 is to identify other high risk girth welds associated with 3D bend assemblies that could be a potential cracking threat.

- R2. Update pipeline design guidelines, pipeline stress analysis procedures, and/or engineering assessment procedures to include details on what factors should be considered in the analysis and when it is important to consider these factors (e.g., transition joint design, bend radius, maximum girth weld imperfections per API 1104, dynamic operational loads, geometry features like ovalities) to reduce the potential for analysis gaps (RC1).**

Lessons Learned: Detailed stress analysis and EA work performed during the capacity increase projects to mitigate the risk of increased stress at elbows and bends from elevated operating temperatures did not consider hypothetical shallow, surface-breaking flaws at the ID toe of the transition girth welds (which were a possibility based on the findings from the Freeman +4 Incident). Appropriately, the results of the MFL4 girth weld inspections were reviewed, but because the sensitivity of the MFL4 tool was not enough to detect the shallow LOF features that initiated cracking, no girth weld anomalies were identified to be included in the EA. Procedures did not require the evaluation of hypothetical girth weld flaws that could have been missed by inspections nor did they call for targeted inspections of girth welds at elbows and bends identified as potentially higher stress locations to verify that they were free of injurious defects. Additional guidance for what should be considered in stress analyses and EAs will help to reduce the potential for future analysis gaps.

- R3. Develop an integrity verification program (IVP) for potentially high stress pup-to-fitting transition welds, such as those at 3D elbows, to understand and manage integrity threats at these locations (RC1).**

Lessons Learned: The combination of the taper transition joint, 3D elbow, and large, applied bending stress during construction all added to the stress concentrations in GWD 13530. Without any one of these factors, the failure would not have occurred in the timeframe in which it did. Both 3D elbows and taper transition joints are acceptable design choices per codes and standards with the caveat that the implications of these choices on the potential pipeline stresses should be well understood and managed. An IVP for the higher stress bend assemblies will help TC Oil to continue to manage the risks.

- R4. Work with ILI vendors to develop tools with improved capabilities for detection of girth weld cracking threats in bends (RC1).**

Lessons Learned: The 2018 MFL4 ILI, which was used to identify anomalous conditions at girth welds, did not detect any anomalies within GWD 13530 or GWD 13520. Though the MFL4 tool was configured to detect some anomalous girth weld conditions, the vendor noted that the probability of detection (POD), probability of identification (POI), and sizing accuracies are affected within a bend. In addition, girth weld cracks need to have an opening of at least 0.01-inch (0.25 mm) to achieve a high POD, and Anderson reported that the crack surface was coated with high-temperature oxides (magnetite) which can impede flux leakage. These factors likely limited the ability of the MFL4 tool in detecting the cracking within GWD 13530 (G59B). Therefore, working with ILI vendors to improve girth weld flaw detection capabilities will enhance TC Oil's ability to manage this threat in the future.

- R5. Look for potential indicators of ovality, wrinkles, buckles, and ripples in raw caliper ILI data or the stand-off data from ultrasonic wall measurement (UTWM) tools to identify other locations where ovalization or wrinkles may be present as the result of a large bending load (RC2).**

Lessons Learned: Several factors during construction may have contributed to the large bending stress applied to the TAG 98 bend assembly that caused it to ovalize. The introduction of the ovality during construction without it being identified points to lapses in construction oversight and control of construction quality processes to minimize pipeline bending stress. Similar lapses in construction oversight may exist at other fabricated bend assemblies replaced in 2010 and therefore R8 is one method for identifying other locations with potentially high construction-related bending loads.

- R6. For large scale fitting replacement projects, such as what occurred along the Cushing Extension, consider the benefits of running another construction caliper**

ILI to detect areas where plastic deformation (ovalization or wrinkles) may have occurred due to construction-related bending loads (RC2, RC3).

Lessons Learned: A construction caliper inspection was completed in October 2010, before the replacement fittings were installed, to address any pipe damage that may have occurred during construction. However, the construction caliper inspection was not repeated after completing the fitting replacement project even though thousands of feet of pipe (and hundreds of fittings) were replaced. Had another caliper tool been run at that time, it likely would have detected the 9% ID restriction in the TAG 98 bend assembly (BND 350) and therefore could have been corrected at the construction contractor's expense.

- R7. Update ILI data analysis procedures to include criteria for response to ovalities within elbows (that extend beyond the elbow itself) such as performing stress analysis, engineering assessments, or defining when NDE of girth welds might be required (RC4).**

Lessons Learned: In March 2013 the Pipe Integrity team investigated the ID restriction at TAG 98 (BND 350) reported by the 2012 BHI profile caliper ILI to address valid integrity concerns about the ability to run future ILI tools through the restriction. The ID restriction was found to be due to an ovality in the TAG 98 bend assembly. The Pipe Integrity team took measurements and discussed with the ILI vendor how best to proceed for future inspections. No other activities were performed at the time to understand the cause of the ovality. Concerns about the feasibility of running future integrity inspections were appropriate but may have led the Pipe Integrity team to overlook the potential integrity risks associated with ovality itself. Additionally, procedures did not require analyses to understand the integrity impacts of the ovality nor require opportunistic NDE of the upstream and downstream transition girth welds to verify that they were defect free.

- R8. Require NDE of transition girth welds at 3D elbows when exposed during integrity digs to identify any potential flaws that may have been missed during prior radiographic or ultrasonic inspections (RC4).**

Lessons Learned: In 2013, pipeline anomaly field investigation procedures did not require opportunistic NDE of transition girth welds at 3D elbows to verify that they were defect free. Considering the Freeman +4 and MP 14 Incidents, future excavations could benefit from opportunistic examination of transition girth welds to identify and remediate potentially injurious defects.

Several recommendations (R) are proposed for TC Oil's consideration based on the contributing factors (CTF) identified for the MP 14 Incident.

- R9. Update welding specifications for bend assemblies to include scenario-based considerations when minimum code requirements may not be enough to ensure a weld will be appropriate for the service conditions. For example, define assembly designs that may have inherently higher stress girth welds and the additional provisions (e.g. tighter NDE requirements, detailed FEA to determine acceptable flaw sizes; redesign to reduce stresses) that are needed to ensure that weld workmanship aligns with the expected stresses (CTF1, CTF2).**

Lessons Learned: The selected welding process and NDE methods required at the fabrication shop did not consider the higher stress girth welds associated with the TAG 98 elbow assembly design. Therefore, additional precautions beyond API 1104 requirements were not instituted to ensure that the weld workmanship and flaw detection sensitivity were acceptable for the service in which it was placed.

- R10. For elbows identified as potentially high stress locations when operating the Cushing Extension at increased capacity, reanalyze them to also consider fatigue from combined thermal and pressure cycles. For elbows that do not meet defined stress or strain criteria, consider performing girth weld NDE to verify that welds are defect free and/or limiting operating conditions (as had been done previously) so that stresses remain at acceptable levels (CTF3, CTF4).**

- R11. For future stress analyses and engineering assessments of Cushing Extension 3D elbows with taper transitions, perform sensitivity studies to understand the stress implications of hypothetical girth weld flaws that could have been missed by the MFL4 tool, by NDE in the shop, or by assuming a flaw that would still be acceptable per code requirements (i.e., girth weld misalignment of 3 mm (1/8-inch) (CTF5, CTF6).**

Lessons Learned (R10 and R11): Though stress analysis and EAs were performed to understand and mitigate any potential increases in pipeline stress from the capacity increase projects, shortcomings were identified in the methodologies used. Specifically, hypothetical girth weld imperfections were not included in the analyses. For the elbow that failed, it experienced temperature and pressure cycles that alone may not have been a concern. However, in combination with a shallow, surface breaking LOF at the toe of the girth weld, the design of the 3D elbow and taper transition, and a large bending stress, the cyclic stresses were enough to grow a crack to failure. In absence of reliable girth weld crack detection ILI in the near term, TC Oil should consider revisiting the parameters used in stress analyses and EAs to define factors to include at 3D elbows with transition welds (e.g., girth weld imperfection, high-low, dynamic loads) or the need for targeted girth weld inspections.

Page Intentionally Left Blank

Table of Contents

1	Introduction	1
2	Background.....	2
2.1	Cushing Extension (Keystone Phase 2)	2
2.2	Special Permit	2
2.3	Affected Segment.....	3
2.4	Synopsis of the Incident.....	5
2.5	PHMSA Corrective Action Order.....	9
2.6	Elbow Replacement Program (2010).....	10
2.7	Investigative Excavation of ID Restriction (2013).....	12
2.8	Capacity Increase Program (2016-2020).....	14
2.9	Capacity Increase Program (2020-Present)	15
3	Root Cause Failure Analysis (RCFA) Process	16
3.1	Objective of the RCFA.....	16
3.2	Confidential RCFA Team	17
3.3	RCFA Methods and Scope	17
3.4	RCFA Terminology.....	18
3.5	Personnel Interviews.....	18
3.6	Event Timeline.....	19
4	Supporting Analyses.....	21
4.1	Metallurgical Failure Investigation.....	21
4.2	Stress Analyses.....	32
4.2.1	Ovalization and Wrinkle	33
4.2.2	Crack Initiation	43
4.3	Fatigue Analysis	46
4.3.1	Analysis of Pressure Data	46
4.3.2	Analysis of Temperature Data	49
4.3.3	Combining Pressure and Temperature Cycles	51
4.3.4	Stress Concentration Factors (SCFs)	52
4.3.5	Crack Initiation and Growth Thresholds	53
4.3.6	Crack Growth	54
5	Root Cause Failure Analysis.....	56
5.1	Stresses Exceeded Girth Weld Strength	57
5.1.1	TAG 98 (BND 350) Bend Assembly Design.....	58
5.1.2	TAG 98 (BND 350) Bend Assembly Manufacture.....	68
5.1.3	TAG 98 (BND 350) Bend Assembly Fabrication.....	73
5.1.4	TAG 98 (BND 350) Bend Assembly Installation.....	85
5.1.5	Operations.....	102

5.2	Assessments and Monitoring	111
5.2.1	2012 BHI Profile Caliper ILI	112
5.2.2	2013 BH GEMINI™ Caliper ILI	116
5.2.3	2018 BHGE MFL4 ILI	117
5.2.4	2020 NDT Eclipse ILI	120
5.2.5	Post-Incident Reviews	120
5.2.6	Causal Factors, Root Causes, Contributing Factors, and Items of Note – Assessments	122
5.3	Control Center Response	123
6	Conclusions and Recommendations	124
6.1	Causal Factors, Root Causes, Contributing Factors, and Items of Note	125
6.1.1	Causal Factors and Root Cause Summary	127
6.1.2	Contributing Factors	129
6.1.3	Items of Note	130
6.2	Applicability of Findings and Lessons Learned to Other Locations within TC Oil's Liquid Pipeline Operations	132
6.3	Recommendations	132
6.3.1	Causal Factors and Root Causes:	132
6.3.2	Contributing Factors:	135
6.3.3	Potential Improvement Opportunities	136
7	References	137
8	Appendix A – Event Timeline	A-1
9	Appendix B – Cause & Effect Trees	B-1
10	Appendix C – As-Built Alignment Sheet and Bending Strain Plots	C-1
11	Appendix D – Stress Analysis	D-1
12	Appendix E – Temperature and Pressure Cycle Histograms	E-1

List of Tables

Table 1. Summary of Crack Dimensions in GWD 13530	23
Table 2. Summary of FE Analyses	33
Table 3. Summary of FEA Results	34
Table 4. Loading Combinations for Operational Load Analysis	35
Table 5. Loading Combinations for Lack of Support Analysis	37
Table 6. Loading Combinations for Cantilever Soil-Pipe Interaction Analyses	40
Table 7. Maximum Equivalent Stress in Empty Pipe [psi]	42
Table 8. Pressure Cycle Characterization at MP 14	47
Table 9. Temperature Cycle Characterization at Steele City Discharge	50
Table 10. Loading Scenarios for Pressure and Temperature Stress Range Analysis	52
Table 11. Stress Concentration Factors	53

Table 12. Threshold Conditions for Fatigue Crack Propagation.....	54
Table 13. Stress Concentration Factors.....	56
Table 14. Keystone Pipeline Design Parameters – US Portion ⁶⁰	58
Table 15. Net Effects from Moving Girth Welds Farther from the Bend Vertex and the Reduced Thrust Force.....	62
Table 16. Crack Growth Over the Operational Life (12-years) for Various Designs	65
Table 17. Summary of Causal Factors and Root Causes – Design	67
Table 18. Summary of Contributing Factors – Design	67
Table 19. Summary of Items of Note – Design	67
Table 20. Summary of Items of Note – Manufacturing of TAG 98.....	73
Table 21. Summary of Contributing Factors – Fabrication of TAG 98	84
Table 22. Summary of Items of Note – Fabrication of TAG 98.....	85
Table 23. Construction Equipment On Site December 2010.....	96
Table 24. Summary of Causal Factors and Root Causes – Installation of TAG 98	102
Table 25. Summary of Contributing Factors – Operations	110
Table 26. Summary of Items of Note – Operations.....	110
Table 27. ILI History for KS10	111
Table 28. Deformation Detection and Sizing for BHI Profile Tool.....	112
Table 29. Summary of Causal Factors and Root Causes – Integrity Assessments	123
Table 30. Summary of Contributing Factors – Integrity Assessments	123
Table 31. Summary of Causal Factors and Root Causes	128
Table 32. Summary of Contributing Factors	130
Table 33. Summary of Items of Note.....	131

List of Figures

Figure 1. Map of Keystone Pipeline System	2
Figure 2. Map of Construction Spread 9C.....	3
Figure 3. Overview of Release Area Showing the Location of GWD 13530	5
Figure 4. Aerial View of the Release Site Looking South from North of Mill Creek – December 9, 2022	6
Figure 5. Pipeline Profile Schematic Looking East (pipeline flows north to south) ²³	7
Figure 6. Excavated Failure Feature Showing Girth Weld Crack – December 14, 2022.....	7
Figure 7. Wrinkle Feature Upstream of GWD 13520 – December 17, 2022.....	8
Figure 8. Excavated Bend Assembly – December 16, 2022	8
Figure 9. Pipe Segment Sent to Anderson for Metallurgical Evaluation (December 18, 2022)....	9
Figure 10. TAG 98 Bend Assembly (BND 350) During Replacement (December 10, 2010)	11
Figure 11. TAG 98 Bend Assembly (BND 350) During March 2013 Excavation to Investigate ILI- Called ID Restriction (March 1, 2013)	13
Figure 12. TAG 98 Bend Assembly (BND 350) ILI-Called Ovality and Actual Measurements...	13
Figure 13. Timeline of Key Events Leading up to the MP 14 Incident.....	20
Figure 14. View of Downstream (Pup Side) of the Exposed Fracture.....	22
Figure 15. Magnified View of Crack 1 in GWD 13530 (G59B).....	23
Figure 16. Magnified View of Crack 2 in GWD 13530 (G59B).....	23

Figure 17. Magnified View of Crack 3 in GWD 13530 (G59B).....	24
Figure 18. Images and Metallographic Sections Showing the Location of Repairs in GWD 13530 (G59B) Between Fatigue Crack Locations.....	24
Figure 19. High-Low Measurements at GWD 13530, GWD 13520, and GWD 13510	25
Figure 20. Post-Incident PAUT Results for GWD 13510, GWD 13520, and GWD 13530	26
Figure 21. Low Magnification SEM Showing the Center Region of Crack 1 (most prominent crack arrest lines identified with yellow arrows).....	27
Figure 22. (a) Low Magnification SEM Fractograph Showing the ID Region of GWD 13530, Crack 1 and (b) Higher Magnification SEM Fractograph Showing that the Fracture Surface near the ID of GWD 13530, Crack 1 had been Consumed by Oxidation	27
Figure 23. (a) Low Magnification SEM Fractograph of GWD 13530, Crack 1 Showing Multiple Crack Arrest Lines (crack arrest lines identified with the yellow arrows) and (b) Higher Magnification SEM Fractograph of GWD 13530, Crack 1 Showing a Band of Dimpled Rupture Associated with a Crack Arrest Line Near the Shear Overload Region	28
Figure 24. Metallographic Cross Section Through GWD 13530, Crack 1.....	29
Figure 25. Photo Montage of Optical Micrographs Showing GWD 13530, Crack 1 (left 12.5x, top right 12.5x, and bottom right 50x).....	30
Figure 26. Metallographic Section of an Intact Portion of GWD 13530 at 139° from TDC Consistent with PAUT Indication 2	31
Figure 27. Optical Micrographs Showing a Scale-Filled, ~200 µm long LOF at the Pipe Side Weld Toe of GWD 13530 (a) 100x and (b) 500x	31
Figure 28. FEA von Mises Stresses with Elbow Elements and Lower-Bound Soil Properties (worst-case)	35
Figure 29. Schematic of the FEA Model for the Weak Support and Settlement Scenario.....	37
Figure 30. Hypothetical Ground Settlement Profile.....	37
Figure 31. FEA Longitudinal Stresses with Elbow Elements and Lower-Bound Soil Properties (a) Side Boom Load Only, (b) Settlement Load Only, and (c) Side Boom and Settlement Loads... ..	38
Figure 32. Use of Sidebooms During Replacement of TAG 98 (December 10, 2010)	39
Figure 33. Schematic of the FEA Model for the Cantilever Scenario with End Deflection.....	40
Figure 34. Schematic of the Cantilever Model with Sliding Displacement	40
Figure 35. FEA (a) Longitudinal Stresses with 6-ft End Deflection and (b) von Mises Stresses with 6-ft End Deflection (Elbow Elements and Lower-Bound Soil Properties)	41
Figure 36. FEA (a) Longitudinal Stresses with 6-inches of Sliding Displacement and (b) von Mises Stresses with 6-inches of Sliding Displacement (Elbow Elements and Lower-Bound Soil Properties).....	41
Figure 37. Region on the Crack 1 Fracture Surface with Corrosion Indicating Crack Initiation Early in the Life of the Crack	44
Figure 38. PAUT Indicated Flaw Depths for GWD 13520 and GWD 13530	45
Figure 39. Comparison of Cross-Sections for GWD 13530 with PAUT Findings (a) 139° from TDC and (b) 270° from TDC.....	45
Figure 40. Pressure Spectrum for the Steele City Discharge and Hope Suction (January 2011 to December 7, 2022)	46
Figure 41. Annual Equivalent 80% SMYS Cycles at MP 14	48

Figure 42. Pressure Cycle Counts for the MP 14 Location (January 2011 to December 7, 2022)	48
Figure 43. Temperature Spectrum for the Steele City Discharge (January 2011 to December 7, 2022)	49
Figure 44. Annual Equivalent Temperature Cycles at Steele City	50
Figure 45. Temperature Cycle Counts for the Steele City Discharge (January 2011 to December 7, 2022)	51
Figure 46. Combined Pressure and Temperature Cycle Counts (January 2011 to December 7, 2022)	51
Figure 47. Histogram of Stress Ranges for the Combined Pressure and Temperature Cycles (January 2011 to December 7, 2022)	52
Figure 48. Sensitivity of Crack Growth Relative to the Paris Law exponent	55
Figure 49. Simplified Cause and Effect Tree – MP 14 Incident	57
Figure 50. Simplified Cause and Effect – Stresses Exceeded Girth Weld Strength	58
Figure 51. TAG 98 As Built Drawing Showing Design Requirements and Bevel Details	60
Figure 52. Acceptable Design for Unequal Wall Thickness (MSS SP-75, Figure 3)	63
Figure 53. As-Built Bevel Details for the TAG 98 Butt Weld	64
Figure 54. As-Fabricated Bevel Length for the TAG 98 Butt Weld Joint at Crack 2	64
Figure 55. Local Weld Joint SCF, Effect of Elbow Wall Thickness and High-Low	66
Figure 56. Fittings Dimensional Inspection and Brinell Hardness Test Report Highlighting TAG 98 Elbow (Item # 174469)	70
Figure 57. Seam Weld Radiographic Examination of TAG 98 Elbow (Item # 174469)	71
Figure 58. TAG 98 (BND 350) Bend Assembly Design for Fabrication	74
Figure 59. Incomplete Fusion at Root of Bead of Top of Joint (IF)	75
Figure 60. ITP Excerpt for Bend Assembly Fabrication at RCT	77
Figure 61. Example of Incomplete Weld Inspection Report for TAG 114C (BND 349)	78
Figure 62. Schematic of SWE/SWV Radiography Technique Used on GWD 13530	79
Figure 63. RT Report for TAG 98 Girth Welds G59B and G59A (November 19, 2010)	80
Figure 64. RT Report to Reexamine Portions of TAG 98 Girth Welds G59B and G59A (November 20, 2010)	81
Figure 65. Summary of Elbow Assembly Fabrication, Weld Radiography, and Hydrostatic Testing at RCT (November 16-26, 2010)	82
Figure 66. Summary of TAG 98 Installation Timeline (December 3-17, 2010)	85
Figure 67. Installation of TAG 98 (December 10, 2010)	86
Figure 68. Key Girth Weld Installation Dates – Approximately 158 ft Between GWD 13530 and Final Tie-In Weld GWD 13590 (photo for illustrative purposes only, it is not from the time of construction)	88
Figure 69. Schematic of Trenching, Pipe Support, and Backfill Requirements	89
Figure 70. Geotechnical Assessment Near MP 14	90
Figure 71. Historical Weather Conditions in Steele City, Nebraska (December 5-18, 2010)	91
Figure 72. Photos Showing Soil Support Beneath TAG 98 (March 1, 2013)	92
Figure 73. Utility Inspector Observations on December 11, 2010	93
Figure 74. Final Tie-In Weld GWD 13590 (9GT-035) Reports Indicating Fit-Up	95

REDACTIONS MADE BY TC OIL - Pending PHMSA Review

TC Oil

**CONFIDENTIAL – Protected from release under
FOIA Exemptions 4 and 7(F), 5 USC 552(b)(4)
and (b)(7)(F).**



ACRONYMS

AUT	Automatic Ultrasonic Testing	MTR	Material Test Report
AYS	Actual Yield Strength	MVC	Micro-Void Coalescence
BHGE	Baker Hughes General Electric	NCR	Nonconformance Report
BND	Bend	NDE	Nondestructive Evaluation
BPD	Barrels per Day	NDT	Nondestructive Testing
BPH	Barrels per Hour	NRC	National Response Center
CAO	Corrective Action Order	NRCS	National Resources Conservation Services
CCSI	Commercial Coating Services International	NWT	Nominal Wall Thickness
CF	Causal Factor	OD	Outside Diameter
CFR	Code of Federal Regulations	P2D	Leak Detection Tool
CGHAZ	Coarse Grained Heat Affected Zone	PAUT	Phased Array Ultrasonic Testing
CST	Central Standard Time	PHA	Process Hazard Analysis
CTF	Contributing Factor	PHMSA	Pipeline and Hazardous Materials Safety Administration
CTOD	Crack Tip Opening Displacement	PM	Project Manager
DBM	Design Basis Memorandum	PO	Purchase Order
DOT	Department of Transportation	POD	Probability of Detection
DRA	Drag Reducing Agent	POI	Probability of Identification
EA	Engineering Assessment	PQR	Procedure Qualification Record
EOC	Emergency Operation Center	PS	Pump Station
EPA	Environmental Protection Agency	PWHT	Post Weld Heat Treatment
FBE	Fusion Bonded Epoxy	QM	Quality Manual
FCAW	Flux Cored Arc Welding	QMS	Quality Management System
FE	Finite Element	RC	Root Cause
FEA	Finite Element Analysis	RCFA	Root Cause Failure Analysis
FFS	Fitness for Service	RCT	RC Technical Welding & Fabrication
FGHAZ	Fine Grained Heat Affected Zone	ROW	Right of Way
GMAW	Gas Metal Arc Welding	RSI	RSI Pipeline Solutions
GWD	Girth Weld	RT	Radiographic Testing
HAZ	Heat Affected Zone	SCADA	Supervisory Control and Data Acquisition
HCA	High Consequence Area	SCF	Stress Concentration Factor
ID	Inside Diameter	SEM	Scanning Electron Microscope
ILI	Inline Inspection	SME	Subject Matter Expert
IMU	Inertial Mapping Unit	SMYS	Specified Minimum Yield Strength
INGAA	Interstate Natural Gas Association of America	SPAC	Standards, Policies and Administrative Controls
ION	Item of Note	SWRA	System Wide Risk Assessment
IQI	Image Quality Indicator	TDC	Top Dead Center
ITP	Inspection & Test Plan	TMCP	Thermo-Mechanically Controlled Processing
JIP	Joint Industry Project	TOC	Threat of Concern
LDS	Leak Detection System	TOFD	Time of Flight Diffraction
LOF	Lack of Fusion	US	United States
LPCC	Liquids Pipeline Control Center	USDA	United States Department of Agriculture
MADT	Maximum Allowable Discharge Temperature	UT	Ultrasonic
MFL	Magnetic Flux Leakage	UTCD	Ultrasonic Crack Detection
MOC	Management of Change	UTWM	Ultrasonic Wall Measurement
MOP	Maximum Operating Pressure	VIV	Vortex Induced Vibration
MP	Milepost	WOF	Weather and Outside Force
MPI	Magnetic Particle Inspection	WPS	Welding Procedure Specification
MST	Mountain Standard Time	YS	Yield Strength

Page Intentionally Left Blank

1 Introduction

About 20:01, Mountain Standard Time (MST), on December 7, 2022, the 36-inch diameter Keystone crude oil pipeline, owned and operated by TransCanada Keystone Pipeline, LP (TransCanada, now TC Oil), ruptured just south of Mill Creek near MP 14 in Washington County, Kansas. The rupture occurred when fatigue cracking in girth weld GWD 13530 (G59B) reached a depth at which the remaining ligament could no longer support the applied loads. The release was detected by the Liquids Pipeline Control Center (LPCC) through the supervisory control and data acquisition (SCADA) system and leak detection system (LDS) the evening of December 7, 2022. Approximately 12,937 barrels¹⁰ (543,350 gallons) of crude oil were released. The incident did not result in any injuries, ignition, or evacuation and no high consequence areas (HCA) were impacted.

PHMSA issued CAO CPF No. 3-2022-074-CAO on December 8, 2022, finding that continued operation of the affected segment¹¹ is or would be hazardous to life, property, or the environment without corrective measures. The CAO outlined specific corrective actions to be taken by TC Oil to protect the public, property, and the environment. Item 5 of the CAO specified that within 90 days following receipt of the CAO, TC Oil must complete an RCFA and submit a final report of the RCFA to the PHMSA Central Region Director. The RCFA must be supplemented or facilitated by an independent, third-party vendor acceptable to the Director. The RCFA must document the decision-making process and all factors contributing to the failure. In addition, the final report must include findings and any lessons learned and whether the findings and lessons learned are applicable to other locations within TC Oil's pipeline system. RSI Pipeline Solutions (RSI) was selected to be the independent third-party vendor and approved by the Director. An Amended Corrective Action Order (ACAO) CPF No. 3-2022-074-CAO¹² was issued on March 7, 2023, outlining additional corrective actions that TC Oil must take as well as a comprehensive list of factors that must be included in the RCFA.

RSI reviewed and evaluated data about the sequence of events, testing and examination of the failed bend assembly, the information available to company personnel, and decisions made prior to, during, and after the incident to develop the conclusions and recommendations provided in this report.

¹⁰ <https://www.tcenergy.com/incident/milepost-14-incident/> accessed on February 10, 2023.

¹¹ PHMSA defines "affected segment" as the approximately 96 miles of TC Oil's Keystone Pipeline that contains 36-inch diameter pipe from Steele City PS (MP 0.0) to Hope PS (MP 95.7). The "affected segment" traverses Jefferson County Nebraska, Washington County Kansas, Clay County Kansas, and Dickinson County Kansas. The affected segment is part of the 36-inch diameter Cushing Extension (Keystone Phase 2) that runs from Steele City, Nebraska to a terminal facility in Cushing, Oklahoma. The affected segment is contained within construction Spread 9C and piggable segment KS10.

¹² Amended Corrective Action Order (ACAO) CPF No. 3-2022-074-CAO, March 7, 2023.

2 Background

2.1 Cushing Extension (Keystone Phase 2)

The Cushing Extension (Keystone Phase 2) pipeline system originates at Steele City, Nebraska and terminates at the Cushing Tank Farm in Cushing, Oklahoma. The Cushing Extension was built between April 2010 and November 2010 and commissioned into operation by TC Oil in February 2011¹³. The Cushing Extension consists of approximately 298 miles of 36-inch diameter by 0.465-inch nominal wall thickness (NWT) line pipe, four pump stations throughout Nebraska, Kansas, and Oklahoma, and a tank terminal facility in Cushing, Oklahoma. The Keystone pipeline has a current capacity of approximately 656,000 barrels per day (BPD) (104,400 m³/day) although projects were ongoing to increase pipeline capacity to approximately [REDACTED]. Figure 1 shows a map of the Keystone pipeline system, including the Cushing Extension and location of the MP 14 Incident.

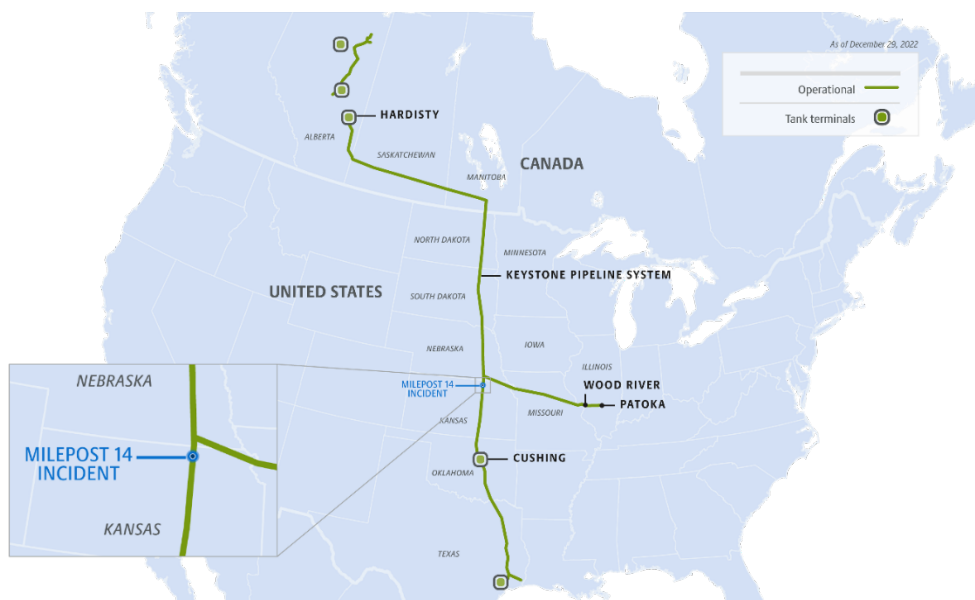


Figure 1. Map of Keystone Pipeline System¹⁴

2.2 Special Permit¹⁵

PHMSA issued a Special Permit on April 30, 2007, with 51 conditions to which Keystone must adhere to allow the pipeline to operate at a stress level up to 80% of the steel pipe's specified minimum yield strength (SMYS), whereas the Code of Federal Regulations (CFR) Title 49 Paragraph 195.106 normally limits the operating stress level for hazardous liquid pipelines to 72% of SMYS. The conditions within the Special Permit required Keystone to implement more rigorous design, inspection, testing, and oversight processes for pipe manufacturing and

¹³ <https://www.tcenergy.com/announcements/2011/2011-02-08keystones-cushing-extension-begins-deliveries-to-oklahoma/> accessed February 10, 2023.

¹⁴ <https://www.tcenergy.com/siteassets/incident/milepost-14/tc-energy-milepost-14-keystone-pipeline-system-map-12-14-2022-hi-res.png> accessed January 13, 2023.

¹⁵ https://www.phmsa.dot.gov/sites/phmsa.dot.gov/files/docs/TC_Keystone_2007-04-30_508compliant.pdf accessed January 13, 2023.

pipeline construction as well as implement state-of-the art SCADA and leak detection systems. The Special Permit also requires TC Oil to more closely inspect and monitor the Keystone pipeline over its operational life than similar pipelines operated at a lower percent of SMYS that do not require a Special Permit. The affected segment complied with the conditions of the Special Permit even though it never operated above a hoop stress level of 72% SMYS.

2.3 Affected Segment

The affected segment is contained within construction Spread 9C which was constructed by [REDACTED] between April 2010 and November 2010. As shown in Figure 2, Spread 9C is a 107.9-mile segment that originates at the Steele City PS (MP 0.0) and terminates on the south side of 290th Street (MP 107.9) in Marion, Kansas.

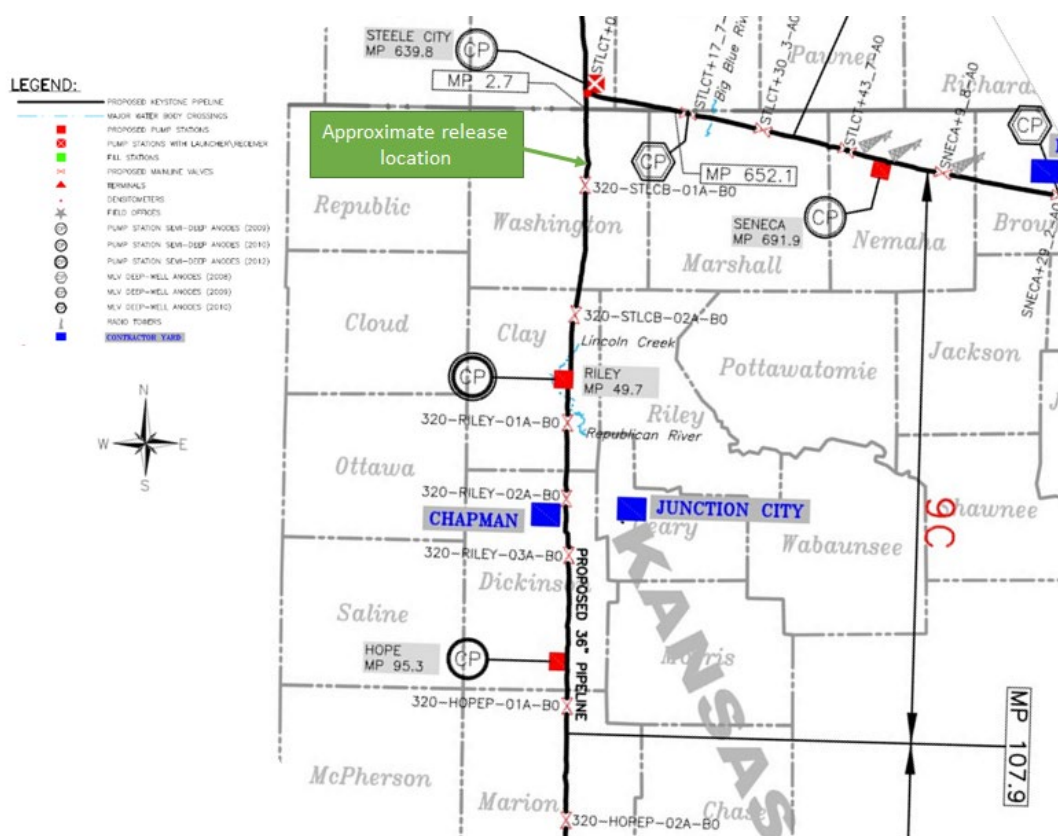


Figure 2. Map of Construction Spread 9C

The affected segment spans from Steele City PS (MP 0.0) to Hope PS (MP 95.3). The pipe segment that failed was part of a fabricated bend assembly, referred to as TAG 98 or BND 350, consisting of a 3D, 30°, 36-inch diameter, WPHY-70-W elbow and two pups¹⁶ manufactured from a single joint of 36-inch OD, 0.515-inch NWT, Grade X70 pipe. The elbow was manufactured by [REDACTED], in Becancour, Quebec to meet MSS SP-75-2008¹⁷ and

¹⁶ A pup is a short length of pipe generally used to fill a gap between fittings and/or pipe joints.

¹⁷ MSS SP-75-2008, Specification for High-Test, Wrought, Butt-Welding Fittings, 2008.

TC Energy's specification for high yield carbon steel butt welding fittings, TES-FITG-LD-US¹⁸. The pipe used for the pups was manufactured by [REDACTED] to meet API 5L, 44th Edition¹⁹ for PSL 2, SAWL, Grade X70 pipe and TC Energy's specification for SAW pipe, TES-PIPE-SAW-US²⁰. The welding process used to join the pups to the elbow was in accordance with specification TES-WELD-AS-US²¹. The bend assembly was fabricated at [REDACTED] in Stafford, Texas and shipped to [REDACTED] in Conroe, Texas for application of the liquid epoxy coating. The design maximum operating pressure (MOP) of the affected segment is 1,440 psig (80% SMYS) and was established by hydrostatic testing performed in December 2010, as it pertains to the release location. Since operations began, the affected segment has never operated above 72% SMYS.

An as-built alignment map of the location where the leak occurred is provided in Appendix C and shows the pipeline profile, Mill Creek crossing, and the location of the 30°, 3D overbend where the failure occurred (station 732+57). The rupture occurred approximately 90 feet downstream and upslope from Mill Creek. The crude oil release entered Mill Creek and was carried downstream for approximately three miles. The oil was contained using multiple containment booms, skimmers, and underflow dams. Figure 3 provides an overview of the release area showing some key pipeline features, including the release site (GWD 13530), bend locations, and creek. The release did not occur within an HCA, and Mill Creek is not connected to any drinking water sources.

The affected segment is contained within piggable segment KS10 which runs between the Steele City PS (MP 0.0) and Burns Pig Trap Station (MP 144.5). Piggable segment KS10 has been regularly inspected with in-line inspection (ILI) technologies since operations began in February 2011. Caliper inspections were completed in 2010, 2012, 2013, and 2018, high-resolution magnetic flux leakage (MFL) and inertial mapping unit (IMU) inspections were completed in 2013 and 2018 and an ultrasonic axial crack detection (UTCD) inspection was completed in September 2020. Both the 2012 and 2013 caliper tools reported a [REDACTED] and [REDACTED] ID restriction (a [REDACTED] ovality in 2012 and [REDACTED] ovality in 2013), respectively, at the failure location. The ID restriction was investigated in the field in March 2013 and determined to be non-injurious at the time. Wall thickness and dimensional measurements were taken but no coating was removed, and the site was subsequently backfilled. Internal leak detection and cleaning tools are also run annually. The most recent in-line leak detection survey of KS10 using the P2D technology was ongoing at the time of the incident. The P2D tool had recently passed the failure location and was approaching the Hope PS when the rupture occurred. Aerial patrols have also been conducted along KS10 a minimum of 26 times per year since operations began.

¹⁸ TES-FITG-LD-US, Specification for High Yield Carbon Steel Butt welding Fittings, February 9, 2007.

¹⁹ API 5L, 44th Edition, Specification for Line Pipe, October 1, 2008.

²⁰ TES-PIPE-SAW-US, Specification for SAW Pipe, Rev 1, June 24, 2009.

²¹ TES-WELD-AS-US, Welding of Assemblies and Station Piping, Rev 01, November 25, 2009.



Figure 3. Overview of Release Area Showing the Location of GWD 13530

2.4 Synopsis of the Incident

On December 7, 2022, at 20:01 MST the [REDACTED] alarm announced indicating a leak the size of which exceeded the 400 m³/hr (2,500 BPH) detection threshold over a two-minute averaging window along with a secondary pressure leak trigger. Approximately 27 minutes prior to the rupture, at 19:34 MST the flowrate on the Cushing Extension was reduced to approximately 3,500 m³/hr (22,000 BPH) to prepare to bypass the Hope PS and allow passage of the P2D leak detection and cleaning ILI tool. Slowing of the Cushing Extension and bypass of the Hope PS caused a transient pressure wave upstream increasing pressures from approximately 1,000 psig (6,900 kPa) to 1,212 psig (8,360 kPa), which was normal for this type of operation. In the two minutes prior to the rupture, at 19:59 MST, the Hope PS was bypassed. Between 20:01 and 20:07 the pressure dropped from 1,212 psig (8,360 kPa) to less than 900 psig (6,205 kPa). At 20:07 MST the LPCC made the decision to perform an emergency shutdown due to a suspected leak and isolation valves were commanded closed. Isolation of the affected segment²² between the Steele City PS and Hope PS was achieved by 20:20 MST.

²² PHMSA defines “affected segment” as the approximately 96 miles of TC Oil’s Keystone Pipeline that contains 36-inch diameter pipe from Steele City PS (MP 0.0) to Hope PS (MP 95.7). The “affected segment” traverses Jefferson County Nebraska, Washington County Kansas, Clay County Kansas, and Dickinson County Kansas.

Around 20:16 MST, regional on-call Technicians were dispatched to locate the release. Between 20:12 and 20:31 MST notifications were made to the on-call Control Center Operations Coordinator, Oil Scheduling, the Regional Emergency Operations Center (EOC), and the Corporate EOC. At approximately 23:15 MST the Technicians noticed a hydrocarbon odor north of US Highway 36 at mainline valve STLCB-01A. The failure location was confirmed to be approximately two miles north of the highway crossing. At 23:28 MST the National Response Center (NRC) was notified (NRC Report #1354442) of the release.

On December 8, 2022, incident response teams were mobilized to the release site and oil containment, recovery, and cleanup began. The area was cordoned off and only accessible by authorized personnel through security checkpoints. Representatives from PHMSA, the Environmental Protection Agency (EPA), and local responders arrived on site to monitor the response, cleanup, and recovery efforts. Calls were also made to the construction contractor, non-destructive evaluation (NDE) personnel, and welders to install a stopple upstream of the release site to further isolate the affected segment in consideration of the elevation profile. An aerial view of the release site on December 9, 2022, prior to excavation of the pipeline and stopple installation, is shown in Figure 4.



Figure 4. Aerial View of the Release Site Looking South from North of Mill Creek – December 9, 2022²³

²³ Internal Memo, Geotechnical Assessment of NPS 36 Keystone Mainline Leak at MP 14, January 16, 2023.

On December 13, 2022, the failure feature was first exposed. As shown schematically in Figure 5, the failure feature was confirmed to be a large crack in the girth weld (see Figure 6) connecting a 3D, 30° overbend to an approximately 8.5-foot-long pup (downstream) within a fabricated bend assembly (TAG 98). Upon further excavation, a wrinkle was also found just upstream of the overbend as shown in Figure 7. Between December 17 and 18, 2022, the bend assembly containing the failure feature and wrinkle was cut-out, removed, and prepared for shipment to Anderson & Associates (Anderson) of Houston, Texas for metallurgical evaluation to determine the direct cause of the rupture (see Figure 8 and Figure 9). The remaining pipe ends were prepared for welding of a new bend assembly as preparations for restarting the pipeline and cleanup operations continued. Restart of the pipeline began on December 29, 2022, under a temporary 20% pressure reduction in the actual operating pressure immediately prior to the failure on December 7, 2022 along the entire length of the affected segment.

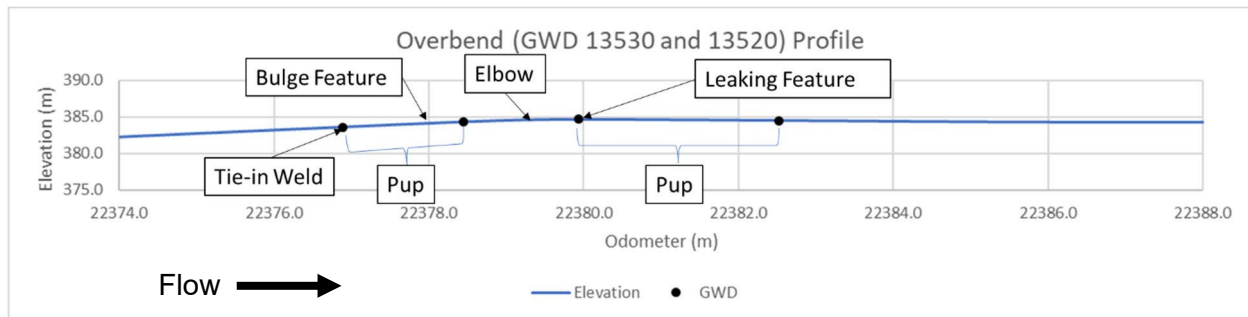


Figure 5. Pipeline Profile Schematic Looking East (pipeline flows north to south)²³



Figure 6. Excavated Failure Feature Showing Girth Weld Crack – December 14, 2022



Figure 7. Wrinkle Feature Upstream of GWD 13520 – December 17, 2022



Figure 8. Excavated Bend Assembly – December 16, 2022



Figure 9. Pipe Segment Sent to Anderson for Metallurgical Evaluation (December 18, 2022)

2.5 PHMSA Corrective Action Order

On December 8, 2022, PHMSA issued CAO CPF No. 3-2022-074-CAO²⁴ outlining specific actions to be taken by TC Oil to understand the cause of the incident, verify that the causal condition does not exist elsewhere in the affected segment, and prevent recurrence of the incident in the future.

Item 5 of the CAO specifies that TC Oil conduct an RCFA. Root causes are deficiencies or gaps in management or control systems, such as procedures, training, communications, or oversight, to name a few, that allow a causal factor to occur or exist. The CAO stipulated that an independent third-party acceptable to the PHMSA Director be selected to supplement or facilitate the RCFA. RSI was selected to be the independent third-party vendor and worked with TC Oil representatives from design, manufacturing and fabrication, construction, integrity, operations, and engineering throughout the RCFA process to collect relevant data and conduct interviews. RSI also relied on the findings from the metallurgical analysis and testing of the failed bend assembly conducted by Anderson (Item 4 of the CAO). The findings of the metallurgical analysis were submitted on February 7, 2023, and are summarized in Section 4.1 of this report.

²⁴ Corrective Action Order, CPF No. 3-2022-074-CAO, December 8, 2022.

The CAO stipulated that the RCFA must document the decision-making process used in the analysis and all factors contributing to the failure. Furthermore, the final report must include findings and any lessons learned and whether the findings and lessons learned are applicable to other locations within TC Oil's pipeline system. The CAO requires that the final RCFA report be submitted to the PHMSA Director within 90 days of its issuance. A two-week extension to this deadline was requested by RSI and granted by the PHMSA Director to give more time to thoroughly review the Anderson metallurgical analysis.

Subsequent to the extension request, an Amended Corrective Action Order (ACAO) CPF No. 3-2022-074-CAO²⁵ was issued on March 7, 2023, outlining additional corrective actions that TC Oil must take. As part of this amendment, requirements were added to the RCFA portion (amended Item 4) that "the RCFA must be comprehensive, including but not limited to: consideration of pipe and fitting design, specification and manufacture of materials, material acquisition, material quality assurance & quality control, fabrication and construction history, girth weld joint design, welding procedures and qualification, previous non-destructive examinations and testing, inline inspection history, operating parameters and pressure cycling, external loading, previous evaluation of land movement, and any prior remediation or repairs." The deadline for submission of the RCFA report to the PHMSA Director was extended to 45-days from issuance of the ACAO.

2.6 Elbow Replacement Program (2010)²⁶

During commissioning hydrostatic testing for the Cushing Extension in the fall of 2010, a fitting (elbow) manufactured by Canadoil Asia was noted as having experienced coating disbondment during the final visual inspection. The fitting was removed and tested to determine the cause. The mechanical testing showed that the actual yield strength of the fitting was [REDACTED], [REDACTED] less than the minimum design yield strength of [REDACTED]. TC Oil initiated an investigation into the root cause of the low yield strength fitting and determined that the fitting had not been adequately quenched which prevented it from being properly heat treated. The investigation discovered equipment issues with the quench tank and furnace used to heat treat the fittings which were not corrected prior to accepting and releasing the fittings. During manufacture of the fittings for the Cushing Extension in March 2010, over 50% of the mechanical tests used to generate the material test reports (MTRs) required retesting due to low or highly variable tensile test results. The process for retesting was substandard and was being performed without an approved procedure. Canadoil Asia did not notify the Keystone project that they were conducting retests, nor did they provide a procedure to TC Oil for review and approval. Ultimately, the root cause was determined to be a failure of Canadoil Asia to follow their Quality Management System (QMS) regarding final product verification, specifically related to their lack of approved re-testing procedures. Based on the investigation results, TC Oil determined that the strength of the 109 fittings supplied under the same purchase order (PO) could not be guaranteed to meet the project's design specification. Therefore, TC Oil decided to replace all 109 fittings supplied by Canadoil Asia.

²⁵ Amended Corrective Action Order (ACAO) CPF No. 3-2022-074-CAO, March 7, 2023.

²⁶ TransCanada Keystone Pipeline, LP, Root Cause Analysis Report: Low Yield Strength 3D Pipeline Fittings Supplied by Canadoil Asia to the Keystone Cushing Extension Project, December 3, 2010.

The replacement fittings were manufactured by [REDACTED] in Becancour, Quebec between February and November 2010. Fabrication of the elbow assemblies was done by Canadoil, who contracted the work to TC Oil approved fabricators. TC Oil supplied the pipe material for fabrication. TC Oil arranged for inspection during construction and fabrication activities. Onsite construction was performed by [REDACTED], for both the original construction and fitting replacement program.

The elbow specific to this investigation (number 174469) was manufactured in November 2010 and the associated pups (number 0031378) were manufactured by [REDACTED] in April 2010. The bend assembly, TAG 98, was fabricated by [REDACTED] on November 19, 2010, and installed at the Mill Creek location in December 2010 by [REDACTED]. Figure 10 shows the TAG 98 bend assembly during installation but prior to tie-in. The bend assembly was successfully hydrostatically tested at the fabricator's facility to 94% SMYS and twice in the field to 100% SMYS. Operation of the Cushing Extension began in February 2011.



Figure 10. TAG 98 Bend Assembly (BND 350) During Replacement (December 10, 2010)

2.7 Investigative Excavation of ID Restriction (2013)

The 2012 BHI Profile ILI caliper tool identified a [REDACTED] ID restriction (due to ovality) near the girth weld²⁷ that failed. According to the Pipe Integrity team, excavations for ovalities are only required if there are concerns that ILI tool passage could be impeded, which was the case for this ID restriction²⁸. An excavation was performed in March 2013 to evaluate the restriction (see Figure 11). The ovality was measured using calipers and ultrasonic wall thickness measurements were taken. The ovality was measured in the ditch at [REDACTED] of the OD²⁹ as shown in Figure 12. The ovality³⁰ was determined not to be an integrity concern at the time as it pertained to future ILI runs and the bend assembly was backfilled without any further interventions.³¹

While the excavation was still open, discussions occurred between the Pipe Integrity team and ILI vendor about how best to proceed. They evaluated several possible options including (1) having the ILI vendor modify their tool so that it would pass through the elbow, (2) using a multi-diameter tool, or (3) cutting out the ID restriction. The option to cut out the feature was escalated to senior leadership but determined not to be the most favorable option for safety and logistical reasons. Instead, the vendor agreed that they could navigate the feature with a tool redesign. Subsequent ILI runs have successfully navigated the ID restriction without any significant issues.

²⁷ The 2012 BHI Profile tool reference girth weld number was 1352 which corresponds with GWD 13530 and fabrication weld number G59B.

²⁸ The ILI vendor reported to TC Oil that the cleaning and gauging tools (sent prior to the BHI profile tool) had been damaged by the ID restriction.

²⁹ The maximum ovality OD was measured at [REDACTED] and the minimum ovality OD was measured at [REDACTED].

³⁰ According to the specification TEP-IN-ILI-L In-Line Inspection Data Analysis for Hazardous Liquid Pipelines Engineering Procedure (US), February 1, 2021, an ovality may be considered for investigation and remediation if significant increases in ovality or a new ovality occurs between consecutive inspections. According to Pipeline Construction Specifications for Keystone, May 1, 2009, a [REDACTED] OD ovality (or smaller) in the field after backfill is allowable. Ovality greater than [REDACTED] OD shall be investigated further and remediated.

³¹ Ovalization has not been generally identified as a significant pipeline integrity threat if ILI tools can move through them safely. However, the paper IPC2018-78281, "Integrity Assessment of Pipelines with Ovality", Zhang, F. and Rosenfeld, M., states in its conclusions "... for liquid pipelines with severe pressure cycles, the fatigue life of the detected oval sections should be analyzed ..." The caution could be extrapolated to thermal cycles as well. Ovality also increases susceptibility to buckling due to the increase pipe wall radius of curvature.

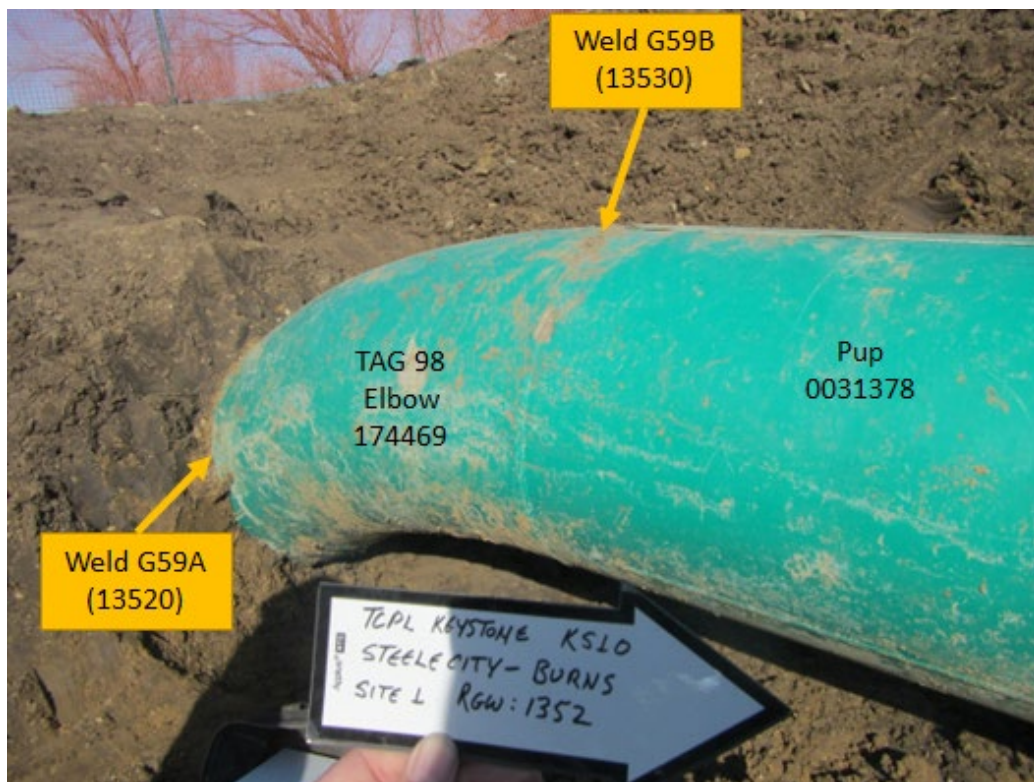


Figure 11. TAG 98 Bend Assembly (BND 350) During March 2013 Excavation to Investigate ILI-Called ID Restriction (March 1, 2013)

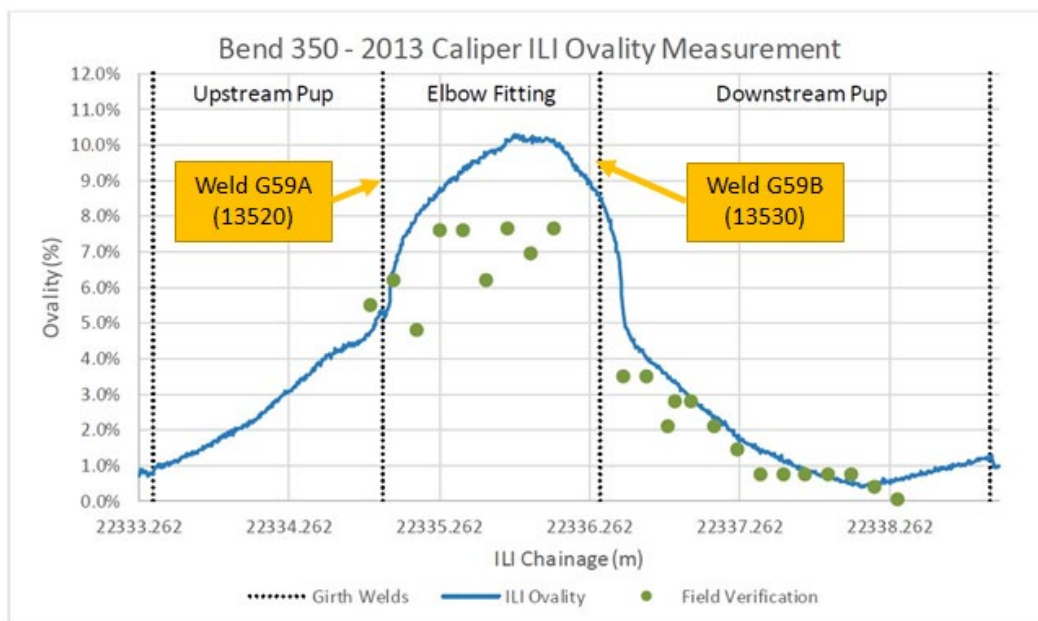


Figure 12. TAG 98 Bend Assembly (BND 350) ILI-Called Ovality and Actual Measurements³²

³² Engineering Assessment of the Combined Stresses from Steele City B PS to Cushing South PS in Consideration of Capacity Increase, Rev 0, March 31, 2021.

2.8 [REDACTED] Capacity Increase Program (2016-2020)³³

In 2016, TC Oil initiated a capacity increase project for the Keystone Pipeline to increase the flowrate from approximately [REDACTED] to [REDACTED] on the portion running from [REDACTED] to [REDACTED] ([REDACTED] and [REDACTED]). Activities to support this project spanned from 2016 to 2021 and included stress analyses and engineering assessments (EA) to understand the impact of the proposed operational change on the pipeline bending stresses, particularly related to the increased operating temperatures associated with the increased flowrate.

An initial study was performed in October 2017 for the two segments that comprise the Cushing Extension, KS10 and KS11, using a linear-elastic, one-dimensional beam in three-dimensional space finite element model. The model evaluated the bending stresses induced by internal pressure, temperature differential, and soil resistance. The acceptability criteria were two-fold:

1. Check the pipeline stress based on allowable design criteria in ASME B31.4:
 - a. Combined equivalent stress (restrained pipeline) $\leq 90\%$ SMYS, and
 - b. Thermal expansion stress (restrained pipeline) $\leq 90\%$ SMYS.
2. Verify that the pipeline stress met a supplemental stress criterion of combined equivalent von-Mises³⁴ stress \leq SMYS.

The operating parameters used in the model included a design pressure of [REDACTED], maximum design temperature of [REDACTED], minimum design temperature of [REDACTED], and installation temperature of [REDACTED].

The initial study identified [REDACTED] bend locations along the Cushing Extension that had a combined equivalent von-Mises stress that exceeded 90% SMYS. Of these [REDACTED] bend locations, [REDACTED]³⁵ locations did not satisfy the second criterion of von-Mises stresses less than SMYS, all at elbow type assemblies. There are a total of [REDACTED] elbow fittings along the Cushing Extension, [REDACTED] on KS10 and [REDACTED] on KS11. The elbow associated with the failure, TAG 98 (BND 350), was not one of the [REDACTED] elbow fittings³⁶ flagged. A recommendation from the initial study was to develop a higher fidelity analysis to predict the elbow stress response more accurately, which TC Oil pursued.

³³ Memo, Keystone MP 14 Leak Site – Historical Pipeline Stress Analyses, January 16, 2023.

³⁴ Von-Mises stress criterion are used to check yield conditions in ductile materials and is suitable for calculating safety factors against failure. The von-Mises stress represents the combination of three principal stresses (axial, radial, and hoop) that can cause yielding, also referred to as the maximum distortion energy criterion. When the von-Mises stress reaches the yield strength, ductile materials can start to yield. The pipeline hoop stress used to define the pipeline MOP (per §195.106 or §195.406) is only one component of the von-Mises stress. The 80% SMYS limit defined in the Special Permit only applies to hoop stress. For equivalent combined stresses a 90% SMYS limit for restrained pipe is acceptable per B31.4, Table 403.3.1-1, American Society of Mechanical Engineers, B31 Code for Pressure Piping, Section 4, "Pipeline Transportation Systems for Liquids and Slurries", B31.4-2016.

³⁵ A total of [REDACTED] locations were identified, but three of the locations appear to have been caused by errors in the pipeline trajectory within the model and not a specific component.

³⁶ The upstream sag bend TAG 114C (BND 349) was identified as one of the [REDACTED] elbows with a combined von-Mises stress exceeding 0.9 x SMYS (96.3% SMYS).

The higher fidelity finite element model used advanced elbow beam elements that can handle large displacements, non-linear material behavior, and account for in-plane ovalization and out-of-plane warping of the pipe cross-section. The more advanced model evaluated the bending stresses induced by internal pressure, temperature differentials, and soil restraint for the previously identified high stress bend locations along the Cushing Extension. A subset of the [REDACTED] bend locations previously identified were modeled, which included [REDACTED] elbow fittings and [REDACTED] cold bends on KS10 and [REDACTED] elbow fittings and [REDACTED] cold bends on KS11. Of the [REDACTED] elbows modelled, [REDACTED] had a von-Mises stress that exceeded 90% SMYS.

In March 2021, an engineering assessment (EA) was completed that evaluated all [REDACTED] elbow fittings along the Cushing Extension and further reviewed potential threat interactions with the nine integrity threats defined in ASME B31.8S. The threat of girth weld anomalies was considered but because the 2018 BHGE MFL4 ILI revealed no reportable girth weld anomalies in the welds joining the elbows to adjacent pipe it was determined that this threat did not degrade the maximum permissible combined stress criterion. This assessment also revealed five elbows with existing ovality deformation which included the TAG 98 (BND 350) elbow. The EA recommended that these elbows be monitored features and to reassess them with the next scheduled high-resolution caliper ILI after increasing the flowrate [REDACTED] and during summer temperatures. In the meantime, an operating temperature limit of [REDACTED] was placed on the KS10 segment.

The EA also evaluated the threat of movement from collapsible or expansive soils but concluded that the amount of pipe or soil movement in these types of soils is self-limiting and is of comparatively lesser concern than geological hazards that impart a potentially unlimited external force (e.g., landslide). As described in the EA, high hazard classifications for these types of soils are related to reports of structural damage to buildings but based on industry experience, these types of soils have not impacted transmission pipeline integrity. TC Oil had revised its threat assessment procedures since the 2012 baseline geological assessment³⁷ which no longer includes collapsible or expansive soils in geologic hazards assessment. After the MP 14 Incident, geohazard subject matter experts (SMEs) evaluated soils in the area and determined them to be clay-colluvium soils³⁸, which are not particularly expansive.

2.9 [REDACTED] Capacity Increase Program (2020-Present)

In 2020, another capacity increase project was initiated to evaluate a capacity increase to [REDACTED] on the [REDACTED] to [REDACTED] portion of Keystone. Another stress analysis was performed to assess bending stresses induced by internal pressure, temperature differentials, and soil restraint for the higher stress bends identified previously. The fitness-for-service acceptability criterion was defined as combined equivalent von-Mises stress less than or equal to SMYS. Like the prior assessment, a non-linear, one-dimensional beam in three-dimensional space finite element model using advanced elbow beam elements was used to remodel the higher stress

³⁷ Golder Associates (2012). Phase I Geologic and Hydrotechnical Hazards Assessment – Keystone Mainline and Cushing Extension Pipelines. Golder Associates.

³⁸ Internal Memo, Geotechnical Assessment of NPS 36 Keystone Mainline Leak at MP 14, January 16, 2023.

bends at the new flowrate³⁹ and associated temperatures. On KS10, [REDACTED] of the [REDACTED] elbows and on KS11, [REDACTED] of the [REDACTED] elbows were remodeled.

In addition, an in-house machine learning regression model⁴⁰ was used to predict the maximum combined stress of bends. A total of [REDACTED] elbows were identified with the machine learning model for further analysis, [REDACTED] of which had not been previously modeled. One of the newly identified elbows was TAG 98 (BND 350) and therefore was included in the FE modeling.

Overall, a total of [REDACTED] elbows were modeled, [REDACTED] of [REDACTED] elbows along KS10 and [REDACTED] of [REDACTED] elbows along KS11. Based on the stress analysis results, [REDACTED] areas were identified where the combined von-Mises stress exceeded 95% SMYS⁴¹. TAG 98 (BND 350) was not one of these five areas. The combined von-Mises stress for TAG 98 (BND 350) was determined to be 86.8% SMYS⁴², which was acceptable per the fitness-for-service criterion of less than or equal to SMYS. Temperature limits were set for the [REDACTED] locations such that the combined von-Mises stress would be less than 95% SMYS. This resulted in temperature limits at Steele City, Hope, Rock, and Ponca City pump stations. At the time of the MP 14 Incident, the operating temperature limit at Steele City PS was [REDACTED].

Ramp up testing to [REDACTED] was initiated in December 2022, only a few days prior to the MP 14 Incident. The goal of the ramp-up test was to collect data on pressures, temperatures, pipe vibration, noise levels, power draw, etc. as well as how the increased flowrate impacted daily operations in the Control Room. The ramp up testing had not been completed prior to the MP 14 Incident.

3 Root Cause Failure Analysis (RCFA) Process

3.1 Objective of the RCFA

An RCFA is an approach for identifying the causal and contributing factors as to why an incident occurred so that the most effective solutions can be identified and implemented to avoid a recurrence. The objective for this investigation was to determine what systems or equipment, or both, were directly causal to crack initiation within girth weld GWD 13530 of the fabricated bend assembly TAG 98 (BND 350), the propagation of the crack until it reached its failure pressure, and the subsequent release of crude oil to the surrounding environment.

³⁹ The model conservatively assumed temperatures associated with a flowrate of [REDACTED] rather than [REDACTED].

⁴⁰ Previously on Keystone Phase 1 bends were predicted as relatively high stress and selected for finite element modeling for evaluation of operating condition changes by matching bend attributes to parametric study cases performed in 2016. The dataset included [REDACTED] bends/FE model results from KS4, KS7, [REDACTED] elbows from KS10, and [REDACTED] elbows from KS11.

⁴¹ This was the target stress level to set the maximum allowable discharge temperature (MADT) limits to protect the pipeline from thermal expansion.

⁴² The hoop stress component was [REDACTED] and the longitudinal stress component was [REDACTED]. The input pressure was [REDACTED], maximum operating temperature was [REDACTED], and minimum operating temperature was [REDACTED].

3.2 Confidential RCFA Team

The investigation team consisted of the following personnel.

Stephanie Flamberg	Principal Engineer	RSI
Bill Amend	Technical Advisor	RSI
Peter Martin	Principal Engineer	RSI
Michael Rosenfeld	Chief Engineer	RSI
Adam Steiner	Senior Engineer	RSI
Benjamin Zand	Principal Engineer	RSI

3.3 RCFA Methods and Scope

An RCFA is a structured approach to investigating an incident. The structure leads to the examining of all factors that could have affected the performance of equipment or personnel that led to the occurrence of the incident. Different methods have evolved for conducting an RCFA including, but not limited to, a timeline analysis, a Cause and Effect tree, or a causal factor diagram. The RCFA team adopted the Cause and Effect Tree and timeline analysis as described in a method developed by ABS Consulting⁴³. The scope of the confidential RCFA is limited to the facts and circumstances of the MP 14 Incident.

The Cause and Effect Tree is an effective tool for incidents that involve multiple-event deficiencies. The technique looks back in time starting with the loss event (the incident) to describe the possible combination of events that had to occur or conditions that had to be present for the incident to happen. Each subsequent factor is then examined to determine what prior conditions or events had to be necessary for it to exist and so on until the most likely root cause(s) is determined. At each level in the tree, the following questions are applied to attain a deeper understanding:

- Why did the event/condition occur?
- Given identified conditions, will the event always occur?
- Are there safeguards that could have prevented the event/condition?
- Are there other potential causes of the event/condition?

Every level within a branch must be supported or eliminated by data. Eventually, by eliminating lines of causes and effects based on data or analyses, the most probable or credible root causes can be identified. The process is complete when there is an understanding of the chain of events or conditions between one or more root causes and the event of interest. Identification of the root causes then leads to recommendations for improved safety and management systems to prevent recurrence.

The RCFA considered a detailed assessment of the following aspects related to the design, manufacture, inspection, fabrication, installation, operation, and integrity management of the

⁴³ ABS Consulting, Root Cause Analysis Handbook (3rd ed. 2008).

TAG 98 bend assembly (BND 350) near Mill Creek as well as the control room response following the rupture.

1. Mechanical and metallurgical testing of the failed component
2. Fitting/pup design and engineering specifications, including materials and joint design
3. Manufacturing, inspections, fabrication, and quality control for the bend assembly
4. Construction methods, oversight, and quality management during installation
5. Testing and inspections performed during commissioning and operations
6. Historical system operations, maintenance, and site influences
7. ILI procedures, tools, verification, findings, and field examinations
8. Integrity management, monitoring, and risk assessment
9. Leak detection and control room response

These subject matter areas were considered within the RCFA scope based on RSI's prior experience in conducting RCFAs. The outcomes of the Cause and Effect Tree process led to the conclusions and recommendations presented in this report.

3.4 RCFA Terminology

Certain terms are commonly used with the RCFA process. These terms are defined below to improve the interpretation of this report. These definitions are consistent with those in the ABS⁴³ process and methodology.

- Causal Factors (CF) are gaps in equipment or personnel performance that cause an incident or allow an incident to become worse. A causal factor may have one or more root causes.
- Contributing Factors (CTF) are underlying reasons why a causal factor occurred but are not sufficiently fundamental to be a root cause.
- Root Causes (RC) are deficiencies in management or control systems, such as procedures, training, internal communications, or procurement that allow a causal factor to occur. A root cause must be within control of management to address.
- Items of Note (ION) are weaknesses discovered during the RCFA that are not directly related to the loss event but, if left uncorrected, could contribute to a future incident. Items of note represent potential opportunities for improvement.
- Barriers or Safeguards are systems or processes designed to avoid, prevent, or mitigate a failure or hazard, such as a specification or an inspection.

3.5 Personnel Interviews

Interviews were conducted with personnel representing design, engineering, construction, integrity management, operations, and project management to gain an understanding of the sequence of events that led to the failure of GWD 13530. Lines of questioning included the timing of events, elbow and joint design, manufacturing and fabrication, welding practices, construction practices, integrity assessments, site conditions, response to events, and possible causes, beliefs, opinions, and judgments related to the incident. Interviewees were asked about their background, experience, and job duties.

REDACTIONS MADE BY TC OIL - Pending PHMSA Review

**CONFIDENTIAL – Protected from release under
FOIA Exemptions 4 and 7(F), 5 USC 552(b)(4)
and (b)(7)(F).**

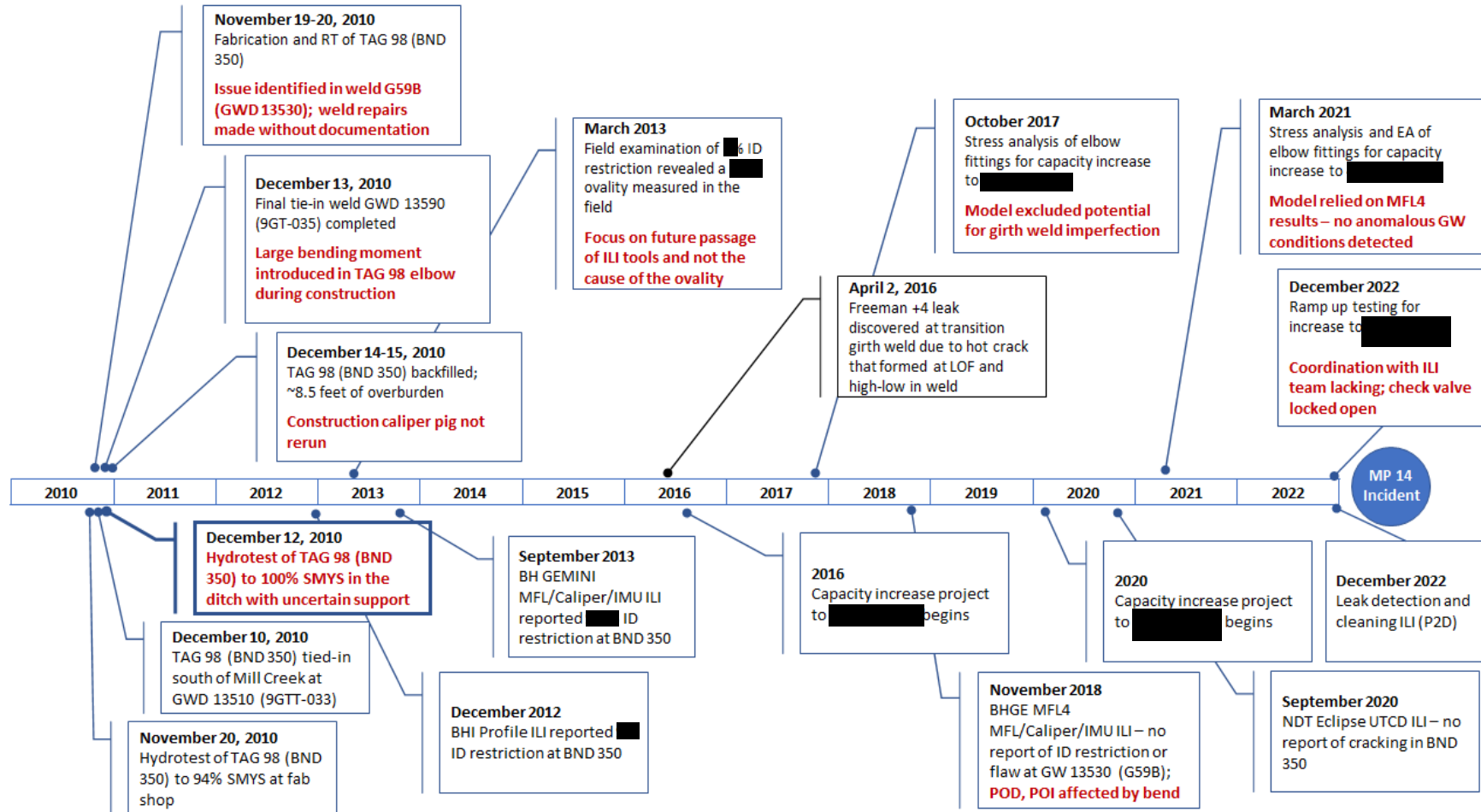


Figure 13. Timeline of Key Events Leading up to the MP 14 Incident

4 Supporting Analyses

This section reviews findings and observations from the metallurgical failure analysis⁴⁴ performed by Anderson in Houston, Texas and the results of finite element analyses (FEA), crack initiation analyses, and fatigue crack growth analyses performed by RSI that were used to aid confirmation of certain potential causal factors to be discussed in Section 5.

4.1 Metallurgical Failure Investigation

Anderson was contracted by TC Oil to perform the metallurgical failure investigation. This investigation included examination and materials testing of the affected bend assembly, including (1) one 3D elbow with 0.866-inch NWT⁴⁵ and (2) two adjacent pups with 0.515-inch NWT. Examinations and tests included, but were not limited to:

- Visual examination of the bend assembly containing the girth weld rupture feature and upstream wrinkle
- Nondestructive Testing (NDT) including radiographic testing (RT), phased array ultrasonic testing (PAUT), ultrasonic wall thickness testing, magnetic particle inspection (MPI), time of flight diffraction (TOFD), and inverse wave field extrapolation (IWEX)
- Laser scan mapping of the OD and ID surfaces
- Characterization of the fracture surface using visual examination, stereoscopic examination, scanning electron microscope fractography (SEM) and energy dispersive x-ray spectroscopy (EDS)
- Characterization of the microstructures in the elbow, pipe, and girth welds
- Metallographic sections of the girth welds
- Material strength tests of the elbow, pipe body, and girth welds
- Toughness tests of the pipe and girth welds
- CTOD tests of the girth welds
- Microhardness tests across the girth welds
- Chemistry analysis of the elbow, pipe body and girth welds

The results are extensive and are not fully reproduced herein, however the most relevant findings are briefly summarized below.

Mode of failure:

According to the Anderson metallurgical analysis, “the cause of the rupture in GWD 13530 was attributed to fatigue (progressive) cracking.” Three individual circumferentially oriented fatigue cracks were identified that originated from a lack of fusion (LOF) region at the inner diameter (ID) toe of the girth weld on the thin-wall side of the weld (pup side). The circumferential orientation of the cracks suggests a bending stress to be the driving mechanism. The cracks then propagated linearly through the thin-wall side of the weld (pup side) via a fatigue

⁴⁴ Anderson & Associates, 220439 TC Energy – Metallurgical Analysis of NPS-36 KS10 MP-14 Pipeline, February 7, 2023.

⁴⁵ Starting plate thickness as noted in the MTR.

mechanism until final overload and subsequent crude oil release occurred when the remaining wall ligament could no longer support the applied load.

The primary evidence that the initiating feature was from LOF was a tightly adhered, high-temperature oxide scale that lined the surfaces of these features. Such oxide scale (magnetite or Fe_3O_4) forms preferentially at higher temperatures, typically higher than 600°C . According to Anderson, this temperature would likely have been achieved and or exceeded during welding operations. The presence of magnetite scale indicates that the surfaces were exposed to an oxygen atmosphere while still at high temperature.

The circumferential nature of the crack features is indicative of local bending stresses. “The fatigue cracks in GWD 13530 appeared to progress via an unstable (brittle) crack extension mechanism consisting of a series of advance/arrest events. There was evidence of dimpled rupture observed coincident with several of the arrest features, indicating there may have been ductile tearing preceding unstable crack extension.”

Visual Examination:

Figure 14 shows the exposed fracture surface on the pup side (downstream) of the failed girth weld (GWD 13530). Note the three distinct elliptical crack features. The top dead center (TDC) of the pipe is marked with the dashed yellow line.

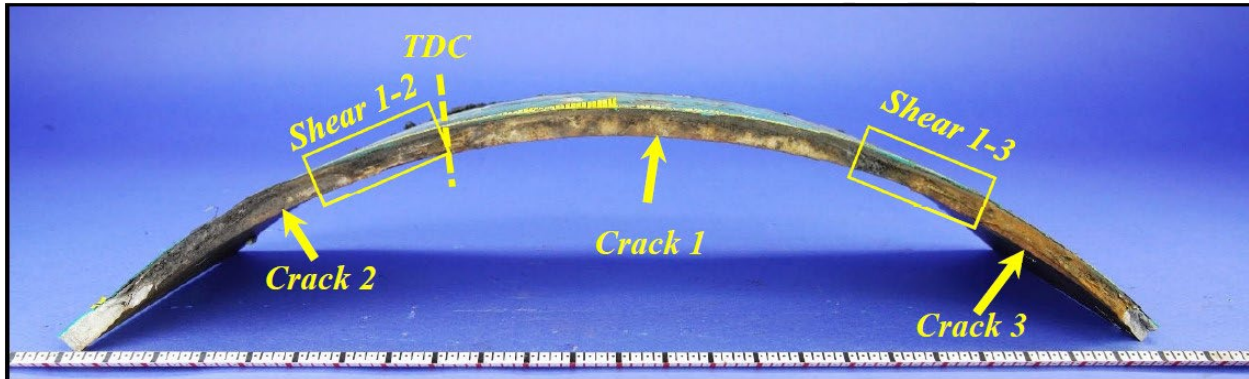


Figure 14. View of Downstream (Pup Side) of the Exposed Fracture.

Figure 15, Figure 16, and Figure 17 show magnified views of the three elliptical crack features that were identified originating from the ID toe of girth weld GWD 13530 (G59B) on the thin wall side of the weld (pup side). The initiating features were coincident with LOF regions at the ID toe with a maximum depth of 0.008-inch (200 μm) and circumferential lengths presumed to extend the full length of each crack feature. LOF defects and fatigue crack extension were observed on both GWD 13530 and GWD 13520. The flat region of each crack exhibited multiple “beach marks” or macroscopic features marking the position of the crack front(s) over time, characteristic of a progressive or fatigue cracking mechanism from the ID surface. As shown in Table 1, the maximum depth of Crack 1 was measured as 0.50-inch (97.1% of the NWT). The total length of the flat, thumbnail feature was approximately 8.7-inches. The wall thickness at the location of the failure was approximately 0.540-inch.

Table 1. Summary of Crack Dimensions in GWD 13530

Crack	Depth [in]	Depth % of NWT	Length [in]	Location (deepest part of feature from TDC)
Crack 1	0.50	97.1%	8.70	14.3°
Crack 2	0.38	73.8%	4.25	346.5°
Crack 3	0.18	34.9%	4.00	41.4°

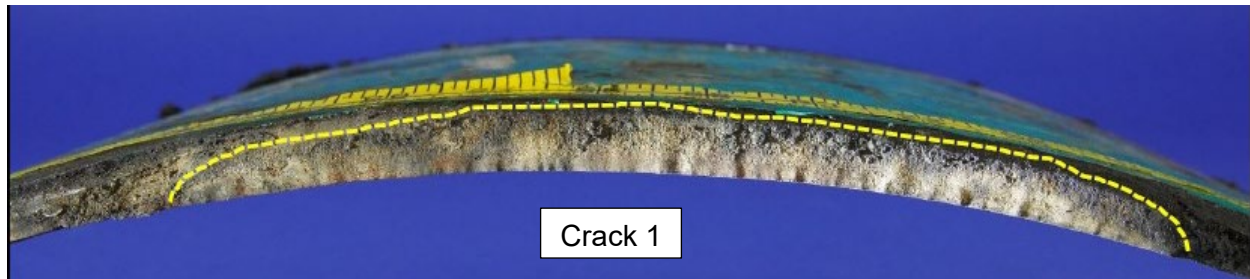


Figure 15. Magnified View of Crack 1 in GWD 13530 (G59B)

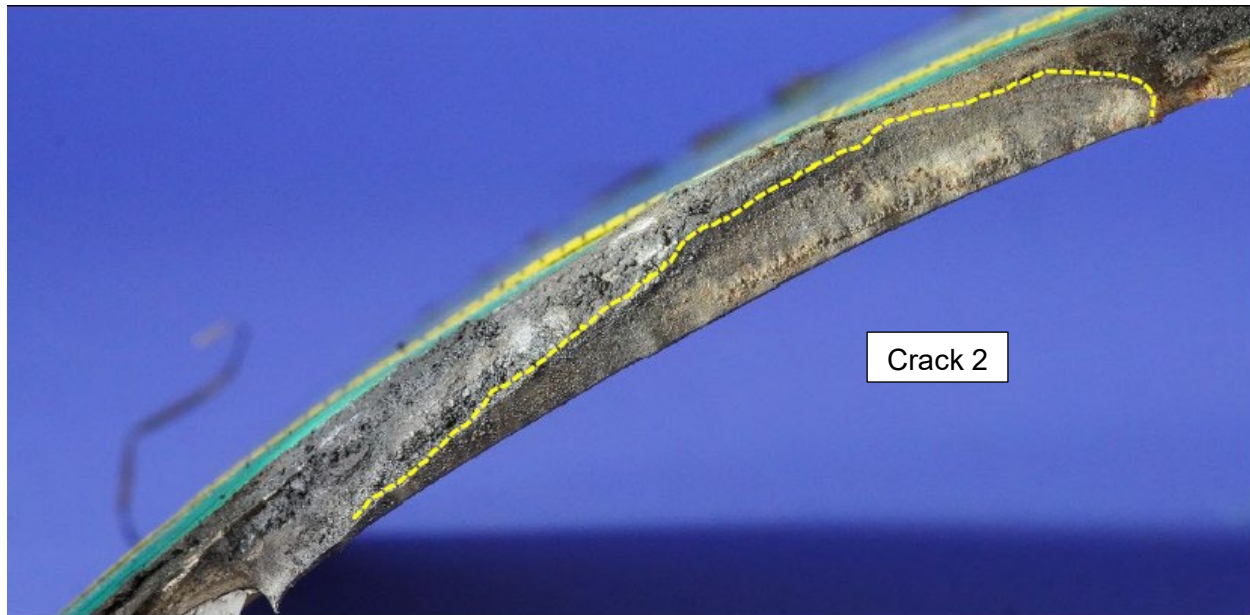


Figure 16. Magnified View of Crack 2 in GWD 13530 (G59B)

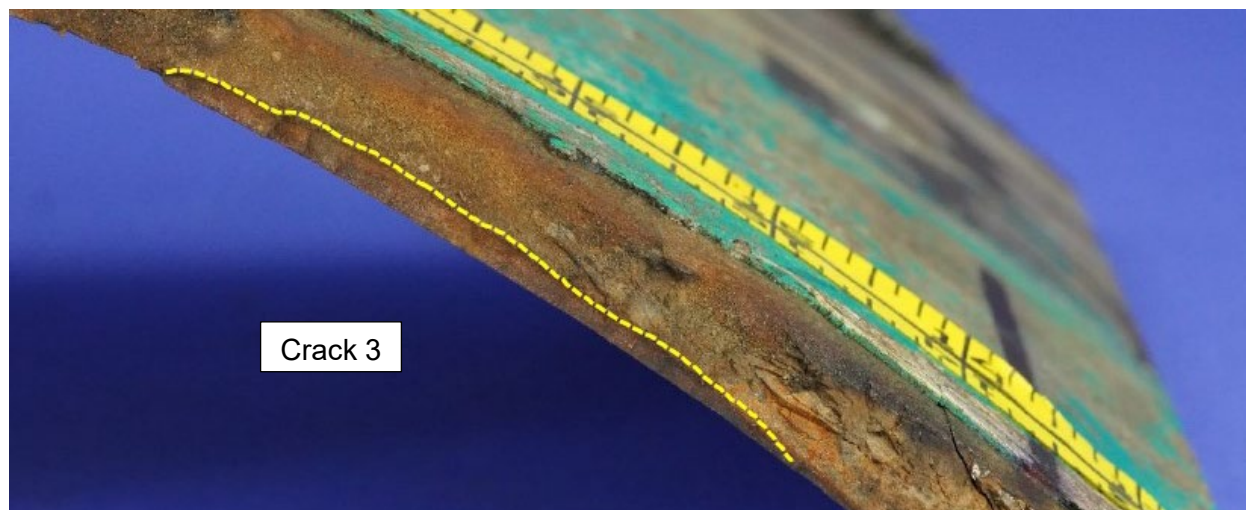


Figure 17. Magnified View of Crack 3 in GWD 13530 (G59B)

As shown in Figure 18, separating Crack 2 and Crack 3 from Crack 1 were two regions exhibiting a shear morphology (fracture surfaces oriented at approximately 45°). Examination of the upstream portion of these regions (weld side) showed that they coincided with weld repairs as confirmed by grind marks and a thicker weld bead.

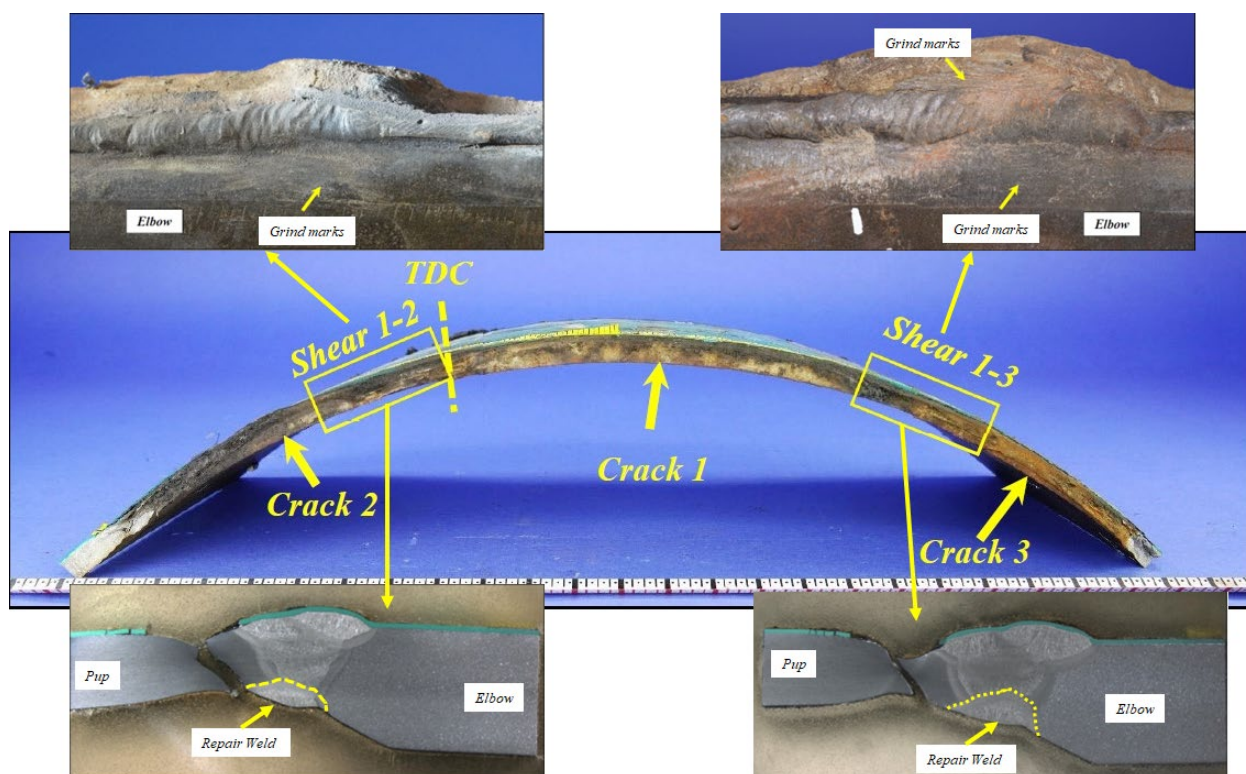


Figure 18. Images and Metallographic Sections Showing the Location of Repairs in GWD 13530 (G59B) Between Fatigue Crack Locations

Nondestructive Examination (NDE):

ApplusRTD was contracted by Anderson to perform NDE of GWD 13530 (G59B) and GWD 13520 (G59A) prior to destructive testing. Full circumference MPI was performed on the OD surface of the elbow, pups, longitudinal seam welds, and girth welds. MPI was also performed on the full circumference⁴⁶ ID root pass and heat affected zone (HAZ) of GWD 13530, GWD 13520, and GWD 13510. Zero-degree ultrasonic (UT) inspection was performed to measure actual wall thickness and to scan for laminations near the weld. PAUT with supplemental TOFD was performed on all three girth welds⁴⁷. Creaform laser scan mapping was completed for both the ID and OD surface. High-low measurements were also taken using a high-low gauge positioned at the centerline of the weld for both the upstream and downstream extents of the three girth welds.

MPI identified linear indications in the upstream weld cap toe on the OD surface, edge of both sides of the root pass on the ID surface, and the edge of the downstream root pass on the ID surface of GWD 13520. Similarly, linear indications were noted at the edge of the downstream root pass on the ID surface of GWD 13530.

As shown in Figure 19, high-low was also noted in all three girth welds with a maximum of 1/8-inch at the 5 o'clock position and 3/32-inch at the 1, 2, 4, and 10 o'clock positions of GWD 13530. A maximum high-low of 5/32-inch was measured at the 1 o'clock position of GWD 13520⁴⁸ and a maximum high-low of 1/16-inch was measured at the 1, 4, and 7 o'clock positions of GWD 13510.

HI-LO READINGS TABLE (IN.)

		13510			13520			13530		
		US	DS	Hi-Lo	US	DS	Hi-Lo	US	DS	Hi-Lo
Clock Position	12	- 1/8	- 1/8	0	- 1/16	- 5/32	3/32	- 1/32	- 3/32	1/16
	1	0	- 1/16	1/16	0	- 5/32	5/32	- 1/8	- 1/32	3/32
	2	- 1/32	- 1/16	1/32	- 1/32	- 5/32	1/8	- 1/32	- 1/16	1/32
	3	- 1/16	- 1/16	0	1/16	- 5/32	3/32	- 1/8	1/32	3/32
	4	- 1/8	- 1/16	1/16	- 1/16	W	-	- 1/8	1/32	3/32
	5	- 1/16	- 1/32	1/32	0	W	-	- 1/32	- 5/32	1/8
	6	- 1/16	- 1/32	1/32	- 1/16	W	-	- 1/16	- 1/16	0
	7	- 1/16	0	1/16	0	W	-	- 1/32	- 1/32	0
	8	- 3/32	- 1/16	1/32	1/16	W	-	- 1/32	0	1/32
	9	- 1/16	- 1/32	1/32	- 1/32	W	-	- 1/16	1/32	1/32
	10	- 1/32	- 1/32	0	1/16	- 1/16	0	- 1/8	- 1/32	3/32
11	- 1/32	- 1/16	1/32	- 3/32	- 1/16	1/32	- 1/32	- 3/32	1/16	

Coating & Tape Interference

W

Measurement Not Able to be Taken Due to Presnece of Wrinkle

Figure 19. High-Low Measurements at GWD 13530, GWD 13520, and GWD 13510

⁴⁶ GWD 13530 was only assessed with MPI for approximately 75% of the circumferential extent to avoid introducing any contaminants in the fracture region.

⁴⁷ The PAUT inspection post-failure exceeded the minimum requirements specified in API 1104 for flaw detection thresholds.

⁴⁸ The high-low could not be measured between the 4 o'clock and 9 o'clock positions on the bottom of the pup at GWD 13520 because of the presence of the wrinkle.

As shown in Figure 20, PAUT noted incomplete root fusion, intermittent root fusion, and root toe cracking in the portions of GWD 13530 that could be scanned. Similarly, root toe cracking and intermittent root fusion was noted in GWD 13520. Welding flaws were noted, however, the post-incident inspection used parameters that exceeded API 1104 requirements to improve flaw detection sensitivity and therefore the results are not indicative of the flaw indications that may have been present at the time of fabrication. Intermittent interpass LOF and slag inclusions were noted in GWD 13510 but nothing that exceeded acceptance criteria in API 1104. All indications identified by PAUT were verified metallographically, according to Anderson.

EXAMINATION DETAILS AND RESULTS													
GIRTHWELD NUMBER	NOMINAL WALL THICKNESS (IN.)	AXIAL LOCATION (FT.)	SKEW	FEATURE NUMBER	SCAN LENGTH (IN.)	START OF INDICATION (IN.)	END OF INDICATION (IN.)	LENGTH (IN.)	HEIGHT (IN.)	DEPTH START (IN.)	DEPTH END (IN.)	ACTUAL THICKNESS (IN.)	DISCONTINUITY TYPE
GW 13510													
13510	0.550	0.00	90	1	117.008	0.102	2.833	2.731	0.138	0.268	0.406	0.542	Intermittent Interpass LOF
13510	0.550	0.00	90	2	117.008	5.399	24.840	19.441	0.093	0.356	0.449	0.537	Intermittent Interpass LOF
13510	0.550	0.00	90	3	117.008	58.104	98.592	40.489	0.086	0.396	0.485	0.540	Intermittent Interpass LOF
13510	0.550	0.00	90	4	117.008	113.293	113.568	0.275	0.040	0.484	0.523	0.542	Slag Inclusion
GW 13520													
13520	0.550 - 0.850	0.00	90	1	117.008	7.370	15.311	7.941	0.149	0.718	0.867	0.863	Intermittent Root Toe Crack
13520	0.550 - 0.850	0.00	90	2	117.008	16.842	32.294	15.452	0.149	0.701	0.850	0.850	Root Toe Crack
13520	0.550 - 0.850	0.00	90	3	117.008	35.017	61.911	26.894	0.106	0.749	0.855	0.855	Root Toe Crack
13520	0.550 - 0.850	0.00	90	4	117.008	69.102	96.551	27.449	0.113	0.748	0.861	0.861	Intermittent Root Fusion
GW 13530													
13530	0.550 - 0.850	0.00	90	1	117.008	31.119	33.639	2.519	0.071	0.461	0.532	0.532	Incomplete Root Fusion
13530	0.550 - 0.850	0.00	90	2	117.008	38.797	46.204	7.407	0.076	0.444	0.520	0.520	Intermittent Root Fusion
13530	0.550 - 0.850	0.00	90	3	117.008	48.694	57.091	8.397	0.138	0.415	0.553	0.553	Root Toe Crack
13530	0.550 - 0.850	0.00	90	4	117.008	62.369	66.808	4.439	0.089	0.458	0.547	0.547	Root Crack
13530	0.550 - 0.850	0.00	90	5	117.008	70.166	86.421	16.255	0.116	0.426	0.542	0.542	Intermittent Root Crack
NOTES													
Due to the complex geometry of the part examined and significant wall thickness variation, depth and height positioning is an estimate based on a theoretical approximation of how the ultrasonic signals propagated through the area of inspection. Assessment of GW13510 was deemed acceptable per API 1104 criterion. Assessment of GW13530 in the area around the thru-wall fracture was impeded by the presence of coating and non-uniform surface condition. Reported indications are those which have the highest confidence of being "real" due to the presence in both PAUT and supplementary ToFD. Additional ultrasonic responses are present, however, can not be reported with confidence due to the lack of confirmation by supplementary inspection methods.													

Figure 20. Post-Incident PAUT Results for GWD 13510, GWD 13520, and GWD 13530

Scanning Electron Microscopic Examination:

The fracture surfaces of the three cracks were examined at low and high magnification by SEM. An SEM image of Crack 1 is presented in Figure 21. Common features to the three elliptical cracks are (1) each crack appeared to initiate at or near the ID surface and had multiple, radially oriented crack initiation features (also known as "ratchet marks"); and (2) each showed evidence of progressive cracking in the form of multiple crack arrest features. Crack 1 and Crack 2 each contained 10 to 15 distinguishable arrest lines or "beach marks".

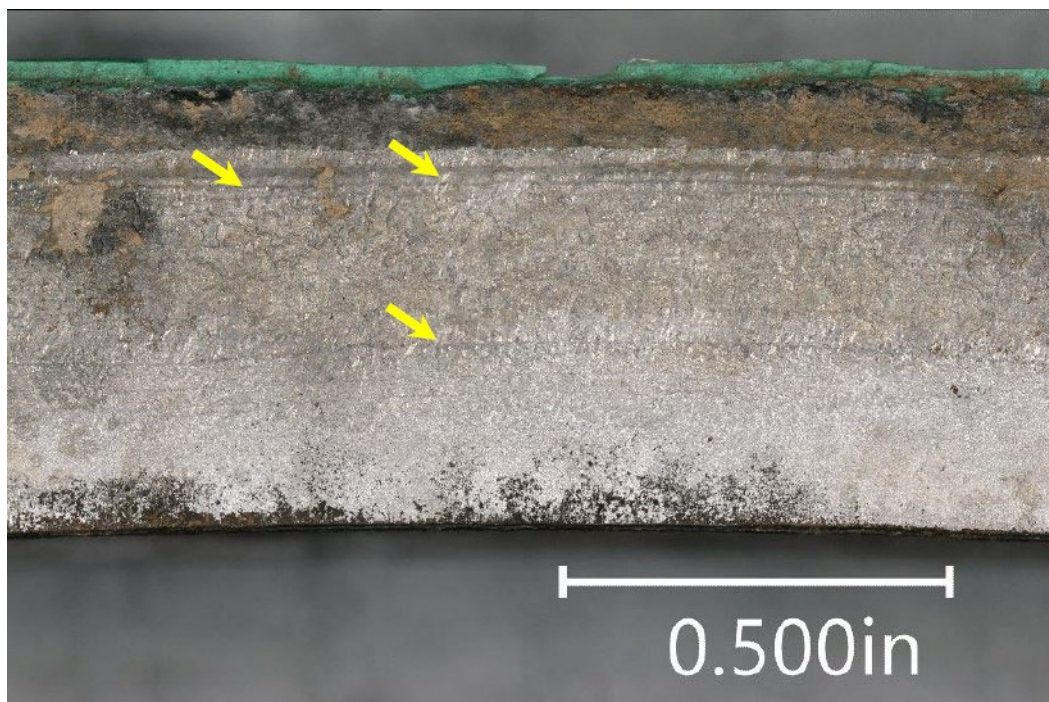


Figure 21. Low Magnification SEM Showing the Center Region of Crack 1 (most prominent crack arrest lines identified with yellow arrows)

A “ratchet mark” identified by the yellow arrow in Figure 22(a) is emanating radially from the edge of the LOF (the region between the dashed yellow lines) onto the fracture surface. Ratchet marks occur where a fracture initiates at multiple sites that are not quite coplanar. They disappear where the individually initiated crack surfaces merge to a common plane. Figure 22 (b) shows the fracture morphology near the ID of GWD 13530, Crack 1 to have been consumed by oxidation.

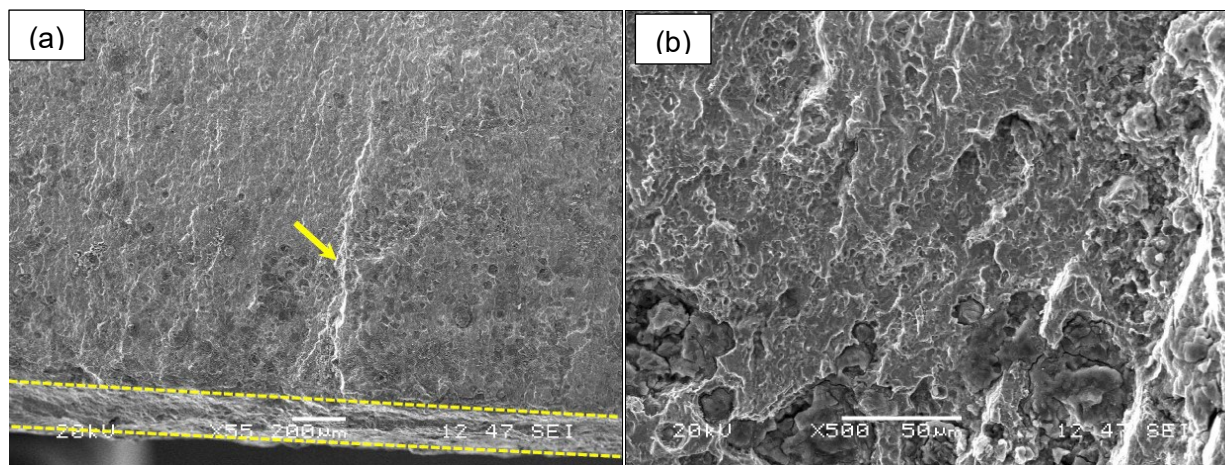


Figure 22. (a) Low Magnification SEM Fractograph Showing the ID Region of GWD 13530, Crack 1 and (b) Higher Magnification SEM Fractograph Showing that the Fracture Surface near the ID of GWD 13530, Crack 1 had been Consumed by Oxidation

The fracture surface near the mid-wall to OD surface of Crack 1 showed several distinct crack arrest lines near the transition to shear overload (denoted by the yellow arrows in Figure 23(a)) with thin bands of micro-void coalescence (MVC) or dimpled rupture between some of the crack arrest lines (region between the dashed yellow lines in Figure 23(b)). According to Anderson, the space between the crack arrest lines appeared to be brittle with no evidence of striations (incremental cyclical crack growth). The shear overload region consisted of MVC which is consistent with ductile overload. RSI considers that the featureless fracture surfaces between the arrest marks are inconclusive as to mode of fracture due to corrosion. The surfaces do not entirely resemble the one region of cleavage fracture identified. The mechanism for stable but brittle crack advance defined by periodic ductile arrest marks is also not obvious. The arrest marks are spaced approximately 0.040-inch on average (0.500-inch / 12 marks), while the estimated plastic zone size assuming a fracture toughness derived from the average weld metal CTOD values (which were lower than the HAZ values), even assuming a constrained plain-strain condition is four times larger. Stable incremental non-ductile crack advance might occur if the crack is forced to extend into a compressive residual stress zone in the weld by periodic high loadings, but this is speculation. The Anderson metallurgical report (see Figure 33 of the Anderson report) identified a single, narrow band of cleavage fracture surface 0.040-inch in radial dimension on Crack 2. No similar feature was observed anywhere else on Crack 2 or any other crack. Its cause is unknown but could have occurred in a zone affected by a transient, nonoptimal welding condition over a short arc length of weld deposit. There is no evidence in the weld CVN or CTOD test results that would suggest a tendency for brittle fracture at the construction or operating temperatures. Since no similar feature was observed on the other fractures and it was very small in radial extent it was concluded to not have significantly influenced the formation or growth of the crack.

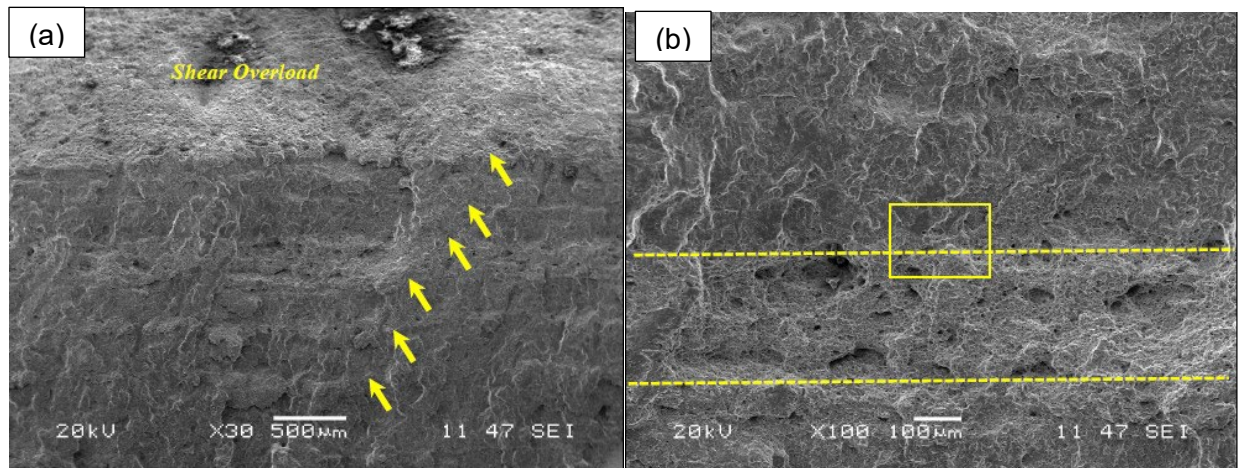


Figure 23. (a) Low Magnification SEM Fractograph of GWD 13530, Crack 1 Showing Multiple Crack Arrest Lines (crack arrest lines identified with the yellow arrows) and (b) Higher Magnification SEM Fractograph of GWD 13530, Crack 1 Showing a Band of Dimpled Rupture Associated with a Crack Arrest Line Near the Shear Overload Region

Metallographic Sections:

Anderson examined the microstructures of the pups, elbow, welds, and HAZ. The microstructure of the pups was consistent with high strength steel pipe manufactured using thermo-mechanically controlled processing (TMCP). The microstructure of the elbow was consistent with low-alloy steels that had been quenched and tempered. The microstructures of the weld and HAZ confirmed that they had not been post-weld heat treated (PWHT)⁴⁹. Evidence to support this finding is that the weld microstructure consisted of large columnar grains of acicular ferrite and carbide and the root pass and lower hot passes appeared to be heavily tempered from subsequent weld passes while the cap pass did not show any evidence of tempering. The HAZ on both the elbow and pup sides exhibited coarse and fine-grained microstructures (CGHAZ and FGHAZ, respectively), which are typically developed during welding and are attributed to the temperature profile.

Metallographic cross sections were prepared across the fractured and intact portions of GWD 13530 (G59B) and the intact GWD 13520 (G59A). Figure 24 is a section across the fractured weld at Crack 1. Figure 25 is a montage of the fracture at higher optical magnification. The crack grew from a small angular feature (lip) in the root pass at the inner toe of the girth weld. The prominent lip was observed at the ID intersection of the crack and appeared to parallel the fusion line. The lip feature was approximately 0.008-inch (200 µm) in length. The crack enlarged in a single radial plane which is typical of fatigue cracks enlarged by cyclic loading conditions. The final fracture occurred by ductile shear represented by the slanted fracture in the outer portion of the weld cap.

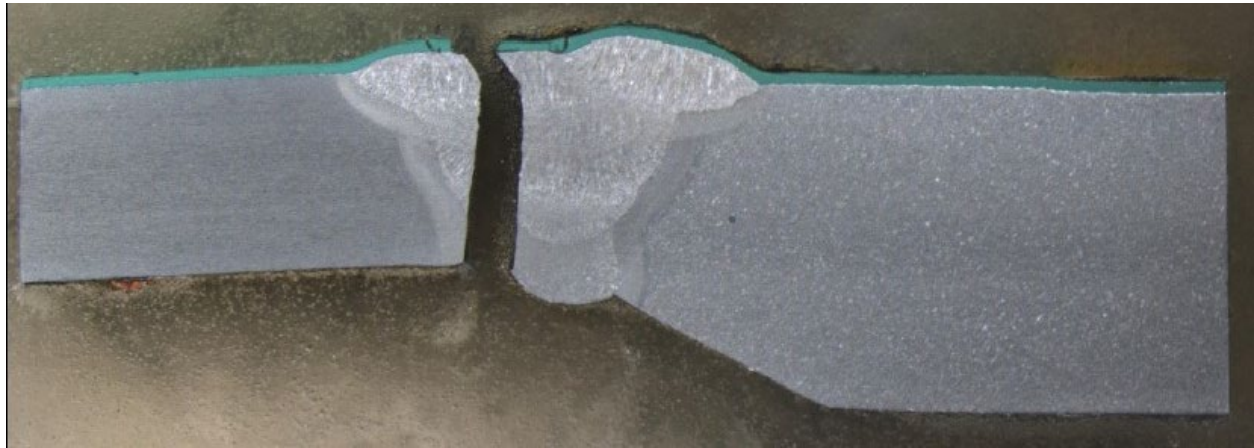


Figure 24. Metallographic Cross Section Through GWD 13530, Crack 1

⁴⁹ Per the welding procedure used to fabricate the bend assembly, WPS RCT-280, PWHT was not permitted and therefore no evidence of PWHT would be expected.

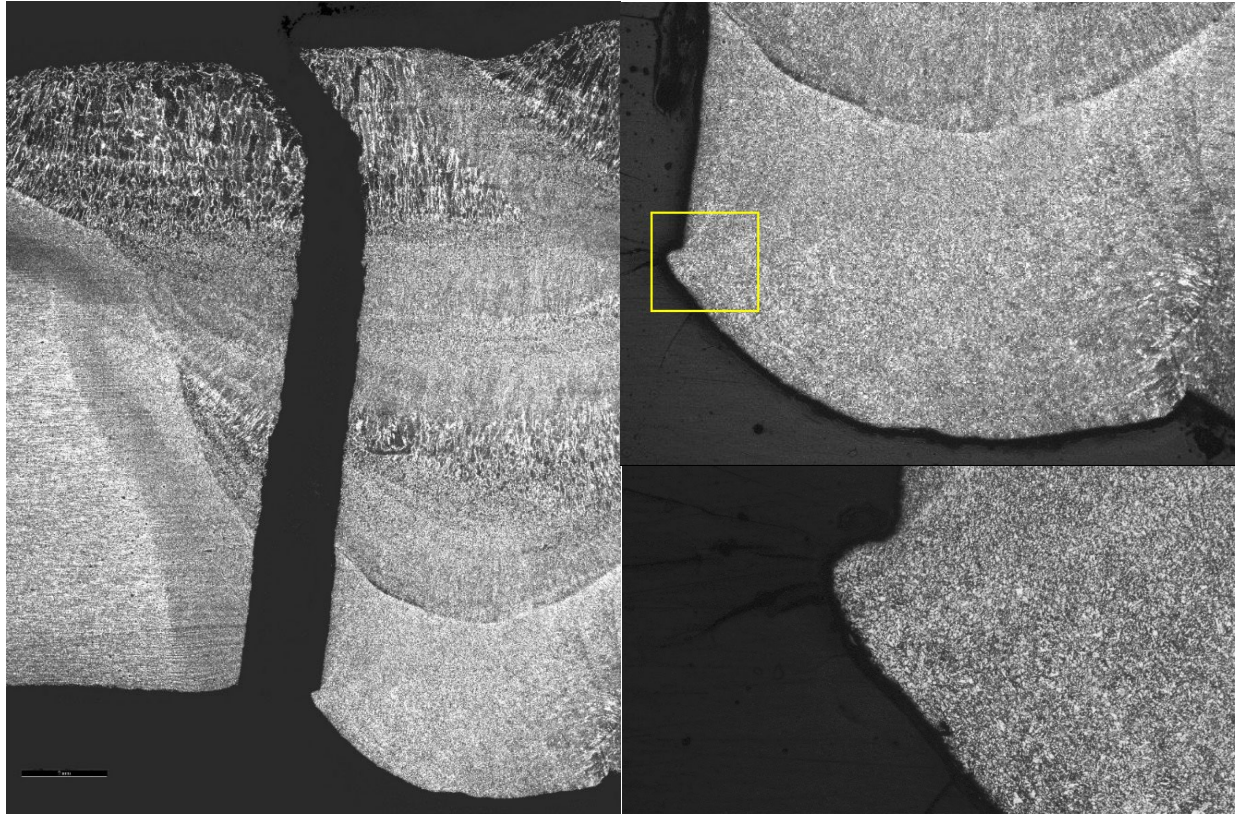


Figure 25. Photo Montage of Optical Micrographs Showing GWD 13530, Crack 1 (left 12.5x, top right 12.5x, and bottom right 50x)

Figure 26 presents a metallographic section of an intact portion of GWD 13530 (G59B) at 139° from TDC which was coincident with a PAUT indicated feature. As shown in Figure 27(a), there was an indication consistent with a LOF defect identified at the toe of the girth weld on the pup side of GWD 13530. Figure 27(b), shows a magnified view at the upward curvature of the defect at the terminal end which may be due to the onset of fatigue cracking. The higher magnification micrograph shows dense, tightly adhered oxide scale lining the surfaces of the LOF which is consistent with formation at the time of welding. Similar LOF defects (which also showed evidence of fatigue) and repairs of the ID weld root pass were also noted in GWD 13520, which did not fail.

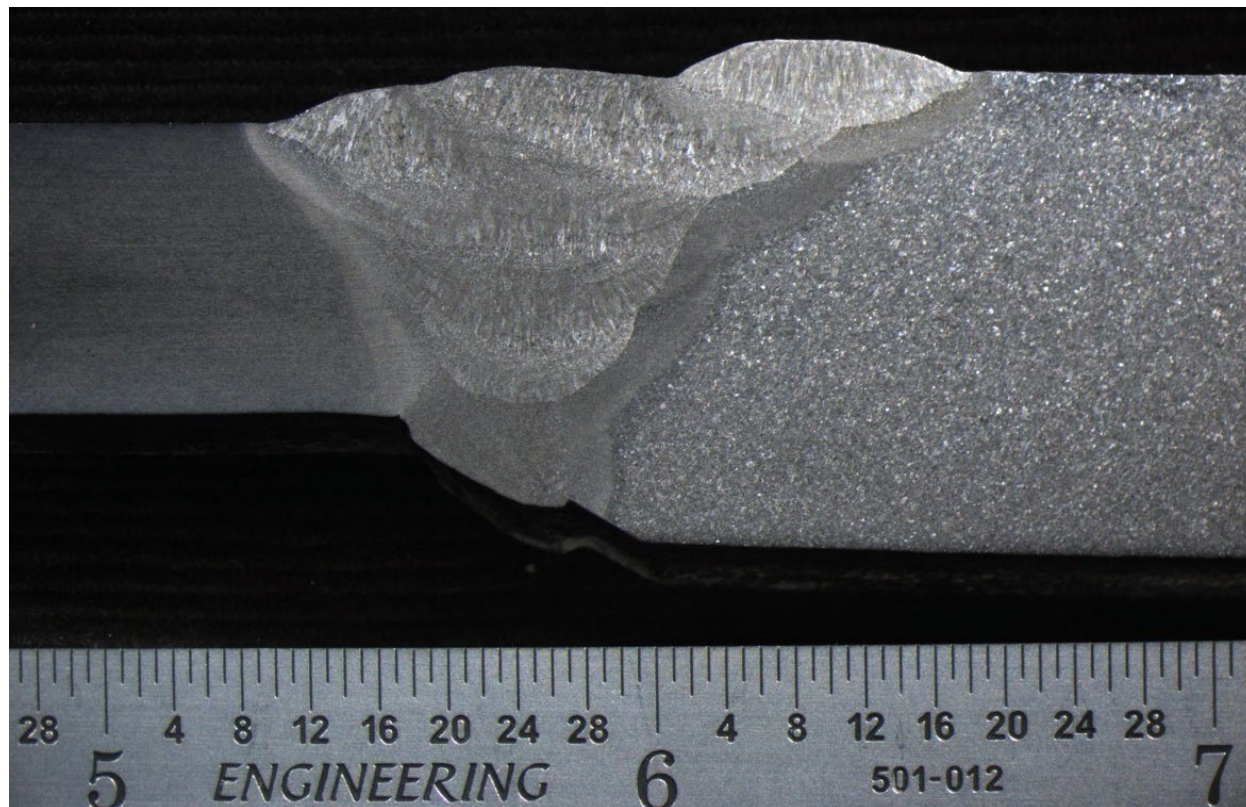


Figure 26. Metallographic Section of an Intact Portion of GWD 13530 at 139° from TDC Consistent with PAUT Indication 2

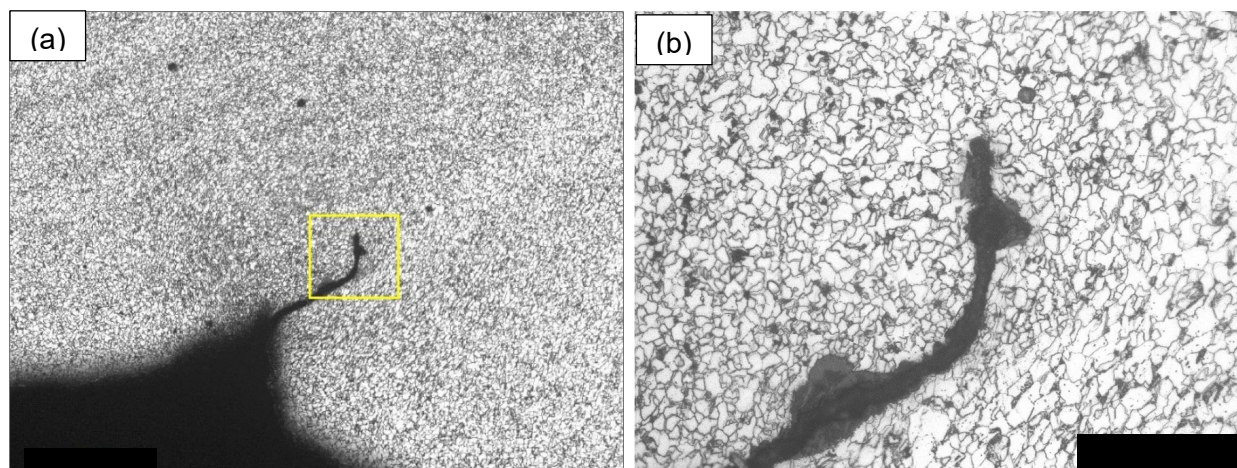


Figure 27. Optical Micrographs Showing a Scale-Filled, ~200 μm long LOF at the Pipe Side Weld Toe of GWD 13530 (a) 100x and (b) 500x

Pup, Elbow, and Girth Weld Material Properties:

Anderson noted that there was no evidence to support that the pipe, elbow, or weld materials were deficient. The microstructure of the pups consisted of finely banded, fine-grained ferrite and pearlite, typical of a low carbon, micro-alloyed steel used to fabricate high strength line

pipe. The bulk weld microstructure appeared sound, though there were intermittent imperfections (i.e., interpass LOF, gas porosity, and slag entrapment) separate from the LOF identified at the ID weld toes. These imperfections were determined to be acceptable per the post-incident inspection report prepared by ApplusRTD.

The mechanical properties and chemical composition of the pipe met the minimum specifications for API 5L grade X70 PSL 2, though there was evidence that some of the HAZ hardness exceeded the maximum set forth for grade X70. Similarly, cross-girth weld mechanical testing showed there were no deficiencies with the mechanical properties of GWD 13530 and GWD 13520 with respect to the minimums set forth in API 1104. The exception to this was one HAZ notched CTOD specimen from GWD 13520 (439-20-16) exhibited 0.0047-inch CTOD which marginally did not meet the minimum CTOD value of 0.005-inch. Since all other results significantly exceeded the specified minimum, it is still reasonable to consider the weld to have adequate ductility. Note that the weld did not fail due to a low-ductility condition. The mechanical properties and chemical composition of the elbow met the minimum specifications for MSS SP-75-2004.

4.2 Stress Analyses

Stress analyses using finite element (FE) modeling were completed by RSI to understand how and when the bending load was applied to the TAG 98 bend assembly (BND 350) to cause it to ovalize and wrinkle as well as to understand the necessary loading conditions for crack initiation and growth. The following scenarios were examined:

- 1) Potential causes of the ovality and wrinkle, including:
 - a) Accidental loads being applied during the 2010 fitting replacement, such as during hydrostatic testing, fit-up, backfill, and compaction activities.
 - b) Operating loads, such as internal pressure and temperature differentials.
- 2) Stress cycles resulting from temperature differential and pressure fluctuations.
- 3) Stress concentration factors due to imperfect elbow geometry (i.e., out-of-roundness, wall thickness transition, and LOF).

Several different analytical models were used to determine the most likely sequence of events. These analyses are summarized in Table 2. Detailed analyses are provided in Appendix D.

Table 2. Summary of FE Analyses

Analysis	Type	Objective	Model Size	Model Details
Beam Bending	Analytical using fixed and cantilever beam equations	Estimate span lengths and load levels as well as corresponding beam deflections required to yield the elbow during construction	Pipe lengths from 1 to 150 ft	Analytical, linear elastic, small strain, and deformations
Operating Loads	Soil-pipe interaction FEA	Calculate stresses in the elbow under operating loads (P=0 and 1,250 psig; ΔT=45°F, 25°C and 110°F, 61.1°C)	Pipe length ~4,900 ft from each side of the elbow	Numerical, nonlinear, finite strain, pipe elements and Elbow290 elements, upper- and lower-bound soil properties
Post-construction outside force (lack of support, settlement, and vehicle loads)	Soil-pipe interaction FEA	Calculate stresses in the elbow when there is a gap or weak soil under the pipe leading to settlement along the south slope coupled with construction vehicle loads		
Cantilever bending – End deflection during hydro or fit-up	Soil-pipe interaction FEA	Calculate stresses in the elbow from end deflection during the hydrostatic test or fit-up of the replacement segment	Pipe length from 695 ft upstream to 165 ft downstream of the elbow	
Cantilever bending – Sliding displacement during hydro or fit-up	Soil-pipe interaction FEA	Calculate stresses in the elbow from sliding displacement during the hydrostatic test or fit-up of the replacement segment		
Operating Load Cycles	Soil-pipe interaction FEA	Calculate stress ranges in the elbow from ΔP = 500 and 1,000 psi and ΔT = ±40°F (22.2°C) and ±80°F (44.4°C)	Pipe length ~4,900 ft from each side of the elbow	
SCF	Elastic FEA	Calculate SCF values due to wall thickness transition and elbow out-of-roundness	TAG 98 (BND 350) and pups	Numerical, elastic, shell elements, small strain, and deformation
Surface Loading	Elastic-plastic FEA	Calculate effects from surface loading from a high concentrated load on the elbow (e.g., plate compactor)	TAG 98 (BND 350) and pups	Numerical, elastic-plastic, shell elements, finite strain

4.2.1 Ovalization and Wrinkle

The TAG 98 elbow and pups (BND 350) were under sufficient loads to cause permanent ovalization of the entire assembly and a wrinkle in the upstream pup. Minor pipe ovalization is not unusual and in most circumstances is not a cause for concern. However, when combined with the geometry of the elbow, a shallow, surface breaking LOF in the girth weld, and cyclic operational stresses, the loads that caused the ovality and wrinkle were enough to eventually lead to the failure of GWD 13530 (G59B).

The FEA showed that one possible scenario that could have caused the ovality was cantilever bending (deflection or sliding displacement) of the pipe during the hydrostatic test or fit-up when the downstream end of the pipe was not yet fixed. Another possible scenario was from post-construction outside forces causing settlement displacements of the pipe due to overburden.

Scenarios related to operating loads, construction vehicle loads during various stages of backfill, and highly concentrated loads from a plate compactor acting on the elbow to cause ovalization were also evaluated but determined to be unlikely. The results of these analyses are summarized in Table 3 and are discussed in detail below.

Table 3. Summary of FEA Results

Analysis Scenario	Model Assumptions	Maximum Predicted Combined Stress to SMYS Ratio	Permanent Deformation Probability
Operating Loads (Pressure and Temperature)	Static loads, 2 fixed ends, soil support	0.99	Unlikely
Post-construction outside force – construction vehicle load only	2 fixed ends, poorly supported by soil, soil overburden, vehicle loads	0.94	Unlikely
Post-construction outside force – settlement only		1.14	Possible
Post-construction outside force – construction vehicle loads and settlement		1.14	Possible
Cantilever bending – end deflection	1 fixed end, unsupported by soil, pipe filled with water, no soil overburden	1.12	Possible
Cantilever bending – sliding displacement	1 fixed end, pipe filled with water, no soil overburden	1.20	Possible
Surface Loading – Construction Vehicles	2 fixed ends, various amounts of soil overburden, vehicle loads	0.52	Unlikely
High Concentrated Load – Plate compactor	2 fixed ends, concentrated load near elbow	0.41	Unlikely

4.2.1.1 Operating Loads

The pipeline stresses were calculated under operating loads, which included differential temperature and operating pressure, to determine if the operating loads could have caused the observed wrinkle and ovality in the TAG 98 (BND 350) elbow. The models that were developed for this analysis are described in Appendix D. The first model used pipe elements and the second model used elbow elements to account for elastic ovalization. The loading combinations that were applied to each model are listed in Table 4.

Table 4. Loading Combinations for Operational Load Analysis

Loading Case No.	Internal Pressure [psig]	Differential Temperature [°F]	Differential Temperature Applied to Replacement Length, [°F]
1	1,250	0	0
2	0	65 (36.1°C)	110 (61.1°C)
3	1,250	0	45 (25°C)
4	1,250	65 (36.1°C)	110 (61.1°C)

The worst-case results for the four loading combinations are shown in Figure 28 (model using elbow elements and lower-bound soil conditions). The purple boxes in Figure 28 show the locations of the upstream (TAG 114C; BND 349) sag bend and the TAG 98 (BND 350) overbend and the dashed dotted red line shows the 90% SMYS longitudinal stress limit for restrained pipe. The longitudinal stress results indicate maximum compressive stresses of 38.1 ksi (263 MPa) and maximum strain of 0.14% for the TAG 98 (BND 350) overbend. The maximum equivalent stress is high (69.6 ksi; 99.4% SMYS), and, although it exceeds the allowable combined stress for the pipe material, it is insufficient to cause permanent deformation in the form of ovalization and a wrinkle.

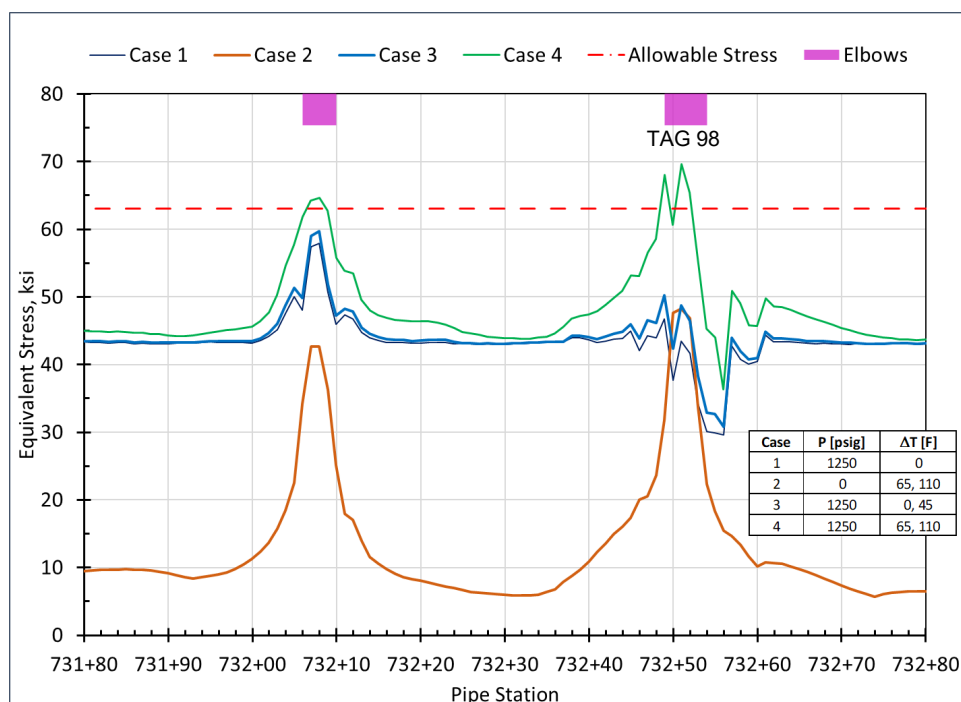


Figure 28. FEA von Mises Stresses with Elbow Elements and Lower-Bound Soil Properties (worst-case)

4.2.1.2 Post-Construction Outside Force

RSI considered the effect of a gap or weak soil underneath the replacement pipe segment after final tie-in, which would allow the pipeline to sag once backfilled (see Figure 29). The potential to have weak soil support is feasible since TAG 98 was replaced in the winter when temperatures were below freezing. Over excavation and the potential for frozen or partially frozen soil to be used as foundational support increases the likelihood for weak pipeline foundational support. This scenario also considered the possibility of surface loading from a large construction vehicle (side boom) crossing the pipeline near the elbow after backfilling was complete. A soil-pipe interaction FEA was used for this assessment with a soil overburden of 8-ft and mass density of 130 lbm/ft³. The weight of the pipe and product were also considered in the analysis. The assumed settlement profile is shown in Figure 30. The models that were developed for this analysis are described in Appendix D.

Three sets of analyses were performed to examine the effects of the side boom and settlement loads, namely (1) side boom surface loading with no settlement, (2) settlement with no side boom surface loading, and (3) settlement and side boom surface loading. Table 5 shows the three loading combinations that were analyzed for each analysis. The longitudinal stress results of the post-construction outside force FEA analyses are shown in Figure 31. The results show that surface loading from a side boom alone would not induce high enough stress levels to plastically deform the elbow. In contrast, post-construction soil settlement could have produced enough bending and axial stresses to cause yielding⁵⁰ in the elbow assembly.

The post-construction settlement or gap under the pipeline can explain the out-of-roundness of the elbow. However, this scenario does not explain the wrinkle as the amount of compressive stress at the elbow is not excessive. For ground settlement to cause a wrinkle, the amount of movement should be around 24-inches or more. It is also possible that the wrinkle was formed later due to thermal cycles or ground movement, but that would require two independent coincidences both affecting the same location of the pipeline at different times, which although is possible it decreases the overall likelihood of the scenario. In addition, the bending strain analysis from the IMU data and assessments by Geotech SMEs did not find evidence of ground movement near the TAG 98 elbow.

⁵⁰ As reported by Anderson, the actual yield strength of the elbow was near [REDACTED] and of the downstream pup was [REDACTED].

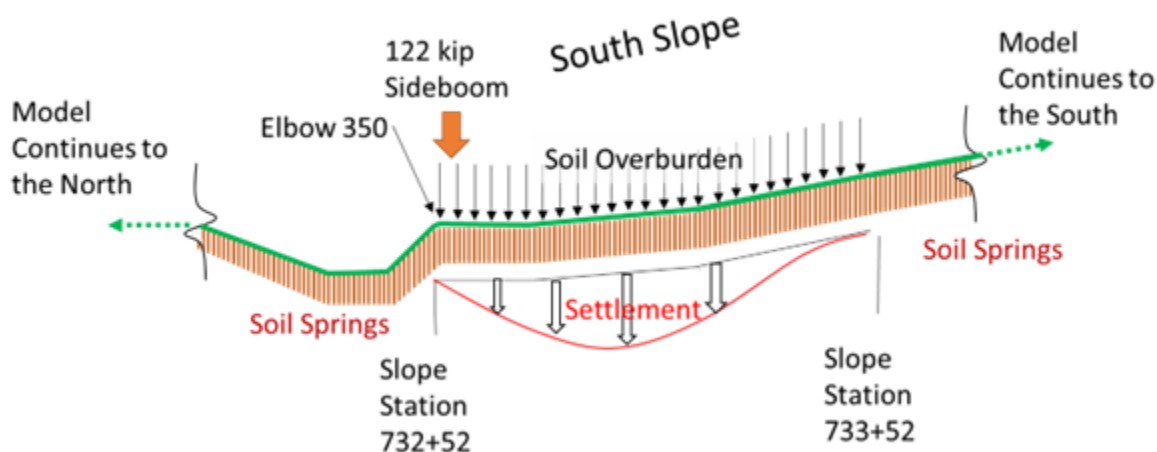


Figure 29. Schematic of the FEA Model for the Weak Support and Settlement Scenario

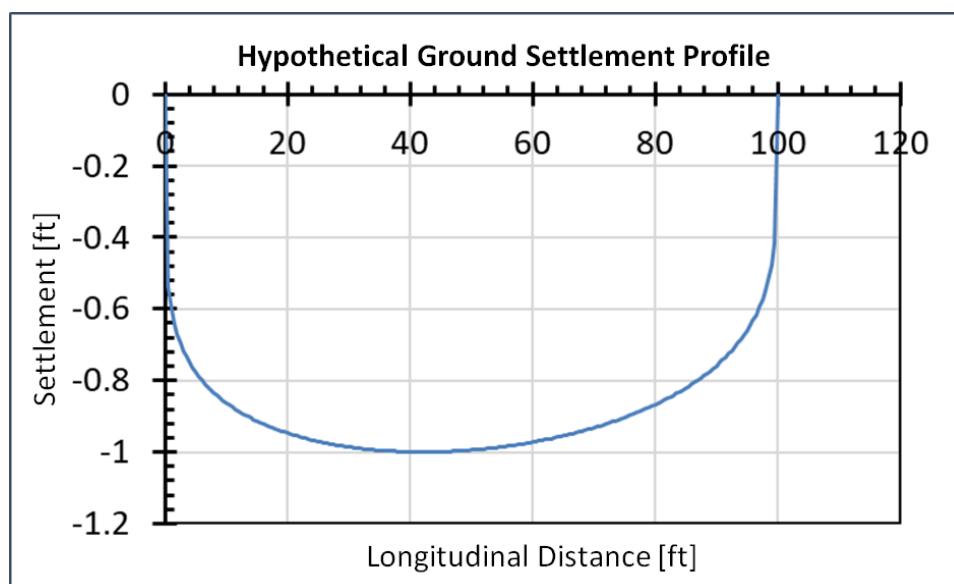


Figure 30. Hypothetical Ground Settlement Profile

Table 5. Loading Combinations for Lack of Support Analysis

Loading Case No.	Internal Pressure [psig]	Differential Temperature [°F]	Differential Temperature Applied to Replacement Length [°F]	Overburden Soil Cover [ft]
1	0	0	0	8
2	1,200	65 (36.1°C)	110 (61.1°C)	8
3	1,200	0	45 (25°C)	8

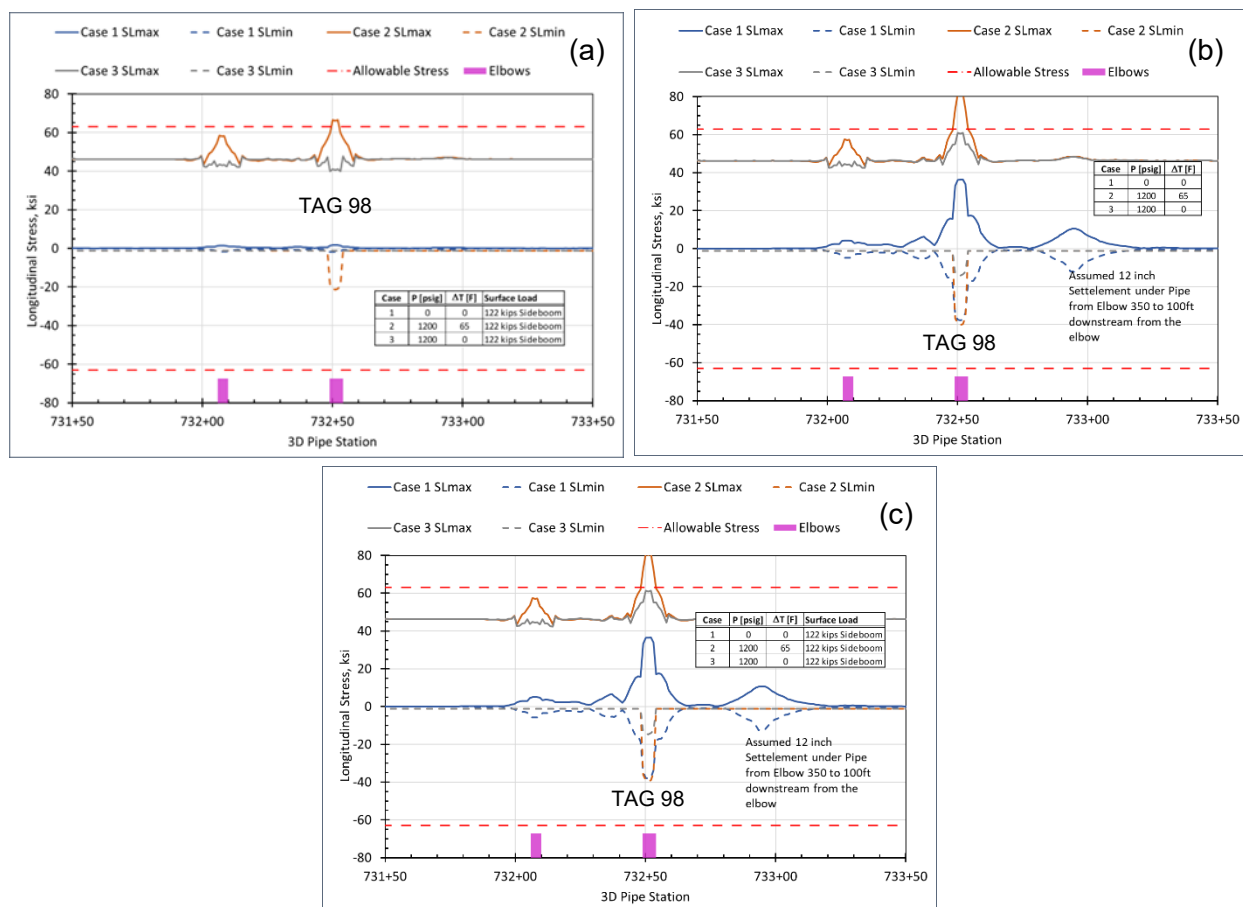


Figure 31. FEA Longitudinal Stresses with Elbow Elements and Lower-Bound Soil Properties (a) Side Boom Load Only, (b) Settlement Load Only, and (c) Side Boom and Settlement Loads

4.2.1.3 Cantilever Bending

Another possible scenario considered was the potential for cantilever bending of the replacement segment after the upstream tie-in weld (GWD 13510) was complete but before the final tie-in weld (GWD 13590) was made downstream. The creek section of the replacement was moved into place on December 10, 2010. Once placed, crews backfilled the creek section and trenched the south side of the creek to weld in the 168-ft long overbend section (containing TAG 98). The overbend section and creek section were filled with water and hydrostatically tested for four hours the afternoon of December 11, 2010. During dewatering later that evening crews encountered difficulties because the dewatering pig froze in the line. On December 12, 2010, the pipe was warmed using heaters and air compressors to jar the pig loose. The dewatering pig was finally removed from the test section on the evening of December 12, 2010. The final tie-in weld (GWD 13590; 9GT-035) on the south side of Mill Creek was completed on December 13, 2010, and was located approximately 158-ft downstream of the failed girth weld GWD 13530 (G59B).

A review of photographs during the December 2010 replacement shows that two side booms were used to hold the overbend section above the ground over the south-slope (see Figure 32).

The creek portion was buried but the downstream overbend section was most likely exposed during the hydrostatic test and free to move because the final tie-in weld had not yet been made. A note in the daily inspection report from December 11, 2010, suggests that the side booms may have been demobilized prior to the hydrostatic test, however, these records are unclear as to how the pipeline was placed in the ditch and supported during the hydrostatic test. Discussions with the Field Engineer onsite during the hydrostatic test indicated that the side booms would have been removed and the pipe supported with cribbing or soil supports. The potential for inadequate support during the hydrostatic test or fit-up creating a cantilever beam-bending effect was studied to estimate the potential bending stresses.



Figure 32. Use of Sidebooms During Replacement of TAG 98 (December 10, 2010)

RSI evaluated two scenarios: (1) the possibility that a 158-ft long portion of the pipeline downstream of the TAG 98 elbow was unsupported during the hydrostatic test allowing the pipe to undergo cantilever bending until the end experienced enough deflection to close the gap (see Figure 33); and (2) sliding displacement downhill (see Figure 34). The models that were developed for this analysis are described in Appendix D. Table 6 shows the two loading combinations that were analyzed. The first loading condition represents the unpressurized pipe filled with hydrostatic water and the second loading condition represents the effects from hydrostatic test pressure.

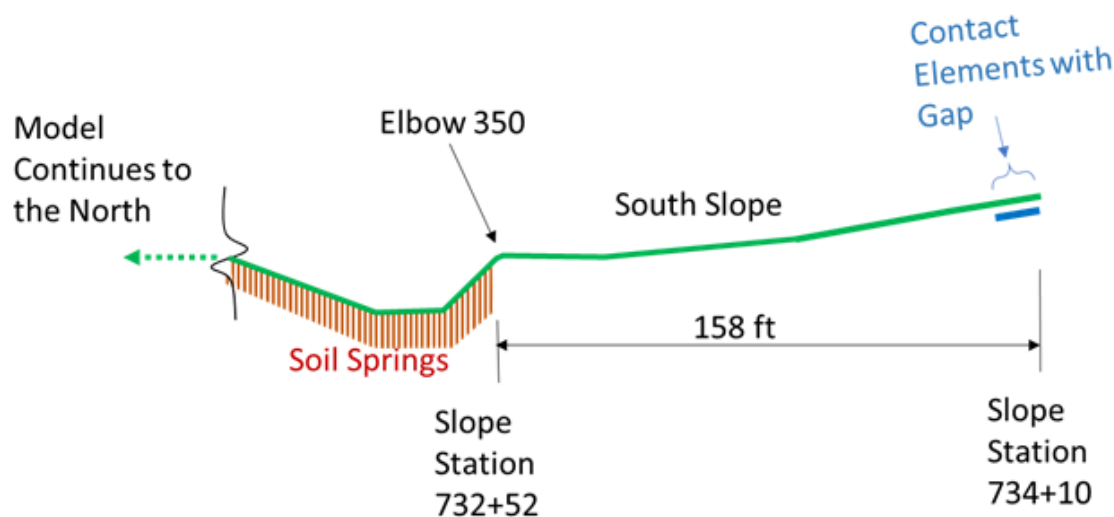


Figure 33. Schematic of the FEA Model for the Cantilever Scenario with End Deflection

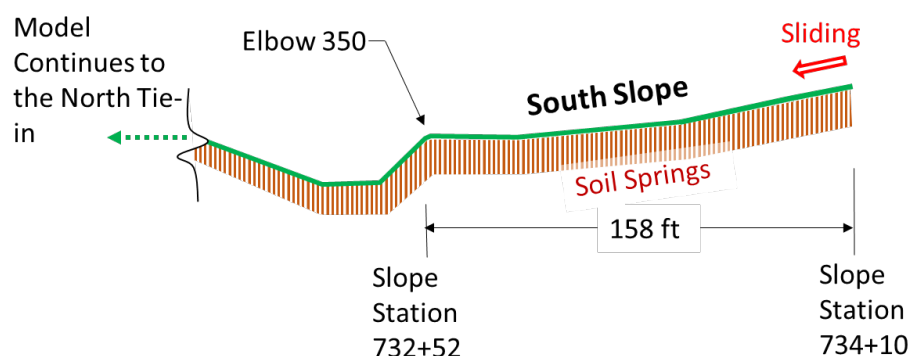


Figure 34. Schematic of the Cantilever Model with Sliding Displacement

Table 6. Loading Combinations for Cantilever Soil-Pipe Interaction Analyses

Loading Case No.	Internal Pressure [psig]	Differential Temperature [°F]	Differential Temperature Applied to Replacement Length [°F]	Overburden Soil Cover [ft]
1	0	0	0	0
2	1,850	10 (5.6°C)	10 (5.6°C)	0

The results of the FEA for the end deflection scenario are shown in Figure 35. Various amounts of gap in the contact elements (cantilever end deflection) were examined to determine how much end deflection would be required to overstress the elbow. The results of the cantilever model with a 6-ft gap are shown in Figure 35(a) for the longitudinal stresses and Figure 35(b) for the equivalent stresses. The results show that cantilever action could have over-stressed the

TAG 98 (BND 350) elbow if the end deflection was at least 6-ft. This amount of end deflection is excessive and could only happen if the pipe length on the south slope was supported above ground before the hydrostatic test and lost the support after it was filled with water. This type of movement would have been noticeable by construction crews and most likely would have resulted in a safety shutdown (which there is no evidence of in the daily inspection reports).

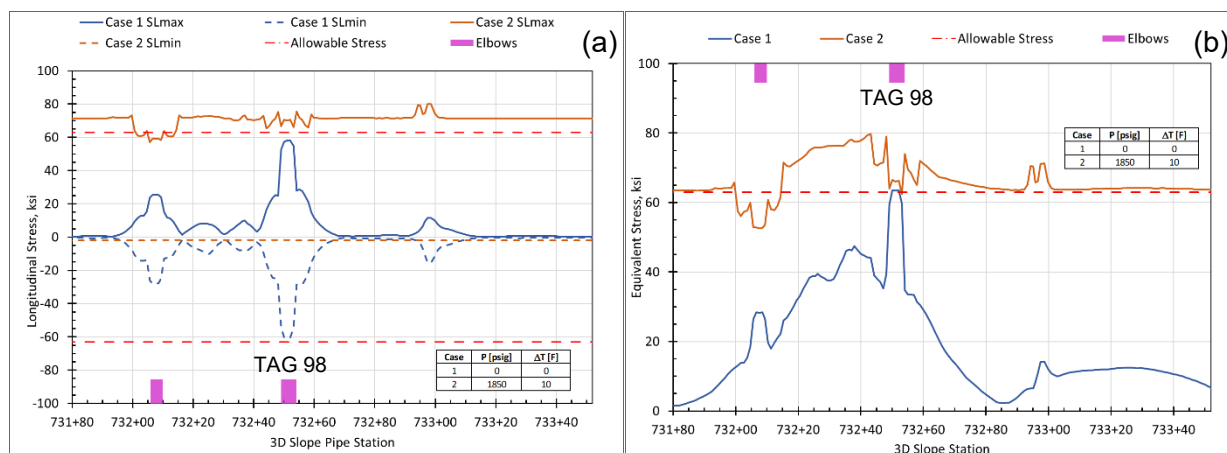


Figure 35. FEA (a) Longitudinal Stresses with 6-ft End Deflection and (b) von Mises Stresses with 6-ft End Deflection (Elbow Elements and Lower-Bound Soil Properties)

The results of the FEA for the sliding displacement scenario are shown in Figure 36. A sliding displacement of 6-inches in the downhill direction was applied to the end of the cantilever length and the model was run to calculate stresses. The results of this analysis are shown in Figure 36(a) for the longitudinal stresses and Figure 36(b) for the equivalent stresses. The results show that sliding of the pipeline down the slope can also create excessive bending stress at the elbow; however, the weight of the pipe filled with hydrostatic water is insufficient to cause the sliding. In other words, some outside loading had to act on the pipeline to force it to slide.

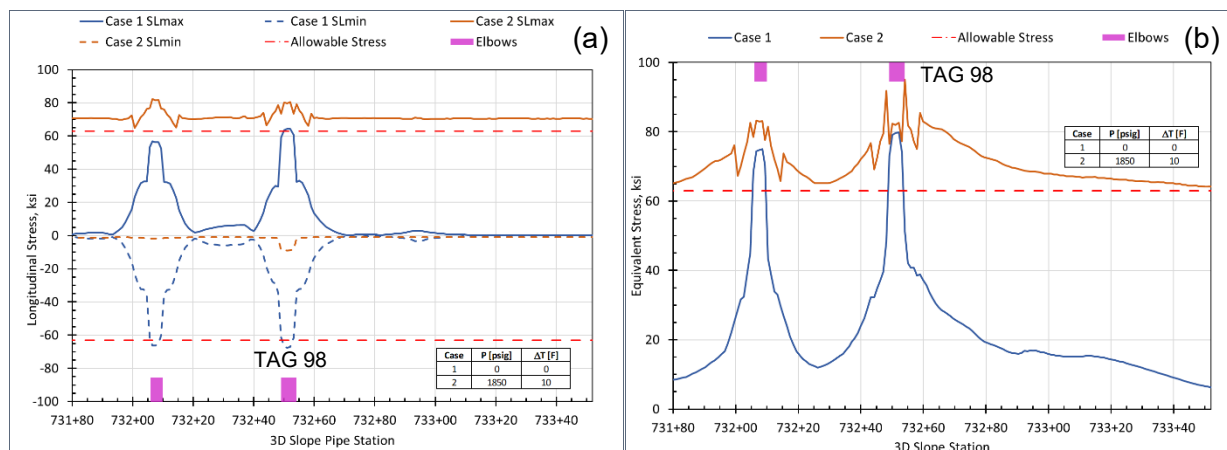


Figure 36. FEA (a) Longitudinal Stresses with 6-inches of Sliding Displacement and (b) von Mises Stresses with 6-inches of Sliding Displacement (Elbow Elements and Lower-Bound Soil Properties)

In summary, RSI analyzed two possible cantilever-type scenarios to determine the potential for high bending stresses to have occurred during hydrostatic testing (1) end deflection and (2) sliding displacement. Under Scenario 1 it was assumed that the pipeline was supported (e.g. with side booms or cribbing) at some distance above the ground and undergoes cantilever bending due to loss of this support. Under Scenario 2, the pipeline was assumed to slide down the hill. Compared to the post-construction outside force scenario discussed in Section 4.2.1.2, the cantilever action (Scenario 1) required a large amount of end deflection, but it explained the ovality as well as the wrinkle (the compressive stress in Figure 35 is at 90% SMYS at the elbow). The sliding action (Scenario 2) also explained the ovality and wrinkle but required a large outside force to overcome ground friction and bending resistance of the elbow to initiate sliding. The post-construction outside force scenario, on the other hand, does not require excessive pipe deflection or outside force, but requires the presence of a long gap or soft soil layer under the pipeline or post construction settlement (or a combination thereof).

4.2.1.4 Surface Loading

The objective of the surface loading analysis was to determine if the weight of the construction equipment crossing the unpressurized pipeline could have caused excessive stress in the elbow. RSI performed a surface loading analysis using the Canadian Energy Pipeline Association (CEPA) model⁵¹ to calculate surface loading induced stresses in the pipe. The CEPA model assumes that the pipe is straight and therefore does not account for stress concentration at the elbow. As such, the results are approximate. Table 7 shows the resulting stresses in the unpressurized straight pipe under surface loading from three different construction vehicles that were onsite during the replacement project for cover depths ranging from 2-ft to 8-ft. The results in Table 7 show that the surface loading induced stresses are not high enough to cause excessive deformation of the pipe – none of the stresses approach SMYS.

Table 7. Maximum Equivalent Stress in Empty Pipe [psi]

Vehicle Model	Cover Depth = 2 ft	Cover Depth = 3 ft	Cover Depth = 4 ft	Cover Depth = 6 ft	Cover Depth = 8 ft
345 GC Excavator	34,859	25,353	19,795	14,954	14,954
CAT 594H Sideboom	36,446	26,708	21,025	16,150	16,150
CAT 583 Sideboom	14,939	11,482	9,716	8,752	8,752

⁵¹ D. J. Warman and D. J. Hart, "Development of a pipeline surface loading screening process & assessment of surface load dispersing methods," Kiefner and Associates, Inc. for Canadian Energy Pipeline Association (CEPA), June 17, 2005.

D. J. Warman, J. Cherney, M. Reed and J. Hart, "Development of a pipeline surface loading screening process (IPC2006-10464)," in 6th International Pipeline Conference, Calgary, Alberta, Canada, September 25-29, 2006. ENV-6-1 Report RP-218-104509, "Field validation of surface loading stress calculations for buried pipelines - Milestone 2," Pipeline Research Council International, Inc (PRCI), Authored by Zand, B., Branam, N. and Webster, W., April 2018.

4.2.1.5 Concentrated Loading (Plate Compactor)

Another FEA was conducted to explore the effect of a potentially high concentrated load on the elbow (e.g., from a plate compactor) – see Appendix D.8 for details. A shell model was used with elastic-plastic constitutive models for the pipe and the elbow. The Ramberg-Osgood elastic-plastic stress-strain curves used in the analysis were based on tensile test data provided in Anderson's metallurgical analysis. A vertical concentrated load of 100,000 lbf was applied to a 10-inch by 20-inch area of the pipe surface right next to the elbow. The results show a maximum von Mises stress of 28.6 ksi in the elbow, which is insufficient to cause plastic deformations.

4.2.1.6 Summary

Overall, the above analyses suggest that high amounts of outside load/displacement would be required to cause the observed ovality and wrinkle. If the pipe segment did, in fact undergo such drastic loading conditions it seems unrealistic that these scenarios would have gone unnoticed. A more likely scenario is that a combination of several factors led to the overstress of the elbow. For example, it is possible that the elbow received some bending during the hydrostatic test and fit-up. Then, the bending increased after the overburden was placed due to presence of gap or weak soil under the pipeline. Finally, the elbow, which already had some level of locked-in bending stress, overstressed during the first year or two after operations began due to soil settlement and operating loads. The difference between the laser-scanner ovality and the ovality measured during operation (i.e., 2012 ILI, the subsequent field investigation, 2013 ILI, and 2018 ILI) shows that the elbow was under relatively high locked-in bending moment at various times during operation. This observation is consistent with the scenarios described above. In contrast, if the ovality was formed by an accidental load during the replacement (i.e., excessive concentrated load from a plate compactor) then the amount of ovality would be expected not to change significantly after the elbow was cut out.

4.2.2 Crack Initiation

As described in Section 4.3.5, fracture mechanics calculations were performed to understand when a crack may have initiated. The intent of this modeling was to try to understand the sequence of events related to crack initiation and growth – and to help narrow down if the crack initiated when high bending loads were applied during construction and/or from operational loads.

Although the surface has been altered by corrosion, the initial 0.040-inches of the fracture surface has a greater concentration of pitting than the remaining 0.500-inch (see areas highlighted by the yellow box in Figure 37). These corrosion pits indicate an 'older' surface that had been exposed to a corrosive environment (e.g., water and product). As discussed previously, the bending load that was applied during construction was sufficiently high to cause permanent plastic deformation of the TAG 98 (BND 350) bend assembly. This load likely exceeded the crack initiation threshold from the LOF already present and initiated the crack at that time (or at a minimum opened the root bead LOF allowing a crack to start sooner). Once a crack initiated, the subsequent thermal and pressure cycles caused the crack-front to progress over the 12-years of operation.

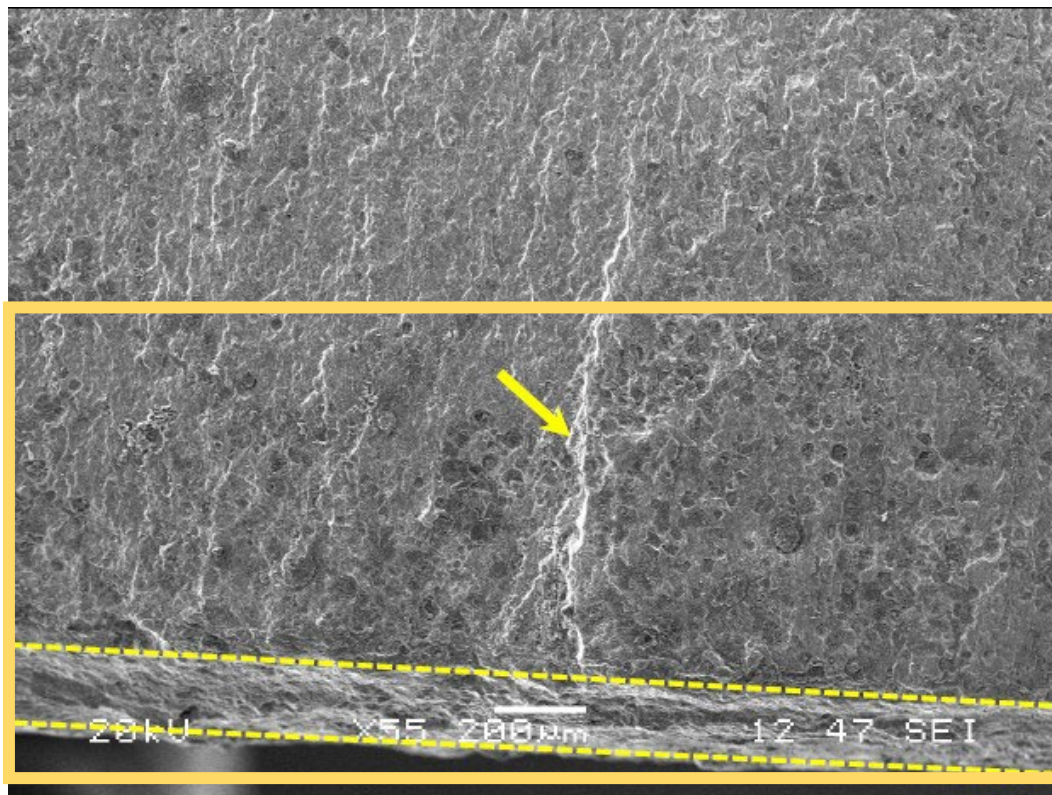


Figure 37. Region on the Crack 1 Fracture Surface with Corrosion Indicating Crack Initiation Early in the Life of the Crack

RSI also examined the indicated flaw depth data from the PAUT NDE performed at Anderson (see Figure 38 for GWD 13530 and GWD 13520). The magnitudes and pattern of indications are similar for both welds. Since the indications appear on the intrados of both welds, they are unlikely to represent initial tearing or overload from loads applied when TAG 98 was installed. They are also unlikely to have been caused by thermal fatigue because the intrados would have been in compression under these loads. The left-hand side of the x-axis represents the TDC of the pipe and the scan direction is clockwise. The flaw depth measurements tend to decrease at the intrados and increase at the extrados which may be evidence of some influence of bending from the installation or thermal loads.

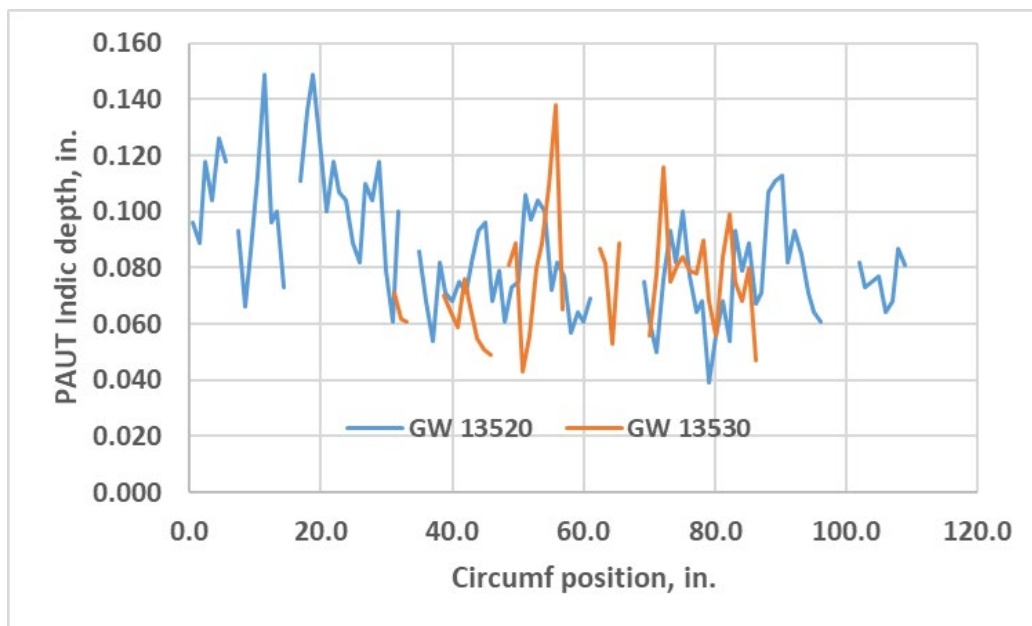


Figure 38. PAUT Indicated Flaw Depths for GWD 13520 and GWD 13530

The fracture surfaces were not clear enough to discern if there was a region of initial tearing when the installation load that caused the ovality was applied, but it is plausible. Additionally, in comparison with actual cross-sections, the PAUT likely over-predicted depths by a factor of 2x to 10x. As shown in Figure 39, the depth of both flaws is approximately 0.008-inch (200 μ m) but the nearby PAUT indications are noted as (a) 0.055-inch and (b) 0.080-inch⁵². So, even where the PAUT indicates flaws that were much larger in GWD 13530 they in fact were similar in size to the LOF that initiated cracking and does not refute the fact that flaws were not reported by radiography at the fabrication shop.

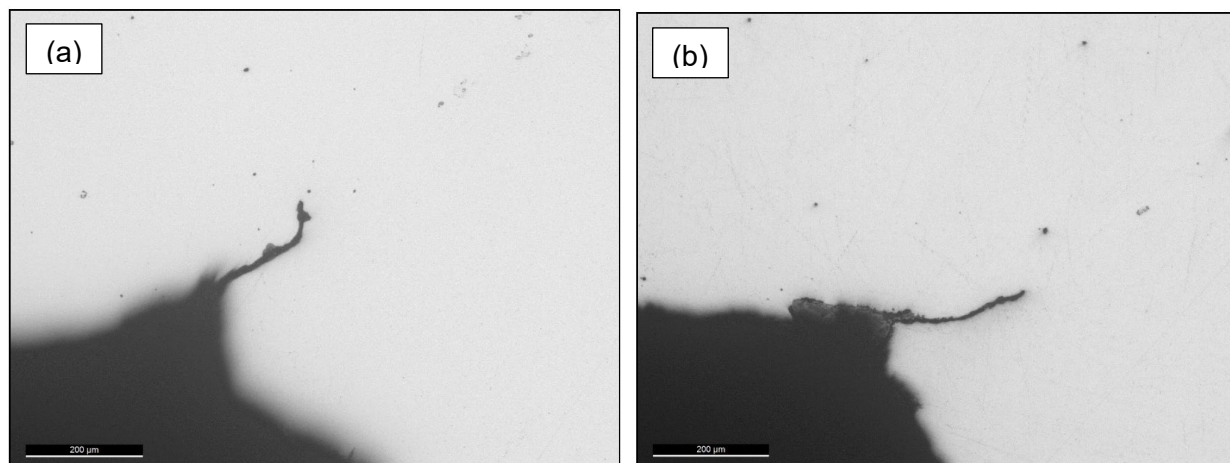


Figure 39. Comparison of Cross-Sections for GWD 13530 with PAUT Findings (a) 139° from TDC and (b) 270° from TDC

⁵² At 139° (43.67-inch) from TDC the PAUT indication was at 43.797-inch from TDC and at 270° (84.82-inch) from TDC the PAUT indication was at 85.116-inch.

4.3 Fatigue Analysis

Fatigue cracking in a girth weld can be affected by variables such as the crack initiation site, weld geometry, pipe and weld material properties, loading conditions, and residual stresses. As noted by Maddox and Zhang⁵³, increased fatigue crack initiation and growth in girth welds was found where weld root bead profiles were poor such as where weld beads were relatively high, sharp corners formed at the weld toe, and cold lap-type flaws formed due to local LOF. The main portion of the fatigue cracks were presumed to be due to a combination of temperature and pressure cycle fatigue. Crack initiation and crack growth life analyses were performed by RSI to determine what parameters likely prevailed consistent with the observed 11.8-year service time to failure. These analyses were supported by detailed FEA to determine elastic SCFs to be used with crack initiation and crack growth calculations. In addition, pressure and temperature cycles were combined using the SCADA time stamp to simulate the combined cyclic loading at the girth weld.

4.3.1 Analysis of Pressure Data

TC Oil provided pressure data from SCADA for the Steele City and Hope pump stations from initial operation through the failure incident. Figure 40 presents the condensed pressure record graphically.

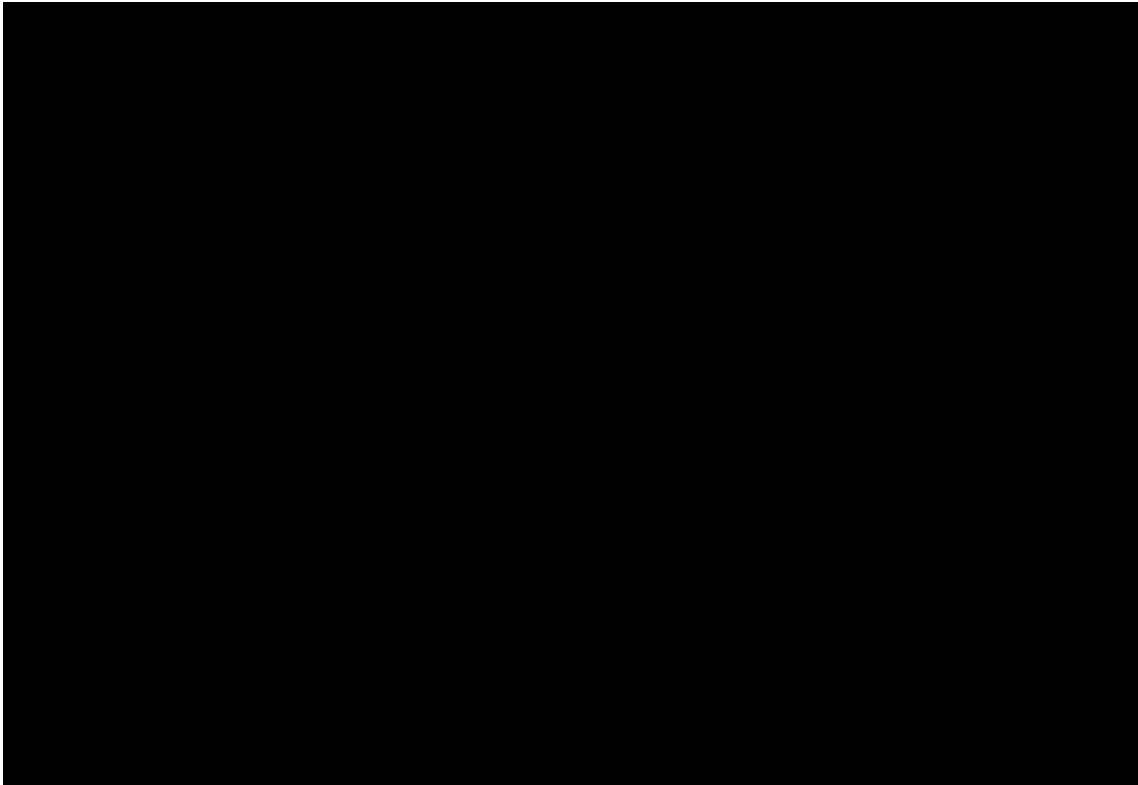


Figure 40. Pressure Spectrum for the Steele City Discharge and Hope Suction (January 2011 to December 7, 2022)

⁵³ <https://www.twi-global.com/technical-knowledge/published-papers/comparison-of-fatigue-of-girth-welds-in-full-scale-pipes-and-small-scale-strip-specimens> accessed on March 1, 2023.

The pressure data was analyzed using actual pressure pairs and a “rainflow” cycle-counting procedure in accordance with standard practices.⁵⁴ The analysis decomposes the stochastic pressure signal in terms of the magnitude, number of occurrences, and sequence of pressure cycles. A linear pressure gradient between the upstream (Steele City PS discharge) and downstream (Hope PS suction) pressure reading locations was assumed to calculate the cycle magnitudes at MP 14. The pressure data at MP 14 was interpolated using basic head loss equations for pipe⁵⁵ that considers location, elevation, and specific gravity of the product. The pressure cycle sequence was then used with incremental crack growth calculations. The number and magnitude of cycles can be expressed in terms of equivalent uniform magnitude cycles using linear cumulative damage concepts (e.g., Miner’s Rule). These metrics are summarized in Table 8 and presented graphically in Figure 41. The pressure cycle counts for MP 14 for the operational life of the pipeline is presented in Figure 42 (histograms for individual years are provided in Appendix E).

Table 8. Pressure Cycle Characterization at MP 14

Year	Equivalent Number of Full-MOP cycles/year at MP 14
2011	
2012	
2013	
2014	
2015	
2016	
2017	
2018	
2019	
2020	
2021	
2022 (a)	
Annualized	

Notes: (a) Eleven months ending December 7, 2022.

⁵⁴ American Society for Testing and Materials, “Standard Practices for Cycle Counting in Fatigue Analysis”, ASTM E1049-85.

⁵⁵ Fox, R. W., and McDonald, A. T., “Introduction to Fluid Mechanics”, John Wiley and Sons, Inc., New York, 1998.

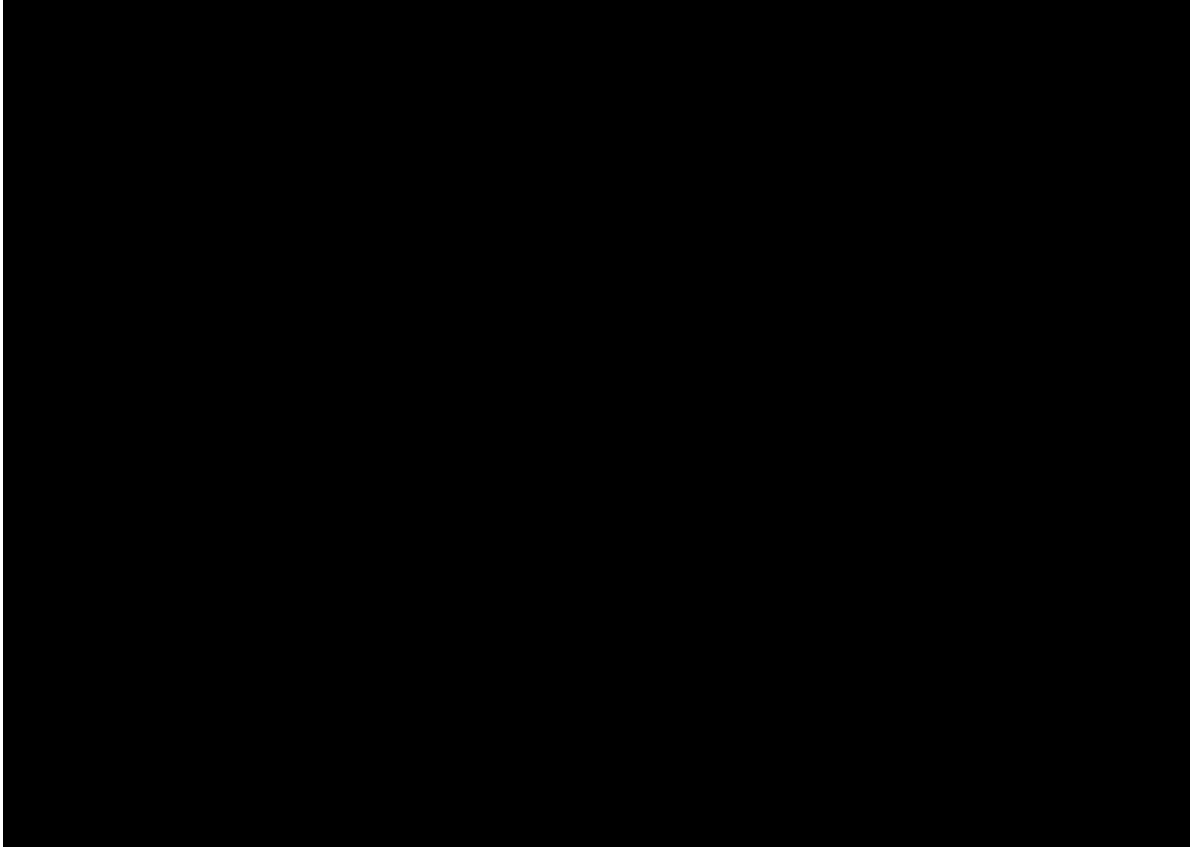


Figure 41. Annual Equivalent 80% SMYS Cycles at MP 14

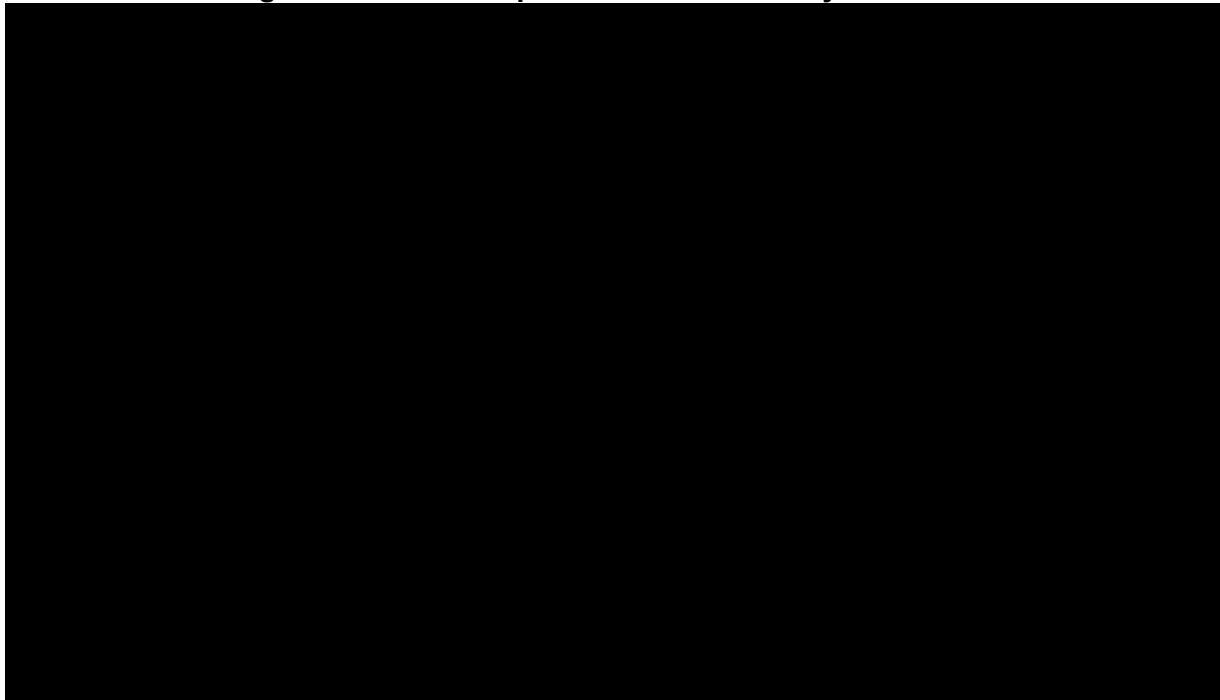


Figure 42. Pressure Cycle Counts for the MP 14 Location (January 2011 to December 7, 2022)

4.3.2 Analysis of Temperature Data

TC Oil provided temperature data from SCADA for the Steele City and Hope pump stations from initial operation through the failure incident. As shown in the Figure 43 temperature spectrum, operating temperatures have been increasing over time. Like the pressure data, the temperature data were analyzed as temperature pairs and using a “rainflow” cycle-counting procedure. The temperature cycle sequences were included in incremental crack growth calculations. The number and magnitude of temperature cycles was also expressed in terms of equivalent uniform magnitude cycles using linear cumulative damage concepts. These metrics are summarized in Table 9 and presented graphically in Figure 44. The temperature cycle counts for the operational life of the affected segment are presented in Figure 45 (histograms for individual years are provided in Appendix E).

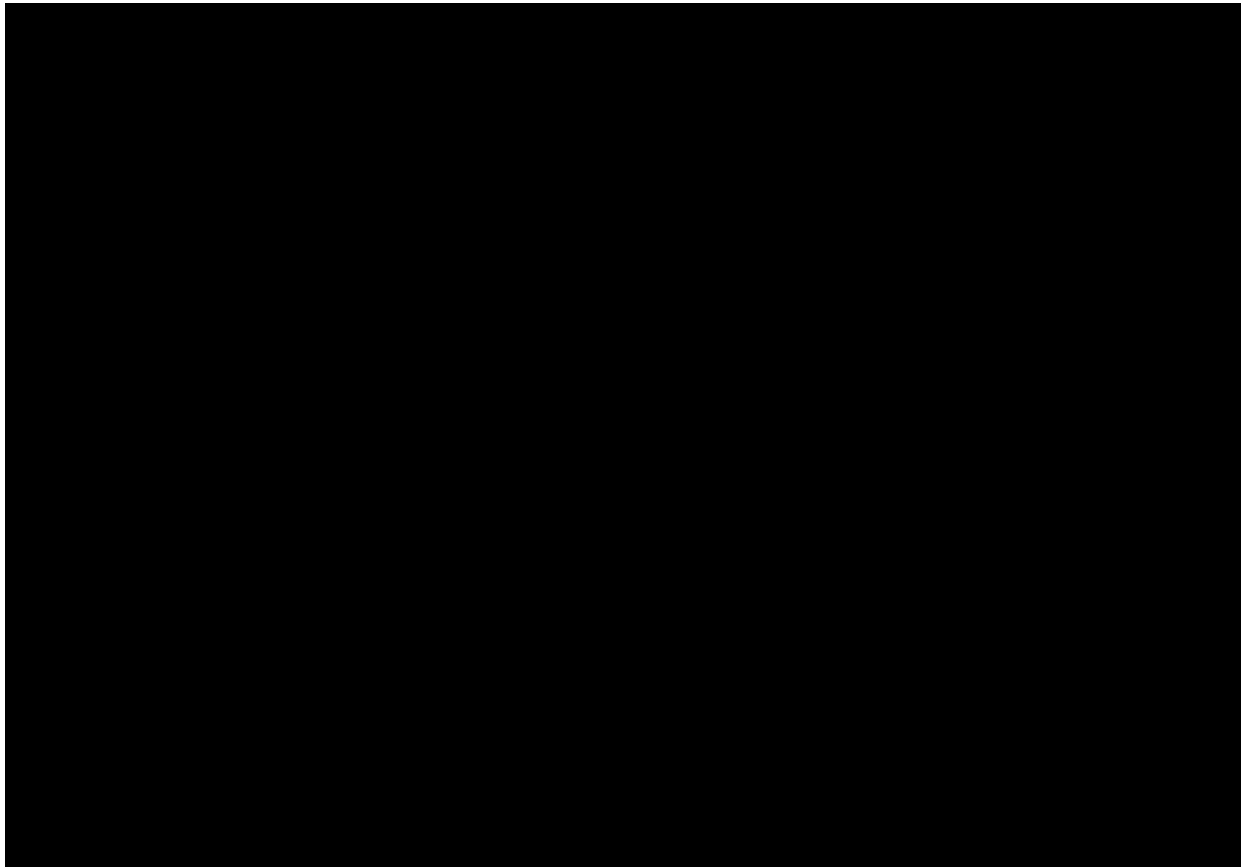
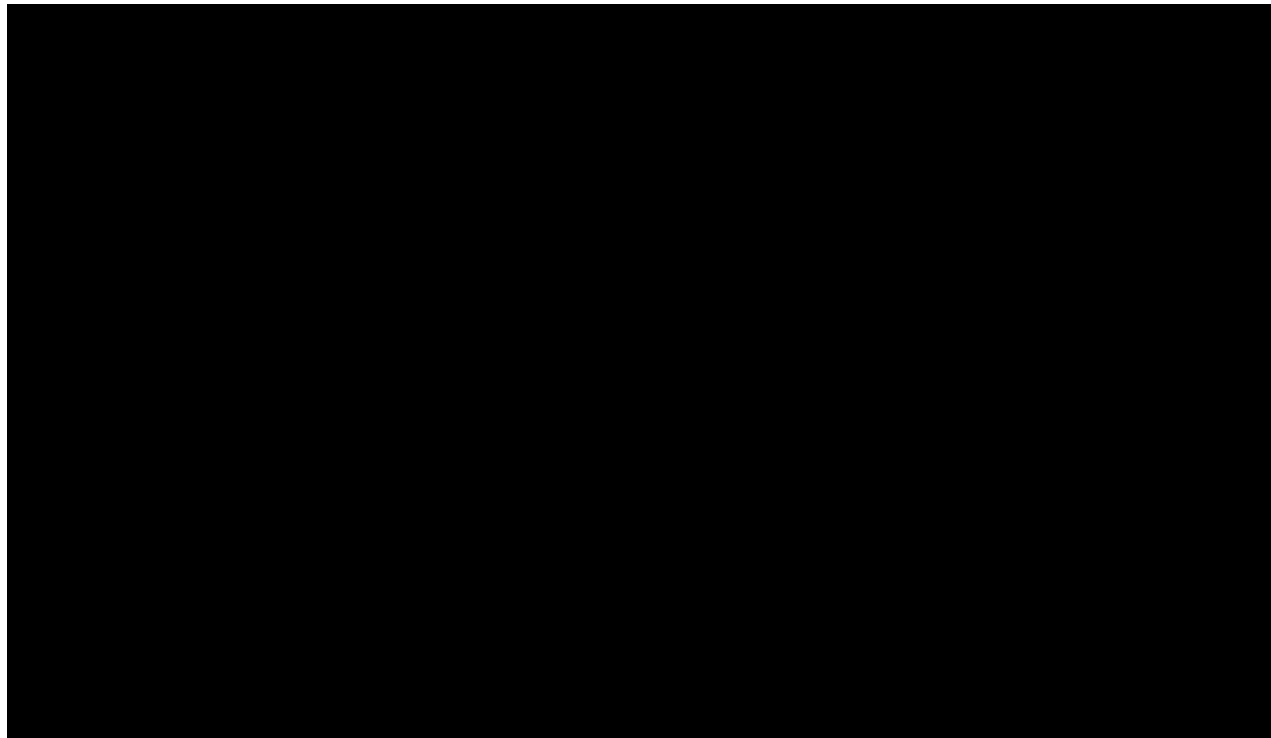


Figure 43. Temperature Spectrum for the Steele City Discharge (January 2011 to December 7, 2022)

Table 9. Temperature Cycle Characterization at Steele City Discharge

Year	Equivalent Number of 40°F (22.2°C) cycles/year	Equivalent Number of 80°F (44.4°C) cycles/year
2011		
2012		
2013		
2014		
2015		
2016		
2017		
2018		
2019		
2020		
2021		
2022 (a)		
Annualized		

Notes: (a) Eleven months ending December 7, 2022.

**Figure 44. Annual Equivalent Temperature Cycles at Steele City**

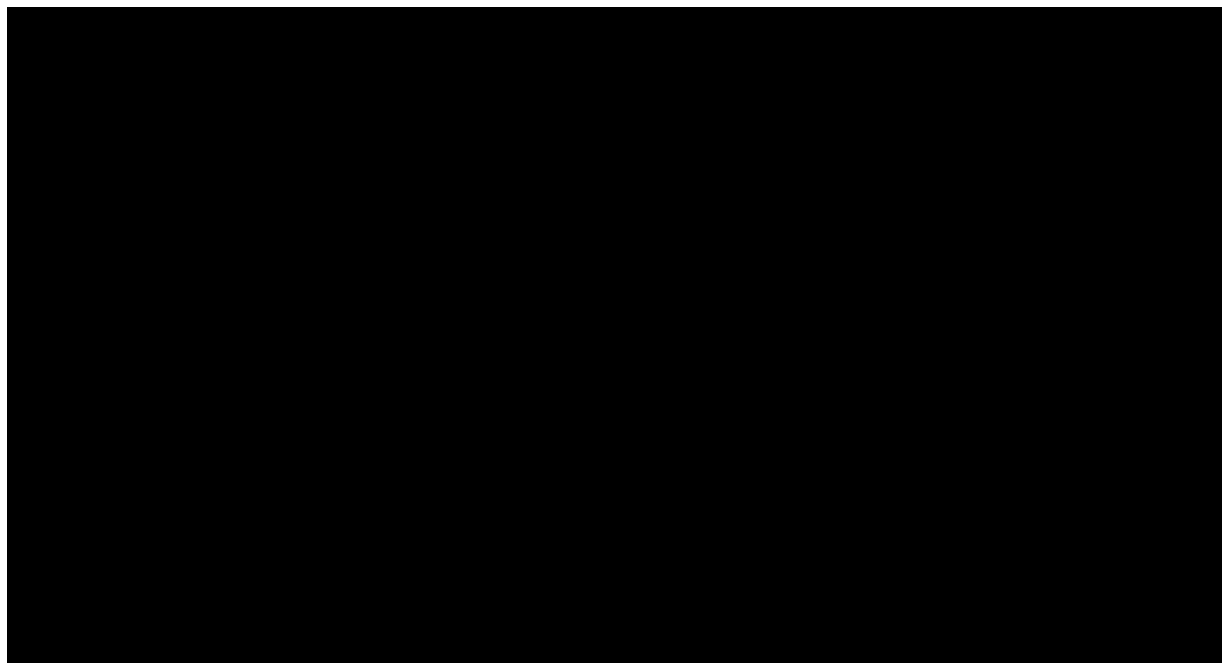


Figure 45. Temperature Cycle Counts for the Steele City Discharge (January 2011 to December 7, 2022)

4.3.3 Combining Pressure and Temperature Cycles

RSI converted the temperature cycles to an equivalent pressure cycle using the correlation between pressure and temperature cycles and the resulting longitudinal stress (see Figure D.42 and Figure D.43 in Appendix D). The resulting cycle counts are shown in Figure 46.

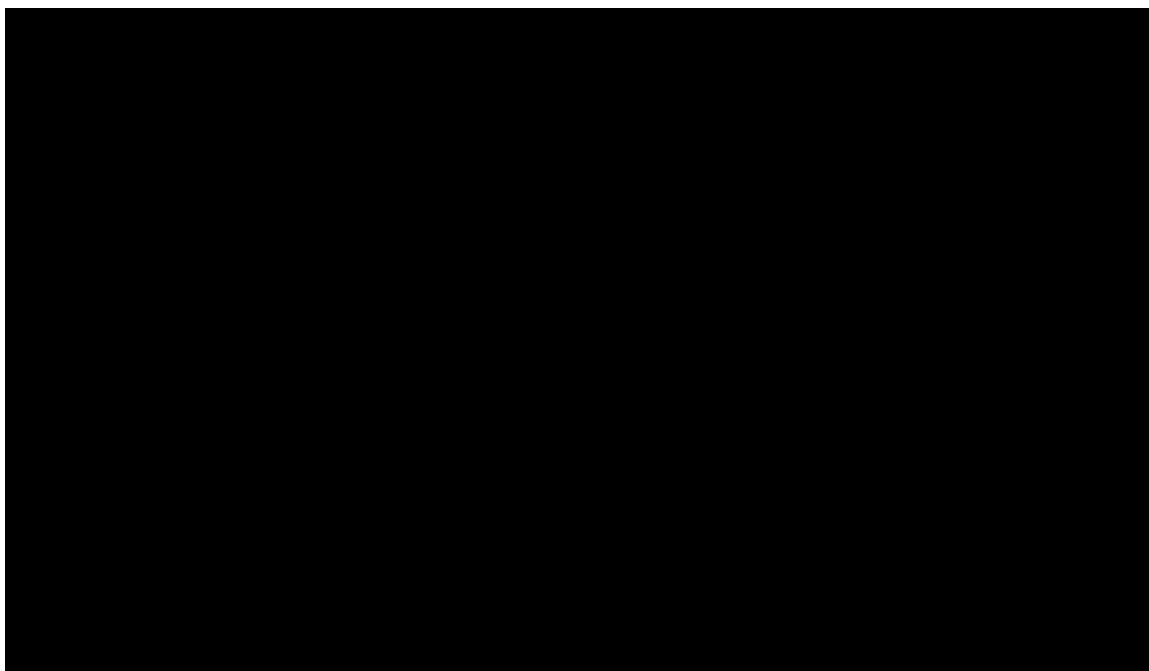


Figure 46. Combined Pressure and Temperature Cycle Counts (January 2011 to December 7, 2022)

The cycle count results shown in Figure 46 were used for S-N fatigue analysis. However, for crack growth analysis with Paris Law, since the order of the stress cycles can affect the end results, the actual SCADA pressure pairs were used which tends to preserve the order of the pressure cycles. These pressure pairs were converted to equivalent longitudinal stress ranges, and then used in the crack growth analysis. Figure 47 shows a cumulative histogram of the stress ranges.

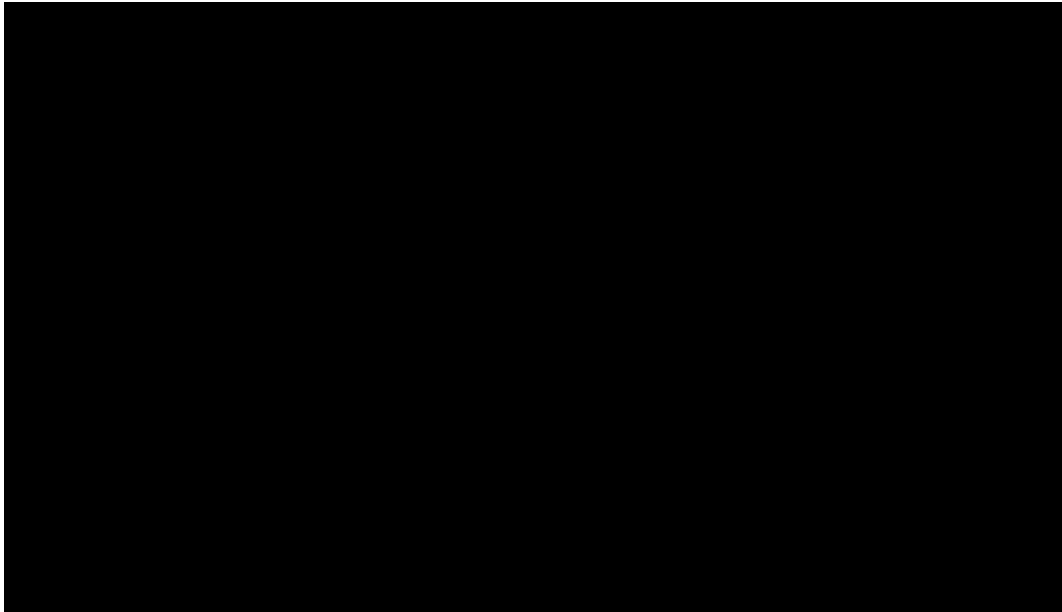
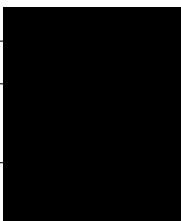


Figure 47. Histogram of Stress Ranges for the Combined Pressure and Temperature Cycles (January 2011 to December 7, 2022)

4.3.4 Stress Concentration Factors (SCFs)

As discussed above, the TAG 98 bend assembly has been subjected to pressure and temperature fluctuations over its operational life. A soil-pipe interaction FEA model was used to determine the stress ranges for fluctuating pressures and temperatures. Two different pressure changes of 500 and 1,000 psig, and two different temperature changes of 40°F (22.2°C) and 80°F (44.4°C) were used in the analysis. Table 10 provides a summary of the loading scenarios and the results of the analysis. The last column of this table ($\Delta\sigma_L$) contains the calculated longitudinal stress ranges at the subject girth-weld (GWD 13530).

Table 10. Loading Scenarios for Pressure and Temperature Stress Range Analysis

Loading Type	ΔP [psig]	ΔT [°F]	$\Delta\sigma_L$ [ksi]
Pressure	500	0	
Pressure	1000	0	
Thermal	0	40 (22.2°C)	
Thermal	0	80 (44.4°C)	

The detailed FEA models were used to estimate SCF for the MP 14 girth weld geometry due to elbow out-of-roundness, wall thickness taper transition, and high-low. Elastic analysis SCFs were used for crack initiation calculations while elastic-plastic analyses were used for crack growth calculations. The SCFs are summarized in Table 11. The elastic SCFs were used with the API 579 stress intensity solution for a part-wall circumferential crack.

Table 11. Stress Concentration Factors

Scenario	SCF
Installed Out-of-Roundness	[REDACTED]
Out-of-Roundness after Cut-Out	
Wall Thickness Taper Transition ⁵⁶	
Overall	

4.3.5 Crack Initiation and Growth Thresholds

The tendency to initiate a fatigue crack is inversely proportional to the radius of a geometric stress concentrating feature. A crack will initiate more quickly from a sharp notch or reentrant corner than from a rounded feature. The LOF at the base of the fatigue crack was not rounded in its condition as found by the metallurgical investigation. An empirical relationship for the initiation threshold is $(\Delta K/\sqrt{\rho})_{th} = 10\sqrt{\sigma_{YS}}$ where ρ is the notch tip radius and values are ksi and inch units.⁵⁷ Substituting an average base metal yield strength of [REDACTED] (from the Anderson report) and the observed notch tip radius 3×10^{-4} inch (based on Figure 27 of this report) results in an initiation threshold stress intensity of $1.0 \text{ ksi}(\text{in})^{0.5}$ which is quite low. A cyclic stress of 6 ksi acting on the 0.008-inch-deep (200 μm) LOF would be sufficient to initiate a fatigue crack, without including the local SCF of 2.3 to 4.015 from the joint geometry.

If the crack tip stress intensity is below a threshold value for growth, the crack will remain stable and will not enlarge by fatigue. The growth threshold varies from approximately 2 to 6 $\text{ksi}(\text{in})^{0.5}$, estimated as $\Delta K_{th} = 6.4(1 - 0.85R)$ where R is the ratio of minimum to maximum fluctuating stress.⁵⁷ Stresses fluctuate so R varies as well. The typical R for pressure loading was estimated as

$$R = \frac{(P_{Mean})_{RMS} - 0.5(\Delta P)_{RMS}}{(P_{Mean})_{RMS} + 0.5(\Delta P)_{RMS}}$$

Applying the annualized RMS P_{mean} and RMS ΔP for the Steele City discharge for the past five years of operation gives $R = [REDACTED]$. The threshold crack tip stress intensity was estimated to be $\Delta K_{th} = 4.6 \text{ ksi}(\text{in})^{0.5}$, approximately. When the applied cyclical crack tip stress intensity is less than this value then the crack is presumed to not extend by fatigue. (Note that environment, microstructure, residual stress, or other factors could affect the threshold.). A similar evaluation was performed using the temperature data for the past five years of operation to estimate $R = [REDACTED]$, resulting in $\Delta K_{th} = 1.6 \text{ ksi}(\text{in})^{0.5}$ for cyclic thermal loading.

⁵⁶ The wall thickness taper transition SCF also includes high-low and taper length.

⁵⁷ Barsom, J.M. and Rolfe, S.T., Fracture and Fatigue Control in Structures, 3rd Edition, 1999.

The cyclic crack tip stress intensity was estimated as $\Delta K_{RMS} = 1.12(SCF)(\Delta\sigma_{RMS})\sqrt{\pi a/Q}$ according to a standard solution. In this expression, $\Delta\sigma_{RMS}$ may represent the cyclical thermal bending stress or the longitudinal component of internal pressure taken as half the hoop stress due to proximity of the elbow. The SCF is the stress concentration factor according to the FEA, the 1.12 factor applies to a surface defect, D is the pipe diameter, t is the wall thickness, a is the crack depth, and Q is a flaw shape parameter approximated by various relationships as 1.0 for the aspect ratio and applied stress in this case.

The pipe-soil structural interaction analyses described in Appendix D determined that the cyclic bending stress due to thermal expansion is approximately [REDACTED]. The cyclic longitudinal stress due to pressure cycles is half the hoop stress, or [REDACTED]. Locally at the initiation point the SCFs from Section 4.3.4 apply ([REDACTED] to [REDACTED] depending on out-of-roundness) but will diminish as the crack enlarges. The fatigue propagation threshold stress as magnified by the SCF, the corresponding event cycle magnitude, and the approximate typical number of annual events of that magnitude or greater are listed in Table 12. The magnitudes and frequency of occurrences of thermal and pressure cycles are sufficient to initiate and propagate a fatigue crack from the LOF features observed in the metallographic sections.

Table 12. Threshold Conditions for Fatigue Crack Propagation

Condition	ΔK_{th} , ksi(in) ^{0.5}	SCF× $\Delta\sigma_{th}$, ksi	SCF = 2.3		SCF = 4.015	
			Cycle size	Annual exceedances	Cycle size	Annual exceedances
Thermal	1.6	9.0	12 °F (6.7°C)	86/yr	6.7 °F (3.7°C)	165/yr
Pressure	4.6	26.0	647 psig (4,460 kPag)	212/yr	370 psig (2,550 kPag)	293/yr

4.3.6 Crack Growth

The crack growth time to failure was estimated using an incremental crack growth rule (the Paris Law) given as $da/dN = C\Delta K^m$ where da/dN represents the increment of crack growth with each load cycle; ΔK is the cyclic stress-intensity at the crack tip which is a function of the cyclic stress, the crack size, and geometry factors that depend on crack aspect ratio and depth; and C and m are material crack-growth parameters. The crack growth is calculated for each stress cycle in sequence until the calculated flaw size is determined to exceed the critical flaw size. There is a threshold for crack tip stress intensity, below which crack growth is negligible. This type of analysis is commonly applied to predicting crack growth times to failure for pipelines (and other structures).

Crack growth assessment was conducted by applying the stress cycles from the pipeline operating loads and using the Paris law to calculate the amount of successive crack growth, following the API 579⁵⁸ procedure for a circumferential crack. The combined pressure and

⁵⁸ API 579-1/ASME FFS-1, "Fitness for Service", 2016.

temperature cyclic stresses (see Section 4.3.3) covering pipeline operation from 2011 to 2022 were enhanced by the elastic SCF magnitude corresponding to the geometry of GWD 13530. Values of [REDACTED] corresponding to the laser-scanner elbow geometry and [REDACTED] corresponding to [REDACTED] ovality as measured by caliper ILI were used. The times to failure were determined starting with an initial flaw depth of 0.008-inch (200 μm) until the flaw reached a final depth that matched the depth determined from the Anderson report (the initial flaw size of 0.008-inch (200 μm) was selected based on the depth of the LOF identified in the Anderson report at the base of the fracture). Using default values for C equal to 8.61×10^{-10} for ΔK in units of $\text{ksi}(\text{in})^{0.5}$ and m equal to 3.0 for steel in nonaggressive environments.⁵⁸ These values produced calculated times to failure that were longer than the observed time to failure when the SCF value of [REDACTED] was used, and shorter than the observed time to failure when the SCF value of [REDACTED] was used. Revising the value of m to [REDACTED] with the SCF value of [REDACTED] resulted in calculated times to failure for the MP 14 transition weld geometry around 12 years. Revising the value of m to [REDACTED] with the SCF value of [REDACTED] resulted in calculated times to failure for the MP 14 transition weld geometry around 12 years.

To show the sensitivity of the calculated crack growth to the Paris Law exponent m , several additional crack growth assessments were conducted using the SCF value of [REDACTED] and the resulting growth was plotted against the exponent in Figure 48.

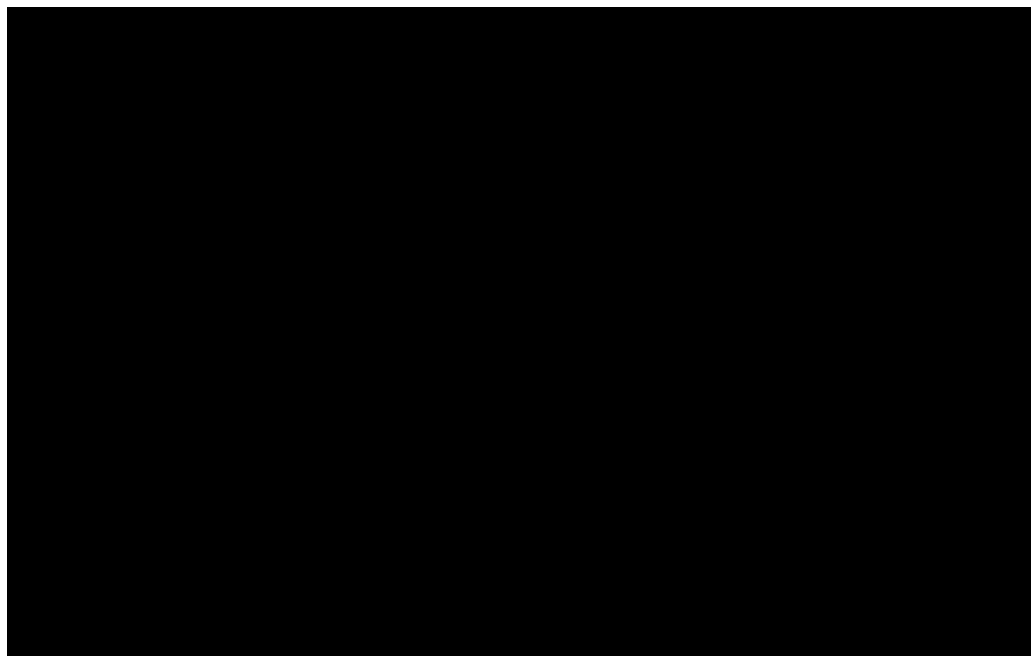
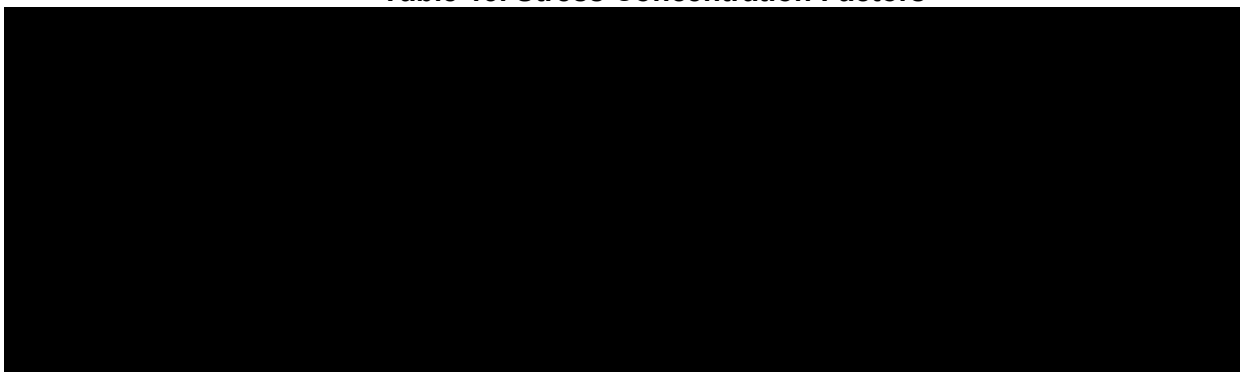


Figure 48. Sensitivity of Crack Growth Relative to the Paris Law exponent

RSI performed further assessment to explore the effect of the SCF values from pipe out-of-roundness and wall-thickness transition to determine if the failure would have happened without either of them occurring (see Table 13). The results of this assessment suggest that the failure could have happened without the pipe out-of-roundness, but it would have taken much longer (i.e. several decades). Conversely, the failure most likely would not have occurred without the presence of the wall-thickness-transition SCF.

Table 13. Stress Concentration Factors

Finally, a fatigue assessment using the S-N resistance method was conducted to determine the effect of the initial LOF that served as the fatigue crack initiation site. The calculations followed the BS 7608 methodology with a fatigue resistance class D curve and the SCF value of [REDACTED] (corresponding to [REDACTED] ovality). The cumulative fatigue damage index was calculated as [REDACTED]⁵⁹, indicating that a fatigue crack would have eventually developed even without the observed LOF, although it would take another decade before failure would occur.

The crack growth mechanism was concluded to be high cycle fatigue, in the absence of definitive proof from the fracture surface, because the analyses were unable to determine sufficient crack growth from known loadings to explain the failure in a low number of cycles.

5 Root Cause Failure Analysis

The loss event was defined as the failure of GWD 13530 (G59B) that resulted in the unintentional release of crude oil to the environment. For a crack to develop in GWD 13530, the applied stresses had to exceed the girth weld strength. For a perfectly sound weld, the stresses must be quite high; however, with the presence of a weld imperfection or defect the required stresses to cause failure are lowered. Several lines of inquiry were evaluated to determine if there were deficiencies in design, manufacturing, fabrication, construction, or operations that led to crack development and growth in GWD 13530. Lines of inquiry were also followed related to integrity assessments not identifying the crack and post-assessments that may have underestimated the risk.

The simplified Cause and Effect Tree shown in Figure 49 and detailed Cause and Effect Trees provided in Appendix B serve as the basis for the conclusions drawn in this report. The evidence that supports the lines of inquiry evaluated during this investigation are provided in the following sections of the report.

⁵⁹ Fatigue failure is defined as the index reaching unity.

For the Cause and Effect Trees, the events are color coded to aid interpretation as follows:

- Gray = Events or steps in event sequence;
- Orange = Inconclusive: causes or causal factors that are neither confirmed nor eliminated by available data or evidence;
- Yellow = Eliminated: causes or causal factors that are eliminated by available data or evidence;
- Purple = Confirmed but not a factor: causes or causal factors that are confirmed as factual but determined to not be causal;
- Light blue = Contributing factor: underlying reasons why a causal factor occurred, but not sufficiently fundamental to be causal.
- Light green = Confirmed: causes or causal factors that are confirmed by available data or evidence;
- Dark green = Root cause: conditions that are confirmed as root causes or near-root causes.

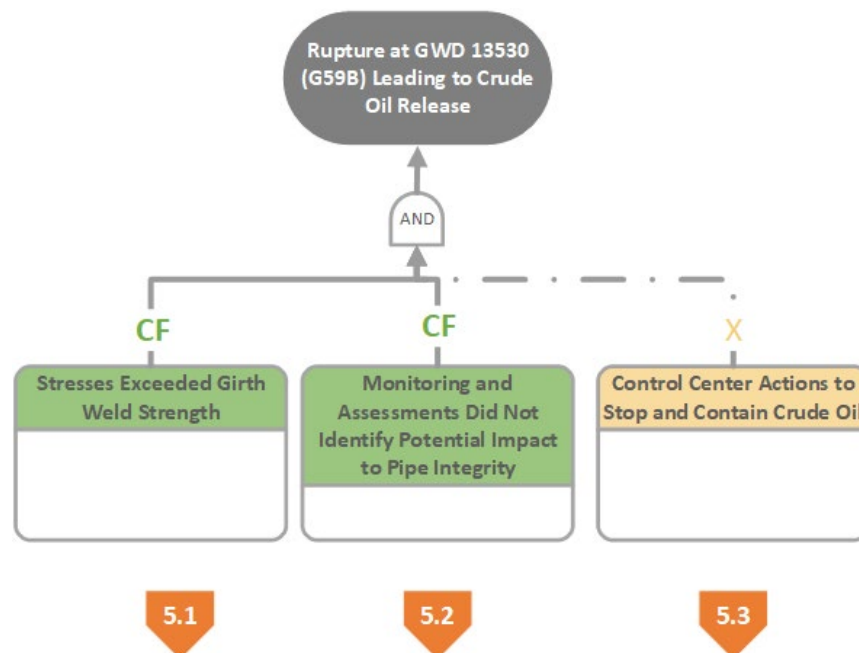


Figure 49. Simplified Cause and Effect Tree – MP 14 Incident

5.1 Stresses Exceeded Girth Weld Strength

Anderson determined that the direct cause of the GWD 13530 (G59B) failure was fatigue (progressive) cracking. The fatigue cracks initiated from a LOF region at the ID toe of the girth weld on the pup side. The circumferential orientation of the cracks suggested a bending stress as the driving mechanism. The fatigue cracks then propagated linearly through the pup side of the weld until the remaining ligament could no longer support the applied load. These findings suggest several possible areas of investigation including the design of the elbow assembly, manufacturing of its components, its fabrication and welding, its installation in the field, and the

Parameter	Design Value

Based on the above design basis values, the maximum temperature differential for the US portion of the buried pipeline is [REDACTED]⁶¹. The stated ultimate system design capacity, which includes the Cushing Extension expansion phase is 104,400 m³/day (656,000 BPD). The design conditions included the assumption that no chemical drag reducing agents (DRA) will be added. Per the DBM, the original design factor for the US portion was 0.72 but the document also mentions that Keystone was applying for a waiver from PHMSA for operation at a design factor of 0.80. Section 7.2.2.2 of the DBM states that “[REDACTED] [REDACTED] As an item of note, no updates were ever applied to the DBM after the PHMSA design factor waiver was granted nor after the capacity increase projects went into effect. Though it was determined not to be causal to this incident, having a master design basis document that is updated to reflect changes that have been made to key design parameters (design factor, flow capacity, use of drag reducing agents, etc.) is beneficial for future process hazard analysis (PHA), risk analysis, and management of change (MOC) activities.

In addition, a stress analysis for the construction spread containing the affected segment (Spread 9C) was completed in May 2010. The analysis evaluated stresses during construction, commissioning, and operating phases in support of using alternative acceptance criteria in Appendix A of API 1104 for mechanized welding. This analysis identified that the highest stresses occurred during lowering-in of concrete coated piping. The highest stresses during operation were from curvature in the pipeline with an overburden of six feet operating at the MOP. The stress analysis considered thermal stress but only in terms of the maximum assumed thermal differential of [REDACTED] between [REDACTED] construction [REDACTED] and product temperatures [REDACTED]. This thermal differential assumption is lower than what the TAG 98 bend assembly had experienced in operation⁶².

Shown in Figure 51, the elbow used in the bend assembly was designed in accordance with the DBM, TES-FITG-LD-US, Rev 0 and MSS SP-75-2008 (see Figure 51). Review of the material

⁶¹ The maximum oil flowing temperature of [REDACTED] minus the below grade temperature of [REDACTED].
⁶² TAG 98 was replaced in the winter with temperatures below freezing. The temperature when the final tie-in weld was made on the south side of Mill Creek was [REDACTED]. The maximum product temperature recorded at the Steele City discharge (STLCB_B0_TMLD) was 1 [REDACTED]. Therefore, the maximum temperature differential was closer to [REDACTED].

test report (MTR)⁶³ and quality surveillance documentation⁶⁴ confirmed that the elbow met the requirements for weldability, pressure rating, materials, chemical composition, tensile properties, bend tests, CVN toughness, fitting dimensions at the ends, and welding tolerances included in the specifications. The MTR for the pipe pup also confirmed that it met the requirements for pressure rating, materials, chemical composition, tensile properties, CVN toughness, and dimensional tolerances.

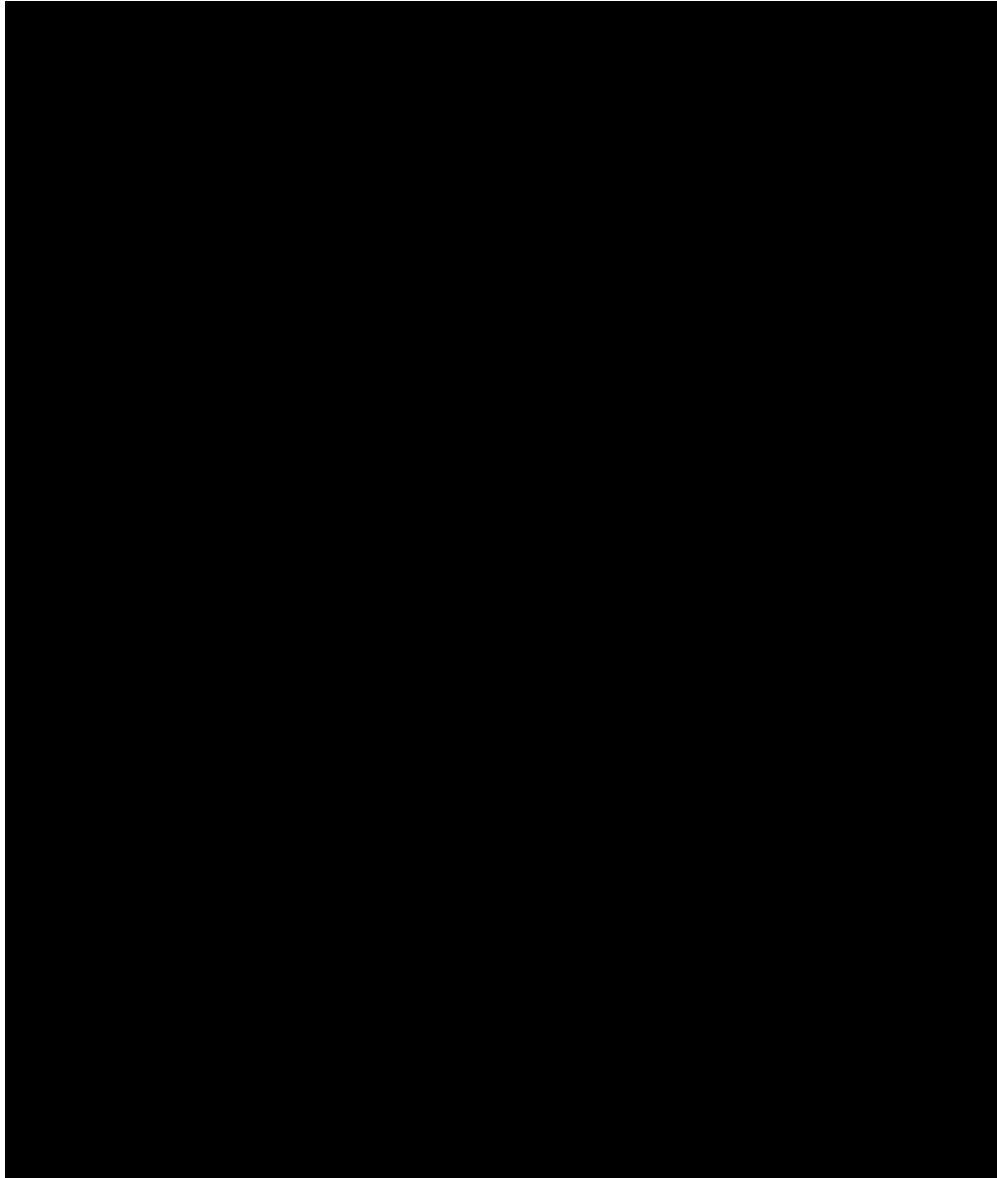


Figure 51. TAG 98 As Built Drawing Showing Design Requirements and Bevel Details

⁶³ [REDACTED], Material Test Report for Heat NOP-C, Piece Number 174469, Certificate Number 6235, November 15, 2010.

⁶⁴ Form SQ-221, Quality Surveillance Report for Keystone Pipeline Replacement Fittings, QSR Number 25472-100-YQA-PV04-1D005, Rev 1, November 12 and 15, 2010.

Along the KS10 segment there are 1 elbow fittings. The design choice of a 3D⁶⁵ elbow for the overbend section (TAG 98) was acceptable per the DBM requirements, and the TAG 98 bend assembly remained within the design guidelines. Wrought or forged elbows manufactured to meet MSS SP-75 are accepted components for use in 49 CFR Part 195 and ASME B31.4.

The selection of the tighter 3D bend radius was likely necessary to accommodate the terrain changes at the Mill Creek crossing. As discussed in the joint industry project (JIP) Guidance for Field Segmentation and Welding of Induction Bends and Elbows⁶⁶, “segmented induction bends and elbows are located at points of inflection, or at changes in topography, which tend to be more susceptible to high stresses from bending loads caused by pipeline movement due to soil settlement. The use of segmented induction bends and elbows often involves transition welds between dissimilar wall thickness materials, which tend to concentrate stresses due to bending. The use of segmented induction bends and elbows often involves the need to cope with high-low misalignment because of out-of-roundness and/or diameter shrinkage of the segmented fitting, which also tend to concentrate stresses due to bending.”

RSI considered whether the selection of a 3D elbow over a larger radius bend could have contributed to the bending stresses experienced by TAG 98 (BND 350). The larger associated bend radius has two effects; (1) the tangent points of the arc, where the girth welds are located, move further away from the vertex thus reducing the bending moment; and (2) it spreads the thrust forces from thermal expansion and contraction over a larger area. However, according to interview statements, the larger bend radius⁶⁷ forged fittings for a 36-inch OD pipe were not practical considering the width of the permitted construction workspace (permanent and temporary) along the right-of-way (ROW) at a water crossing. Additionally, the engineering team did not feel that they could achieve the needed material consistency from heat treatment with induction bends.

Absent the weld flaw and bending moment applied during construction, the 3D elbow was an acceptable choice. Yet, a larger radius induction bend (such as 5D, 7.5D or 10D) would have significantly reduced the stress at GWD 13530 and extended its fatigue life, if it could have been practically used at the Mill Creek location. Estimates of the effect of bend radius on the SCF and fatigue life are shown in Table 15.

⁶⁵ A 3D elbow is defined as a bend in which the bend radius is three times the pipe diameter.

⁶⁶ DNV, Phase 2 Final Report, Guidance for Field Segmentation and Welding of Induction Bends and Elbows for JIP on Welding of Field Segmented Induction Bends and Elbows for Pipeline Construction, December 6, 2011.

⁶⁷ The DBM

Table 15. Net Effects from Moving Girth Welds Farther from the Bend Vertex and the Reduced Thrust Force⁶⁸

Bend Radius (R/D)	Impact A: Girth Welds Further from Bend Vertex		Impact B: Thermal Expansion Thrust Force Reduction			Net Result
	Bending Moment Ratio C_x/C_{x_3}	Fatigue Life Ratio NF1	Thrust Force Ratio $(D/R)^{0.637}$	Stress Concentration Factor Ratio SCF/SCF_3	Fatigue Life Ratio NF2	Fatigue Life Ratio NF_Net (NF1 x NF2)
3D	1.000	1.000	0.496	1.000	1.000	1.0
5D	0.934	1.228	0.359	0.722	2.654	3.3
7.5D	0.854	1.604	0.277	0.558	5.761	9.2
10D	0.778	2.122	0.231	0.464	9.982	21.2

Compared to a 3D elbow, a 5D induction bend would reduce the SCF to a factor of 0.72 and larger radius induction bends (7.5D or 10D) would reduce the SCF to about 0.60 and 0.47, respectively for thrust forces from thermal expansion (Impact B). Since the fatigue life is a function of $(\Delta\text{Stress})^{-n}$ with $n = 3$ (approximately), the fatigue life from thermal expansion (NF2) would be increased by a factor of approximately six to ten with a 7.5D- or 10D-radius bend, respectively.

A secondary benefit of a larger-radius bend is that, for a given angle or direction change (e.g., 30 degrees), the girth welds are moved farther out from the apex of the bend, with some reduction of the bending stress at the position of the welds (Impact A). An approximation for this effect was made considering the pipe to be a beam on elastic foundation represented by medium-stiffness soil, with the thrust force from thermal expansion or end-cap pressure acting as a concentrated load at the bend apex^{69,70}. So, having the girth welds positioned farther from the bend apex could approximately double the fatigue life (NF1) with an induction bend having R/D between 7.5 and 10.0, compared with the elbow.

⁶⁸ Rosenfeld, M.J., Hart, J.D., and Zulficar, N., "Acceptance Criteria for Mild Ripples in Pipeline Field Bends", Pipeline Research Council International, Inc., PR-218-9925, Catalog No. L51994, August 2008.⁶⁹ The distribution of bending moment with increasing normalized distance x from the bend apex varies as $C(x) = e^{-x}(\cos x - \sin x)$. In this expression, $x = s/\lambda$ with s being the actual position of the weld, taken as half the subtended arc length of the bend, and λ is the characteristic of the beam-on-soil system, $\lambda = [k_{\text{soil}}/(4EI)]^{0.25}$. For a medium-stiffness soil having $k=2,000$ psf and moment of inertia for the nominal pipe, $\lambda=0.0017$ in.⁻¹. The term $C(x)$ represents the bending moment at the girth weld relative to the maximum bending moment at the bend apex. The term $C(x)/C(x)_{\text{Elbow}}$ is the bending moment at the girth weld in a bend having the R/D as listed relative to that of the elbow.

⁶⁹ The distribution of bending moment with increasing normalized distance x from the bend apex varies as $C(x) = e^{-x}(\cos x - \sin x)$. In this expression, $x = s/\lambda$ with s being the actual position of the weld, taken as half the subtended arc length of the bend, and λ is the characteristic of the beam-on-soil system, $\lambda = [k_{\text{soil}}/(4EI)]^{0.25}$. For a medium-stiffness soil having $k=2,000$ psf and moment of inertia for the nominal pipe, $\lambda=0.0017$ in.⁻¹. The term $C(x)$ represents the bending moment at the girth weld relative to the maximum bending moment at the bend apex. The term $C(x)/C(x)_{\text{Elbow}}$ is the bending moment at the girth weld in a bend having the R/D as listed relative to that of the elbow.

⁷⁰ The reduction in bending stress moving away from the bend vertex, as well as the reduction in bending stress with using a larger-radius bend have been confirmed by more detailed analyses, for example "Longitudinal Stress in Buried Pipelines Near Bends or End Caps", Zhang, F. and Rosenfeld, M., The Journal of Pipeline Engineering, June 2018.

The combined effect of the thrust force reduction and bending stress reduction would extend the fatigue life by a factor of 3.3 for a 5D induction bend. For larger radius induction bends the expected net increase in the fatigue life would be significantly more: 9x for 7.5D and 21x for 10D.

5.1.1.2 Transition Weld Joint Design

The TAG 98 (BND 350) elbow was manufactured in accordance with TransCanada's specification TES-FITG-LD-US, Rev 0 (2007) and MSS SP-75-2008 for grade WPHY 70 materials. According to these specifications, [REDACTED]

[REDACTED]. Figure 53 shows the as-built bevel details for the TAG 98 elbow. The transition joint design followed US industry standards, including ASME B31.4, ASME B31.3, ASME B16.25, and MSS SP-75 as well as Company specifications and recommendations from the JIP on Guidance for Field Segmentation and Welding of Induction Bends and Elbows⁷¹. It appears, however, that the taper transition length of approximately 0.78-inch in the metallographic section prepared through GWD 13530 at Crack 2 (see Figure 54) is less than the minimum requirement of 1.00-inch from Figure 3 of MSS SP-75-2008 (see Figure 52). The shorter transition length can increase stress concentrations in the girth weld.

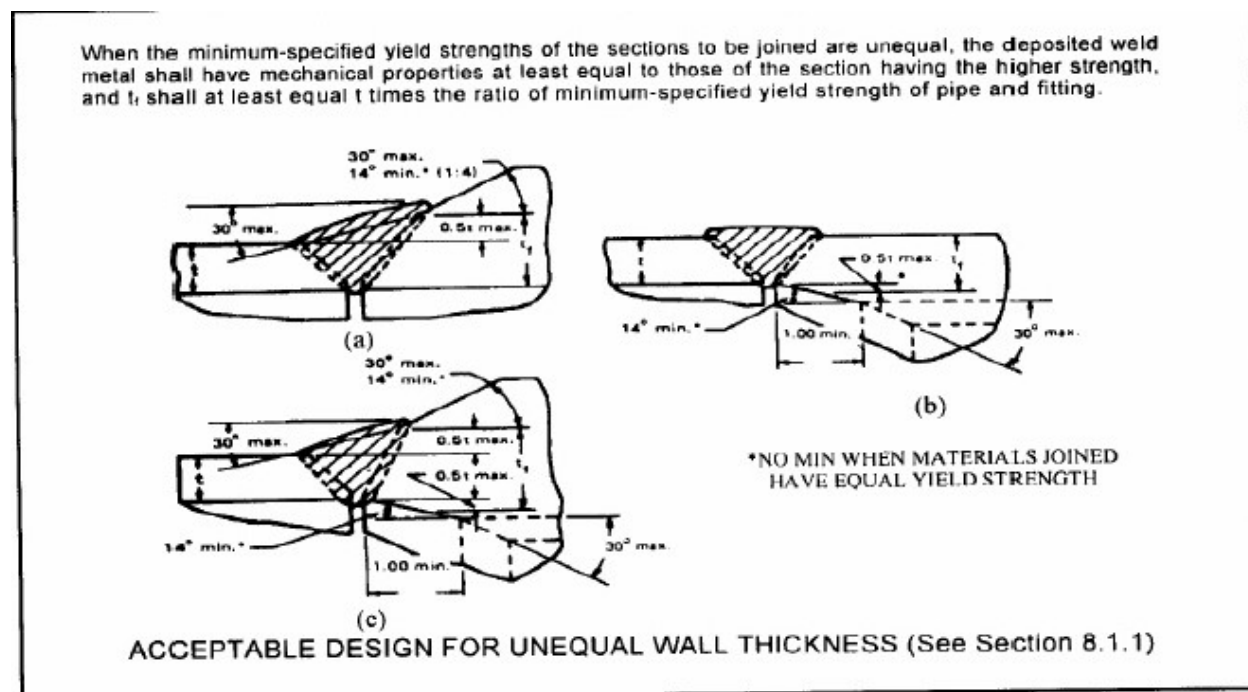


Figure 52. Acceptable Design for Unequal Wall Thickness (MSS SP-75, Figure 3)

⁷¹ JIP final Summary Report, Enhanced Girth Weld Performance for Newly Constructed Grade X70 Pipelines, May 29, 2020.

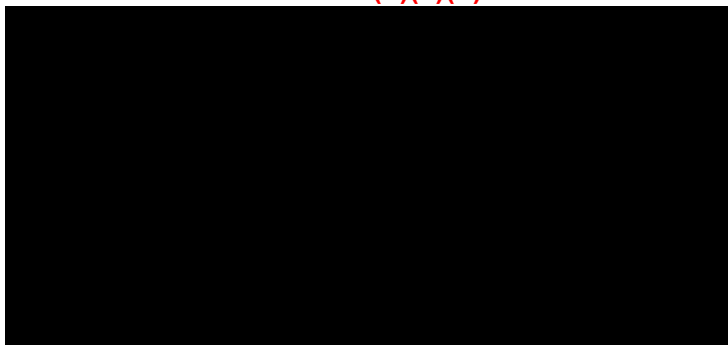


Figure 53. As-Built Bevel Details for the TAG 98 Butt Weld

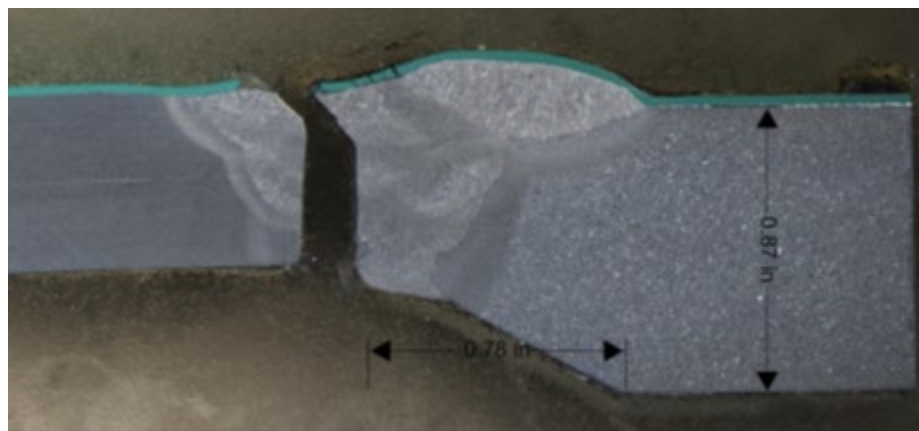


Figure 54. As-Fabricated Bevel Length for the TAG 98 Butt Weld Joint at Crack 2

According to TC Oil's specification for welding of assemblies at the time of fabrication, TES-WELD-AS-US, Rev 1, butt welds between items of unequal wall thickness must be made using a transition designed in accordance with TEP-MECH-TRAN-US⁷², which for fittings [REDACTED] the [REDACTED] of a [REDACTED]⁷³. Moreover, Section 8.20 of TES-WELD-AS-US states that the [REDACTED]

[REDACTED]. According to interview statements, analyses were not performed to understand the SCF for pup-to-elbow fitting welds. EAs were performed for mainline pipe transition welds and guidance was provided regarding SCFs for different butt weld joint configurations (taper versus counterbore and tapered) but similar analyses were not performed for fitting-to-pup butt weld configurations because the design followed US industry standards.

⁷² TEP-MECH-TRAN-US, Selection of Transition Pieces and Joining Methods, Rev 0, October 15, 2009.

⁷³ The current version of TEP-MECH-TRAN-US r [REDACTED]

In the case of TAG 98, both conditions were met. In addition, [REDACTED]

[REDACTED] will not adversely affect the structural integrity of the pipeline.

As seen in the bevel details and joint design images, the pup-elbow joints were designed with a taper transition joint. As discussed in the Freeman +4 RCFA report⁷⁴, taper transitions for unequal wall thickness joints can result in higher stresses over a counterbore and taper design. This thought is echoed in the JIP for enhanced girth weld performance for newly constructed Grade X70 pipelines which recommends that transition welds between pipes of the same grade but different wall thicknesses be made using pipe that is counterbored which eliminates the SCF due to wall thickness differences on either side of the girth weld. Though the use of taper transitions is acceptable per 49 CFR 195, ASME B31.4, and MSS SP-75-2008 weld imperfections and bending loads can lead to increased stress in the joint. And much like the use of larger radius induction bends, a counterbore and taper transition⁷⁵ would have significantly reduced the stress at GWD 13530 and extended its fatigue life by an order of magnitude as shown in Table 16.

Table 16. Crack Growth Over the Operational Life (12-years) for Various Designs

Crack Depth	Baseline (MP 14 Geometry)	Counterbore and Taper (no WT transition)	5D Bend	7.5D Bend	10D Bend
Stress Reduction Ratio	1.00	0.48	0.72	0.56	0.46
Initial crack depth, a ₀ [in]	0.008	0.008	0.008	0.008	0.008
Final crack depth, a [in]	0.500	0.009	0.015	0.010	0.009
Final crack depth, a [%WT]	93%	1.7%	2.8%	1.9%	1.7%

Adding to the stress at the taper joint was the fact that the elbow wall thickness was higher than the minimum acceptable plate thickness for manufacturing (starting plate thickness of [REDACTED] per the MTR). The range of acceptable plate thicknesses was from 0.644-inch to 1.125-inch⁷⁶ per the as-built drawing in Figure 51. The thicker the elbow in comparison to the pup, the greater the stress concentrating effect at the thinner wall side of the taper transition joint. The weld joint SCF (calculated as described in Appendix D) varies as shown in Figure 55, with the actual configuration circled.

In hindsight, it is easy to question a design choice without knowing all the variables that went into that decision. Both 3D elbows and taper transition joints are acceptable design choices per codes and standards with the caveat that the implications of these choices on the potential pipeline stresses should be well understood and managed. The combination of the taper transition joint, 3D elbow, and large, applied bending stress during construction (see Section 5.1.4) were determined to be causal to this incident, in that they all added to the stress concentrations in GWD 13530 and accelerated its time to failure.

⁷⁴ Kiefner and Associates, Inc, Root Cause Failure Analysis of Transition Girth Weld 4B-CTT-1 Leak at Freeman +4, September 6, 2016.

⁷⁵ A counterbore an taper transition design could have been achieved with an induction bend but not an elbow fitting (0.50 design factor for fabricated assemblies) unless heavy wall pups with matching wall thickness to the elbow starting plate thickness were used.

⁷⁶ The design drawing for fabrication at [REDACTED] states a starting plate thickness of 0.644-inch to 0.875-inch as shown in Figure 46. It is unclear why the maximum plate thickness is different between the two documents.

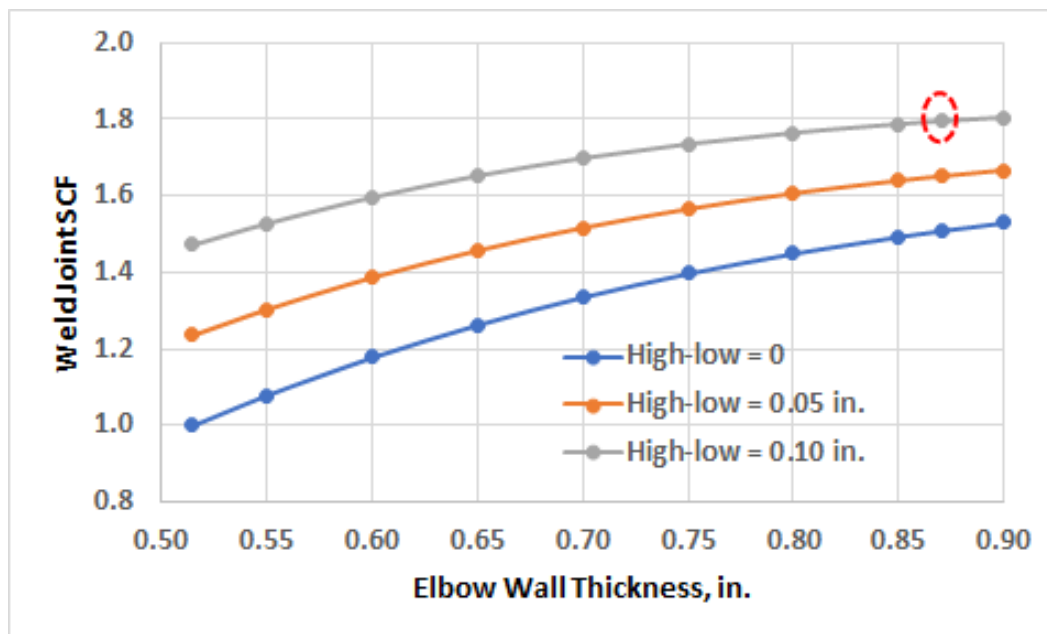


Figure 55. Local Weld Joint SCF, Effect of Elbow Wall Thickness and High-Low

5.1.1.3 Causal Factors, Root Causes, Contributing Factors, and Items of Note – Design

At no time during the twelve years of operation have the operating conditions along the Cushing Extension exceeded the pressure or temperature design limits. Although the flow rates have exceeded the original system design capacity⁷⁷, extensive stress analyses, hydraulic modelling, and engineering assessments (EA) were completed prior to the capacity increases to ensure that the pressure and temperature limits remained within the pipeline's design basis and that operating stress levels remained within acceptable limits. The effect of the increased flow rate is accounted for in the temperature spectra used in the fatigue analyses (see Section 4.3) which contributed to the time to failure.

The selection of the 3D elbow with a taper transition joint (in compliance with ASME B31.4) for the TAG 98 bend assembly was determined to be causal to this incident, in that these acceptable design choices led to high stress concentrations in GWD 13530 (CF1). Without any one of these factors, the failure would not have occurred in the timeframe in which it did. The associated root cause is that Company standards, policies, and administrative controls (SPAC) for the design of bend assemblies did not effectively address the impacts of added stress at the girth weld from the use of 3D elbows and taper transition joints under real-world conditions like the joint's susceptibility to accidental construction loads, weld imperfections, or cyclic operational loads (RC1). In addition, the taper transition length was shorter than the minimum specified in MSS SP-75-2008 which also increased the stress concentration in the girth weld (CTF1)

⁷⁷ The DBM stated a system design capacity of [REDACTED]. Around 2016 the system capacity was increased to [REDACTED] and shortly before the incident TC Oil was performing a ramp test to determine the feasibility of increasing the system capacity to [REDACTED].

Two items of note were also identified. The first is that the DBM was never updated once the PHMSA waiver was granted nor when the capacity increase projects went into effect. The DBM was intended as a 'living document' but no updates were made after the original draft document was published (ION1). Having a master design basis document that is updated to reflect changes that have been made to key design parameters (design factor, flow capacity, use of drag reducing agents, etc.) is beneficial for future PHA, risk analysis, and management of change (MOC) activities.

The second item of note is that although the DBM states that a stress analysis shall be conducted on all high-pressure piping to ensure that overstress and pipe movement does not cause concerns, it was only in relation to facilities. A similar requirement was not contained within the pipeline design basis section, though stress analyses were performed to identify construction, commissioning, and operational stresses along the Cushing Extension. The lack of detail on what should be considered in a pipeline stress analysis during design can result in analysis gaps (ION2).

Table 17. Summary of Causal Factors and Root Causes – Design

Effect	Causal Factors	Root Causes
Elbow Assembly Design Enhanced SCFs at GWD 13530	CF1: The selection of a 3D elbow with a taper transition (in compliance with ASME B31.4) for the TAG 98 elbow-pup joint led to high stress concentrations in the girth weld.	RC1: Gaps in SPAC for design of bend assemblies did not effectively address the impacts of added stress at the girth weld from the use of 3D radius elbows and taper transition joints under real-world conditions like the joint's susceptibility to accidental construction loads, weld imperfections, or cyclic operational loads.

Table 18. Summary of Contributing Factors – Design

Effect	Contributing Factors
Taper Transition Length	CTF1: The taper transition length on the TAG 98 (BND 350) elbow was less than the 1.00-inch minimum requirement in Figure 3 of MSS SP-75-2008 which can enhance stress concentration in the girth weld.

Table 19. Summary of Items of Note – Design

Effect	Items of Note
Design Basis Memorandum (DBM) not Kept Current	ION1: The DBM was intended as a 'living document' but no updates were made after the original draft document was published.
[REDACTED]	ION2: Though the DBM states [REDACTED]

5.1.2 TAG 98 (BND 350) Bend Assembly Manufacture

The replacement elbow fittings were manufactured by [REDACTED] in Becancour, Quebec and associated replacement pups were manufactured by [REDACTED] in Milan, Italy. To offset the potential for off-specification materials leaving the manufacturer, a quality management system (QMS) was in place that included visual inspections, NDE, and mechanical testing to ensure the components met applicable industry standards and internal Company specifications. In addition, TC Oil had surveillance personnel on site to witness specific quality activities and to confirm that procedures and specifications were being followed. Extra scrutiny was placed on the manufacture of the elbow fittings at [REDACTED], including increased number and frequency of inspections and mechanical testing, due to the previously identified manufacturing issues at their Asia facility.

5.1.2.1 Elbow Manufacture

The TAG 98 (BND 350) elbow was manufactured in accordance with TransCanada's specification TES-FITG-LD-US, Rev 0 (2007) and MSS SP-75-2008 for grade WPHY 70 materials. The MSS SP-75-2008 fitting specification is a widely accepted document and the Company-specific specification for fittings was more stringent in areas related to weld tension retesting requirements and CVN test temperatures ([REDACTED] rather than 20°F). The elbow also complied with Special Permit (SP) Conditions 13⁷⁸ and 14⁷⁹.

Interview statements confirmed that extra measures were taken to ensure that the newly fabricated fittings met design and quality specifications, including extra temperature monitoring on each fitting, testing of furnaces, temperature measurement in quench tanks, increased frequency of mechanical testing, and increased inspections and surveillance. In addition, [REDACTED] Quebec facility was ISO 9001 and ANSI/ISO/ASQ Q9001 certified for the manufacture of carbon steel fittings which aligns with requirements in Section 1.5 of TES-FITG-LD-US that the manufacturer must have a documented Quality Program that is registered with an independent registrar.

The material properties listed in the MTR⁸⁰ confirm that the elbow met the MSS SP-75-2008, TES-FITG-LD-US, Rev 0, and the Special Permit requirements for chemistry, tensile properties, toughness properties, hardness properties, and dimensional checks which was also confirmed by Anderson post-incident. The microstructure of the elbow was consistent with low-alloy steels that had been quenched and tempered. According to the MTR, elbow number 174469 (heat NOP-C) was quenched and tempered to [REDACTED] for [REDACTED] minutes and air cooled. However, the actual tempering time for the elbow did not comply with MSS SP-75-2008. Per Section 9.1.3, fittings shall be tempered by "reheating to a temperature below the transformation range, but not

⁷⁸ Condition 13, certification records of factory induction bends and/or factory weld bends must be obtained and retained. In addition, all bends, flanges, and fittings must have carbon equivalent (CE) equal to or below 0.42 or a pre-heat procedure must be applied prior to welding CE above 0.42. The WPS required a minimum preheat temperature of 50°F and maximum interpass temperature of 500°F. Welding inspection documentation was never located for the TAG 98 (BND 350) bend assembly to confirm the preheat temperature but it is reasonable to assume that pre-heating was applied prior to welding per the WPS and PQR.

⁷⁹ Condition 14, all pressure rated fittings and components must be rated for a pressure rating commensurate with the MOP of the pipeline.

⁸⁰ [REDACTED], Material Test Report, Heat NOP-C, Piece Number 174469, November 15, 2010.

less than 1000°F, held at temperature for a minimum of one hour per inch of maximum thickness, but not less than one-half hour and cooled in the furnace or in air.” As confirmed by Anderson, the maximum wall thickness of the elbow was [REDACTED] which would have required a minimum of 54-minutes at temperature to meet the requirements of Section 9.1.3 of MSS SP-75-2008.

In September 2011, an audit⁸¹ was conducted for the large diameter, high grade fittings produced at the [REDACTED] Becancour facility. There were two major findings (1) the tempering duration for fittings greater than 0.500-inch in thickness was shorter than that required by MSS SP-75-2008; and (2) annual surveys of the austenizing furnace were not being conducted by the manufacturer. Nonconformance reports (NCRs) were issued, and corrective actions were put in place immediately by the manufacturer to re-temper and re-test 24 fittings that were not in compliance with specifications, to increase tempering times to meet specifications, and to complete annual furnace surveys. Though these audit findings were after completion of the Cushing Extension, [REDACTED] did study the effects of tempering time on the mechanical properties of grade X70 heat treated steel with four different plate thicknesses ranging from 0.625-inch to 1.500-inch and concluded that the mechanical properties for fittings using a tempering time of 30-minutes do not differ significantly from fittings that comply with the longer tempering time requirements in the specifications. This finding was subsequently confirmed by review of the MTR and the post-incident mechanical testing conducted by Anderson in which the mechanical properties (strength⁸² and toughness⁸³) of the elbow met requirements for grade WPHY-70 materials.

5.1.2.1.1 Fitting Quality Inspections and Testing

As shown in Figure 56, [REDACTED] performed dimensional checks of the ID, wall thickness, and bevel angle at both ends as well as hardness measurements of the elbow. [REDACTED] also performed radiographic testing (RT) of the longitudinal seam weld (see Figure 57). All inspections and tests met MSS SP-75-2008 and TES-FITG-LD-US, Rev 0 specifications⁸⁴ (measurements for out-of-roundness⁸⁵ throughout the body of the elbow were not uncovered during the investigation). According to MSS SP-75-2008, the out-of-roundness tolerance for the NPS 36 elbow was [REDACTED] and per TES-FITG-LD-US, the minimum ID at any

⁸¹ Final Auditing Report: Auditing Production of Large Diameter High Grade Fittings at Canadoil Forge Becancour Quebec Facility, KXL Pipeline Project (PO 25472), October 11, 2012. Note, this audit was performed after the Phase 2 Cushing Extension was complete and in operation.

⁸² Per MSS SP-75-2008 and TES-FITG-LD-US, Rev 0 the minimum yield strength requirement for WPHY-70 material is 70 ksi and minimum tensile strength requirement is 82 ksi. The actual yield strength of the elbow was 93 ksi and the actual tensile strength of the elbow was 114.2 ksi.

⁸³ Per TEST-FITG-LD-US, Rev 0, the CVN absorbed energy values for the parent and weld metal shall be a minimum of [REDACTED]. Per the metallurgical analysis report, the average CVN absorbed energy value for the elbow was [REDACTED]. Per the MTR, for heat NOP-C the average CVN absorbed energy value for the body was [REDACTED] and [REDACTED] for the seam weld at [REDACTED].

⁸⁴ Per MSS SP-75-2008 Table 3 the ID at the end of the fitting shall be +/-0.09-inch and out of roundness tolerances shall be 1% of the diameter (0.36-inch) at the ends and 2.5% (0.90-inch) throughout the body of the elbow. Per Section 13.5 of TES-FITG-LD-US, the minimum ID at any location in a 3D elbow must be at least [REDACTED] of the nominal OD of the matching pipe. The maximum out-of-roundness was [REDACTED] at End A and minimum WT at the bevel End B was [REDACTED] with a bevel angle of [REDACTED] at both ends.

⁸⁵ According to MSS SP-75-2008, Table 3 “Out-of-roundness tolerances shall be the difference between the maximum and minimum diameters measured on any radial cross-section.”

location in a 3D elbow must be at least [REDACTED] of the nominal OD of the matching pipe. As discussed in Section 2.7, a [REDACTED] ID restriction was discovered during the 2012 profile caliper ILI within the TAG 98 bend assembly. Although during manufacturing out-of-roundness measurements appear to have only been taken at the ends, the field investigation in 2013 demonstrated that the ovality extended from the elbow into the attached pups both upstream and downstream, and therefore it is unlikely that the ovality was present because of manufacturing issues.

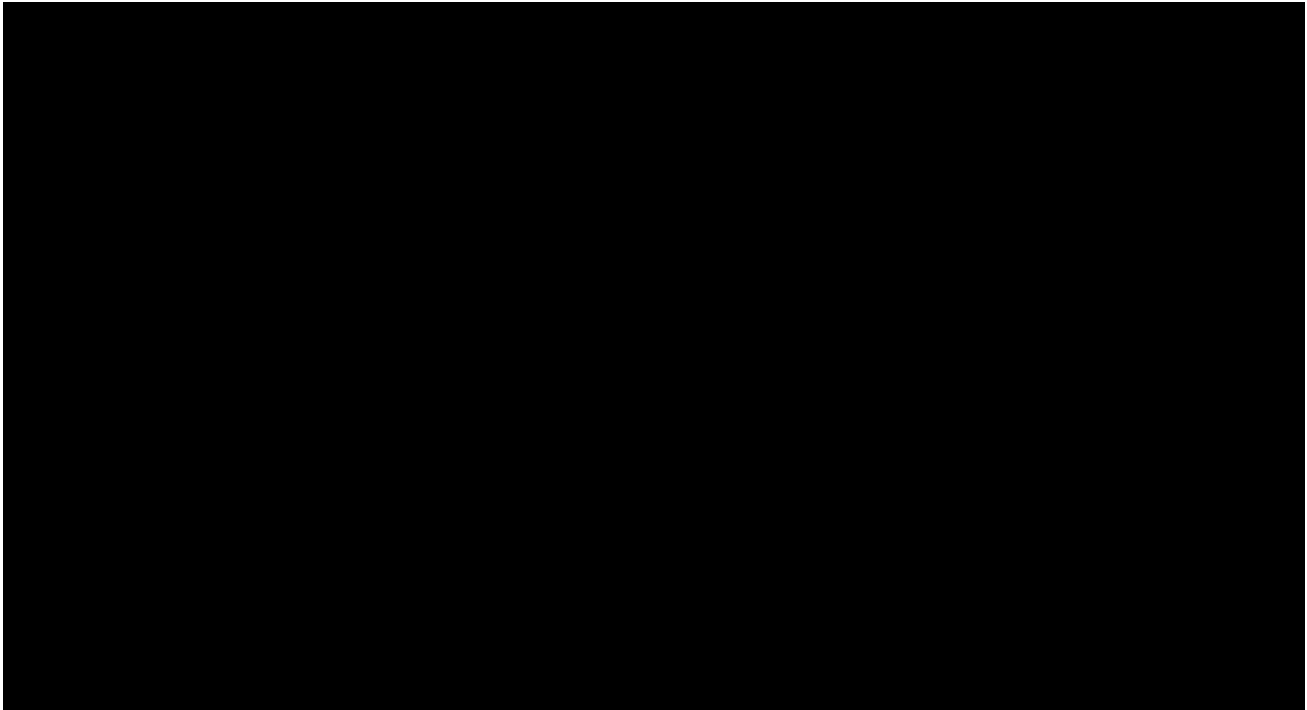


Figure 56. Fittings Dimensional Inspection and Brinell Hardness Test Report Highlighting TAG 98 Elbow (Item # 174469)

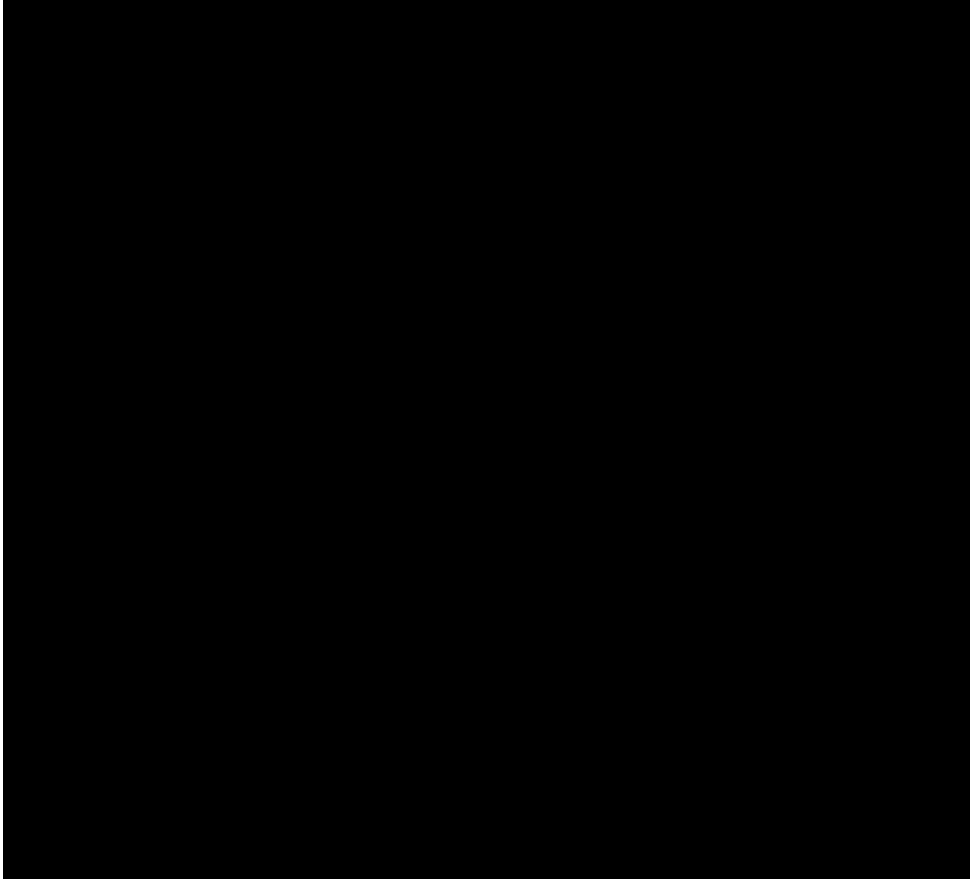


Figure 57. Seam Weld Radiographic Examination of TAG 98 Elbow (Item # 174469)

5.1.2.1.2 Fitting Quality Surveillance

A third-party engineering firm provided surveillance for TC Oil at the fitting manufacturer. As required by the PO, an inspection and test plan (ITP) was developed for the manufacture of the elbows. The ITP covered inspections of incoming plate material, cutting, identification and traceability, forming, assembling, welding, heat treatment, cleaning, radiographic inspections, chemical and mechanical testing, beveling, dimensional and visual inspections, stamping, and final third-party inspections.

A third-party inspection representative traveled to the [REDACTED] facility in Becancour, Quebec on November 12 and 15, 2010 to conduct final quality surveillance on items completed against the PO and to report the findings. A total of [REDACTED] elbows were examined, including elbow 174469 (TAG 98) which was examined on November 15, 2010⁸⁶. A visual examination of the elbows was performed to identify linear defects. All elbows were found to be free of loose mill scale, foreign matter, oil, and grease and were clean and dry on both the inside and outside. The formed sections were noted to be smooth, true to plane and profile, free of creases and without dents, flat spots, or burrs; no injurious surface defects were noted.

⁸⁶ Form SQ-221, Quality Surveillance Report, Keystone Pipeline Replacement Fittings for 25350-100-POA-PF01-U1001, November 12, 15, 2010.

Welding of the longitudinal seam was carried out by semi-automated media and certified welders (recently tested and approved) meeting the TES-FITG-LD-US, Rev 0 specification requirements. Welding was verified for appearance and size and was found to correspond to standard procedures. Hardness testing was carried out on each fitting and found to comply with TES-FITG-LD-US. Radiographic inspection of the longitudinal seam weld was performed by [REDACTED] and the film was reviewed and accepted. The third-party inspector also verified that the end dimensions and bevel angles complied with specifications. Fittings were loaded on a flatbed truck for shipment to the fabricator RCT. No manufacturing quality-related issues were noted for the TAG 98 elbow.

5.1.2.2 Pup Manufacture

The pup for the TAG 98 (BND 350) elbow assembly was manufactured in accordance with API 5L 44th Edition (2007), TES-PIPE-SAW-US, Rev 1, and manufacturing-related conditions in the Special Permit. The API 5L specification is a widely accepted standard for the manufacture of line pipe and the TC Oil specification is in alignment with API 5L requirements with more stringent requirements in certain areas such as carbon equivalents and material toughness. [REDACTED] maintained a certified QMS that met ISO 9001:2008, ISO/TS 16949, ISO 14001, and OHSAS 18001 to ensure that materials and manufacturing practices met the specification requirements.

The pipe (pipe number 031378) used for the pups was a [REDACTED] ft length of pipe tested to 1,890 psig (94% SMYS) for 10 seconds at the mill. [REDACTED] generated an MTR for the pipe that demonstrates compliance with API 5L, 44th Edition, TES-PIPE-SAW-US, Rev 1, and the Special Permit for chemistry, tensile strength, yield strength, toughness, hardness, and dimensional checks. Post incident, Anderson confirmed that the pups complied with specifications. As discussed in the Anderson metallurgical analysis report, “there was no evidence found to support a finding that the pipe material was deficient. The microstructure of the pups consisted of finely banded, fine-grained ferrite and pearlite, typical of a low carbon, microalloyed steel used to fabricate high strength line pipe. The weld microstructure appeared sound and free from any internal defects such as porosity or slag inclusions. The mechanical properties and chemical composition of the pipe met the minimum specifications for API 5L grade X70 PSL 2, though there is evidence that some of the HAZ hardness exceeded the maximum set forth for grade X70.”

5.1.2.3 Item of Note - Manufacturing

No causal factors were identified related to manufacturing of the TAG 98 bend assembly. Anderson did not find any evidence that the pipe, elbow, or weld materials were deficient. As discussed in Section 4.1, the microstructure of the pups was consistent with low carbon, microalloyed steel used to fabricate high strength line pipe. The microstructure of the elbow was consistent with low-alloy steels that had been quenched and tempered. The bulk weld microstructure appeared sound. The mechanical properties and chemical composition of the pipe met the minimum specifications for API 5L grade X70 PSL 2, though there is evidence that some of the HAZ hardness exceeded the maximum set forth for grade X70. The mechanical properties and chemical composition of the elbow met the minimum specifications for MSS SP-75-2008 and TES-FITG-LD-US.

One item of note was identified related to the tempering time requirements for the elbow. The TAG 98 elbow (heat NOP-C) was tempered for [REDACTED]-minutes which does not align with MSS SP-75-2008 or TES-FITG-LD-US, Rev 0 requirements to temper fittings for 1-hour per inch of maximum wall thickness. The maximum wall thickness of the TAG 98 elbow was [REDACTED]-inch which would have required a minimum tempering time of [REDACTED]-minutes to meet specifications (ION3). Though it did not comply with the specification requirements, MTRs and post-incident mechanical testing confirmed that the material properties met design requirements and played no role in this incident.

Table 20. Summary of Items of Note – Manufacturing of TAG 98

Effect	Items of Note
Elbow Tempering Duration did not Comply with Specifications	ION3: The TAG 98 elbow (heat NOP-C) was tempered for [REDACTED]-minutes which does not align with MSS SP-75-2008 or TES-FITG-LD-US, Rev 0 requirements to temper fittings for 1-hour per inch of maximum wall thickness. The maximum wall thickness of the TAG 98 elbow was [REDACTED]-inch which would have required a minimum tempering time of [REDACTED]-minutes to meet specifications.

5.1.3 TAG 98 (BND 350) Bend Assembly Fabrication

The TAG 98 bend assembly (BND 350) was fabricated by [REDACTED] in Stafford, TX. [REDACTED] was responsible for the fabrication of [REDACTED] of the [REDACTED] bend assemblies being replaced.

The TAG 98 bend assembly consisted of the 30°, 3D elbow and two 8-ft pups cut from a single pipe joint and welded to both ends of the elbow (see Figure 58) using a taper transition. The metallurgical analysis identified multiple fatigue cracks within GWD 13530 (G59B) that initiated at LOF regions at the ID toe of the weld. There are several possible causes for LOF during welding including inadequate heat input, poor joint preparation, misalignment, and poor workmanship. To offset the potential for girth weld flaws leaving the fabricator, a QMS was in place that included visual inspections, NDE using radiography, and hydrostatic testing of the finished assembly. In addition, TC Oil had surveillance personnel on site to witness specific quality activities and to confirm that procedures and specifications were being followed. Although several safeguards were in place to prevent a potentially injurious girth weld flaw from reaching the field, shallow LOF imperfections in GWD 13530 escaped detection at the fabricator and entered service.

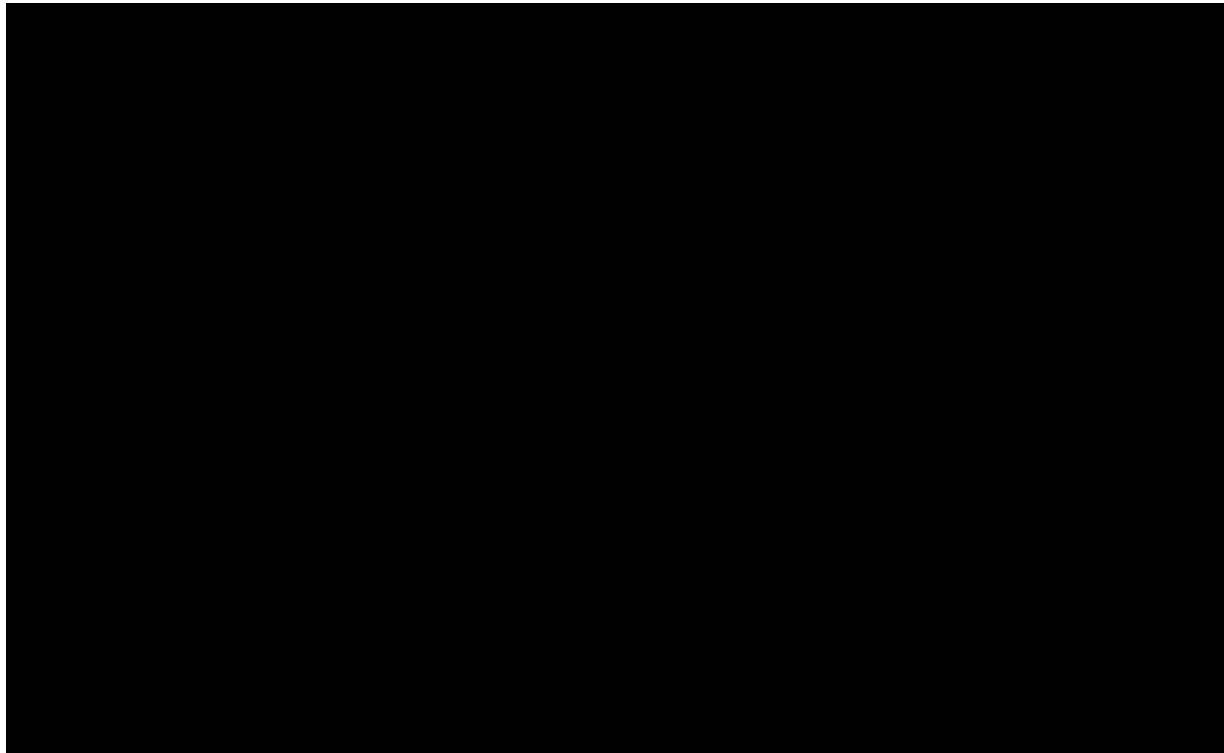


Figure 58. TAG 98 (BND 350) Bend Assembly Design for Fabrication

5.1.3.1 Weld Workmanship

The TAG 98 girth welds were fabricated using a semi-automated process at [REDACTED] fabrication facility. As described in the Freeman +4 RCFA⁸⁷, the installation of a good weld relies on several factors:

- Engineering specifications that set appropriate criteria for design and materials;
- Procurement and quality control practices that assure that materials conform to engineering requirements;
- Installation practices that verify welds conform to design specifications, fit-up of joints meet spacing and offset requirements, and welding is performed in accordance with approved procedures by qualified individuals; and
- External conditions are appropriately controlled during weld installation.

These factors were evaluated to determine where safeguards may have been inadequate or missing that allowed a high stress weld with LOF imperfections to enter service.

The shop welding procedure and procedure qualification record were reviewed. The welding procedure specification (WPS) RCT-280⁸⁸ for groove and fillet welds was applicable for welding grade X70 pipe in wall thicknesses ranging from 0.500-inch to 1.000-inch. WPS [REDACTED]-280 was qualified on November 14, 2010, using 36-inch diameter, 0.500-inch wall thickness, grade X70 pipe materials and low-hydrogen welding processes. The root pass was produced using a

⁸⁷ Kiefner and Associates, Inc, Root Cause Failure Analysis of Transition Girth Weld 4B-CTT-1 Leak at Freeman +4, September 6, 2016.

⁸⁸ [REDACTED] Welding & Fab, Welding Procedure Specifications (WPS), [REDACTED]-280, Groove and fillet welds, November 14, 2010.

semiautomatic, short-circuiting arc, gas metal arc welding (GMAW) process (which can have a higher propensity for LOF) while the filler and cap passes were produced using a semiautomatic, spray arc, flux cored arc welding (FCAW) process. The procedure qualification record⁸⁹ (PQR) verified that the WPS produced acceptable mechanical properties in the weld, which was verified post-incident by Anderson - no deficiencies in the mechanical properties of GWD 13530 and GWD 13520 were found with respect to the minimums set forth in API 1104.

As noted by Anderson, “the initiating features appeared consistent with lack-of-fusion at the ID toe approximately 200 μ m in length. Lack-of-fusion and cracking extending from the LOF was observed on both GWD 13530 and 13520.” Per Section 9.3.4 of API 1104, “Incomplete fusion (IF) is defined as a surface imperfection between the weld metal and the base material that is open to the surface.” This condition is shown schematically in Figure 59. According to API 1104, “IF shall be considered a defect should any of the following conditions exist: (a) The length of an individual indication of IF exceeds 1-inch (25 mm); (b) The aggregate length of indications of IF in any continuous 12-inch (300 mm) length of weld exceeds 1-inch (25 mm); or (c) The aggregate length of indications of IF exceeds 8% of the weld length in any weld less than 12-inch (300 mm) in length.”

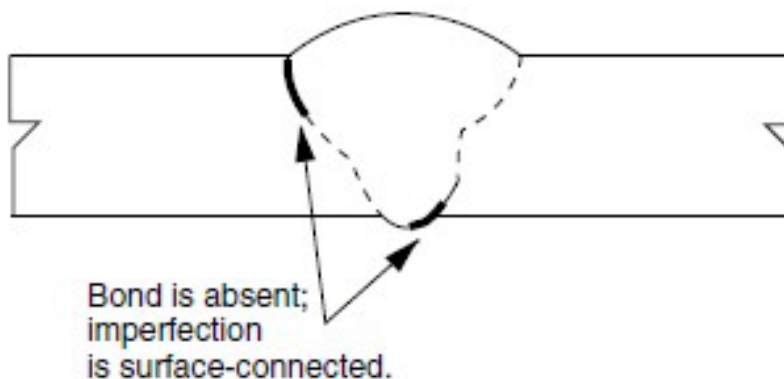


Figure 59. Incomplete Fusion at Root of Bead of Top of Joint (IF)⁹⁰

There are several potential causes of LOF in gas metal arc welds, especially in root passes made using the short-circuiting arc variant of the process. Among the most common include:

- inadequate heat input (voltage, current, and/or travel speed);
- improper gun angle relative to the joint (i.e., gun tilted to one side or the other or the angle parallel to the direction of welding varies from a normally targeted range of about 0° to 15°); or
- poor joint preparation; either machining problems or surface contamination.

In general, mechanized welding makes it easier to set and maintain constant heat input and torch angle, but it is also less able to accommodate small variations in the root gap and radial alignment, so fit-up is critical. The approved WPS and quality monitoring reports do not indicate

⁸⁹ [REDACTED] Welding & Fab, Procedure Qualification Record (PQR), [REDACTED]-280, Groove weld, Single V-Groove, November 14, 2010.

⁹⁰ API Standard 1104, 20th Edition, Welding of Pipelines and Related Facilities, April 2010.

how fit-up between pup and elbow was maintained. Per the governing specification at the time of fabrication, TES-WELD-AS-US, [REDACTED] weld alignment options were provided [REDACTED] or [REDACTED]⁹¹. Based on input from TC Oil, due to the nature of the welding configuration (elbow to pup), the use of tacks was likely once alignment and gaps were achieved. As discussed previously, the post-incident NDE inspection noted some high-low conditions⁹² in GWD 13530 and GWD 13520. The welding operator can make small adjustments to accommodate some misalignment while welding but might not have the same flexibility as would a manual welder. The WPS was qualified on thinner pipe (0.500-inch wall thickness) than the actual wall thicknesses for the TAG 98 (BND 350) girth welds and used only API 5L Grade X70 pipe rather than API 5L Grade X70 pipe and a thicker wall WPHY 70 fitting. This can also increase the possibility for fusion problems because the thicker pipe (elbow) is a more effective heat sink. The WPS maximum heat input is listed as 45.36 kJ/in for the root pass which would not be expected to contribute to LOF; however, the listed maximum heat input may not be representative of the actual heat input at the time the weld was made. Records to confirm welding parameters used for the TAG 98 bend assembly were never uncovered during the investigation.

The length of the original LOF regions were not reported by Anderson but based on the post-incident MPI and PAUT inspections, they likely exceeded the API 1104 defect criteria and should have been rejected if found⁹³. Since repair welds were discovered in GWD 13530 post-incident between the three distinct crack fronts, it is possible that some defects were discovered at the time of fabrication but not all.

5.1.3.2 Quality Control at Fabricator

Quality control during bend assembly fabrication included a combination of visual inspections, radiographic testing, and hydrostatic testing of the finished bend assembly to check for leaks. According to the [REDACTED] Quality Manual (QM)⁹⁴, [REDACTED] was responsible for setting the quality objectives which included verification, validation, monitoring, inspection, testing, and generation of records to provide evidence that the processes used and resulting products met requirements. A separate QM was not uncovered for [REDACTED], but individual quality documents and procedures were reviewed. All inspection and testing activities were to be executed per the identified procedures and ITP. The ITP represents a chronological checklist to show the status of all necessary inspection and testing activities required by the fabricator. An excerpt of the only completed ITP for fabrication of the bend assemblies at [REDACTED] is shown in Figure 60. The

⁹¹ Per the governing specification at the time of fabrication TES-WELD-AS-US Welding of Assemblies and Station Piping US-MEX it outlines [REDACTED] weld alignment options in [REDACTED]

⁹² Per Section 7.2 of API 1104, 20th Edition, "the alignment of abutting ends shall minimize the offset between surfaces. For pipes of the same nominal thickness, the offset should not exceed 1/8-inch (3 mm). Larger variations are permissible provided the variation is caused by variations of the pipe end dimension within the pipe purchase specification tolerances, and such variations have been distributed essentially uniformly around the circumference of the pipe."

⁹³ Per Table 3 of TES-WELD-AS-US Welding of Assemblies and Station Piping, the acceptance criterion for LOF using radiography is [REDACTED]. Because the depth of the LOF in GWD 13530 was less than the IQI of [REDACTED], it would not have been detectable. Thus, GWD 13530 would have been an acceptable weld per the code since there were no evident imperfections.

⁹⁴ Canadoil Forge, LTD, Quality Manual According to ISO-9001-2000, January 15, 2002.

ITP activities align with surveillance requirements in the PO and reporting requirements in TES-WELD-AS-US, Rev 01. [REDACTED] supplied a document package to TC Oil containing [REDACTED] ITP, completed as-built drawings, fabrication spool sheets, pressure test logs and charts, weld map, radiograph reports and procedure, and WPS/PQR records.

Even though an ITP was used, it was not specific to individual bend assemblies and was completed on the day that fabrication started (November 16, 2010). No other ITP documentation for [REDACTED] was found. This clearly shows that the ITP was used as a planning document but not as an actual indicator of acceptable completion of the specific tasks for each assembly. No complementary records were found for TAG 98 to indicate that fit-up, weld preparation, or welding operations complied with procedures. An individual weld inspection record documenting welding parameters (amps, volts, travel speed, heat input) for the TAG 98 fitting was not found. Weld inspection reports were found for only two of the 22 bend assemblies fabricated by [REDACTED] but appear to be incomplete as shown in Figure 61.

The missing weld inspection records for TAG 98 indicate weaknesses in recordkeeping, at a minimum, and could be an indication of more general quality control issues during fabrication of the bend assemblies.

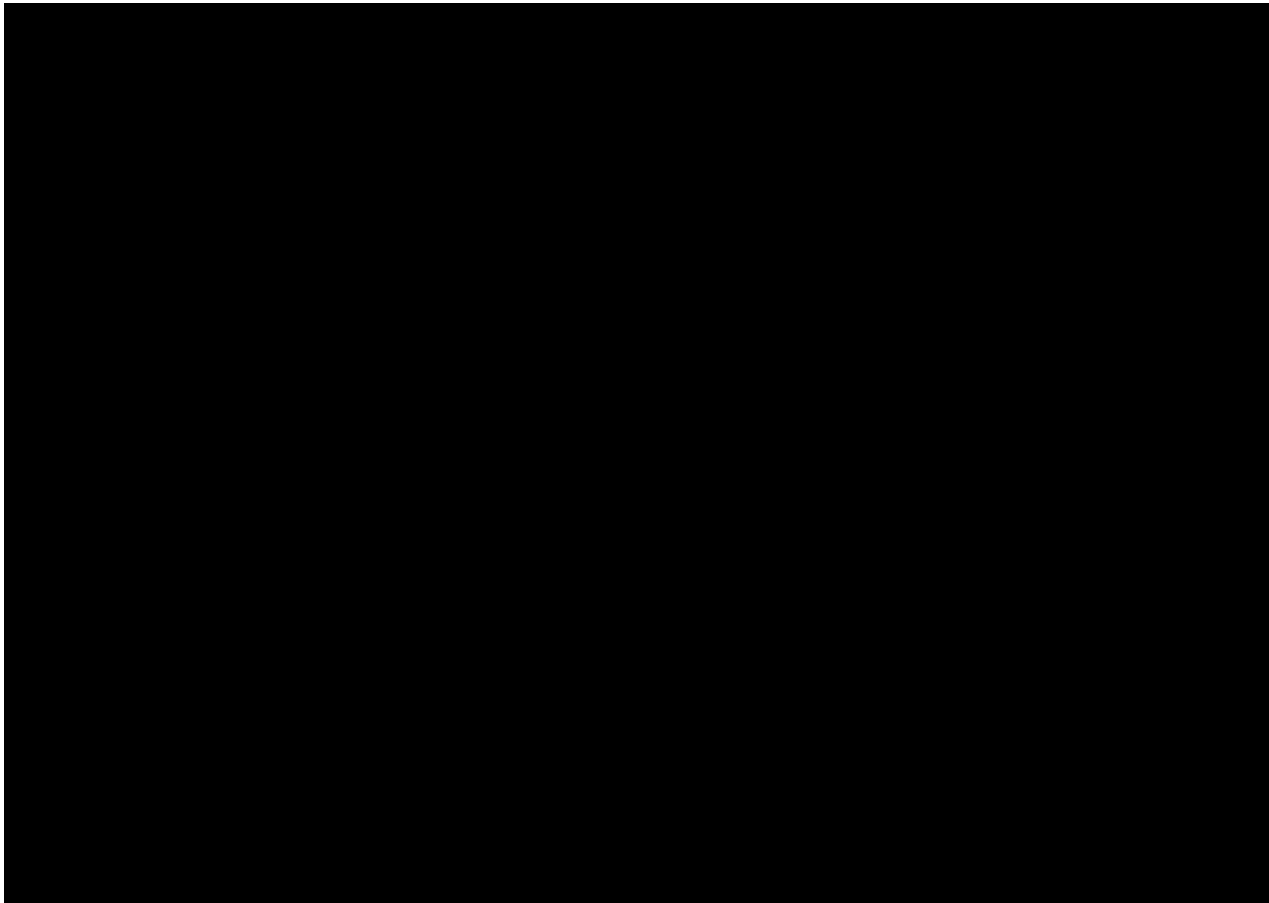


Figure 60. ITP Excerpt for Bend Assembly Fabrication at [REDACTED]

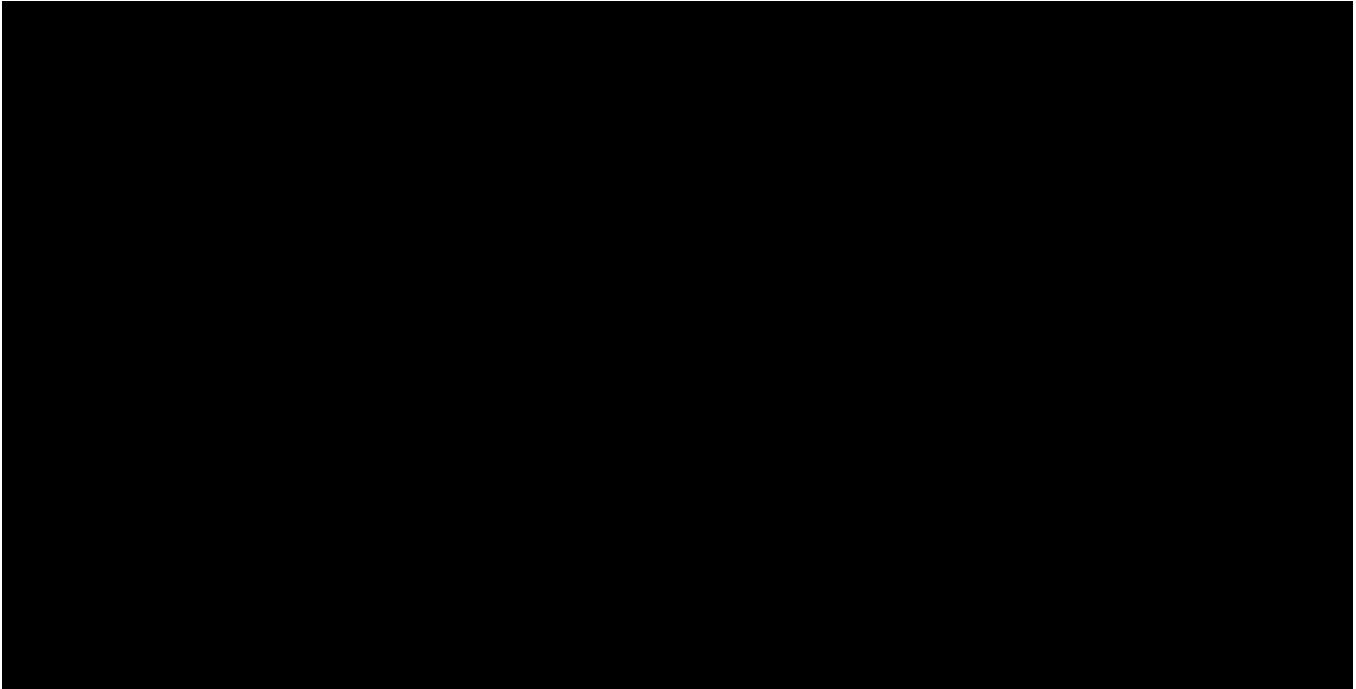


Figure 61. Example of Incomplete Weld Inspection Report for TAG 114C (BND 349)

5.1.3.2.1 Weld Inspections – Visual

Though an ITP was completed on November 16, 2010, and signed off by the [REDACTED] inspector there were no separate sign offs by [REDACTED] or a third-party inspector representative. The ITP requires verification of material certificates and checking measurement and test equipment prior to their use. For welding, the ITP requires checks for fit-up, verification that welders and operators are up to date with qualifications, checks of filler materials for compliance with procedures, verification of weld preparations in accordance with shop details, and observation of welding operations to verify compliance to procedures (including checks for proper preheat, voltage/current/travel speed/back gouging, slag removal, and removal of tack welds). Inspectors were required to visually inspect welds for proper size, visual quality, dimension or reinforcement, and welder identification.

A weld inspection report was never found for TAG 98 indicating that at a minimum, recordkeeping procedures were not followed and at worst that the weld inspections were never performed. Although quality surveillance documents were not located for the TAG 98 bend assembly, visual inspections for general workmanship likely took place because both weld G59A and weld G59B were reexamined with radiography at three locations the next day (November 20, 2010) as will be discussed in the next section.

5.1.3.2.2 Weld Inspections - Radiography

Radiography is a common and accepted industry practice for girth weld inspections. Radiography was performed on GWD 13530 (G59B) and GWD 13520 (G59A) by a certified Level II Technician on November 19, 2010, using the single wall exposure/single wall viewing (SWE/SWV) technique (see Figure 62). An image quality indicator (IQI) is placed between the pipe and film to verify the sensitivity of the inspection. For weld thicknesses ranging between

0.500-inch and 0.750-inch an IQI wire diameter of 0.016-inch is required to show that the sensitivity of the radiograph is at least equal to 2%.

Radiography works best for blunt flaws and for assessing weld workmanship but has some difficulty detecting sharp flaws like cracks or LOF.⁹⁵ Note that the radiograph need only to have enough sensitivity to detect and image a specified wire diameter in a standard IQI. For TAG 98, that essential wire diameter is 0.016-inch, therefore, flaws shallower than 0.016-inch might not be detectable using conventional RT techniques defined in codes and standards such as API 1104. In addition, for welds joining pipe with a sizeable difference in wall thickness, the radiographic film exposure time can also be difficult to optimize for both wall thicknesses. TES-WELD-AS-US, Rev 1 requires NDE for both wall thicknesses when the pipe wall thickness difference is greater than [REDACTED], as was the case for TAG 98 (BND 350).

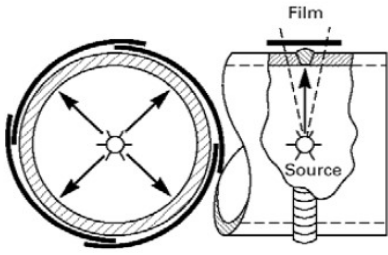
Pipe O.D.	Exposure Technique	Radiograph Viewing	Source-Weld-Film Arrangement		IQI		Location Marker Placement
			End View	Side View	Selection	Placement	
Any	Single-Wall	Single-Wall	 <p>Exposure Arrangement – A</p>		See Figure 4	<div>Source Side</div> <div>Film Side</div>	Either Side

Figure 62. Schematic of SWE/SWV Radiography Technique Used on GWD 13530⁹⁶

As shown in the radiograph report in Figure 63, GWD 13530 (G59B) and GWD 13520 (G59A) were both found to be acceptable. The inspection met the requirements within Condition 21⁹⁷ of the Special Permit and the inspection parameters complied with the [REDACTED] procedure DGIR-0001⁹⁸ and TransCanada's specification TES-NDT-RT-US, Rev 0⁹⁹. The LOF features were approximately 0.008-inch (200 µm) in depth before transitioning to a crack (see Figure 27). Therefore, it was approximately 1.6% of the wall thickness deep at the time of radiography and unlikely to be detectable. Other figures in the metallurgical analysis report showed LOF features that were approximately 0.012-inch (300 µm) deep, which are still below RT detection thresholds. Because the initial LOF depths were below the sensitivity of the RT inspection, it is

⁹⁵ Reed, R.P., et al, Fitness-For-Service Criteria for Pipeline Girth Weld Quality, National Bureau of Standards, NBSIR 83-1695, November 1983.

⁹⁶ Boccard USA Corporation, Radiographic Testing RT-1, Revision 1, March 29, 2010.

⁹⁷ Condition 21 of the SP states that a construction QA plan for quality standards and controls must be maintained throughout the construction phase with respect to: inspection...welding, NDE of girth welds...backfilling. All girth welds must be NDE by radiography or alternative means. The NDE examiner must have all current required certifications.

⁹⁸ DGIR-0001, General Procedure for Radiographic Examination, Diamond G Inspection, Rev 1, August 30, 2010

⁹⁹ TES-NDT-RT-US, Rev 0, Radiographic Examination of Welds, June 15, 2007.

not surprising that the LOF region was not detected. However, as noted in 4.2.2, PAUT conducted post-incident reported flaws with depths 2x to 10x the LOF depth at locations in the weld that would have been unaffected by installation and thermal loads. So, it is possible that flaws larger than the 0.008-inch (200 µm) LOF were present and might have been detectable but Section 4.2.2 also shows that the post-incident PAUT significantly overcalled actual feature depths.

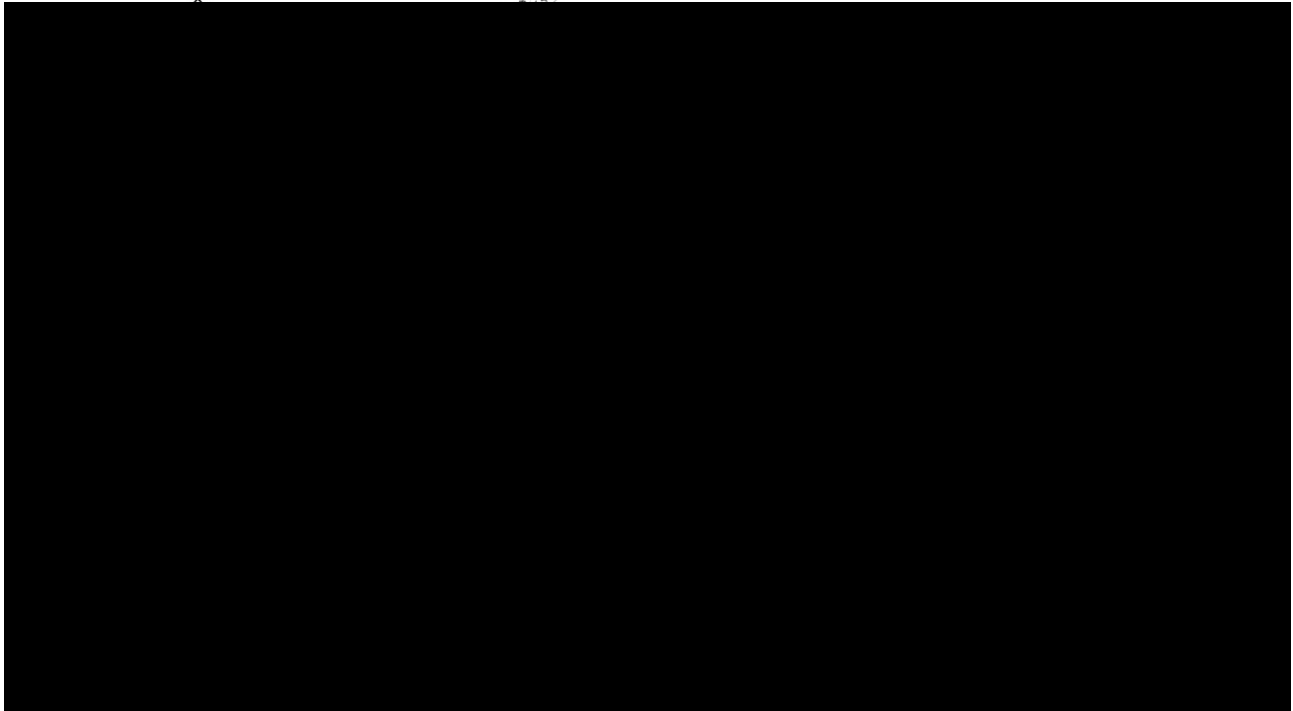
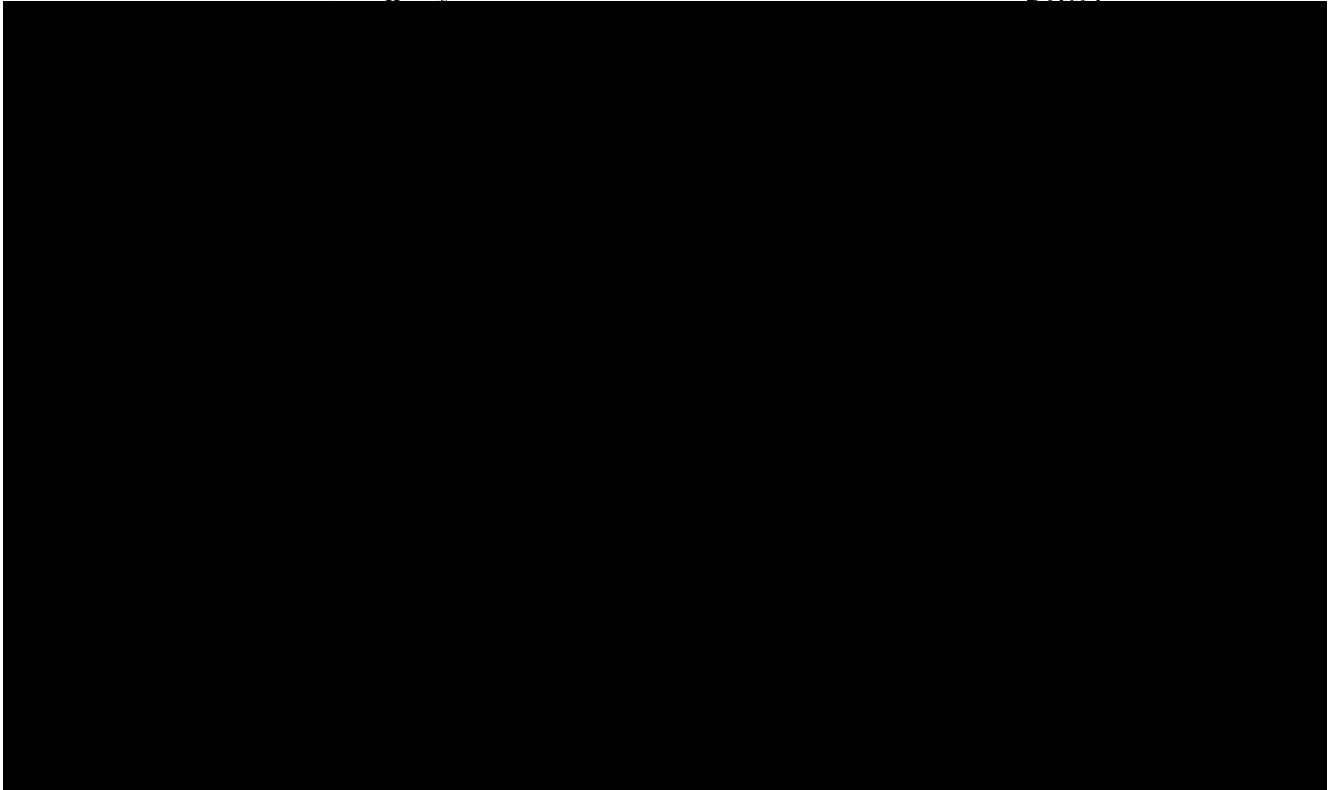


Figure 63. RT Report for TAG 98 Girth Welds G59B and G59A (November 19, 2010)



**Figure 64. RT Report to Reexamine Portions of TAG 98 Girth Welds G59B and G59A
(November 20, 2010)**

On a separate note, the day that TAG 98 was fabricated (November 19, 2010), three other bend assemblies were also fabricated, TAG 138F, TAG 126A, and TAG 126. Except for TAG 98, the other three bend assemblies were found to have weld defects requiring repair. TAG 138F and TAG 126A were repaired and re-radiographed the same day and TAG 126 was repaired and re-radiographed the following day (November 20, 2010). Portions of the TAG 98 girth welds were also re-radiographed the following day (see Figure 64) and the only note to indicate potential reasons why is the statement “offsets for customers”. It is unclear if this statement is related to offsetting the radiation source to get better views (although the source-to-object distance is the same for both radiographs) or if an offset, or misalignment condition was discovered in the TAG 98 girth welds. When asked, Company representatives responded that it is reasonable to assume that the TAG 98 reshoots were using a source offset. This conclusion was drawn from the fact that the shot locations only accounted for a third of the weld circumference. Offsets may have been requested to better balance density variations in the film due to the transition weld geometry or potentially to confirm the presence of a mis-oriented flaw. At the time of fabrication, no defects were noted even though it is clear from the Anderson metallurgical analysis that repairs were made on GWD 13530 and GWD 13520. The [REDACTED] radiographic inspections and results are summarized in Figure 65.

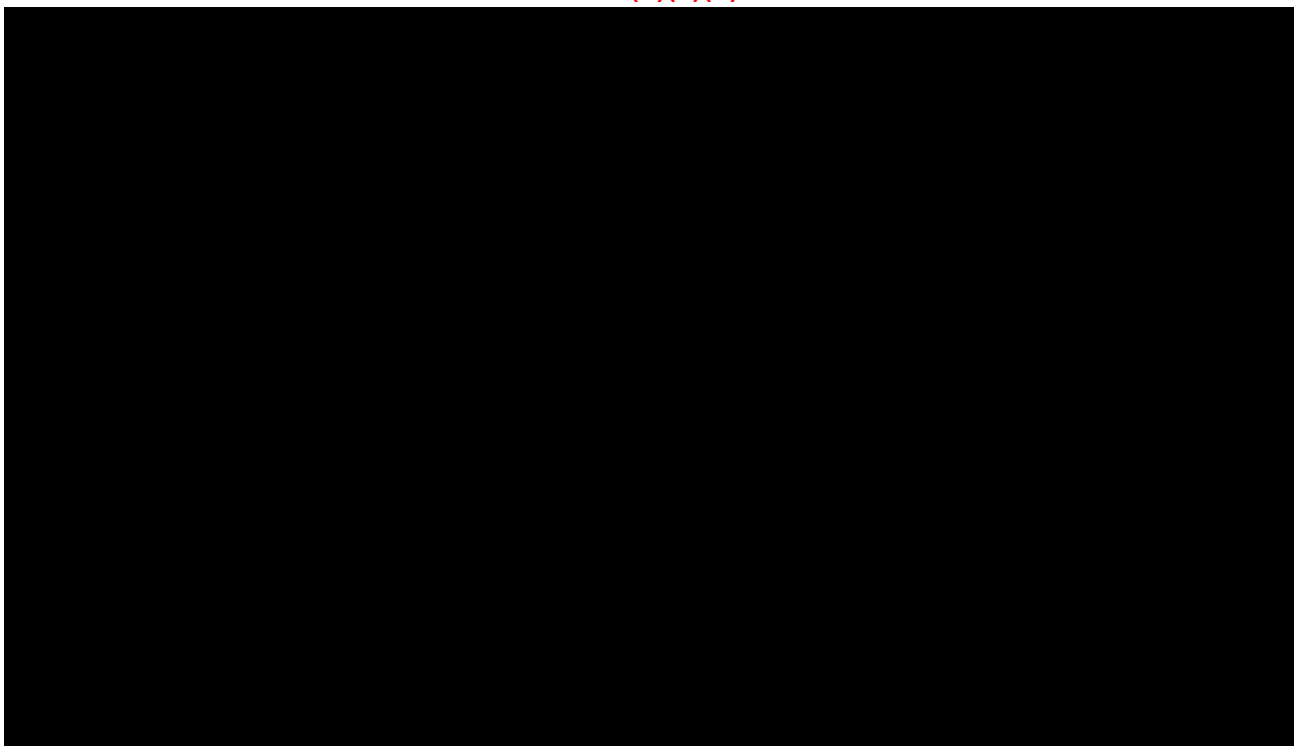


Figure 65. Summary of Elbow Assembly Fabrication, Weld Radiography, and Hydrostatic Testing at RCT (November 16-26, 2010)

Clearly, the weld repair rate on the day that TAG 98 was fabricated was higher than other days on which replacement bend assemblies were being fabricated. Three assemblies were noted as needing repair in radiography records and post-incident TAG 98 was also found with weld repairs. However, because weld inspection records and quality surveillance records are unavailable for TAG 98, the reason for the higher repair rate could not be determined.

5.1.3.2.3 Hydrostatic Test of Bend Assembly

On November 20, 2010, after welding and inspections had been completed on TAG 98, the bend assembly was hydrostatically tested to a minimum test pressure of 1,880 psig (94% SMYS) for four hours. The assembly was visually inspected for leaks for the duration of the test. The test was successfully completed in accordance with procedures¹⁰⁰ and no leaks were noted.

5.1.3.2.4 Weld Repairs

As noted by Anderson and shown in Figure 18, the three primary fatigue cracks were separated by two shear regions that were coincident with weld repairs in the original weld root pass. Further evidence of repair was the observation of grind marks on the elbow bevel and remnant pipe as well as a thicker weld bead in these areas. The [REDACTED] Weld Repair Procedure¹⁰¹ was a one-page document that provided steps for repairing improper start & stop welds, undercuts, insufficient weld cap, and RT-directed repairs. All repairs required grinding to sound metal or a

¹⁰⁰ [REDACTED] Hydrostatic Leak Test Procedure, [REDACTED] ([REDACTED]-12117), 36" SCH XS Pipe Spools, Undated.

¹⁰¹ [REDACTED], Repair Procedure, Job No. 12117.

smooth surface then using low-hydrogen welding methods to apply filler metal. Any excess weld fill was to be ground off to “blend” with the welding pattern followed by visual inspections to check welding workmanship. The only time RT was required after a repair was when the repair was directed by findings from the original RT examination.

Section 9 of TES-WELD-AS-US, Rev 01 allows for the repair of defects in the root pass detected by visual inspection prior to NDE provided that all repair work is approved by the Company, welding is performed in accordance with the approved WPS, visual inspection is performed after the repair work, and inspectors are trained and qualified. Visual and RT inspection acceptance criteria for LOF defects is that no evident imperfection is found. This likely was the case for the LOF region in GWD 13530 (G59B) which was smaller than the RT IQI for the wall thicknesses inspected.

As discussed in Section 5.1.3.2, weld inspection reports and the third-party surveillance checklist for TAG 98 (BND 350) were missing and therefore could not be examined for possible clues as to why repair welds were needed or what the visual inspections found. Figure 65 provides a summary of the dates on which the 22 bend assemblies fabricated by [REDACTED] were produced, associated radiography results, and hydrostatic testing results. Of note is the day that TAG 98 was fabricated, Friday, November 19, 2010. On that day a total of four bend assemblies were fabricated, three of which were reported to have a weld defect in subsequent RT inspections (TAG 138F, TAG 126A, and TAG 126). The welds on these bend assemblies were noted as being repaired and re-radiographed the same day or the following day. Curiously, TAG 98 was also re-radiographed the following day (November 20, 2010) despite no defects being noted in the original RT report.

Though none of the records show that weld defects were found in TAG 98, it is plausible that root bead workmanship flaws were visually detected by the welder and repaired but not recorded. In this situation, the repair would have been considered as “rework” per API 1104 and not an official “repair” that could trigger special documentation or perhaps the use of a dedicated repair procedure. It is also plausible that inspections did not identify all weld conditions requiring repair which allowed the LOF defects to leave the shop undetected. Because of the missing records, RSI could not determine the reason why repairs were needed.

5.1.3.2.5 Surveillance at the Fabricator

The fabrication work performed at [REDACTED] was to comply with the quality requirements defined in the PO. [REDACTED] had developed an ITP to comply with the minimum quality surveillance requirements. TC Oil also developed a third-party surveillance checklist (TEF-SCL-FITG-US) to verify drawings, material traceability, material properties, welding procedures, compliance with inspection requirements, markings, and verification of records and documentation prior to release of the fitting for shipment. As part of the surveillance activities, welding inspectors should have witnessed each approved WPS. If the WPS results were satisfactory, subsequent witness by in-process inspection would have been on a random basis throughout the fabrication cycle. Related to fit-up and welding of pupping, surveillance inspectors were to review the work environment for factors that could affect compliance with the WPS, verify welding personnel

qualifications, consumable storage and weld temperature controls, verify material cleanliness, confirm and report that WPS/PQR essential variables are being followed, and visual inspection of welding for general workmanship.

A completed TEF-SCL-FITG-US form and weld inspection report for TAG 98 (BND 350) was never uncovered during the investigation. Therefore, the investigation was unable to determine whether these surveillance activities were completed for the TAG 98 (BND 350) elbow assembly. At a minimum, there were lapses in recordkeeping for fabrication of the TAG 98 elbow assembly and at the most, key weld inspection and verification steps were missed for TAG 98 (BND 350).

5.1.3.3 Contributing Factors and Items of Note - Fabrication

Though specific quality documents for TAG 98 were missing, the records that were available confirmed that RT inspections and hydrostatic testing had been completed. In addition, it is plausible that visual inspections took place that identified weld locations requiring repair as evidenced by the two weld repair regions that bifurcated the LOF into three separate regions. However, contributing to the failure, the selected welding process and NDE methods used at the fabrication shop did not consider the higher stress girth welds associated with the TAG 98 elbow assembly design. Therefore, additional precautions beyond API 1104 minimum requirements were not instituted to ensure that the weld workmanship and flaw detection sensitivity were acceptable for the service in which it was placed (CTF2).

As an item of note, the weld inspection report and quality surveillance records (TES-SCL-FITG-US) were missing for the TAG 98 bend assembly (ION4). In addition, for bend assemblies where records were found, they appear to be incomplete. Records retention is a key component of quality management systems to provide evidence of conformity to requirements and processes. The urgency to replace the [REDACTED] fittings likely was a factor in the recordkeeping lapses even though the importance of quality control was at the forefront of the fitting replacement project. Not maintaining key quality records to confirm that procedures and specifications were followed opens the possibility for future problems during operation.

Table 21. Summary of Contributing Factors – Fabrication of TAG 98

Effect	Contributing Factors
LOF Flaw in GWD 13530 (59B)	CTF2: The selected welding process and NDE methods used at the fabrication shop did not consider the higher stress girth welds associated with the TAG 98 elbow assembly design. Therefore, additional precautions beyond API 1104 minimum requirements were not instituted to ensure that the weld workmanship and flaw detection sensitivity were acceptable for the service in which it was placed.

Table 22. Summary of Items of Note – Fabrication of TAG 98

Effect	Items of Note
Missing Quality Surveillance Records and Inadequate Recordkeeping	ION4: The weld inspection report and quality surveillance records (TES-SCL-FITG-US) were missing for the TAG 98 bend assembly. In addition, for bend assemblies where records were found, they appear to be incomplete. Records retention is a key component of quality management systems to provide evidence of conformity to requirements and processes. The urgency to replace the [REDACTED] fittings likely was a factor in the recordkeeping lapses even though the importance of quality control was at the forefront of the fitting replacement project.

5.1.4 TAG 98 (BND 350) Bend Assembly Installation

Construction along the Cushing Extension had been largely completed by the end of October 2010 and was a month ahead of schedule. TC Oil was preparing for dry commissioning when the low yield fitting problem was discovered. TC Oil made the decision to replace [REDACTED] fittings along construction spreads 9C, 10C, and 11C. TC Oil worked with [REDACTED] to manufacture the replacements and to find fabricators that could manufacture the assemblies within a tight schedule yet still maintain the quality standards that were expected. As discussed previously, the TAG 98 (BND 350) elbow assembly was cut-out and replaced in December 2010 by the construction contractor [REDACTED]. The following narrative was compiled from Daily Inspection Check List, Welding Inspector's Daily Report, and Daily Inspection Report records. These events are summarized in Figure 66.

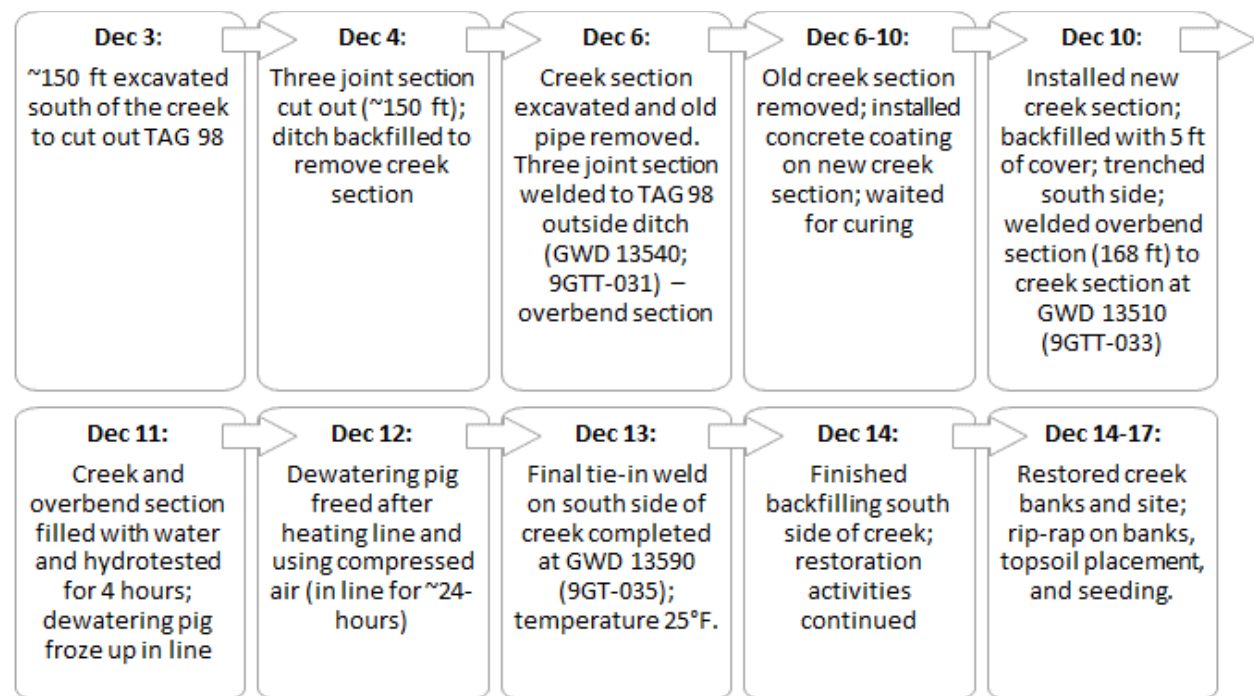


Figure 66. Summary of TAG 98 Installation Timeline (December 3-17, 2010)

Around November 23, 2010, construction activities began in the Mill Creek area to remove the old creek section and associated elbows and prepare the site for the replacement fittings. Initial activities included installing truck mats on the ROW and removing topsoil to prepare the site. Fabrication of the new section to be installed beneath the creek was started on November 30, 2010, outside of the ditch. Open cut excavation on the north side of Mill Creek began on December 1, 2010, along with topsoil and rip-rap¹⁰² removal on the south side of Mill Creek. On December 3, 2010, approximately 150-ft of the ROW was excavated on the south side to expose the pipe and cut-out the old overbend fitting (presumed to be TAG 98). On December 4, 2010, a three joint section (approximately 150-ft in length) was cut out on the south side. After its removal, the ditch was backfilled, and mats were placed to begin excavating the creek. On December 6, 2010, the creek section was excavated, and the old pipe and fittings were removed. The three joint section removed on December 4, 2010 was also welded to the downstream side of the TAG 98 bend assembly (GWD 13540; 9GTT-031). In addition, a 6-ft pup was attached downstream of the three joint section (GWD 13580; 9GT-030) presumably to facilitate fit-up at the final tie-in weld. The total length of this section, referred to as the 'overbend section', was approximately 168-ft in length, including the TAG 98 elbow assembly. The 'overbend section' held up by two side booms is shown in Figure 67 prior to it being welded to the creek section.



Figure 67. Installation of TAG 98 (December 10, 2010)

Between December 6 and 10, 2010, construction crews removed the old creek section, installed concrete coating on the new creek section, and excavated the creek to prepare for its installation. The construction contractor had to wait about four days for the concrete coating to

¹⁰² Loose stone used to form a foundation to protect the creek bank from scour and erosion.

cure on the creek section before it was moved into place on December 10, 2010. Once placed, crews backfilled the creek section (inspection reports note 5-ft of cover at the center of the creek) and trenched the south side of the creek to weld in the overbend section to the creek section. The trench was excavated approximately 20-ft upstream and 150-ft to 200-ft downstream¹⁰³ of the creek. The approximately 168-ft long overbend section was then welded to the creek section at transition girth weld GWD 13510 (9GTT-033). The overbend section and creek section were filled with water and the four-hour hydrostatic test began at 2:30 PM CST on December 11, 2010. The hydrostatic test was completed at 6:30 PM CST and dewatering operations began at 7:45 PM CST the same day. During dewatering crews encountered difficulties when the dewatering pig froze in the line. On December 12, 2010, the pipe was warmed using heaters and air compressors to jar the pig loose. The dewatering pig was finally removed from the test section at about 6:20 PM CST. The final tie-in weld (GWD 13590; 9GT-035)¹⁰⁴ on the south side of Mill Creek was completed on December 13, 2010. As shown in Figure 68, the final tie-in weld was approximately 158-ft downstream of the failed girth weld (GWD 13530; G59B). The construction contractor began and finished backfilling the trench and restoring the Mill Creek banks on December 14, 2010. French drains were installed, and the creek banks were restored with rip-rap material. Installation of rip-rap on the banks, topsoil placement, and seeding were completed by December 17, 2010.

¹⁰³ Daily Inspection Check List for Fitting # 108, MP 13.6, Spread 9C, December 17, 2010, and Daily Inspection Report, Form C37, Utility Inspector, December 4, 2010.

¹⁰⁴ Note, there was a 24-hour delay between completion of the final tie-in weld GWD 135990 (9GT-035) and NDE with radiography and automatic ultrasonic (AUT) inspection techniques. No flaws noted.

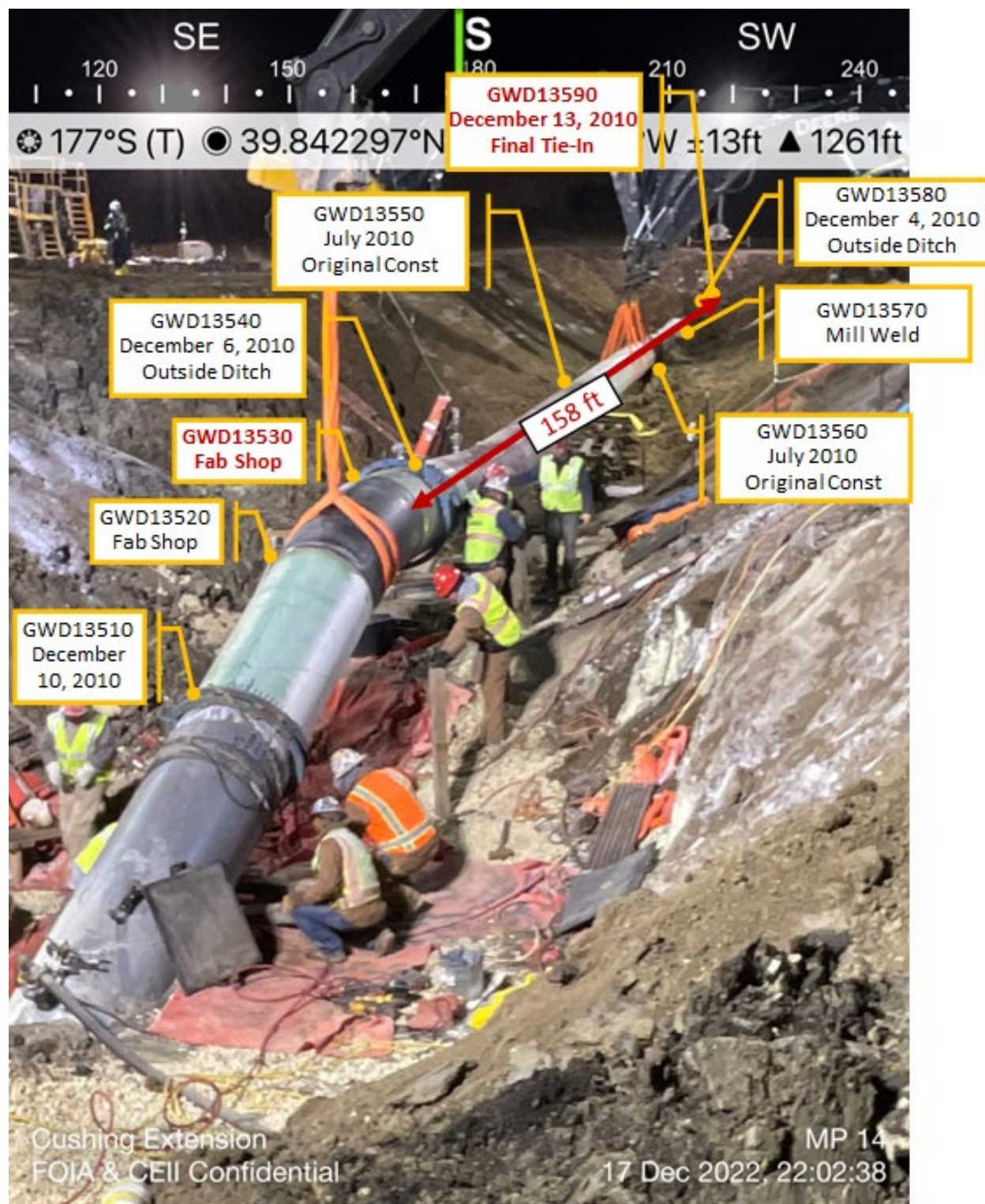


Figure 68. Key Girth Weld Installation Dates – Approximately 158 ft Between GWD 13530 and Final Tie-In Weld GWD 13590 (photo for illustrative purposes only, it is not from the time of construction)

5.1.4.1 Soil Support Beneath Pipe

Figure 69 is a schematic showing general pipe support details for construction of the Cushing Extension. Assuming that this same standard was used when TAG 98 was replaced, the pipe would have been placed on [REDACTED] inches of loose earth padding with [REDACTED] maximum particle size in the bottom of the ditch. No specific supports like sandbags or foam pillows were used as there were no remnant materials from these types of materials identified during the post-incident repair work. Other specific pipe support details from the elbow replacement project were not found during the investigation.

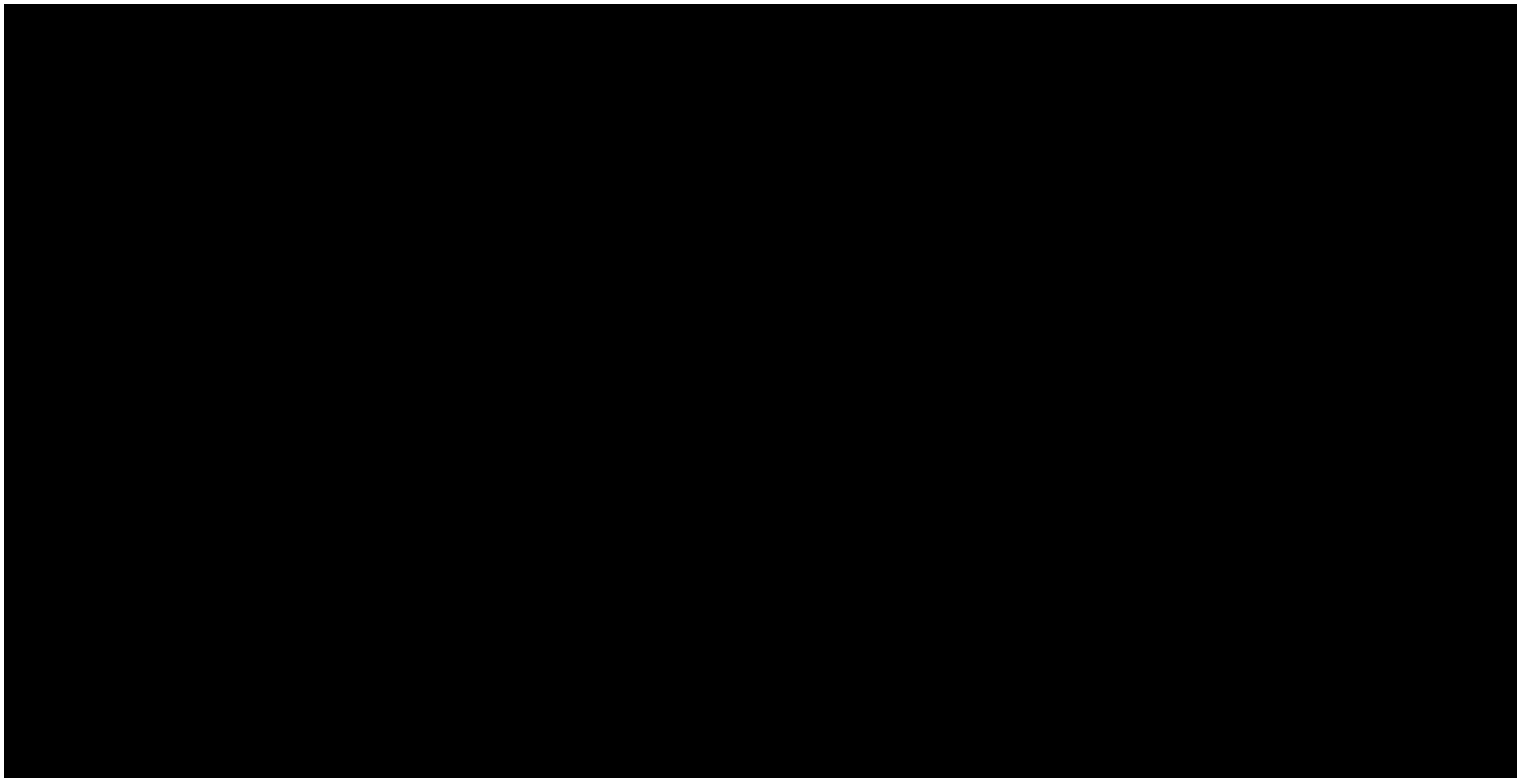


Figure 69. Schematic of Trenching, Pipe Support, and Backfill Requirements¹⁰⁵

As shown in Figure 70, the dominant soil types are fluvial/colluvium deposits in the area south of Mill Creek. This was confirmed by the Geotechnical SMEs onsite where they found clay-colluvium soils throughout. The US Department of Agriculture, Natural Resources Conservation Service (USDA NRCS) publishes a web soil survey¹⁰⁶ providing information on local soil data to make land use and management decisions. One of many soil data categories that is reported is soil susceptibility to compaction. The area south of Mill Creek is rated as 'medium' for soil compaction which indicates that the potential for compaction is significant and after compaction the soil can support standard equipment with only minimum increases in soil density. The area also has a moderate rating for frost action which is "the likelihood of upward or lateral expansion of the soil caused by the formation of segregated ice lenses (frost heave) and the subsequent

¹⁰⁵ Drawing No. 1862-03-ML-02-605, 36" OD Crude Oil Pipeline Typical Details Pipeline Construction, Rev 0, April 1, 2010.

¹⁰⁶ <https://websoilsurvey.sc.egov.usda.gov/App/HomePage.htm> accessed on February 16, 2023.

collapse of the soil and loss of strength on thawing...silty and highly structured, clayey soils that have a high water table in winter are the most susceptible to frost action.” The evidence supports that the soil in the area is appropriate for pipeline support but also may have been susceptible to frost action.

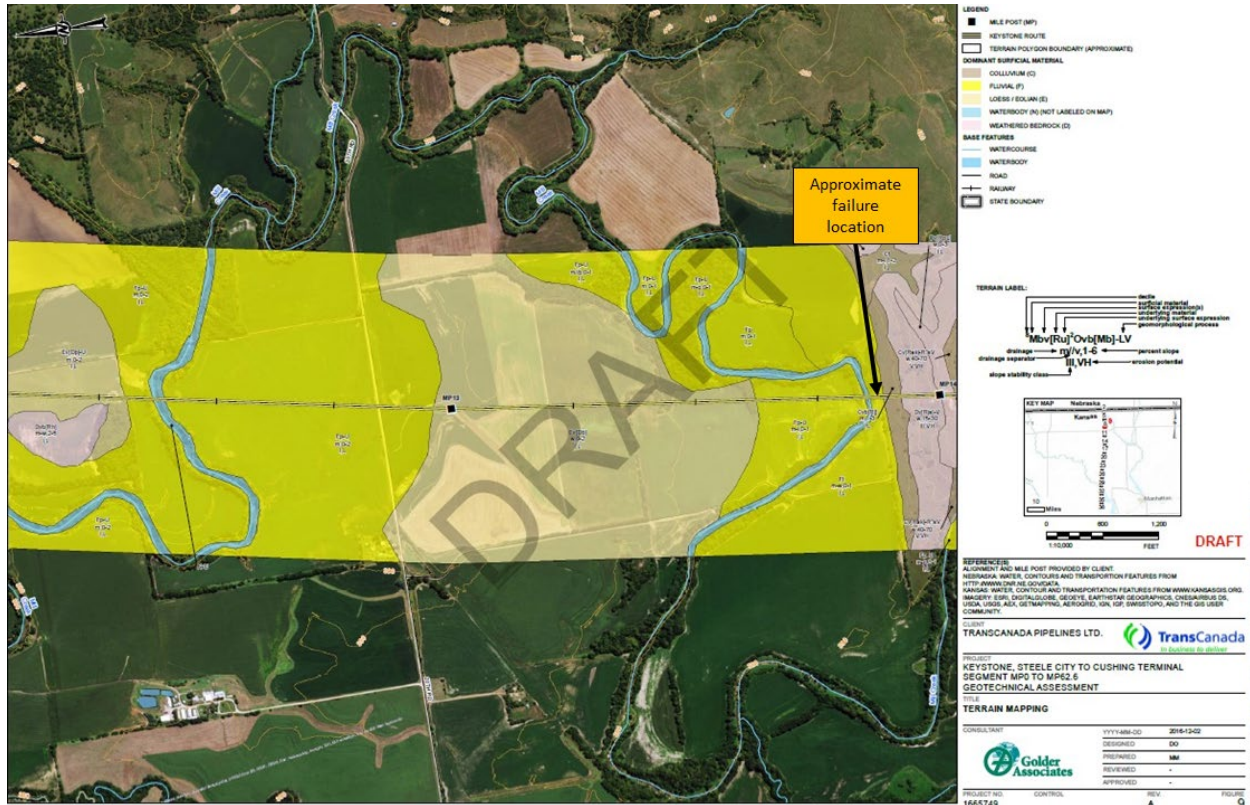
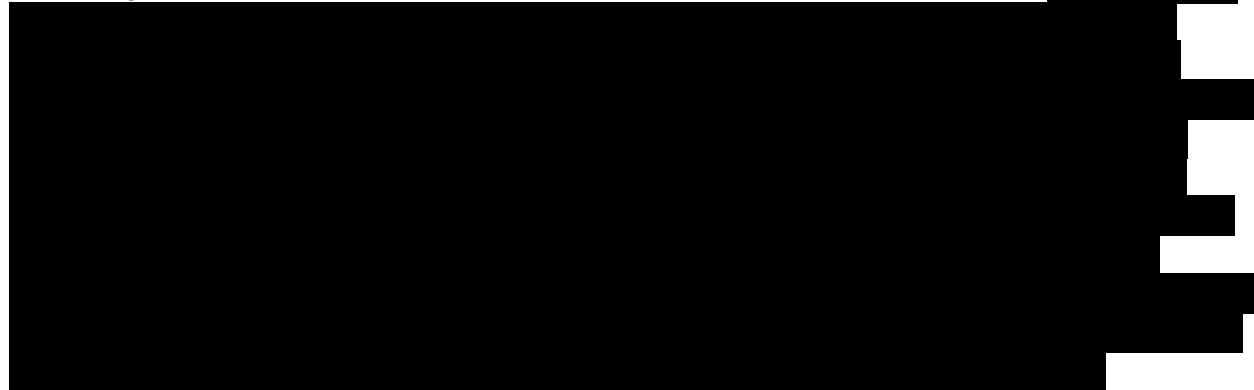


Figure 70. Geotechnical Assessment Near MP 14¹⁰⁷

According to TC Oil's compaction control specification, TES-CT-COMPC-GL¹⁰⁸,



¹⁰⁷ Golder Associates, Preliminary Desktop Mapping and Geotechnical Parameters for Terrain Analyses, TransCanada Keystone Pipeline Project (MP 0 to MP 62.7), December 2016.

¹⁰⁸ TES-CT-COMPC-GL Compaction Control Measures for Pipeline Excavations Specification (CAN-US-MEX), Rev 02, February 1, 2018.

As shown in Figure 71, the average temperature in nearby Steele City, Nebraska did not exceed 25°F (-4°C) between December 10, 2010, and December 14, 2010. The trench on the south side of Mill Creek was excavated December 10th and backfilled December 14th giving four to five days for the excavated soil to potentially freeze. Between those dates the newly installed overbend and creek sections were hydrostatically tested in the ditch with temperature maximums below 20°F (-7°C). No precipitation was noted, so crews were likely not dealing with snow or ice, but there was the potential for the ditch and the soil used as padding/backfill to freeze. The creek section had been backfilled prior to the hydrostatic test but the investigation team believes that the overbend section remained unburied so that any potential leaks at tie-in welds could be visually identified.

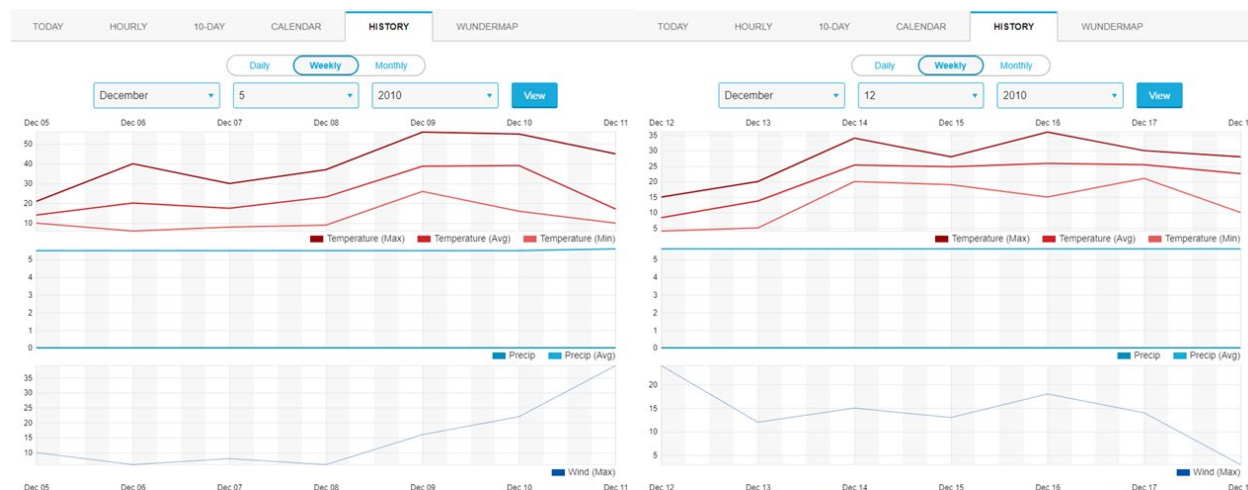


Figure 71. Historical Weather Conditions in Steele City, Nebraska (December 5-18, 2010)¹⁰⁹

Daily inspection reports indicate that a trench was excavated for placement of the new overbend section on the south side of Mill Creek. No further information was received describing the depth of the trench, the need for foundational material, the type of support beneath the pipeline, or the level of compaction achieved prior to backfill. However, because the trench south of Mill Creek was excavated four days prior to backfilling and the temperatures were below freezing for those four days, it is plausible that the in-situ foundational and backfill materials were partially frozen at the time of placement leaving them susceptible to thawing and loss of strength once operations began. There is no clear evidence to support or refute this possibility, except for photos from the March 1, 2013 integrity dig that do not appear to show any significant gaps or voids between the soil support and the elbow (see Figure 72). The FEA analysis in Section 4.2.1.2 showed that with settlement up to 1-ft beneath the pipe, the bending load could result in ovalization of the elbow but may not be sufficient to explain the wrinkle. Though inconclusive, lack of foundational support in the ditch is a potential causal factor.

¹⁰⁹ <https://www.wunderground.com/history/weekly/us/ne/lincoln/KLNK/date/2010-12-12> accessed on February 15, 2023.



Figure 72. Photos Showing Soil Support Beneath TAG 98 (March 1, 2013)

5.1.4.2 Hydrostatic Test Loads

The overbend section and the creek section were hydrostatically tested in the field on December 11, 2010. The minimum hydrostatic test pressure achieved was 1,822 psig (101% SMYS) and no leaks were noted. The total length of the test section was 658-ft. According to daily inspection reports, the creek section had been backfilled on December 10, 2010, but it appears that the pipe on the south side of the creek remained unburied in the trench to visually confirm the hydrostatic test results. The test began at 2:30 PM CST and was completed at 6:30 PM CST on the same day. The ambient temperatures during the test ranged from 17°F to 21°F. Dewatering activities began later that evening; however, crews ran into difficulties when the dewatering pig froze in the line. On December 12, 2010, daily inspection reports note that the dewatering pig never left the launcher. Construction crews used pipeline heaters and compressed air to free the pig approximately 24-hours after completion of the hydrostatic test.

A 158-ft long pipe section filled with water weighs approximately 94,000 lbs¹¹⁰. As shown schematically in Figure 33, backfilling of the creek section prior to the hydrostatic test effectively restrained the pipe upstream of the TAG 98 bend assembly. Assuming TAG 98 and the 158-ft length of pipe downstream had not been backfilled so that crews could visually confirm the success of the hydrostatic test, it would have been unrestrained (per ASME B31.4). As discussed in Section 4.2.1.3, testing in this configuration may have created a cantilever effect at the TAG 98 elbow. Daily inspection reports were not clear as to how the overbend section was supported during the hydrostatic test. As shown in Figure 67, the overbend section is being supported by two side booms prior to it being tied-in to the creek section. But the evidence was inconclusive regarding whether the side booms were used as support during the hydrostatic test. Statements by a Field Engineer onsite during the hydrostatic test indicate that the side booms most likely had been removed and that the pipe was supported with cribbing or earthen

¹¹⁰ The inside cross-sectional area of the pipe is 36-inch – 2 x 0.465-inch = 966 sq-in. The total inside volume is 966 sq-in x 1,896 in (158-ft length) = 1,831,536 cubic in (1,060 cubic ft or 7,930 gallons). The density of water is 8.34 lbs/gal therefore the total weight of the water in the test section is 66,140 lbs. The mass per unit length of steel pipe is defined in API 5L as $t(D-t) \times C$ where C is equal to 10.69. Therefore, the mass of the pipe is 0.465-inch (36"-0.465") x 10.69 = 176.7 lbs/ft x 158 ft = 27,920 lbs of steel. Combining these values gives a total weight of approximately 94,000 lbs (47 tons).

supports in the ditch. A note in the observation section of a Utility Inspectors report (see Figure 73) completed the day of the hydrostatic test (December 11, 2010) but prior to the actual test stated, “Broke down and took out (2) side booms” which also indicates that they were not in place during the test.

Time	Observations and Actions
6:00am	Arrived at Office. Turned in reports and documentation.
7:00am	Meeting with contractor and inspectors on prior days progress and days work schedule.
8:00am	Drove to R-O-W.
9:45am	Arrived at Tag 108 & 109. Unstream side of Mill Creek 3. Contractor had begun filling pie section with water at 9:30am. Broke down and took out (2) sidebooms.
11:30am	Contractor completed filling pie with water and began pressure for test.
2:30pm	Reached pressure for Hydrostatic test. Began test.
6:30pm	Completed test. Test passed and approved. Began plumbing for dewatering.
7:45pm	Began dewatering. Progress slowed due to having to heat manifold because dewatering pig froze up.
11:30pm	Pig locked up in pipe during dewatering. Left R-O-W.

Figure 73. Utility Inspector Observations on December 11, 2010

As summarized in Section 4.2.1.3, the FEA showed that accidental loads that caused significant end deflection (6-ft) or sliding displacement (6-inches) during the hydrostatic test could have been large enough to cause ovalization and wrinkling of the elbow assembly. And, because the elbow was significantly thicker than the pups, stresses would concentrate at the girth weld transitions. The crack tip stress intensity analysis showed that the stress induced when the bending load was applied was likely high enough to open the shallow LOF defect and either cause or contribute to crack initiation. The FEA suggests that high amounts of outside load/displacement would be required to cause the observed ovality and wrinkle. If the pipe segment did, in fact undergo such drastic loading conditions it seems unrealistic that these scenarios would have gone unnoticed. Accidental loads during the hydrostatic test are plausible as a causal factor for the bending load but do not completely explain the observed ovality and wrinkle due to the unrealistic load/displacement conditions needed.

5.1.4.3 Fit-Up During Installation

Per Section 8.6 of TES-WELD-AS-US, [REDACTED]

As shown in Figure 68, the final tie-in (GWD 13590; 9GT-035) on the south side of Mill Creek was completed on December 13, 2010, after the hydrostatic test. Approximately 150-ft to 200-ft had been trenched on December 10, 2010, to replace the overbend section as described in the daily inspection records. Though daily inspection reports state that the fit-up was good and no issues were noted (see Figure 74), there is the potential that additional stress was applied to

TAG 98 when the final tie-in weld was made. Post-incident, as the pipe was excavated it lifted approximately 6-inches indicating that there were external loads acting on the pipeline.¹¹¹

Interview statements acknowledged that replacing the fittings was a challenge because they already had pipe in the ground – they had to be exact and precise with fit-up. Therefore, this was a consideration in the selection of ■■■ pups to minimize the potential for fit-up issues. Backfill of the Cushing Extension had occurred in the summer months (July timeframe) but the new fittings were being installed under winter conditions. Because of the potential for spring back and the amount of pipe that would need to be excavated to alleviate some of the residual stress, the bend assemblies needed longer pup lengths. As such, the pups on the replacement fittings were specified at ■■■ long rather than the typical ■■■ lengths to try to achieve a stress-free fit-up. The Project Engineer onsite at the time the fitting was replaced did not remember any fit-up issues with the tie-in weld.

The FEA showed that a possible cantilever scenario over-stressed the TAG 98 (BND 350) bend assembly. Although there is no direct evidence that fit-up during the final tie-in contributed to the stress applied at GWD 13530 (G59B), it is plausible that a bending moment from the long lever arm (158-ft length of pipe) downstream of the TAG 98 bend assembly (BND 350) could have caused plastic deformation and concentrated stress in the weld.

¹¹¹ TCE Memo, Geotechnical Assessment of NPS 36 Keystone Mainline Leak at MP 14, January 16, 2023.

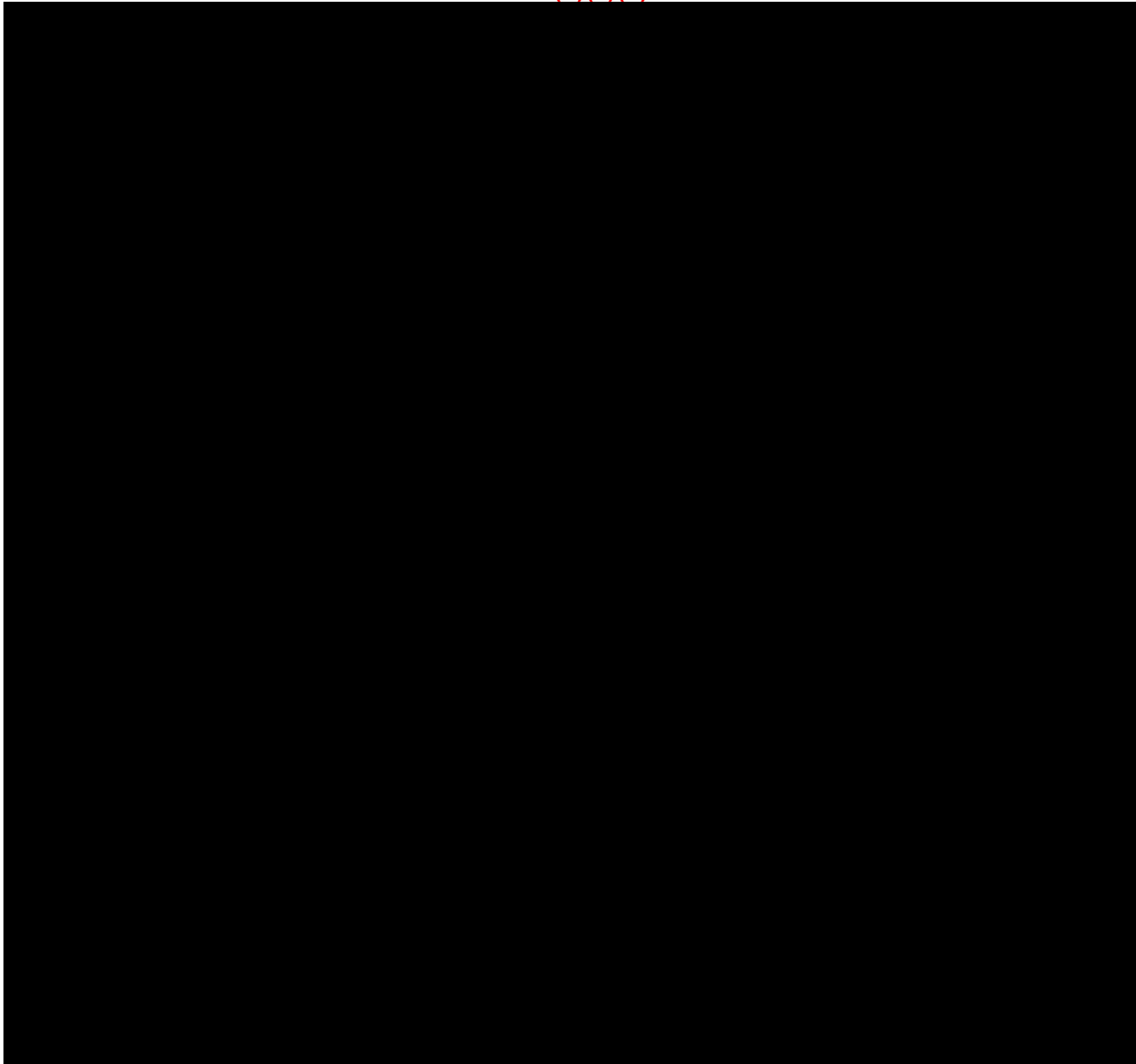
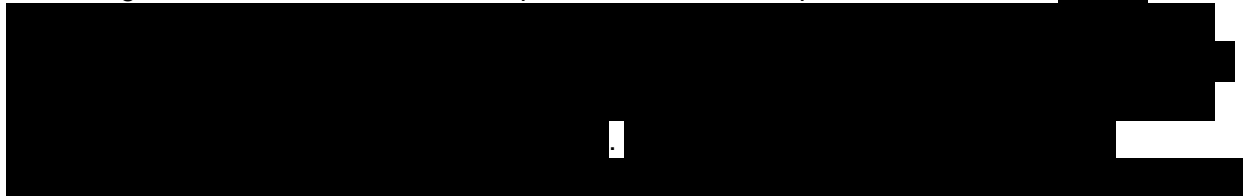


Figure 74. Final Tie-In Weld GWD 13590 (9GT-035) Reports Indicating Fit-Up

5.1.4.4 Lack of Support and Backfilling Loads

According to Section 25.1 of TC Oil's Pipeline Construction Specifications¹¹², the



¹¹² Exhibit F – Pipeline Construction Specifications, Rev 9, May 1, 2009.



Padding and backfilling operations were completed on December 14, 2010, after the final tie-in of the overbend section and creek section. No issues were noted in daily inspection reports during backfilling operations. Based on photographic evidence from December 10, 2010, it is unclear if the overbend section had been placed in a trench prior to backfill. However, based on daily inspection records¹¹⁴ inspectors noted that they began trenching southside of creek to weld the overbend section to the creek section on December 10, 2010, so it is more than likely that the pipe was placed within a trench prior to backfilling.

Several types of construction vehicles were onsite during the replacement project including side booms, track hoes, and bulldozers. Table 23 provides a summary of the vehicles that were onsite as described in daily inspection reports and includes the model numbers, operating weights, numbers on site, and lifting capacity, where applicable. Statements made by the onsite Field Engineer indicated that the side booms would not have been permitted to drive over the pipeline and other construction vehicles would only have been permitted to cross the pipeline only after achieving a certain amount of depth of cover.

Table 23. Construction Equipment On Site December 2010

Equipment Model	Maximum Lifting Capacity [lbs]	Operating Weight [lb]	Total On Site	Assumed Boom Overhang [ft]	Working Lifting Capacity [lb]	Total Working Lifting Capacity [lb]
CAT 583T ¹¹⁵ Side boom	140,000	100,000	2	8	60,000	120,000
CAT 594H ¹¹⁶ Side boom	200,000	121,475	3	8	80,000	240,000
CAT 345GC ¹¹⁷ Track hoe	---	95,500	2	---	---	---
CAT D8T ¹¹⁸ Bulldozer	---	87,733	2	---	---	---

¹¹³



¹¹⁴ Daily Inspection Checklist, Fitting 108/109, MP 13.6, December 10, 2010.

¹¹⁵ CAT 583T Pipelayer brochure found at <https://crosscountryis.com/pdf/CAT583TPipelayer.pdf> on March 20, 2023.

¹¹⁶ CAT 594 Pipelayer brochure found at <https://www.maats.com/wp-content/uploads/2020/09/Brochure-CAT-594H-coloured.pdf> on March 20, 2023.

¹¹⁷ CAT 345GC Hydraulic Excavator found at <https://s7d2.scene7.com/is/content/Caterpillar/CM20181214-35962-39643> on March 20, 2023.

¹¹⁸ CAT D8T Track-Type Tractor brochure found at <https://s7d2.scene7.com/is/content/Caterpillar/C658733> on March 20, 2023.

The depth of cover near the release location was approximately [REDACTED] as recorded during the 2013 integrity dig (see Figure 75) and again in 2017 when a depth of cover survey was performed in the Mill Creek area (see Figure 76). The FEA showed that once the pipe was tied-in and backfilled, the overburden loads with [REDACTED] of settlement below the pipe were large enough to cause ovalization of the TAG 98 bend assembly.

A bending strain analysis was performed post-incident and reported a [REDACTED] vertical bending strain about [REDACTED] downstream of GWD 13530 (see Appendix C). This amount of strain is less than the buckling strain [REDACTED] of an unsupported [REDACTED] long span of [REDACTED]-inch wall thickness pipe – which was confirmed by the lack of a midspan buckle in the caliper data. This amount of strain corresponds to a bending stress of [REDACTED] which is well within the elastic range. The bending moment at the ends of such a span would be of similar magnitude. This magnitude of bending and the [REDACTED] inches of upspring in the pipe upon excavation points to some post-installation soil settlement but not enough to completely explain the deformations seen at the heavy wall elbow and pup. As with the other potential loading scenarios during installation of the replacement fitting, RSI could not conclusively determine if soil settlement was causal to the plastic deformation experienced by the TAG 98 (BND 350) bend assembly.

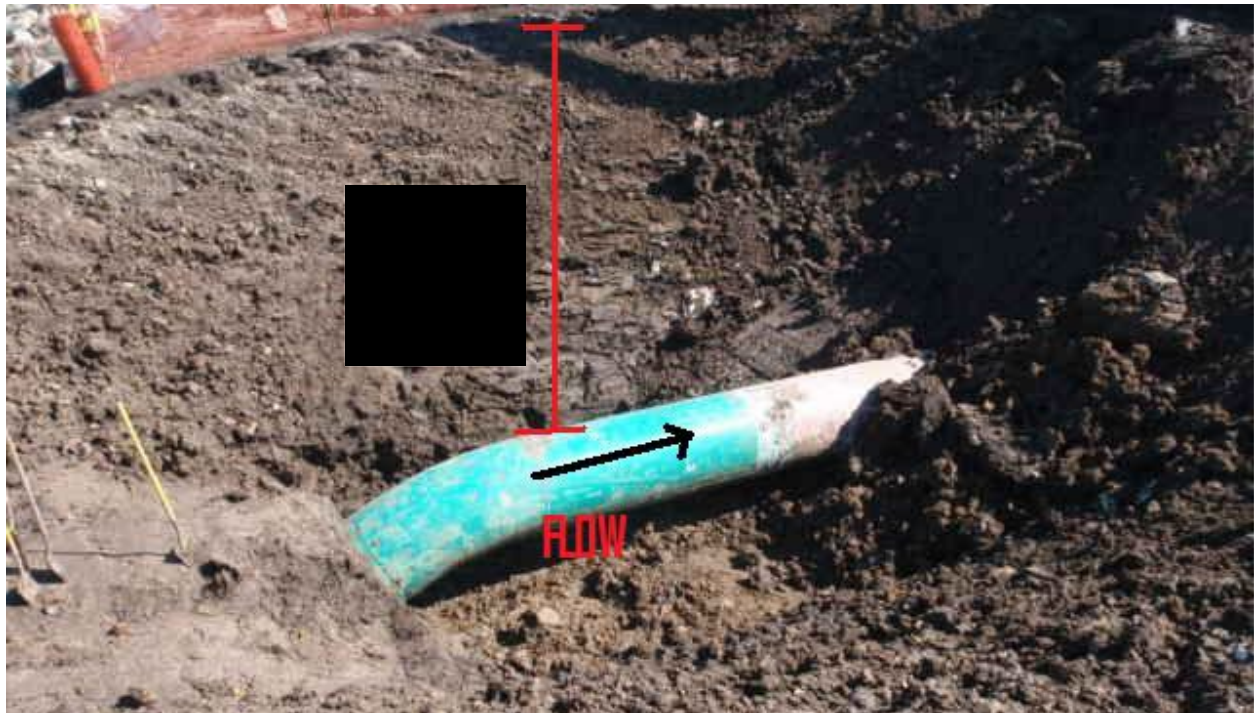


Figure 75. Photo of TAG 98 (BND 350) During March 2013 Integrity Dig Showing a Depth of Cover of [REDACTED]

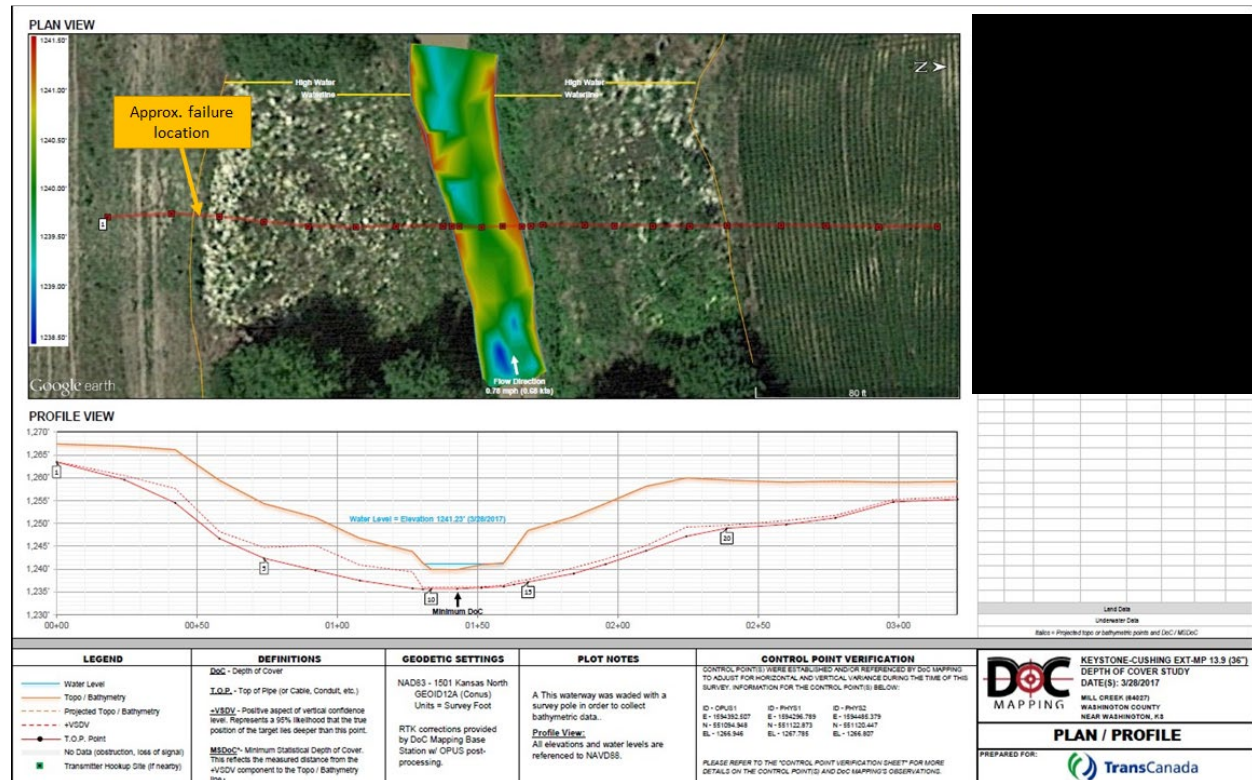


Figure 76. Depth of Cover Survey in the Mill Creek Area (March 28, 2017)

5.1.4.5 Other External Loads

Weather and outside force (WOF) baseline surveys are conducted approximately every 10 years for the Keystone Pipeline. The last survey¹¹⁹ was completed in January 2022. This study identified a low liquefaction¹²⁰ hazard in the floodplain area of Mill Creek based on colluvial sediments. Low liquefaction hazard areas are monitored via the baseline assessments, but no other extra actions are taken. The potential for a landslide event, surface loading from a nearby two-track road, or pipe exposure from scour were evaluated but eliminated as potential causal factors. The evidence to support this conclusion is discussed below. No other geotechnical hazards were identified near the incident location.

5.1.4.5.1 Landslide

Post-incident, geotechnical SMEs travelled to the site to ascertain if the failure may have been caused by ground movement. Based on observations from their site visit¹²¹ on December 13, 2022, the geotechnical SMEs concluded that there were no signs of active ground movement on the hillside that could be impacting pipeline integrity. They further concluded that a landslide would be unlikely because the slope of the hill was not severe (about a 10° slope angle), and the soils are competent, stiff to hard clay. Reviews of prior IMU data were also completed and

¹¹⁹ Golder Associates, Phase I Geologic Hazards Assessment Update, Keystone Mainline and Cushing Extension Pipelines, Midwestern United States, January 18, 2022.

¹²⁰ As reported by Golder, liquefaction involves the transformation of granular material from a solid to a liquefied state as the result of increased pore-water pressure and reduced effective stress, generally during strong seismic events.

¹²¹ TC Energy Memo, Geotechnical Assessment of NPS 36 Keystone Mainline Leak at MP 14, January 16, 2023.

there were no obvious strain changes¹²² or pipeline movement identified between the 2013 and 2018 runs and a bending strain analysis indicated no strain change signals over the 0.1% reporting threshold. In addition, the location of the wrinkle feature in the upstream pup is mechanistically inconsistent with ground movement in the form of landslide activity which would cause tensile forces rather than the compressive forces needed to wrinkle the pipe. For these reasons, ground movement in the form of a landslide was eliminated as a potential cause of the bending loads.

5.1.4.5.2 Vehicle Loads

As shown in Figure 77, a two-track road running east-west crosses the pipeline approximately 9-ft downstream of the release location. The road is “closed” and is not maintained by the township but heavy farm-type equipment (tandem axle semi-truck, tandem axle grain trailer, and John Deere S670 combine; ~36,000-lb loads) crosses the uncased pipeline at a frequency of approximately 12 times per year each¹²³. The cyclic loads from vehicular traffic were considered to determine their potential impact. With a lateral distance 9-ft away and a depth of cover at the TAG 98 bend assembly of [REDACTED], the cyclic loads from vehicular traffic were likely minimal. Therefore, vehicle loads were determined not to be a causal or contributing factor to the MP 14 Incident.



Figure 77. Aerial View of Site Highlighting the Two-Track Road Near the MP 14 Incident

5.1.4.5.3 Pipe Exposure

The Mill Creek crossing used open cut construction methods to install the pipeline and per Section [REDACTED] of the DBM [REDACTED]

[REDACTED] The TAG 98 overbend was installed sufficiently far from the edge of the Mill Creek banks to not be at risk of exposure from avulsion or lateral scour¹²⁴.

The Mill Creek crossing was surveyed in March 2017 and the data was used to perform a screening hydrotechnical analysis of the crossing. The analysis identified that the Mill Creek

¹²² Indications of minor, localized pitch and azimuth changes were apparent in the plots and are also seen in the vertical and horizontal strain plots just upstream of GWD 13520 but were most likely attributed to localized minor differences between the pig trajectory and pipe when the pig traveled through the elbow.

¹²³ TC Energy Form, Excerpt from Heavy Equipment Crossing Information Form, 2023.

¹²⁴ Memo, KeyUS Cushing Extension – MP 13.9 – Mill Creek Crossing (64029), November 2, 2022.

crossing could potentially become exposed in a 1:100-year return period flooding event but without an associated pipe integrity impact. Though the analysis was meant to be conservative, the WOF threat assessment team had some experience where this may not necessarily have been the case. Therefore, a more detailed analysis was conducted which included field assessment results.

The refined assessment included the site visit findings, flood frequency analysis, velocity calculations, and vertical scour depth estimates. This analysis estimated a 1:100-year return period scour depth of 6.9 ft (2.1 m) which is below the top of pipe elevation but not enough to undermine the pipe. As shown in Figure 76, the minimum depth of cover near the center of the creek is approximately [REDACTED] to the top of pipe. Including the pipe diameter of 3 ft (0.9 m), a scour depth of 7.2 ft (2.2 m) would be needed before a portion of the pipe might be exposed. Regardless, the pipe would not be suspended and therefore not susceptible to hydrotechnical hazards such as vortex induced vibration (VIV). Moreover, the creek section contains a concrete coating to minimize buoyancy which, based on Reynolds Number calculations, would be in the turbulent or aperiodic wake regime and therefore not a concern for vibration.

5.1.4.6 Construction Caliper (October 2010)

A caliper ILI was conducted in October 2010 using the TDW caliper technology. The intent of the inspection was to identify any construction-related defects (such as dents or ID restrictions) that exceeded allowable limits. Should any such defect be found, the construction contractor would be responsible for rectifying it. Since the TAG 98 bend assembly was installed in December 2010, this ILI would not have provided any information related to the ID restriction found in 2012. Prior to commencement of operations, another construction caliper was not run after the fitting replacement project nor was it required by procedures¹²⁵. This led to the TAG 98 ovality going unnoticed and unrepaired after replacement construction was complete and was determined to be causal to this incident.

5.1.4.7 Causal Factors and Root Causes - Installation

Factors during construction likely contributed to the large bending stress applied to the TAG 98 bend assembly which in combination with the design of the 3D elbow and taper transition joint most likely caused crack initiation at the LOF in GWD 13530 (CF2). Postulated scenarios included loads introduced during the construction hydrostatic test, fit-up of the final tie-in weld, and backfill and compaction activities with the pipeline poorly supported. First, hydrostatic testing was performed while the creek portion of the new installation was restrained with approximately 5-ft of cover and the TAG 98 (BND 350) bend assembly and downstream piping were unrestrained (per ASME B31.4). This configuration could have allowed for the development of a significant bending moment at the TAG 98 (BND 350) elbow and caused the elbow and pups to ovalize and the upstream pup to wrinkle. Second, though attempts were made to ensure that fit-up during final tie-in was precise, there always remains the possibility that alignment was not precise. Therefore, it is plausible that additional bending stress was

¹²⁵ Regulations, the Special Permit, and TC Oil construction specifications do not contain any requirements for repeating construction caliper ILI if significant changes are made after original construction is complete and a construction caliper ILI tool has already been run,

applied over a long moment arm when the final tie-in at GWD 135990 (9GT-035) was made. Third, some post-construction soil settlement likely occurred as evidenced by the [REDACTED] vertical bending strain identified by IMU and the 6-inch lift observed during post-incident excavation which could also have contributed to the bending loads. Weak foundational support combined with soil overburden and the possibility of construction vehicles driving over the pipeline during restoration could also have caused the bending stress in TAG 98. The postulated scenarios point to lapses in construction oversight and control of construction quality processes to minimize pipeline bending stress (RC2).

The ovality of the elbow and wrinkle in the upstream pup is best explained by certain loadings postulated to have occurred during construction while replacing the elbow at the failure site. It is difficult to provide positive proof that the postulated overload was the primary causal factor, but the overload condition could have contributed to the failure occurring when it did in the following ways:

1. The PAUT NDE of the welds at Anderson Lab appears to show indications of root pass LOF in both welds that were larger around the upper part of the pipe section compared with the lower part, consistent with a large bending load as postulated to have occurred during construction. Although the magnitude of root pass LOF *where metallographic sections were made* did not match the PAUT indicated sizes, the construction loading may still have contributed to opening, extending, or initiating cracking around the upper part of the pipe section.
2. A component of the postulated loading could have persisted as a steady-state or sustained bending moment in tension on the outer portion of the elbow and the girth welds in the upper portion of the pipe section. That sustained tensile stress would be additive to the cyclical stresses due to fluctuations of internal pressure and thermal expansion. While that does not change the magnitudes or frequencies of stress cycles, it would tend to increase the R-factor, the ratio of minimum to maximum stresses, for both pressure and thermal cycles. As R increases, the cyclic crack-tip stress-intensity threshold for fatigue crack propagation decreases. This would allow the smaller-magnitude pressure or thermal stress cycles, which are more numerous than larger cycles, to contribute to crack growth early in the crack growth history while the crack was still quite small. Like an investment growing at a compound interest rate, a slightly larger initial contribution has a large effect when compounded over time. The contribution of even the smallest stress cycles right away would have the effect of higher apparent crack growth rate parameters C and m .

Causal to the ovality not being identified at the time of installation is the fact that a construction caliper run was not repeated (CF3). The original construction caliper ILI was completed October 2010 prior to the TAG 98 replacement. Another caliper run was not completed until December 2012 which identified the ID restriction (due to ovality). Even though it was not a procedural or regulatory requirement, had the construction caliper ILI been repeated at the time of replacement, the ID restriction would likely have been discovered and could have been repaired. Company SPAC did not address the issue of re-running a construction caliper ILI for

significant modifications to the pipeline after completion of the original construction activities to identify construction-related damage (RC3).

Table 24. Summary of Causal Factors and Root Causes – Installation of TAG 98

Effect	Causal Factors	Root Causes
Large Bending Stress Introduced in TAG 98 (BND 350) Initiated Crack at LOF	CF2: Construction practices (e.g., during hydrostatic testing, fit-up, backfilling, and compaction) during the replacement of the TAG 98 (BND 350) elbow assembly led to the introduction of a large bending moment at the overbend.	RC2: Lapses in construction oversight and quality control during the fitting replacement project led to bending stresses going unnoticed.
Construction Caliper Run Not Repeated	CF3: Construction caliper re-run was not required for the fitting replacement project.	RC3: SPAC did not address the issue of re-running a construction caliper ILI after significant pipeline modifications were made along the Cushing Extension to identify construction-related damage.

5.1.5 Operations

Fatigue is a process of incremental subcritical crack growth that occurs due to repeated cycles of applied load or stress. As discussed previously, fatigue crack growth is typically apparent on a fracture surface by the presence of “beach marks” or parallel semi-elliptical markings emanating from one or more points of origin. These mark the progression and direction of incremental crack growth. The fracture surface may also exhibit “ratchet marks” which are small ridges oriented in the direction of crack growth, which represent the convergence of portions of the fatigue crack that are not perfectly aligned in the same plane at the point(s) of origin. Multiple fatigue crack initiation sites (as evidenced by ratchet marks) and [REDACTED] distinct beach marks were identified by Anderson in all three cracks confirming progressive crack growth. SEM examination confirmed that very early incremental crack fronts originated from the shallow LOF regions.

According to API 1104, “the enlargement of weld imperfections due to fatigue is a function of stress intensity, cycles of loading, imperfection size, and the environment at the crack tip.” As reported by Dong, et. al.¹²⁶, factors affecting stress at the weld root include axial misalignment, weld root angle, and root bead width. As summarized in Section 4.3, stress concentration from the bending load at the LOF within the transition weld geometry was sufficient to initiate a crack in GWD 13530. Once the crack initiated, the subsequent thermal and pressure cycles during operation grew the crack until the remaining ligament could no longer support the applied loads.

¹²⁶ Dong, Y., Ji, G., Fang, L., and Liu, X., Fatigue Strength Assessment of Single-Sided Girth Welds in Offshore Pipelines Subjected to Start-Up and Shut-Down Cycles, Journal of Marine Science and Engineering, 2022.

Several lines of inquiry were investigated to determine how fatigue may have contributed to crack initiation and growth at the GWD 13530 (G59B). The investigation evaluated the combined effect of pressure and temperature cycles on crack initiation and fatigue crack growth.

5.1.5.1 Flow Capacity Increases

As discussed previously, in 2016 TC Oil initiated a project to increase the flow capacity of the Keystone Pipeline from [REDACTED] to [REDACTED] and then again to [REDACTED] in 2020 (see Figure 78 illustrating flowrate changes). Ramp up testing to [REDACTED] was initiated in December 2022, only a few days prior to the MP 14 Incident. The goal of the ramp test was to collect data on pressures, temperatures, pipe vibration, noise levels, power draw, etc. as well as how the increased flowrate impacted daily operations in the Control Room. During the ramp up test, a leak detection ILI tool was also being run in the KS10 segment¹²⁷ - this ILI was being run independent of the ramp up test. According to interview statements, a check valve was locked open to allow passage of the ILI tool. Coordination between these project activities did not occur except to make sure that the operating parameters were suitable for the tool being run – both projects were aware of one another, but the overlap of activities was not identified as a concern. The ramp up testing and ILI run could not be completed because of the release.

For each capacity increase, a Project was initiated, and the Project Manager (PM) brought in each engineering discipline under the Project Team. Team members included personnel from facilities, pipeline terminals, electrical infrastructure, instrumentation & controls, engineering, pipeline integrity, hydraulics, control center operations, leak detection, environmental, and emergency response. The work that occurred prior to increasing the system capacity included, but was not limited to, EAs, risk assessments, PHAs, stress analyses, control room workload studies, SCADA and leak detection system studies, and emergency response studies to understand the implications that the capacity change may have on the system. The Project Team evaluated the risks associated with each rate increase and performed engineering studies to determine how to mitigate the risks so that safe operation of the pipeline at the target flowrates was maintained. Execution and mitigation plans were in place prior to conducting ramp up testing and were presented to the senior leadership team for sign off. Then, as ramp up testing commenced, enhanced inspections, awareness, and monitoring were in place to make sure the EAs held true in a real-world scenario – the ramp up test was used to validate all the engineering work.

Of particular concern during the capacity increase projects was the impact on operating temperatures, pressures, and associated pipeline stress (as well as vibration at facilities from higher flow velocities and the potential for increased release volumes should a spill occur). Significant planning went into understanding the impacts on pipeline stress at the new flowrates. Mainline pipe stress analyses had been completed to support the capacity increase projects and operational changes on Keystone. These analyses identified potentially high stress locations

¹²⁷ Timing of ILI tool runs is established to comply with 49 CFR 195.452(j)(3), Assessment Interval, which requires operators to establish five-year inspection intervals, not to exceed 68 months, for continually assessing the line pipe's integrity. An operator must base the assessment intervals on the risk the line pipe poses to the HCA to determine the priority for assessing the pipeline segments.

along the Cushing Extension (primarily elbows), where bending stresses exceeded or nearly exceeded safety factors (von-Mises stress below 95% SMYS). In addition, EAs¹²⁸ were conducted to understand the impact of interacting threats on the FFS of the pipeline at these higher stress locations.

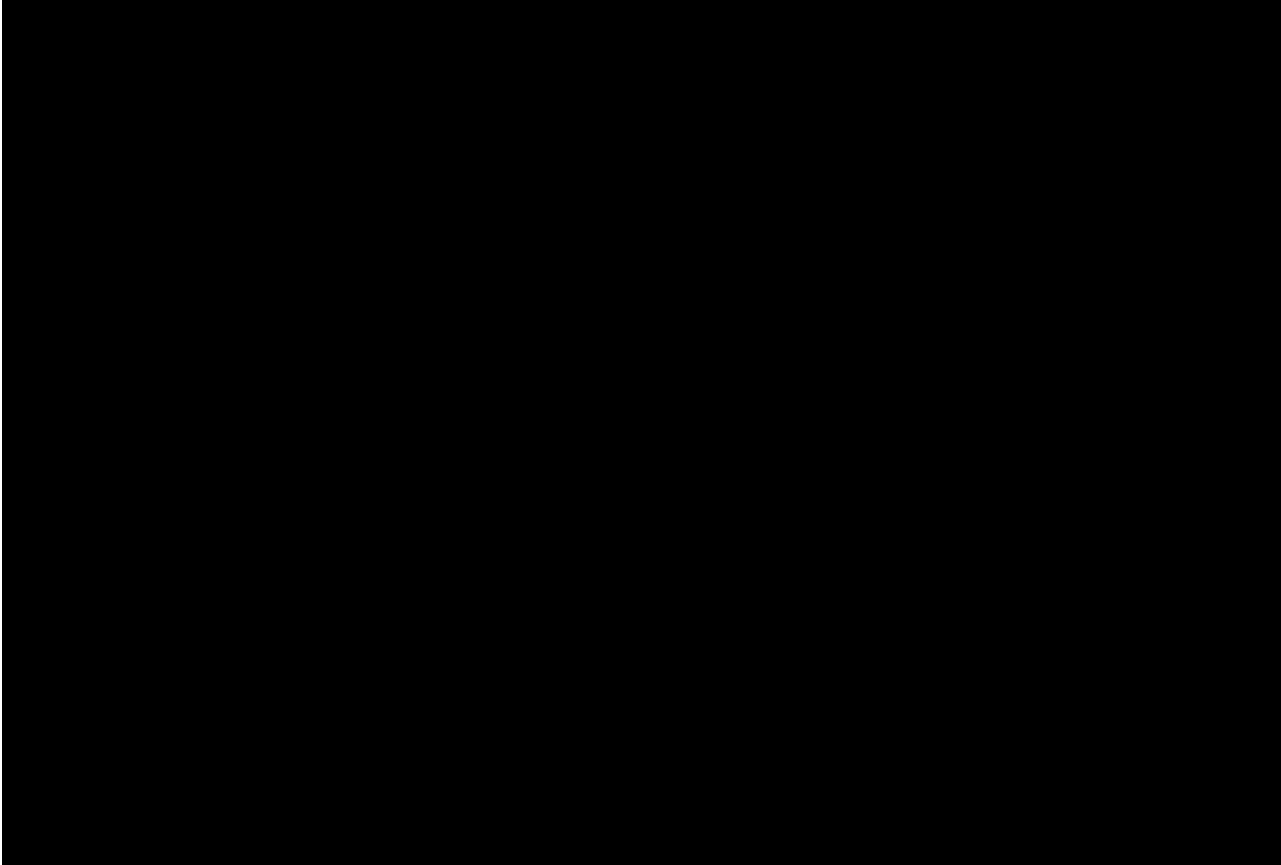


Figure 78. Flowrate Data Steele City to Hope

The EAs considered the potential for girth weld defects from construction based on learnings from the Freeman +4 incident. Analyses used information from the 2018 BHGE MFL4 ILI technology which was configured to detect certain girth weld anomalies, specifically targeted at transition welds. Review of the MFL4 data revealed no reportable girth weld anomalies (cracks or other anomalous volumetric indications) in the welds joining the elbows to adjacent pipe along KS10 and KS11. Therefore, this threat was determined to not degrade the permissible maximum stress criterion. As will be discussed in Section 5.2.3, this tool has fairly broad probability of detection (POD) specifications at the 90% confidence level. Knowing this, it may have been beneficial to run sensitivity analyses to understand how (1) an acceptable girth weld flaw (one that would pass API 1104 criteria) or (2) a girth weld flaw below the POD thresholds of the MFL4 tool might impact the stresses at the higher stress elbows. Or, alternatively, specify a more restrictive safety factor on the acceptable von-Mises stresses such that girth weld imperfections would not be a concern.

¹²⁸ Engineering Assessment of the Combined Stresses from Steele City B PS to Cushing South PS in Consideration of [REDACTED] Capacity Increase, Rev 0, March 31, 2021.

Similarly, the ovality in the TAG 98 (BND 350) elbow was considered in the EA. The ovality was not constrained to only the elbow fitting but spanned across the pup-elbow-pup configuration – evidence of a closing in-plane bending moment in-service. No axial cracks were reported during the 2020 NDT Eclipse crack detection ILI and no girth weld cracks were reported during the 2018 MFL4 ILI. The EA recommended that TAG 98 (BND 350) be reassessed with a high-resolution caliper tool while operating at the increased flows and with peak ground temperatures to determine if the ovality deformation was stable or changing. The failure occurred before this inspection could be completed but even if this inspection did occur, it likely would not have noted any significant changes to the ovality since it was not caused by operational stresses.

The EAs recognized the potential risk of elevated stresses at elbows as system flowrates were increased but did not go far enough to consider the stress concentrating effects at weld imperfections when determining the combined stress level. As such, the safety factor may not have been stringent enough or real-world conditions were not appropriately modeled. The capacity increase projects, and associated analyses, were not causal to this incident. However, had the stress concentrating effects from weld imperfections been included, additional field investigations for the higher stress elbows may have been triggered to ensure that the girth welds were sound prior to commencing with ramp-up activities.

Although not causal, the investigation did find weaknesses in the coordination of the ramp-up testing activities with the leak detection ILI team. The risk of running an ILI tool during the ramp up test was not fully vetted and as such a check valve was locked open on the day of the incident to allow passage of the ILI tool. It is unclear if having check valve locked open contributed to the severity of the release but at the very least, the teams should have been coordinating activities such that they were not being performed concurrently to avoid the potential for increased risks and errors.

5.1.5.2 Thermal Loads

According to the Guidelines for the Design of Buried Steel Pipe¹²⁹, “movement of a buried pipeline can occur at the apex of sidebends, sagbends, and overbends. This movement can be caused by either a net outward force generated by internal pressure, or expansion caused by temperature increases. The resulting forces are resisted by the pipe bending and axial stiffness and by the soil bearing and shear resistance. Soil resistance is a function of burial depth, backfill material type, and level of compaction.”

As identified in the PHA for the [REDACTED] capacity increase project, the Steele City PS has the [REDACTED] in the Keystone Pipeline between [REDACTED] and [REDACTED].¹³⁰ The Project Team evaluated the potential for incremental temperature increase (above [REDACTED] but less than [REDACTED]; [REDACTED] and [REDACTED]) in the pipeline due to the increased flowrates and recommended that stress analyses be performed to understand the effects. Condition 16 of the

¹²⁹ American Lifelines Alliance, Guidelines for the Design of Buried Steel Pipe, July 2001 (with Addenda through 2005).

¹³⁰ Critical Workspace Solutions, Keystone Pipeline [REDACTED] Flow Rate What-If Report, July 18-19, 2022.

Special Permit requires that the pipeline operating temperatures must be less than 150°F (65.6°C). The Pipe Integrity team performed a mainline stress assessment of the entire Keystone Pipeline and created a temperature management plan¹³¹ based on the results. The maximum allowable discharge temperature (MADT) limits at pump stations were set to maintain stress levels at or below 95% SMYS at the identified higher stress elbows and bends. The MADT limits downstream of Steele City were lowered from [REDACTED] to [REDACTED] ([REDACTED] to [REDACTED]) as an enhanced safety margin during the ramp up testing because [REDACTED] bends were found with combined stress levels exceeding 95% SMYS at the higher MADT.

The PHA, supporting stress analyses, and EAs considered the impact of the flowrate change to known pipeline threats, including manufacturing-related flaws, girth weld flaws, and ovalities, among other threats. The TAG 98 elbow combined stress was predicted to be less than 90% SMYS and therefore would not have required any special attention. However, other elbows downstream of Steele City PS did have combined stresses exceeding the 95% SMYS criterion and therefore temperature limits were placed on the pipeline segment.

Though detailed stress analyses and EAs were performed prior to increasing capacity to ensure that the pipeline operating stresses remained within acceptable levels, these analyses failed to consider girth weld imperfections as potential stress concentrating factors and the potential for fatigue to occur at an initiating flaw. As discussed in Section 4.3.5, the magnitudes and frequency of occurrences of thermal and pressure cycles were sufficient to initiate and propagate a fatigue crack from the LOF features observed in the metallographic sections. Improvements to stress analyses and EAs for capacity increase projects should be considered to address when fatigue could be a concern at transition girth welds connecting pups and fittings and the potential need for more stringent safety factors.

5.1.5.3 Internal Pressure Loads

The Steele City discharge pressures for 2022 are shown in Figure 79. Since operations began in February 2011, the KS10 segment has never operated above 72% SMYS. At the time of the rupture the pipeline was operating at 1,210 psig (8,343 kPag) – 84% MOP (67% SMYS). Approximately 12-minutes before the rupture occurred (about 19:39 MST), Controllers placed the Hope PS on bypass mode to allow passage of the P2D ILI which caused a transient pressure wave upstream (normal for this type of operation). Pressures were still increasing at the time of the rupture (see Figure 80) but not more than the MOP. This pressure spike contributed to the failure only because the girth weld fatigue crack had grown large enough that the failure pressure was reached at 1,210 psig.

Condition 44 of the Special Permit required an annual fatigue analysis to validate the pipe reassessment interval for the first five years of operation and Condition 45 required that these analyses be revisited two years after the pipeline in service date on the most severely cycled pipeline section to determine the effect of growth on flaws that passed manufacturing standards and installation specifications. Though TC Oil has an active pressure cycle management

¹³¹ Technical Memorandum, Maximum Allowable Discharge Temperature Limits in Consideration of [REDACTED] Flow Rate Ramp Test, November 4, 2022.

program, pressure cycling is generally not a concern for circumferentially oriented girth weld flaws because of the significantly reduced hoop stress (typically 30% of the actual hoop stress) acting in the axial direction.

The flow capacity increase PHA identified the risk from increased pressure cycling which was evaluated by the Pipe Integrity team. The Pipe Integrity team was monitoring the pressure cycles on the mainline and updating the integrity program as required to maintain the same level of risk (e.g. decreased pipeline inspection intervals). The [REDACTED] ramp up testing was to be used to provide additional information to the Pipe Integrity team on the pressure cycling implications and to recalculate reinspection intervals based on the results. Though pressure cycling was a concern, it was likely only a consideration for axial crack-like flaws and not circumferential crack-like flaws. As discussed in Section 4.3.5, fatigue from thermal and pressure cycling contributed to crack growth. Improvements to stress analyses and EAs for capacity increase projects should be considered to address when fatigue could be a concern at transition girth welds and the potential need for more stringent safety factors.

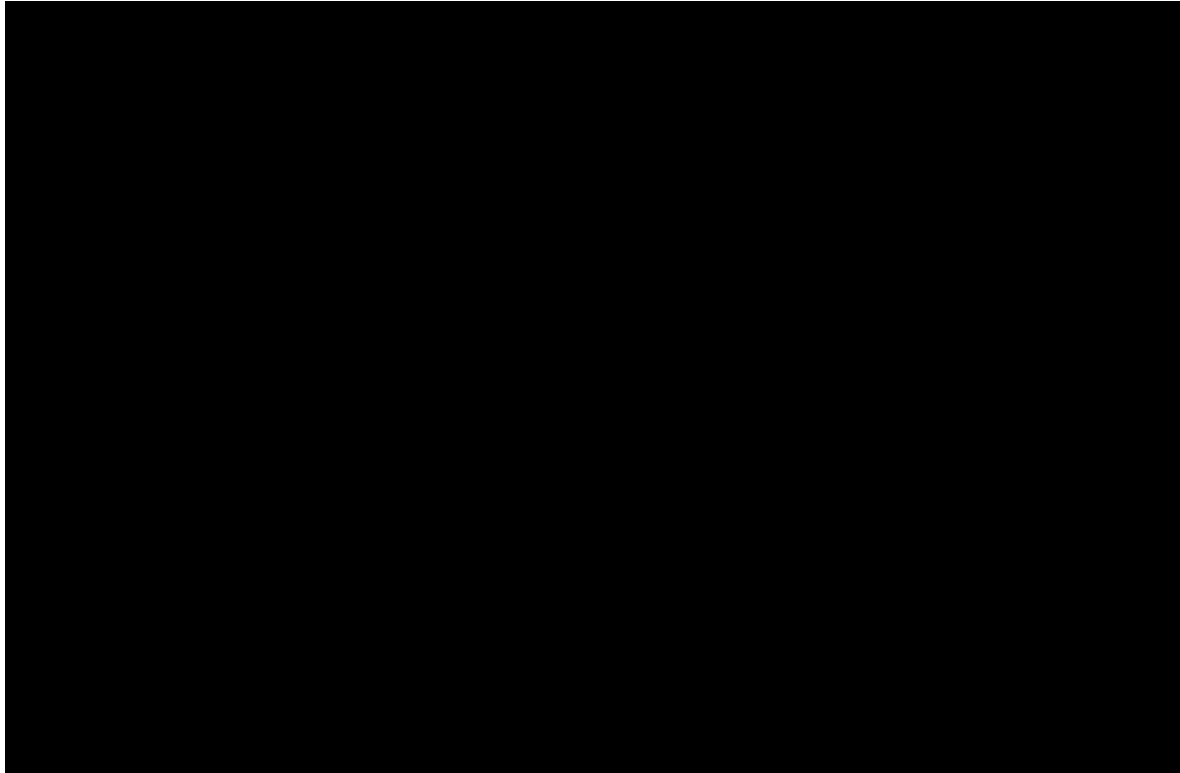


Figure 79. Pressure Spectrum for Steele City Mainline Discharge – 2022

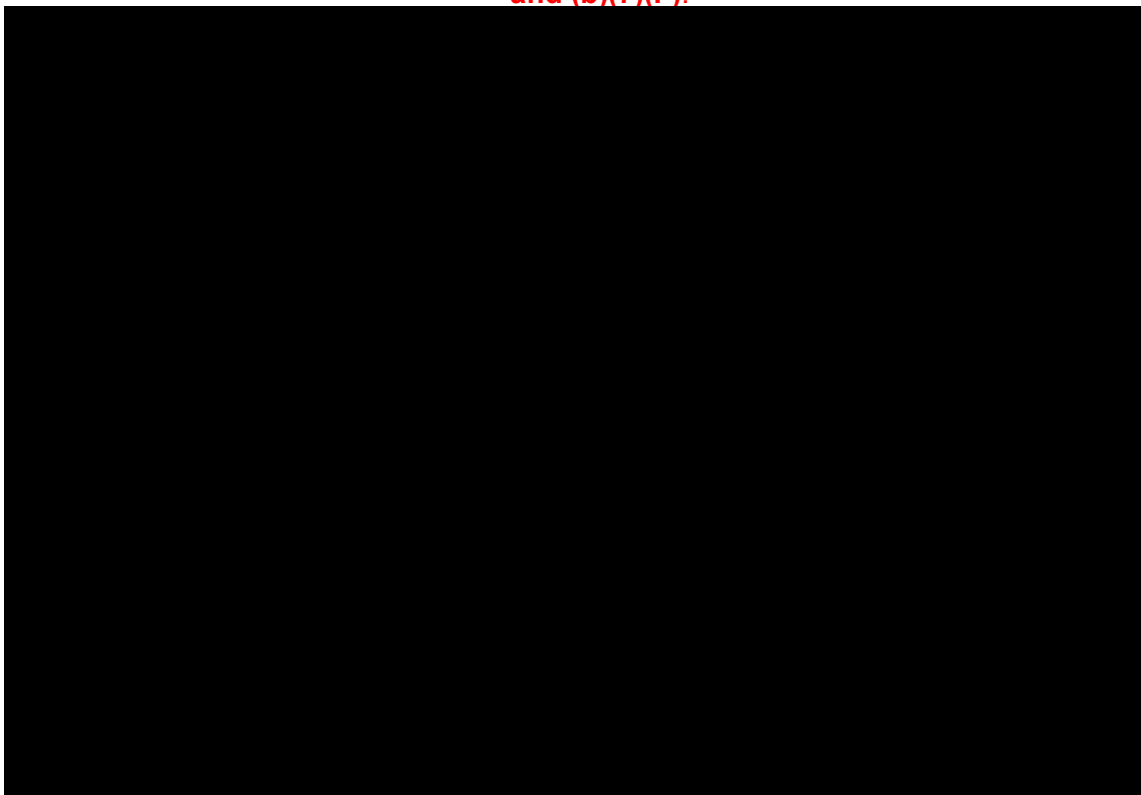


Figure 80. Pressure Profile Just Before Rupture of GWD 13530

5.1.5.4 ILI Loads

The investigation team considered the possibility that inertial loads from running of ILI tools through the TAG 98 (BND 350) elbow could have contributed to the progressive crack growth. Four ILI tools have been run through the KS10 segment, one profile caliper tool, two combined MFL/caliper/IMU tools, and one UTCD tool. In addition, leak detection and/or cleaning tools are sent through the line annually. Therefore, the elbow has been subjected to loads from ILI tools approximately 15 times. The inertial load depends on the weight of the tool, tool speed, and drag. With the weights of typical MFL and UTCD tools, the inertial force through a 30° angle change is not expected to be high enough to contribute to crack growth. RSI considered the weight of a 5,000-lb tool traveling through the bend at a velocity of 6 ft-sec. The resulting thrust loads¹³² were only 1,420 lb in each tangent which results in a trivial axial stress in the pipe. ILI loads are neither large enough nor frequent enough to have contributed to the incident.

5.1.5.5 System Wide Risk Assessment (SWRA)

Given the girth weld failure at Freeman +4, welding or fabrication/construction related defects are initially considered a threat of concern (TOC), pending their baseline assessment using a suitable ILI technology such as the BH MFL4 tool. KS10 was inspected with the MFL4 technology in 2018, and no girth weld anomalies were identified within 500-ft of the incident location.

¹³² RSI was unable to determine the contribution from re-rounding and opening moment forces due to the restriction. These factors depend on a tool's resistance to traversing a deformation in a pipe which can vary with tool design and speed.

TC Oil's System Wide Risk Assessment (SWRA) A large, solid black rectangular redaction box covers the majority of the page content, starting below the title and ending above the final paragraph.

In addition, conventional pressure-cycle-induced fatigue analyses only pertain to axial crack-like flaws. The effect of fatigue in girth welds with defects that elude detection are not considered in the fatigue studies used for the Special Permit application nor in TransCanada's SWRA – which is not unusual. However, at high stress elbows with weld transitions, monitoring of fatigue conditions might be warranted.

5.1.5.6 Contributing Factors and Items of Note - Operations

Though stress analysis and EAs were performed to understand and mitigate any potential increases in pipeline stress, shortcomings were identified in the methodologies used. Specifically, girth weld imperfections were not included in the analyses (CTF4). For the elbow that failed, it experienced temperature and pressure cycles that alone may not have been a concern. However, in combination with a shallow, surface-breaking flaw at the toe of the transition girth weld and a bending stress sufficiently large to initiate a crack, the cyclic stresses were enough to grow a crack to failure (CTF3).

Acknowledging that it is impossible to consider every possible scenario in engineering assessments, at the time the capacity increase projects were started in 2016, the Freeman +4 failure in South Dakota had occurred and been investigated. Findings from that investigation showed there was high-low at a transition weld that caused an area of stress concentration in the weld. As subsequent weld passes were installed, the stresses from heating and rapid cooling during the welding process were high enough to grow a crack from a notch-like LOF feature. The amount of high-low was acceptable per code and radiography also failed to find the tight, angled crack. With this knowledge, the engineering assessments at the elbows along the Cushion Extension should at a minimum have considered the potential for high-low at transition welds and possibly even considered an acceptable depth of weld imperfection per codes. Although the MFL4 tool was run in the affected segment and no notable flaws were found or

reported (even post-incident), the POD, POI, and sizing tolerances can be affected by the elbow geometry. In addition, the MFL4 tool requires cracks with some width (0.025-inch) for detection and the crack that caused this failure may have been below this detection threshold. The potential for missed flaws or flaws below the detection and reporting thresholds was overlooked in the engineering assessment (CTF5).

In absence of reliable girth weld crack detection ILI in the near term, TC Oil should consider revisiting the parameters used in the stress analyses, EAs, and SWRA to determine if they remain useful for future integrity planning based on the learnings from this investigation. The results from this evaluation could be used to define variables to include in future stress analyses or the need for targeted girth weld inspections in the ditch.

Although not causal, the investigation did find weaknesses in the coordination of the ramp-up testing activities with the leak detection ILI team. The risk of running an ILI tool during the ramp up test was not fully vetted and as such a check valve was locked open on the day of the incident to allow passage of the ILI tool. The teams should have been coordinating activities such that they were not being performed concurrently to avoid the potential for increased risks and errors (ION5).

Table 25. Summary of Contributing Factors – Operations

Effect	Contributing Factors
Thermal and Pressure Cycling Led to Crack Growth	CTF3: Thermal and pressure cycles led to crack growth until the critical flaw size was reached.
Stress Analyses and EAs did not Analyze Effects of Girth Weld Imperfections	CTF4: SPAC for stress analyses and EAs for capacity increase projects need improvement to address when girth weld imperfections should be considered or applying more stringent safety factors to account for the uncertainty of these real-world conditions.
Over-reliance on MFL4 Results	CTF5: EAs used the results of the MFL4 ILI to determine that the girth weld threat did not degrade the maximum stress criterion, but the analysis overlooked the potential for missed flaws or flaws below detection and reporting thresholds.

Table 26. Summary of Items of Note – Operations

Effect	Items of Note
Lack of Coordination Between Ramp Up Team and ILI Team	ION5: Ramp up testing and the leak detection ILI run were scheduled to occur at the same time. Coordination between the two project teams was not structured nor were the risks of concurrent activities addressed. Though causal factors were not identified specific to the girth weld failure, check valves were locked open to allow passage of the ILI tool which could contribute to the spill size.

5.2 Assessments and Monitoring

The Pipe Integrity team within TC Oil's Liquids Pipeline Operations Engineering is responsible for assessing pipeline FFS and implementing repair or remediation activities where needed. The Pipe Integrity team relies on several tools to assess pipeline integrity and identify potential threats, the foremost being ILI technologies¹³³. The data received from the inspection reports is used to prioritize and schedule pipeline excavations as well as to inform FFS engineering assessments. Excavations are conducted to evaluate the ILI results, to remediate or repair defects, and to examine the condition of the pipeline segment.

A variety of ILI technologies are routinely used by TC Oil as part of the integrity management program to assess the Cushing Extension for threats like metal loss, mechanical damage, and cracking. Different tools and technologies are employed depending on the type, orientation, and location of expected threats. ILI tools are designed to examine hundreds of miles of pipe for specific integrity threats during a single inspection. Each ILI tool vendor provides specifications that detail the POD and sizing accuracy for specific pipeline threats. Tools also have a POI that represents the uncertainty involved in post-processing and interpretation of the raw data through sizing and selection algorithms as well as feature characterization by data analysts.

Piggable segment KS10 spans the 145-mile length between the Steele City PS and Burns Pig Trap Station. Since operations began in 2011, TC Oil has conducted four different inspections of the affected segment using multiple tool types including: (1) caliper, (2) high-resolution MFL, (3) IMU, and (4) ultrasonic axial crack detection (see Table 27).

Table 27. ILI History for KS10

Tool Type	Tool Technology	Run Date
TDW Caliper	Construction Caliper	October 2010
BHI Profile	Low-Resolution Caliper	December 2012
BH Gemini	High-Resolution MFL, Caliper, and IMU	September 2013
BHGE MFL4	High-Resolution MFL, Caliper, and IMU	November 2018
NDT Eclipse	Ultrasonic Axial Crack Detection	September 2020

Although multiple ILIs of the affected segment were completed between 2010 and 2022, including a metal loss ILI in 2018 that had capabilities to detect some anomalous girth weld conditions, the LOF and fatigue crack in GWD 13530 was not discovered prior to the rupture. The 2012 profile and 2013 caliper surveys did report the ID restriction (due to ovality) and an investigation was performed in March 2013; however, the severity of the threat was underestimated in terms of its potential effect on girth weld integrity. Several possible sequences of events were postulated as shown in Figure 81 (detailed Cause and Effect Trees are provided in Appendix B). Causal factors were identified related to post-analysis of

¹³³ Condition 42 of the Special Permit required that a baseline ILI be performed within three years of placing the pipeline in service using a high-resolution MFL tool. Condition 43 required future ILI inspections on a frequency consistent with 49 CFR 195.452(j)(3) assessment intervals or on a frequency determined by fatigue studies based on actual operating conditions, inclusive of flaw and corrosion growth models.

assessment results. The limitations of ILI technologies in detecting girth weld cracks in a 3D bend was a contributing factor to the cracks not being identified. The selected assessment tools and the frequency of inspections were adequate for the identified threats and therefore determined not to be causal.

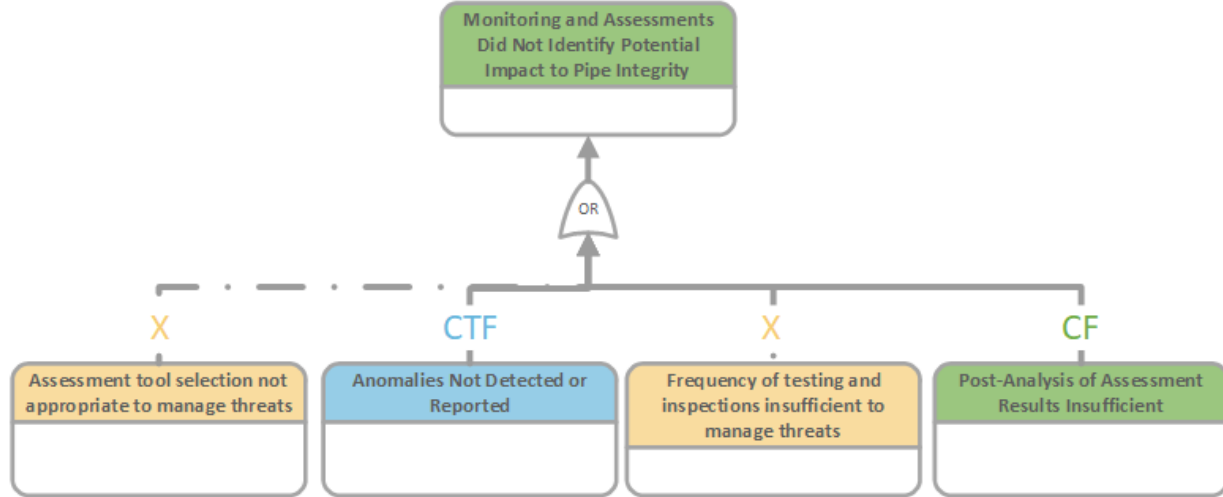


Figure 81. Simplified Cause and Effect – Monitoring and Assessments

5.2.1 2012 BHI Profile Caliper ILI

The BHI Profile caliper ILI was conducted in December 2012 to determine if the high-resolution GEMINI™ tool could successfully travel through KS10 without damage. The specified minimum nominal bore diameter of the tool is 34.25-inch and minimum local bore restriction is 10% OD. Its deformation detection and sizing capabilities are provided in Table 28.

Table 28. Deformation Detection and Sizing for BHI Profile Tool¹³⁴

Parameter	Dent ^(a)	Ovality ^(b)
Depth at POD = 90%	1% OD	
Depth sizing accuracy at 80% certainty	± 0.10-inch	± 0.10-inch
Width sizing accuracy at 80% certainty	± 6.30-inch	N/A
Length sizing accuracy at 80% certainty	± 1.42-inch	± 1.42-inch
Standard minimum reporting threshold ^(c)	2% OD	

(a) Dent = Dnon – Dmin – Ov

(b) Ovality = (Dmax – Dmin)/(Dmax + Dmin)

(c) Lower thresholds available

The 2012 inspection identified a 9% ID restriction (due to ovality) near the girth weld¹³⁵ that failed (see Figure 82) – the ID restriction had damaged the cleaner and gauge tools¹³⁶ sent through the line prior to the caliper inspection. As discussed previously, excavations for ovalities

¹³⁴ 36-inch PROFILE™ Tool, Tool Data Sheet, 2016.

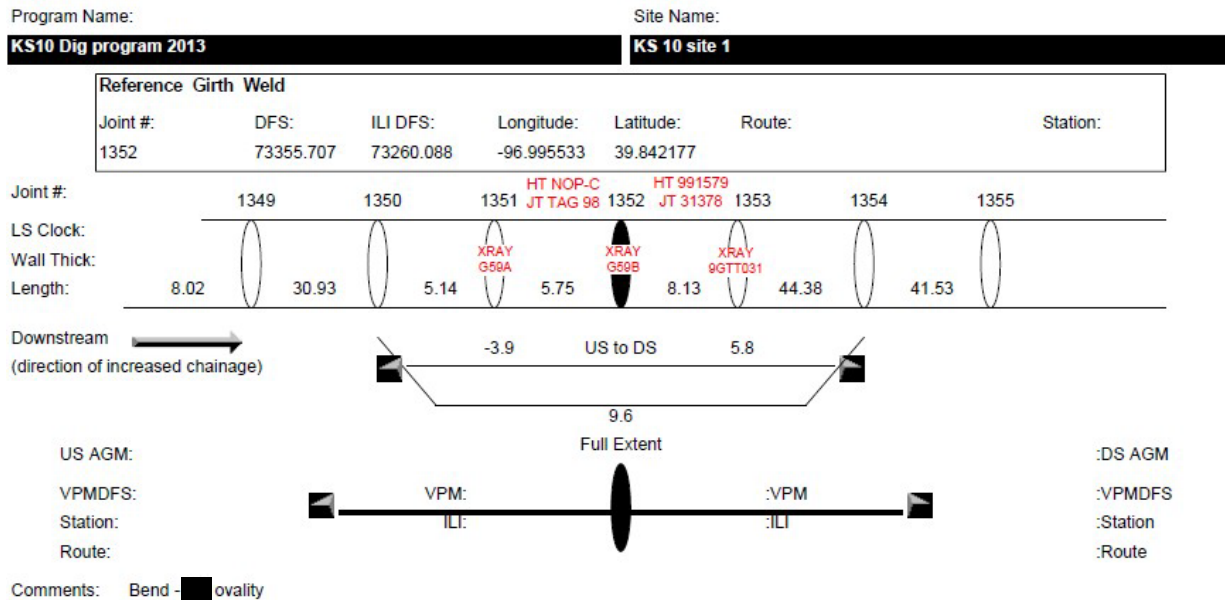
¹³⁵ The 2012 BHI Profile tool reference girth weld number was 1352 which corresponds with GWD 13530 and fabrication weld number G59B.

¹³⁶ When removed from the line, the cleaner tool's urethane cup was cracked and several plates were bent on the gauge tool.

are only required if there are concerns that ILI tool passage could be impeded, which was the case for this ID restriction. Therefore, the ID restriction was excavated in March 2013 to evaluate it (see Figure 83). The ovality was confirmed and measured at [REDACTED] of the OD¹³⁷ in the ditch and was determined not to be an integrity concern at the time. The bend assembly was backfilled without any further intervention.

While the excavation was still open, discussions occurred between the Pipe Integrity team and ILI vendor about how best to proceed. They evaluated several possible options including (1) having the ILI vendor modify their tool so that it would pass through the elbow, (2) using a multi-diameter tool, or (3) cutting out the ID restriction. The option to cut out the feature was escalated to senior leadership but determined not to be the most favorable option for safety and logistical reasons. Instead, the vendor agreed that they could navigate the feature with a tool redesign. Subsequent ILI runs successfully navigated the ID restriction without any significant issues.

Site Information Report - ILI: KS10 Steele City-Burns



¹³⁷ The maximum ovality OD was measured at [REDACTED]-inch and the minimum ovality OD was measured at [REDACTED]-inch

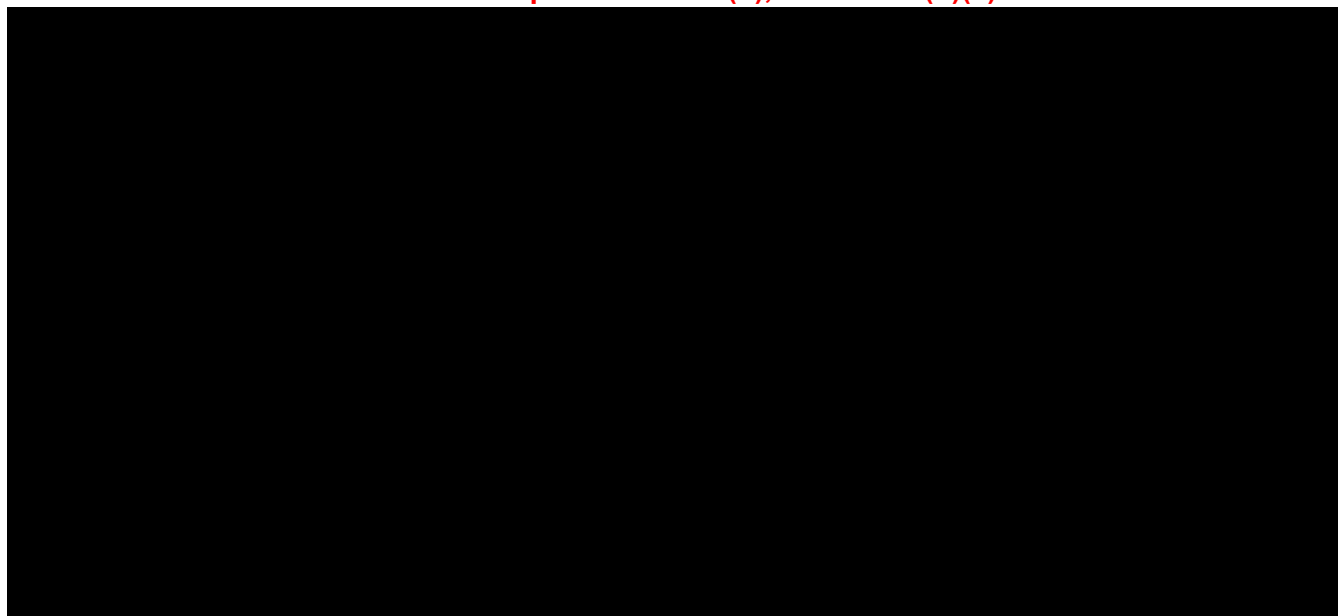


Figure 82. Dig Sheet for [REDACTED] ID Restriction Found at TAG 98

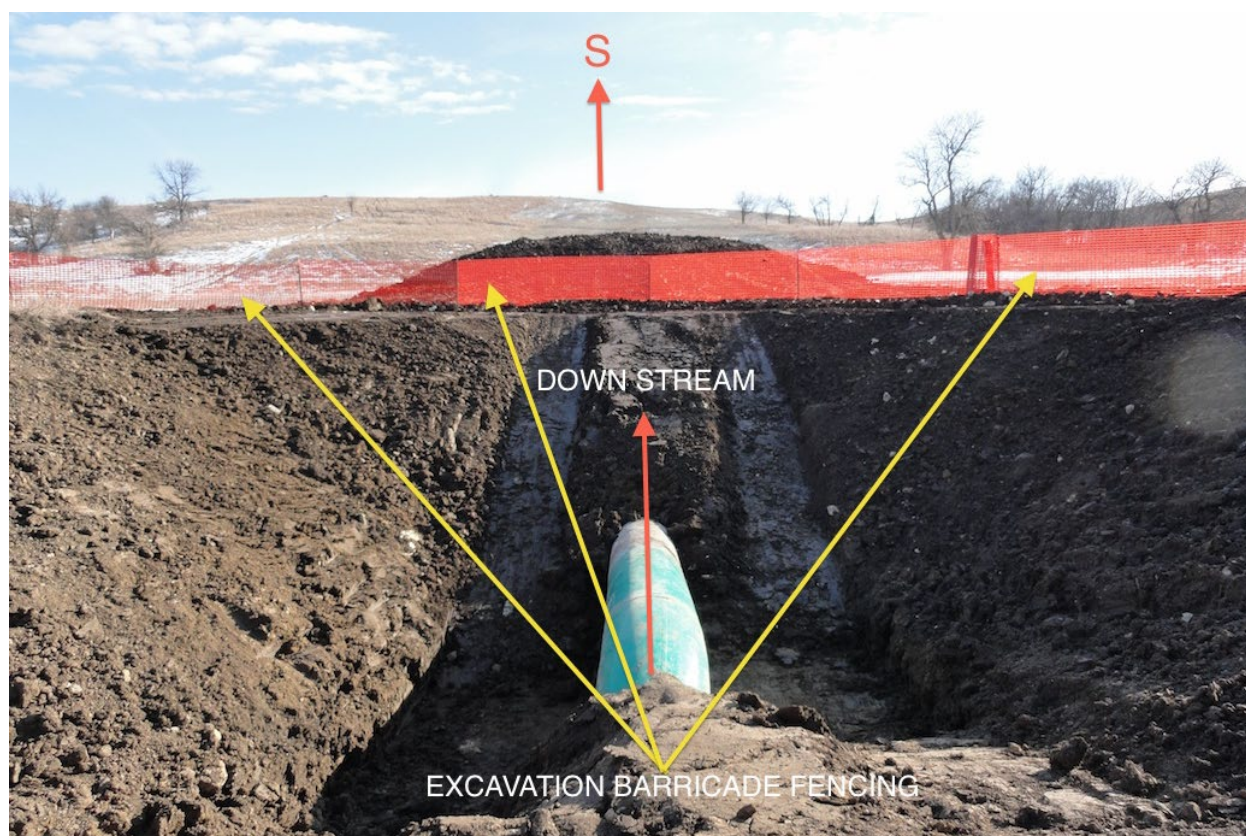


Figure 83. View of TAG 98 Looking South (Downstream) During 2013 Dig

A post-incident review of the 2012 caliper data in the location approximately six inches upstream of GWD 13520 does not show a clear indication of a wrinkle, which was subsequently confirmed by the ILI vendor. The only anomalous data at this location was that the ovality of the pipe at the 3 o'clock and 9 o'clock positions appear to be the greatest where the wrinkle was

later found, when compared to the pup further upstream and downstream. This was a low-resolution tool with only 16 circumferentially spaced caliper arms so there is not a lot of granularity in the data.

Industry standards and regulations do not provide a lot of guidance on how to respond to an ovality within a bend, aside from repairing it if it may interfere with internal inspections. In fact, regulators removed a requirement from the gas rule in 1984 for pipe greater than 4-inch OD that an ovality in a field bend could not exceed 2.5%¹³⁸. Justification for removal of this requirement was (1) it was more restrictive than current industry practice; (2) more stringent than the ovality limitation in pipe manufacturing specifications; and (3) the existing ovality restriction was based on an operating consideration (e.g., passage of internal cleaning and inspection tools) rather than a structural integrity consideration. The Interstate Natural Gas Association of America (INGAA) submitted a letter stating that they were “not aware of ovality being a problem in construction, operation, or safety; in fact, to the best of our knowledge ovality has not been connected with the cause of a single pipeline failure.”

Aside from the discussions during the 2013 dig, no further information was available regarding discussion to understand the cause of the ID restriction, even though it was larger than MSS SP-75-2008 and TES-FITG-LD-US out-of-roundness tolerances. The greater concern was for the passage of future ILI tools without damage rather than investigating the origins of the ovality. Therefore, efforts to understand the stresses in the bend were not performed at that time. Moreover, there were no attempts to opportunistically perform NDE on the girth welds upstream and downstream of the elbow to verify that they were sound and free of potentially injurious flaws (granted, the 2013 dig was prior to the Freeman +4 Incident which involved a leak at a transition girth weld from a notch-like LOF so similar construction issues were likely not on anyone’s radar). Not performing further investigations or assessments as to the cause and implications of the ovality was determined to be causal to this incident.

Another potential complication is that the excavation may have disturbed the soil support beneath the TAG 98 elbow. If proper compaction was not achieved, movement of the elbow during thermal cycles could have exacerbated bending loads over time. TC Oil’s Compaction Control Measures for Pipeline Excavations Procedure (TES-PROJ-COM)¹³⁹, is used to limit bending stress in the pipe when transitioning from an area of consolidated bedding material to an area that is disturbed.

[REDACTED]

[REDACTED] According to interview statements from the Pipe Integrity team, a Tech Memo is issued for each excavation that details the planning and execution of the dig. Within this memo, they specify what the project needs to follow related to pipeline support requirements, especially if it is more extensive than the normal

¹³⁸ Federal Register, Volume 49, No. 212, Notice of Proposed Rulemaking, Transportation of Natural and Other Gas by Pipeline; Ovality of Field Bends in Steel Pipe, October 31, 1984.

¹³⁹ TES-PROJ-COM, Compaction Control Measures for Pipeline Excavations (CDN-US-MEX), Rev 01, April 8, 2011.

procedural requirements. A specific Tech Memo was not found for this dig but photographic documentation (see Figure 11 and Figure 72) shows that the excavation extents were relatively small, and support appeared to be good. The excavation and subsequent backfill/compaction activities in 2013 likely did not contribute to this incident.

5.2.2 2013 BH GEMINI™ Caliper ILI¹⁴⁰

On September 6, 2013, TC Oil performed a high-resolution MFL, caliper, and IMU inspection of KS10 using the 36-inch Baker Hughes (BH) GEMINI™ technology for detection of metal loss and geometry anomalies. The purpose of the caliper and inertial survey inspection was to determine pipeline geometry, which included plan, profile, curvature, pipe wall shape, and deformations. The tool identified [REDACTED]

[REDACTED] The largest ID restriction was measured at 90.5% OD at a bend at absolute distance 73,277.1 ft – this was the TAG 98 elbow. The data plots for the TAG 98 elbow are provided in Figure 84.

Likely, because the Pipe Integrity team was already aware of this ID restriction and had investigated it six months earlier, no additional actions were taken at this time.

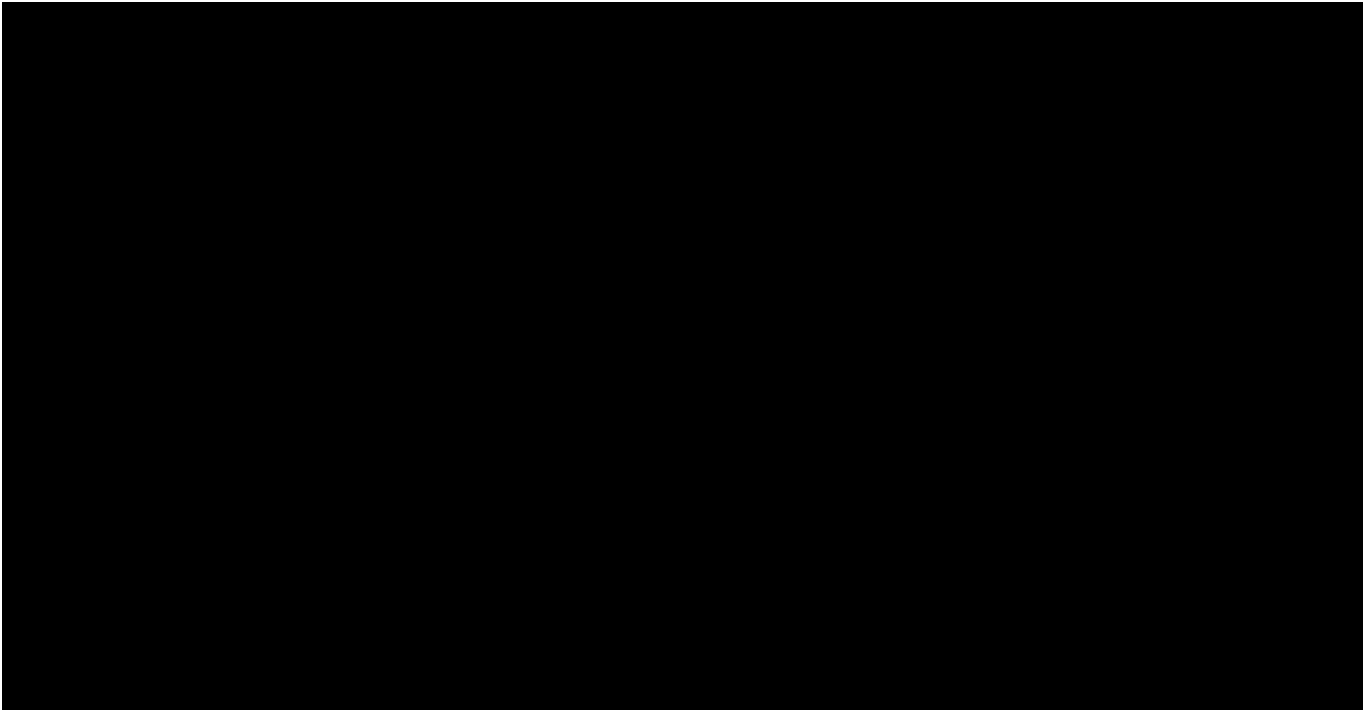


Figure 84. 2013 Axial MFL, ID Profile, Nominal Wall Thickness, and Curvature Radius Plots for TAG 98 (BND 350)³²

The wrinkle upstream of GWD 13520 was not reported by the GEMINI™ tool which was a high-resolution tool (80 circumferentially spaced caliper arms). Post-incident review of the raw caliper data did not show a clear indication of the wrinkle upstream of GWD 13520. There was

¹⁴⁰ Baker Hughes Geometry Inspection Report for TransCanada Pipelines Ltd, 36" GEMINI™ Geometry Inspection NPS 36 KS10 Steele City to Burns, September 6, 2013.

approximately 2 mm (0.08-inch) of variation at the location of the wrinkle which could be attributed to noise in the dataset. The ovality at the 3 o'clock and 9 o'clock positions was less pronounced than in the 2012 assessment at the location where the wrinkle was found. However, the amount of ovalization six to eight inches further upstream had increased slightly. These small variations in the raw data could be attributed to differences in ILI tool resolution, how the tool traveled through the bend, or actual small changes in the pipe geometry.

5.2.3 2018 BHGE MFL4 ILI¹⁴¹

The leak of the Keystone Phase 1 pipeline downstream of the Freeman PS in Hutchinson County, South Dakota on April 2, 2016, caused by an ID toe crack in a transition girth weld, prompted TC Oil to perform an ILI capable of detecting certain girth weld anomalies in November 2018 using the Baker Hughes General Electric (BHGE) MagneScan™ tool, also referred to as MFL4, to inspect KS10. The MFL4 tool is a combination high-resolution MFL, caliper, and IMU inspection vehicle. Aside from inspecting for metal loss and geometry features, it is also capable of screening girth welds for anomalous conditions, including crack-like defects.

The MFL4 tool is a standard MFL tool that also has a specification for detection of girth weld anomalies. The tool has two specifications for girth welds as shown in Figure 85, (1) a POD of 90% for flaws with a peak depth of 50% and circumferential width of 2-inch (50 mm); and (2) a POD of 90% for flaws with a peak depth of 30% and width of 3.1-inch (80 mm), with the caveat that the defects must be open by at least 0.01-inch (0.25 mm). In addition, the POI is estimated at 50% for cracks and only very deep and sharp signals are classified as a crack; otherwise, an anomalous weld signal is classified as a weld anomaly. Girth weld defects that have an opening of less than 0.01-inch (0.25 mm) are included in the assessment, but the POD, POI, and sizing specifications do not apply¹⁴².

¹⁴¹ Baker Hughes, New MagneScan™ Inspection Report for 36 inch Crude Oil Pipeline, KS10 Steele City to Burns, NPS 36 November 9-11, 2018.

¹⁴² Integrity Verification Plan, Corrective Action Order CFP No. 3-2016-5003H, Liquids Pipeline Systems Engineering, May 4, 2016.

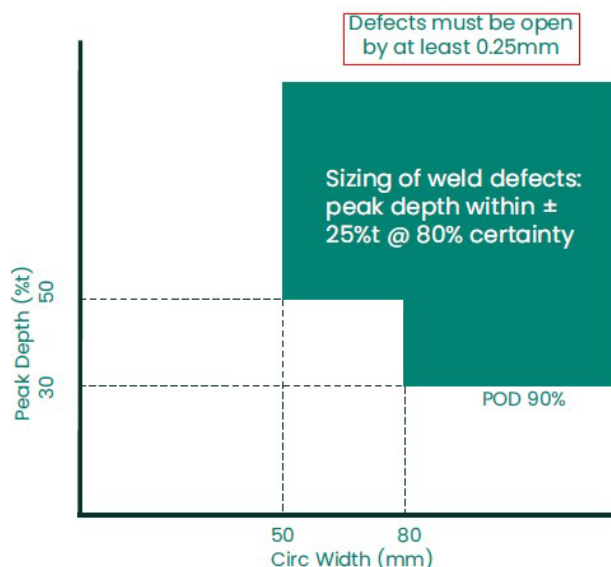


Figure 85. MFL4 Detection and Sizing Capabilities for Girth Weld Anomalies

Analysis of features involves assigning a shape category: (1) narrow, linear features with metal loss signal equal to or less than the width of the girth weld signature and length around the circumference 0.6-inch (15 mm) or greater; (2) circular or oval features with metal loss signal greater than or equal to the width of the girth weld signature and length around the circumference with a ratio less than 2:1 between length and width; or (3) wide linear feature with metal loss signal greater than the width of the girth weld signature and length around the circumference 0.6-inch (15 mm). Then using the shape classification, the analyst selects the most likely hypothesis of the defect. For a LOF defect, the shape category would be a narrow, linear feature as shown schematically in Figure 86.

As shown in Figure 87, there were no indications of any anomalous features at GWD 13530 (G59B) or GWD 13520 (G59A). At the time of the inspection, fatigue Crack 1 would likely have been below 30% in depth and therefore below the 90% POD threshold even if the crack opening was greater than 0.01-inch (0.25 mm). It is unclear why the fatigue crack was not discovered at the time of the inspection except that the elbow and transition weld geometry may have affected the tool's POD, the crack opening was potentially tighter than the minimum tool requirements, or the magnetite¹⁴³ corrosion product affected the MFL signal. The 2018 results were re-reviewed post incident and Baker Hughes came up with the same conclusion – no girth weld anomaly features were detected.

¹⁴³ As described in the USDOT PHMSA Failure Investigation Report for the Plains Pipeline, LP, Line 901 Crude Oil Release in Santa Barbara County, CA, May 2016, magnetite is highly magnetic and can potentially impede flux leakage.

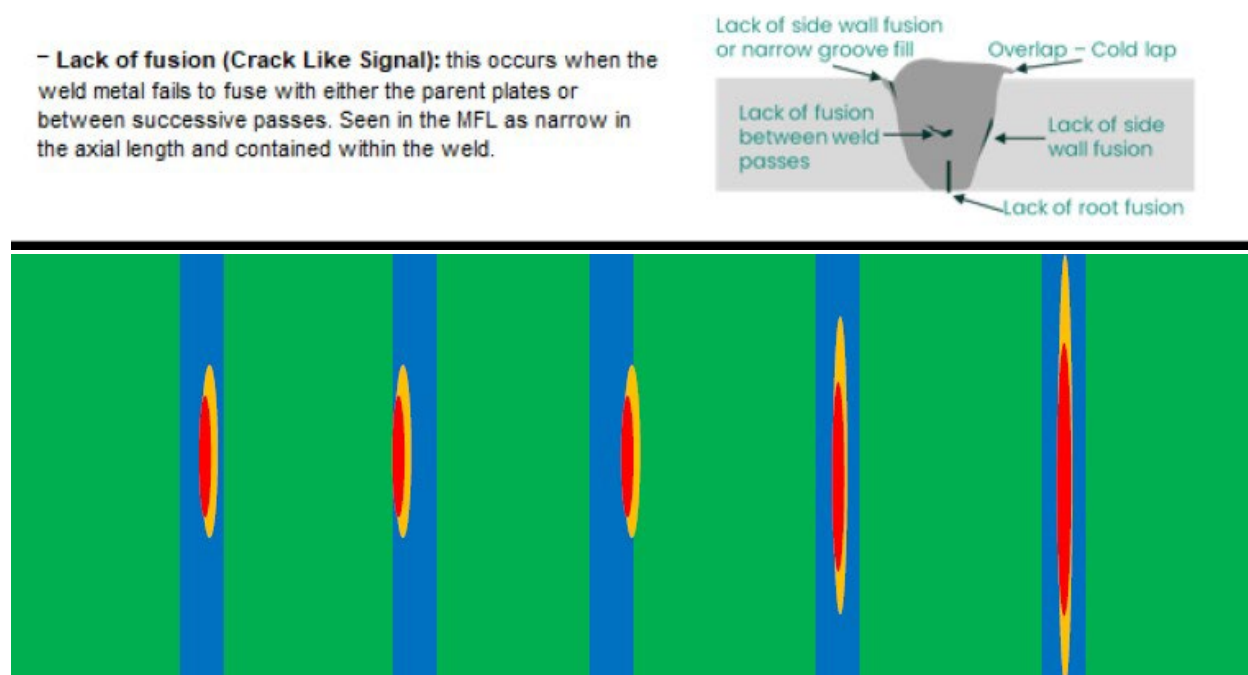


Figure 86. Schematic of Narrow Linear Feature MFL4 Signal Representing Crack-Like or LOF Defects in a Girth Weld¹⁴⁴

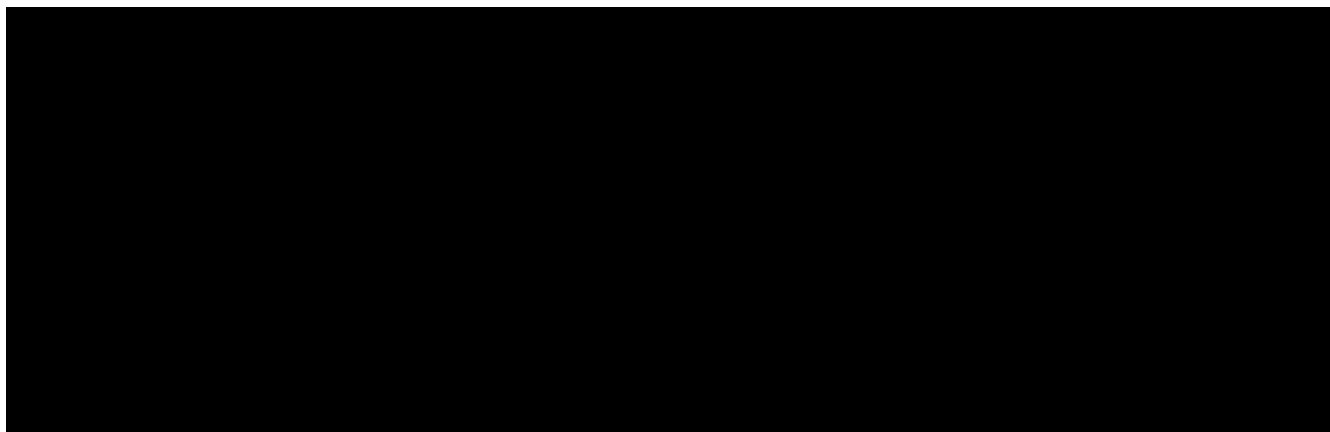


Figure 87. MFL4 Signals for GWD 13520 and GWD 13530

TC Oil had performed tool validation exercises in piggable segments [REDACTED] and [REDACTED] following the Freeman +4 incident in 2016 (the leak was in [REDACTED]). At the time, the girth weld crack that leaked, remained in the line and had been temporarily repaired with a Plidco clamp – the MFL4 tool demonstrated that it could identify the crack that leaked. TC Oil performed several other excavations as part of the validation program and the tool did not report any features as cracks, only girth weld anomalies. When the anomalies were excavated, the vast majority were only areas of high-low or misalignment rather than cracking features.

¹⁴⁴ Baker Hughes, Girth Weld Assessment and Defect Discrimination, 2019.

Curiously, the MFL4 tool did not report the ID restriction that both the 2012 and 2013 caliper tools reported. Post-incident TC Oil inquired why this was the case and was informed by Baker Hughes that the standard reporting for the MFL4 tool does not report ID restrictions at elbows. The rationale was that they would expect to have some sort of restriction at elbows normally and therefore it does not merit reporting; however, they do report ID restrictions within straight pipe. In review of the raw data post incident, the ID restriction was detected and was similar in magnitude as what was reported in 2012 and 2013 but it did not meet the MFL4 reporting requirements at that time. They also noted that there was an indication of a possible wrinkle near TAG 98 in the 2018 data. The height of the wrinkle was more evident and of similar magnitude to that measured in the post failure laser scan dimensional analysis than in the 2012 and 2013 caliper data. This may be an indication of changes over time to the stress in the TAG 98 bend assembly or simply related to differences in tool technologies and how they traversed the bend.

The inspection was successful and achieved the specified quality requirements; however, there were noted limitations in the system performance specification. Though the MFL4 tool was used as a tool to find certain girth weld anomalies, the vendor noted that the POD, POI, and sizing accuracies are affected within a bend. Moreover, girth weld cracks need to have an opening of at least 0.01-inch (0.25 mm) to achieve a high POD. These factors likely limited the ability of the MFL4 tool in detecting the cracking within GWD 13530 (G59B) and therefore contributed to the failure feature not being detected or reported in 2018.

5.2.4 2020 NDT Eclipse ILI¹⁴⁵

The NDT Eclipse tool is designed for detection and sizing of axial cracking threats. No crack-like features were identified in the KS10 segment during the inspection. Since this tool is designed for the detection of axial cracking, it was not meant to identify girth weld cracking threats, the wrinkle, or ovality. Post-incident, TC Oil requested that the data between GWD 13580 and GWD 13800 be reviewed for any indications near the failure site. The re-analysis¹⁴⁶ concluded that the tool selection and configuration were the proper selection for the objectives of the survey, the data quality was appropriate, and the analysis settings and thresholds aligned with the crack procedure. Upon review, the tool did not record data for most of the section in question suggesting that there were no linear indications to report. NDT also reviewed the wall thickness and standoff data to determine if the wrinkle was identified. They noted that for the entire section, there were indications in the standoff data that suggest field bends and that these indications share the patterns from ripples they have analyzed in the past. The wrinkle upstream of GWD 13520 was not identified, however.

5.2.5 Post-Incident Reviews

As discussed previously, the Pipe Integrity team investigated the [REDACTED] ID restriction identified by the 2012 profile caliper ILI to address valid integrity concerns about the ability to run future ILI tools through the restriction. The ID restriction was found to be due to an ovality in the TAG 98

¹⁴⁵ NDT Global, Inspection Report Ultrasonic Crack Survey, TransCanada Keystone Pipeline, LP, 144.78 mi. x 36" KS10 Steele City – Burns, September 15-18, 2020.

¹⁴⁶ NDT Global, DS Customer Response Report, 36" x 233.03 km Steel City – Burns, December 12, 2022.

(BND 350) bend assembly. The Pipe Integrity team took measurements and discussed with the ILI vendor how best to proceed for future inspections. No other activities were performed at the time to understand the cause of the ovality. Concerns about the feasibility of running future integrity inspections were appropriate but may have led the Pipeline Integrity team to overlook the potential integrity risks associated with the ovality itself. In addition, procedures did not require analyses to understand the integrity impacts of the ovality nor require opportunistic NDE of the upstream and downstream transition girth welds to verify that they were defect free. Not performing further investigations or assessments as to the cause and implications of the ovality was determined to be causal to this incident.

Post-incident review of the 2012 and 2013 caliper data did not identify anything that would have been characterized as a wrinkle, but a possible indication of a wrinkle was found in review of the 2018 caliper data. From review of the caliper data, it appears that the formation of the wrinkle (or at least to its final most pronounced height) occurred between 2013 and 2018. Baker Hughes was asked to review all other elbows and pups in KS10 for any other indications of wrinkles and they did not see any indications like the signal seen in the failure elbow.

Though post-incident analysis of the caliper data showed features that correlate with the location of the wrinkle, the caliper tools had reporting thresholds of 1% to 2% for dents that can be degraded by the presence of features such as bends. Because the caliper sensor module of the tool enters the bend and starts to become distorted prior to the location of the wrinkle, it shows up as just a small area where the readings are not quite as distorted in the bottom edge of the pipe as they would have been without the protrusion. It is unlikely that a blind automated assessment of the caliper ILI data would determine this feature to be sufficiently anomalous to call out on a report. However, as demonstrated post-incident manual reviews of the caliper data can identify some of the small changes associated with wrinkle formation. Ultrasonic ILI technology can be more sensitive in finding geometry features, particularly in bends or other areas where caliper tools have reduced sensitivity, by analyzing the sensor stand off from the pipe wall. The increased density of ultrasonic sensors and the way the data is collected allow for easier detection and identification of small dents or geometry features.

Post-incident bending strain analysis¹⁴⁷ was also completed comparing the 2018 and 2013 IMU datasets for an [REDACTED]-ft section encompassing the failure location. The data was analyzed to identify bending strain features stretching more than a pipe joint with a peak value exceeding [REDACTED] strain, excluding bends and angular misalignments at girth welds. [REDACTED] bending strain meeting the reporting requirement was identified as shown in Appendix C. [REDACTED]

[REDACTED]. No such areas were identified. The study concluded that there was no indication that the pipeline leak was caused by excessive bending strain or pipeline movement between the 2013 and 2018 surveys. This conclusion further supports the hypothesis that the bending strain had to be

¹⁴⁷ PipeNav Consulting Ltd., Bending Strain and Pipeline Movement Analysis of TC Energy's 800 ft Section of NPS KS10 Steele City to Burns, January 6, 2023.

introduced during construction – there was no change in the bending strain because it had already been imparted to the pipe prior to the 2013 IMU.

5.2.6 Causal Factors, Root Causes, Contributing Factors, and Items of Note – Assessments

The affected segment has undergone numerous integrity assessments targeting identified threats including corrosion, mechanical damage, and cracking in both the body, longitudinal seam weld, and girth welds. The frequency of inspections is well within the regulatory guidelines and the tools selected are appropriate for the identified threats. Based on the ILI findings, TC Oil has responded promptly to excavate any anomalies of concern, and where needed remediate and repair.

Regulations, IMP procedures, and the industry in general view ovalities as rather benign features. Therefore, the 2012 investigation into the [REDACTED] ID restriction (due to ovality) was short-sighted in that the immediate concern was the potential for passage of future ILI tools and not a broader view of what may have been causing the ovality to occur in the first place (CF6). Rightly so, the special permit and regulations are heavily focused on ILI and the ability to identify, assess, and where needed respond to threats. So, in a situation that might prevent integrity from performing future ILIs, the obvious focus would be on making sure that actions are such that future tool passage is feasible. Yet, this focus may have caused the Pipe Integrity team and senior management to overlook a potential concern of added stress on the elbow and its possible impact to future integrity. Procedures do not provide guidance for further investigation should a significant ovality be discovered in a high stress location, such as MP 14 – a 3D radius bend with transition welds (susceptible to movement and higher stresses) undergoing ramp up testing that pushes the limits of design (RC6). Had these locations been identified as higher risk for failure, the investigation in 2013 might have thought to (1) perform NDE of the nearby girth welds to look for potential injurious flaws that could be affected by increased stress; (2) ensure that backfill and compaction under and around the elbow was such to limit potential movement of the elbow from thermal expansion; and (3) consult with stress analysis and geotechnical experts to ensure that the actions taken align with minimizing stress at the elbow – which might have led to its replacement back in 2013.

Moreover, despite their sophistication, the detection capabilities of ILI tools have limitations. Each tool technology has a stated minimum defect size that can be detected, and tools can be prone to interference from nearby anomalies, geometry features, or weld geometry. In general, girth weld cracks are more challenging to detect because of geometry factors related to the extra weld metal as well as features like high-low, which can alter signal amplitudes. Post-incident, the BHGE MFL4 data set was re-evaluated to determine if a cracking signal could be identified within GWD 13530 (G59B). BHGE concluded that the signals present in the data did not meet criteria for any reportable feature type. The complexity of detecting cracks in transition girth welds near bends was determined to have been a contributing factor to this incident.

Table 29. Summary of Causal Factors and Root Causes – Integrity Assessments

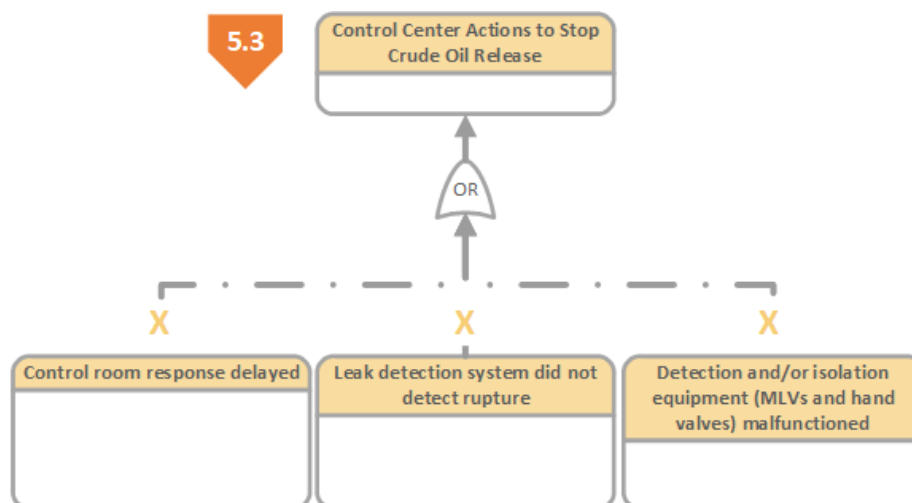
Effect	Causal Factors	Root Causes
Post-Analysis of Caliper Results Insufficient	CF4: Further investigations or assessments as to the cause and implications of the ovality were not performed as part of the March 2013 integrity dig. Focus was on future ILI runs for integrity management rather than cause of the ovality and the risk of increased stress at the transition weld.	RC4: Evaluation and repair criteria for ovalities within bends needs improvement, especially where stresses are known to be high, and the risk of girth weld failure is elevated (weld transitions).

Table 30. Summary of Contributing Factors – Integrity Assessments

Effect	Contributing Factors
Crack in GWD 13530 (G59B) Not Detected by MFL4 ILI	CTF6: Though the MFL4 ILI was used as a tool to find certain types of girth weld anomalies, the vendor notes that the POD, POI, and sizing accuracies are affected within a bend. Moreover, girth weld anomalies need to have an opening of at least 0.01-inch (0.25 mm) to achieve a high POD. These factors likely limited the ability of the MFL4 tool in detecting the flaw indications within GWD 13530 (G59B).

5.3 Control Center Response

Images showing a ductile overload region on the metallographic section substantiate that the cracks in GWD 13530 had not leaked prior to the pipeline rupture. Therefore, the size of the release was dictated by the response of the control room in shutting down and isolating the pipeline. The control room response event sequence is shown in Figure 88. The investigation team determined that the control room response was appropriate and therefore not causal to the release volume.

**Figure 88. Control Room Response Event–Sequence - Cause and Effect Tree**

On December 7, 2022, at 20:01 MST the [REDACTED] alarm announced indicating a leak the size of which exceeded the [REDACTED] detection threshold over a two-minute averaging window along with a secondary pressure leak trigger. Approximately 27 minutes prior to the rupture, at 19:34 MST the flowrate on the Cushing Extension was reduced to [REDACTED] to prepare to bypass the Hope PS and allow passage of the P2D leak detection and cleaning ILI tool. In the two minutes prior to the rupture, at 19:59 MST, the Hope PS was bypassed. As shown in Figure 80, the slowing of the Cushing Extension and bypass of the Hope PS caused a transient pressure wave upstream. Pressures increased from approximately 1,000 psig (6,898 kPa) to 1,212 psig (8,359 kPa). These pressure transients are a normal occurrence during pigging operations and did not exceed the MOP. However, the pressure increase was enough to cause failure of the remaining ligament of the most prominent crack in GWD 13530. Between 20:01 and 20:07 the pressure dropped from 1,212 psig (8,360 kPag) to less than 900 psig (6,205 kPag). At 20:07 MST the Liquids Pipeline Control Center (LPCC) made the decision to perform an emergency shutdown due to a suspected leak and isolation valves were commanded closed. Isolation of the affected segment¹⁴⁸ between the Steele City PS and Hope PS was achieved by 20:20 MST.

Around 20:16 MST, regional on-call Technicians were dispatched to locate the release. Between 20:12 and 20:31 MST notifications were made to the on-call Control Center Operations Coordinator, Oil Scheduling, the Regional Emergency Operations Center (EOC), and the Corporate EOC. At approximately 23:15 MST the Technicians arrived north of US Highway 36 at mainline valve STLCB-01A and detected a hydrocarbon odor. The failure location was confirmed to be approximately two miles north of the highway crossing. At 23:28 MST the National Response Center (NRC) was notified (NRC Report #1354442) of the release.

The SCADA timeline and actions taken by the LPCC during this event were reviewed and showed that all actions taken align with TC Oil procedures and best practices. The Pipeline Controller and LDS Controller worked to diagnose the problem and rapidly respond. The pipeline was shut down within seven minutes of the initial alarm and completely isolated within 10 minutes of the rupture. No major delays in response were found whether from initial notification to shut down; shutdown to isolation; isolation to notification of field technicians; or in initiation of the EOC.

6 Conclusions and Recommendations

Failure of GWD 13530 (G59B) was caused by stresses acting on a shallow LOF region at the ID toe of the weld that were sufficiently high to initiate a crack. The stresses imparted to the 3D elbow assembly concentrated at the girth welds (GWD 13530 and GWD 13520) where the wall thickness transitioned from approximately [REDACTED] in the elbow to approximately [REDACTED] in the pups. The application of a large bending load to the TAG 98 (BND 350) bend assembly during its replacement in December 2010 contributed to the stress in the weld. The bending

¹⁴⁸ PHMSA defines "Affected Segment" as the approximately 96 miles of TC Oil's Keystone Pipeline that contains 36-inch diameter pipe from Steele City PS (MP 0.0) to Hope PS (MP 95.7). The "Affected Segment" traverses Jefferson County Nebraska, Washington County Kansas, Clay County Kansas, and Dickinson County Kansas.

load was large enough to ovalize the bend assembly and to eventually cause plastic deformation (wrinkle) in the upstream pup. FEA modeling showed that the most likely scenarios to have caused such a large bending stress were loads applied during construction. Postulated scenarios include loads introduced during the hydrostatic test on December 11, 2010, during final tie-in of the replacement section on December 13, 2010, or during backfill and restoration activities where pipeline support may have been inadequate and construction vehicles may have driven over the pipeline. Once a crack initiated, subsequent pressure and thermal cycles were large enough to cause the progressive crack growth until the remaining ligament was no longer able to withstand the applied loads and ruptured.

6.1 Causal Factors, Root Causes, Contributing Factors, and Items of Note

Causal factors were identified for events related to (1) the design of the TAG 98 bend assembly that used a 3D elbow joined to pups with a taper transition joint that enhanced stress concentrations in GWD 13530; (2) installation of the TAG 98 elbow assembly in a manner that introduced a large bending stress; (3) the lack of a post-construction caliper tool re-run to identify construction-related damage that may have occurred during the replacement project; and (4) post-analysis of integrity assessment results that underestimated the potential risks of the identified ovality and hypothetical girth weld imperfections. Contributing factors were identified for events related to (1) a taper transition length shorter than MSS SP-75-2008 requirements; (2) introduction of a shallow LOF imperfection during fabrication of TAG 98 that served as a crack initiation site; (3) underestimation of pressure- and thermal-cycle fatigue risks from daily operations; (4) integrity assessments that did not adequately identify the girth weld cracking threat subsequent to the use of the MFL4 technology; and (5) procedures for stress analyses and EAs that did not effectively address uncertainty related to the potential for girth weld imperfections. Event sequences related to the control room response were also investigated but determined not to be causal factors in this incident.

RSI determined that the root causes of the December 7, 2022 rupture near Washington, Kansas were (1) gaps in SPAC for design of bend assemblies that did not effectively address the impacts of added stress at the girth weld from the use of 3D elbows and taper transition joints under real-world conditions; (2) lapses in construction oversight and quality control during the fitting replacement project allowed for construction techniques that introduced a large bending stress in the TAG 98 bend assembly; (3) SPAC that did not address the need to re-run a construction caliper tool after significant pipeline modifications; and (4) weaknesses in evaluation and repair criteria for ovalities in high stress bend locations.

In consideration of the above factors, RSI concludes that the most probable chain of events for the MP 14 Incident are that:

- The primary cause of the rupture was a progressive (fatigue) crack that originated from a shallow LOF at the ID toe of GWD 13530.
- The LOF occurred because of:
 - Weld workmanship that, although it was code compliant, was not sufficient for the higher stress TAG 98 elbow assembly; and

- NDE that was unable to detect such conditions.
- The ovality in the TAG 98 bend assembly most likely occurred when excessive bending loads were applied during its installation in December 2010.
- The LOF initiated a crack when localized stresses from ovalization and the girth weld geometry (3D elbow and taper transition joint) acted as stress concentrators on the LOF flaw.
- The ovality was discovered during the September 2012 caliper survey; however, upon its discovery the ovality was not addressed because:
 - It was not deemed an integrity concern except for the fact that it might prevent passage of subsequent ILI tools;
 - Ovalities are generally not viewed as an integrity threat by the industry; and
 - Further investigations and analyses were not performed to understand the cause and integrity implications of the ovality.
- Fatigue cracking occurred during operation with contributions from both pressure and thermal cycling.
- The fatigue crack was not detected during the 2018 MFL4 ILI targeting girth weld anomalies because:
 - The presence of the elbow geometry may have reduced the tool's POD, POI, and sizing accuracy;
 - The crack opening may have been below detection thresholds; and
 - The high-temperature oxide (magnetite) lining the crack surface may have impeded flux leakage.
- The risk of progressive girth weld cracking was underestimated during the capacity increase projects because:
 - Stress analyses and EA relied on the results of the MFL4 tool run without consideration of POD, POI, or sizing accuracy limitations in bends;
 - Sensitivity analyses were not performed to understand the impact of imperfections in transition welds, such as high-low, acceptable flaws per API 1104, or flaw sizes just below the MFL4 detection threshold under cyclic operational loads.
- The fatigue crack failed when the remaining ligament could no longer support the applied loads.

6.1.1 Causal Factors and Root Cause Summary

Causal factors and root causes were identified during the investigation for events leading to the failure of GWD 13530. The causal factors and root causes are discussed below and summarized in Table 31.

6.1.1.1 Elbow Design Enhanced Stress Concentration in GWD 13530 (CF1, RC1)

The combination of the taper transition joint, 3D elbow, and large, applied bending stress during construction all added to the stress concentrations in GWD 13530. Without any one of these factors, the failure would not have occurred in the timeframe in which it did. A larger bend radius has two effects; (1) the tangent points of the arc, where the girth welds are located, move further away from the vertex thus reducing the bending moment; and (2) it spreads the thrust forces from thermal expansion and contraction over a larger area. The combined effect of the thrust force reduction and bending stress reduction for a larger bend radius would extend the fatigue life by a factor of three to 21 (depending on the bend radius selected). Additionally, the pup-elbow joints were designed with a taper transition which can result in higher stresses over a counterbore and taper design. Adding to the stress at the taper joint was the fact that the elbow wall thickness was higher than the minimum acceptable plate thicknesses for manufacturing (██████████ per the MTR). The thicker the elbow in comparison to the pup, the greater the stress concentrating effect at the thinner wall side of the taper transition joint. In hindsight, it is easy to question a design choice without knowing all the variables that went into that decision. Both 3D elbows and taper transition joints are acceptable design choices per codes and standards with the caveat that the implications of these choices on the potential pipeline stresses should be well understood and managed.

6.1.1.2 Construction Practices Led to Bending Moment (CF2, RC2)

Factors during construction contributed to the large bending stress applied to the TAG 98 bend assembly which in combination with the design of the bend and taper transition joint likely caused crack initiation at the LOF in GWD 13530. Postulated scenarios included loads introduced during the construction hydrostatic test, fit-up of the final tie-in weld, and backfill and compaction activities with the pipeline poorly supported. First, the hydrostatic test was performed while the creek portion of the new installation was restrained with approximately 5-ft of cover and the TAG 98 (BND 350) bend assembly and downstream piping were unrestrained (per ASME B31.4) which could have introduced a bending moment at the elbow. Second, though attempts were made to ensure that fit-up during final tie-in was precise, there always remains the possibility that alignment was not precise. Third, some post-construction soil settlement likely occurred as evidenced by the ██████████ vertical bending strain identified by IMU and the ██████████ lift observed during post-incident excavation which could also have contributed to the bending loads. These combined factors point to lapses in construction oversight and control of construction quality processes to minimize pipeline bending stress.

6.1.1.3 Construction Caliper Not Re-Run (CF3, RC3)

Causal to the ovality not being identified at the time of installation is the fact that a construction caliper run was not repeated. The original construction caliper ILI was completed October 2010 prior to the TAG 98 replacement. Another caliper run was not completed until December 2012 which identified the ID restriction (due to ovality). Even though it was not a procedural or

regulatory requirement, had the construction caliper ILI been repeated at the time of replacement, the ID restriction would likely have been discovered and could have been repaired. Company SPAC did not address the issue of re-running a construction caliper ILI for significant modifications to the pipeline after completion of the original construction activities to identify construction-related damage.

6.1.1.4 Ovality Investigation (CF4, RC4)

The Pipe Integrity team investigated the [REDACTED] ID restriction identified by the 2012 profile caliper ILI to address valid integrity concerns about the ability to run future ILI tools through the restriction. The ID restriction was found to be due to an ovality in the TAG 98 (BND 350) bend assembly. The Pipe Integrity team took measurements and discussed with the ILI vendor how best to proceed for future inspections. No other activities were performed at the time to understand the cause of the ovality. Concerns about the feasibility of running future integrity inspections were appropriate but may have led the Pipeline Integrity team to overlook the potential integrity risks associated with the ovality itself. In addition, procedures did not require analyses to understand the integrity impacts of the ovality nor require opportunistic NDE of the upstream and downstream transition girth welds to verify that they were defect free.

Table 31. Summary of Causal Factors and Root Causes

Effect	Causal Factors	Root Causes
Elbow Assembly Design Enhanced SCFs at GWD 13530	CF1: The selection of a 3D elbow with a taper transition (in compliance with ASME B31.4) for the TAG 98 elbow-pup joint led to high stress concentrations in the girth weld.	RC1: Gaps in SPAC for design of bend assemblies did not effectively address the impacts of added stress at the girth weld from the use of 3D elbows and taper transition joints under real-world conditions like the joint's susceptibility to accidental construction loads, weld imperfections, or cyclic operational loads.
Large Bending Stress Introduced in TAG 98 (BND 350)	CF2: Construction practices (e.g., during hydrostatic testing, fit-up, backfilling, and compaction) during the replacement of the TAG 98 (BND 350) elbow assembly led to the introduction of a large bending moment at the overbend.	RC2: Lapses in construction oversight and quality control during the fitting replacement project led to bending stresses going unnoticed.
Construction Caliper Run Not Repeated	CF3: Construction caliper re-run was not required for the fitting replacement project.	RC3: SPAC did not address the issue of re-running a construction caliper ILI after significant pipeline modifications were made along the Cushing Extension to identify construction-related damage.
Post-Analysis of Caliper Results Insufficient	CF4: Further investigations or assessments as to the cause and implications of the ovality were not performed as part of the March 2013 integrity dig. Focus was on future ILI runs for integrity management rather than cause of the ovality and the risk of increased stress at the transition weld.	RC4: Evaluation and repair criteria for ovalities within bends needs improvement, especially where stresses are known to be high, and the risk of girth weld failure is elevated (weld transitions).

6.1.2 Contributing Factors

Several contributing factors were identified during the investigation that although were not directly causal, were determined to have contributed to the events leading up to the MP 14 Incident. A brief discussion of each contributing factor is provided below and are summarized in Table 32.

6.1.2.1 Taper Transition Length (CTF1)

The measured length of the taper transition was approximately [REDACTED] which is less than the minimum requirement of 1.00-inch specified in Figure 3(b) of MSS SP-75-2008. The shorter transition length can enhance the stress concentration at GWD 13530 due to the weld geometry.

6.1.2.2 LOF Flaw in GWD 13530 (CTF2)

Though specific quality documents for TAG 98 were missing, the records that were available confirmed that RT inspections and hydrostatic testing had been completed. In addition, it is plausible that visual inspections took place that identified weld locations requiring repair as evidenced by the two weld repair regions that bifurcated the LOF into three separate regions. However, contributing to the failure, the selected welding process and NDE methods used at the fabrication shop did not consider the higher stress girth welds associated with the TAG 98 elbow assembly design. Therefore, additional precautions beyond API 1104 minimum requirements were not instituted to ensure that the weld workmanship and flaw detection sensitivity was acceptable for the service in which it was placed.

6.1.2.3 Thermal and Pressure Cycles, Stress Analyses, EAs, and MFL4 Findings (CTF3, CTF4, CTF5, CTF6)

Though stress analysis and EAs were performed to understand and mitigate any potential increases in pipeline stress, shortcomings were identified in the methodologies used. Specifically, hypothetical girth weld imperfections were not included in the analyses. For the elbow that failed, it experienced temperature and pressure cycles that alone may not have been a concern. However, in combination with a shallow, surface breaking LOF at the toe of the girth weld, the design of the 3D elbow and taper transition, and a large bending stress, the cyclic stresses were enough to grow a crack to failure. Though the MFL4 tool was run in the affected segment and no notable flaws were found or reported (even post-incident), the POD, POI, and sizing tolerances can be affected by the elbow geometry. In absence of reliable girth weld crack detection ILI in the near term, TC Oil should consider revisiting the parameters used in stress analyses and EAs to define factors to include at 3D elbows with transition welds (e.g., girth weld imperfection, high-low, dynamic loads) or the need for targeted girth weld inspections.

Table 32. Summary of Contributing Factors

Effect	Contributing Factors
Taper Transition Length	CTF1: The taper transition length on the TAG 98 (BND 350) elbow was less than the 1.00-inch minimum requirement in Figure 3 of MSS SP-75-2008 which can enhance stress concentration in the girth weld.
LOF Flaw in GWD 13530 (59B)	CTF2: The selected welding process and NDE methods used at the fabrication shop did not consider the higher stress girth welds associated with the TAG 98 elbow assembly design. Therefore, additional precautions beyond API 1104 minimum requirements were not instituted to ensure that the weld workmanship and flaw detection sensitivity were acceptable for the service in which it was placed.
Thermal and Pressure Cycling Led to Crack Growth	CTF3: Thermal and pressure cycles led to crack growth until the critical flaw size was reached.
Stress Analyses and EAs did not Analyze Effects of Girth Weld Imperfections	CTF4: SPAC for stress analyses and EAs for capacity increase projects need improvement to address when girth weld imperfections should be considered or applying more stringent safety factors to account for the uncertainty of these real-world conditions.
Over-reliance on MFL4 Inspection Results	CTF5: EAs used the results of the MFL4 ILI to determine that the girth weld threat did not degrade the maximum stress criterion, but the analysis overlooked the potential for missed flaws or flaws below detection and reporting thresholds.
Crack in GWD 13530 (G59B) Not Detected by MFL4 ILI	CTF6: Though the MFL4 ILI was used as a tool to find certain types of girth weld anomalies, the vendor notes that the POD, POI, and sizing accuracies are affected within a bend. Moreover, girth weld anomalies need to have an opening of at least 0.01-inch (0.25 mm) to achieve a high POD. These factors likely limited the ability of the MFL4 tool in detecting the flaw indications within GWD 13530 (G59B).

6.1.3 Items of Note

Several items of note were identified during the investigation that were not causal but indicate a possible weakness. A discussion of each item of note is provided below and summarized in Table 33.

6.1.3.1 DBM Not Current (ION1)

The DBM was never updated once the PHMSA waiver was granted nor when the capacity increase projects went into effect. The DBM was intended as a 'living document' but no updates were made after the original draft document was published. Having a master design basis document that is updated to reflect changes that have been made to key design parameters (design factor, flow capacity, use of drag reducing agents, etc.) is beneficial for future PHA, risk analysis, and management of change (MOC) activities.

6.1.3.2 DBM Stress Analysis Guidance (ION2)

Although the DBM

, it was only in relation to facilities. A similar requirement was not contained within the pipeline design basis section,

though stress analyses were performed to identify construction, commissioning, and operational stresses along the Cushing Extension. The lack of detail on what should be considered in a pipeline stress analysis during design can result in analysis gaps.

6.1.3.3 Elbow Tempering Time (ION3)

The TAG 98 elbow (heat NOP-C) was tempered for [REDACTED] minutes which does not align with MSS SP-75-2008 or TES-FITG-LD-US, Rev 0 requirements to temper fittings for 1-hour per inch of maximum wall thickness. The maximum wall thickness of the TAG 98 elbow was [REDACTED]-inch which would have required a minimum tempering time of [REDACTED]-minutes to meet specifications. Though it did not comply with the specification requirements, MTRs and post-incident mechanical testing confirmed that the material properties met design requirements and played no role in this incident.

6.1.3.4 Missing Quality Surveillance Records and Inadequate Recordkeeping (ION4)

The weld inspection report and quality surveillance records (TES-SCL-FITG-US) were missing for the TAG 98 bend assembly. In addition, for bend assemblies where records were found, they appear to be incomplete. Records retention is a key component of quality management systems to provide evidence of conformity to requirements and processes. Not maintaining key quality records to confirm that SPAC were followed opens the possibility for future problems during operation. The urgency to replace the [REDACTED] fittings likely was a factor in the recordkeeping lapses even though the importance of quality control was at the forefront of the fitting replacement project.

6.1.3.5 Lack of Coordination Between Ramp Up and ILI Teams (ION5)

Ramp up testing and the leak detection ILI run were scheduled to occur at the same time. Coordination between the two project teams was not structured nor were the risks of concurrent activities addressed. Though causal factors were not identified specific to the girth weld failure, check valves were locked open to allow passage of the ILI tool which could contribute to the severity of the incident. Not having an effective system for coordinating concurrent projects can lead to enhanced risks and a greater potential for errors.

Table 33. Summary of Items of Note

Effect	Items of Note
Design Basis Memorandum (DBM) not Kept Current	ION1: The DBM was intended as a 'living document' but no updates were made after the original draft document was published.
[REDACTED]	ION2: Though the DBM states [REDACTED], it was in relation to facilities. A similar requirement was not contained within the pipeline design basis section.
Elbow Tempering Duration did not Comply with Specifications	ION3: The TAG 98 elbow (heat NOP-C) was tempered for 30-minutes which does not align with MSS SP-75-2008 or TES-FITG-LD-US, Rev 0 requirements to temper fittings for 1-hour per inch of maximum wall thickness. The maximum wall thickness of the TAG 98 elbow was 0.892-inch which would have required a minimum tempering time of 54-minutes to meet specifications.

Effect	Items of Note
Missing Quality Surveillance Records and Inadequate Recordkeeping	ION4: The weld inspection report and quality surveillance records (TES-SCL-FITG-US) were missing for the TAG 98 bend assembly. In addition, for bend assemblies where records were found, they appear to be incomplete. Records retention is a key component of quality management systems to provide evidence of conformity to requirements and processes. The urgency to replace the 109 fittings likely was a factor in the recordkeeping lapses even though the importance of quality control was at the forefront of the fitting replacement project.
Lack of Coordination Between Ramp Up Team and ILI Team	ION5: Ramp up testing and the leak detection ILI run were scheduled to occur at the same time. Coordination between the two project teams was not structured nor were the risks of concurrent activities addressed. Though causal factors were not identified specific to the girth weld failure, check valves were locked open to allow passage of the ILI tool which could contribute to the severity of the incident.

6.2 Applicability of Findings and Lessons Learned to Other Locations within TC Oil's Liquid Pipeline Operations

The findings and lessons learned from this incident are potentially applicable to other locations along Keystone where ovalities or ID restrictions have been identified in tight radius (3D) fabricated bend assemblies that contain a taper transition weld between the elbow and pups. In addition, all fabricated 3D bend assemblies that were replaced in 2010 could have similar shallow LOF imperfections as identified for the TAG 98 bend assembly. Therefore, the girth welds for these bend assemblies should be examined with appropriate ILI or NDE techniques based on risk priority to identify any potential girth weld cracking concerns.

6.3 Recommendations

Several recommendations are proposed based on the causal factors and root causes identified in this RCFA.

6.3.1 Causal Factors and Root Causes:

Several recommendations (R) are proposed for TC Oil's consideration based on the causal factors (CF) and root causes (RC) identified for the MP 14 Incident.

- R1. Perform ILI with a validated circumferential crack detection tool or NDE of the girth welds for the 3D bend assemblies replaced in 2010 based on risk priority to determine if any flaws exist that could compromise pipeline integrity (RC1).**

Lessons Learned: Although the welding performed for TAG 98 complied with API 1104 code requirements for workmanship, a shallow LOF region was found in GWD 13530 (G59B) that was undetectable using conventional radiographic inspection techniques. The design of the TAG 98 bend assembly combined with the external bending load applied during construction was such that the stresses imparted to the weld were sufficiently high to initiate a crack at the shallow LOF. Other 3D elbows with taper transition joints are inherently higher stress and may also be susceptible to crack initiation at undetectable,

shallow LOF regions. Therefore, the intent of R1 is to identify other high risk girth welds associated with 3D bend assemblies that could be a potential cracking threat.

- R2. Update pipeline design guidelines, pipeline stress analysis procedures, and/or engineering assessment procedures to include details on what factors should be considered in the analysis and when it is important to consider these factors (e.g., transition joint design, bend radius, maximum girth weld imperfections per API 1104, dynamic operational loads, geometry features like ovalities) to reduce the potential for analysis gaps (RC1).**

Lessons Learned: Detailed stress analysis and EA work performed during the capacity increase projects to mitigate the risk of increased stress at elbows and bends from elevated operating temperatures did not consider hypothetical shallow, surface-breaking flaws at the ID toe of the transition girth welds (which were a possibility based on the findings from the Freeman +4 Incident). Appropriately, the results of the MFL4 girth weld inspections were reviewed but because the sensitivity of the MFL4 tool was not enough to detect the shallow LOF features that initiated cracking, no girth weld anomalies were identified to be included in the EA. Procedures did not require the evaluation of hypothetical girth weld flaws that could have been missed by inspections nor did they call for targeted inspections of girth welds at elbows and bends identified as potentially higher stress locations to verify that they were free of injurious defects. Additional guidance for what should be considered in stress analyses and EAs will help to reduce the potential for future analysis gaps.

- R3. Develop an integrity verification program (IVP) for potentially high stress pup-to-fitting transition welds, such as those at 3D elbows, to better understand and manage integrity threats at these locations (RC1).**

Lessons Learned: The combination of the taper transition joint, 3D elbow, and large, applied bending stress during construction all added to the stress concentrations in GWD 13530. Without any one of these factors, the failure would not have occurred in the timeframe in which it did. Both 3D elbows and taper transition joints are acceptable design choices per codes and standards with the caveat that the implications of these choices on the potential pipeline stresses should be well understood and managed. An IVP for the higher stress bend assemblies will help TC Oil to continue to manage the risks.

- R4. Work with ILI vendors to develop tools with improved capabilities for detection of girth weld cracking threats in bends (RC1).**

Lessons Learned: The 2018 MFL4 ILI, which was used to identify anomalous conditions at girth welds, did not detect any anomalies within GWD 13530 or GWD 13520. Though the MFL4 tool was configured to detect some anomalous girth weld conditions, the vendor noted that the probability of detection (POD), probability of identification (POI), and sizing accuracies are affected within a bend. In addition, girth weld cracks need to have an

opening of at least 0.01-inch (0.25 mm) to achieve a high POD and Anderson reported that the crack surface was coated with high-temperature oxides (magnetite) which can impede flux leakage. These factors likely limited the ability of the MFL4 tool in detecting the cracking within GWD 13530 (G59B). Therefore, working with ILI vendors to improve girth weld flaw detection capabilities will enhance TC Oil's ability to manage this threat in the future.

- R5. Look for potential indicators of ovality, wrinkles, buckles, and ripples in raw caliper ILI data or the stand-off data from ultrasonic wall measurement (UTWM) tools to identify other locations where ovalization or wrinkles may be present as the result of a large bending load (RC2).**

Lessons Learned: Several factors during construction may have contributed to the large bending stress applied to the TAG 98 bend assembly that caused it to ovalize. The introduction of the ovality during construction without it being identified points to lapses in construction oversight and control of construction quality processes to minimize pipeline bending stress. Similar lapses in construction oversight may exist at other fabricated bend assemblies replaced in 2010 and therefore R8 is one method for identifying other locations with potentially high construction-related bending loads.

- R6. For large scale fitting replacement projects, such as what occurred along the Cushing Extension, consider the benefits of running another construction caliper ILI to detect areas where plastic deformation (ovalization or wrinkles) may have occurred due to construction-related bending loads (RC2, RC3).**

Lessons Learned: A construction caliper inspection was completed in October 2010, before the replacement fittings were installed, to address any pipe damage that may have occurred during construction. However, the construction caliper inspection was not repeated after completing the fitting replacement project even though thousands of feet of pipe (and hundreds of fittings) were replaced. Had another caliper tool been run at that time, it likely would have detected the 9% ID restriction in the TAG 98 bend assembly (BND 350) and therefore could have been corrected at the construction contractor's expense.

- R7. Update ILI data analysis procedures to include criteria for response to ovalities within elbows (that extend beyond the elbow itself) such as performing stress analysis, engineering assessments, or defining when NDE of girth welds might be required (RC4).**

Lessons Learned: In March 2013 the Pipe Integrity team investigated the ID restriction at TAG 98 (BND 350) reported by the 2012 BHI profile caliper ILI to address valid integrity concerns about the ability to run future ILI tools through the restriction. The ID restriction was found to be due to an ovality in the TAG 98 bend assembly. The Pipe Integrity team took measurements and discussed with the ILI vendor how best to proceed for future

inspections. No other activities were performed at the time to understand the cause of the ovality. Concerns about the feasibility of running future integrity inspections were appropriate but may have led the Pipe Integrity team to overlook the potential integrity risks associated with ovality itself. Additionally, procedures did not require analyses to understand the integrity impacts of the ovality nor require opportunistic NDE of the upstream and downstream transition girth welds to verify that they were defect free.

- R8. Require NDE of transition girth welds at 3D elbows when exposed during integrity digs to identify any potential flaws that may have been missed during prior radiographic or ultrasonic inspections (RC).**

Lessons Learned: In 2013, pipeline anomaly field investigation procedures did not require opportunistic NDE of transition girth welds at 3D elbows to verify that they were defect free. Considering the Freeman +4 and MP 14 Incidents, future excavations could benefit from opportunistic examination of transition girth welds to identify and remediate potentially injurious defects.

6.3.2 Contributing Factors:

Several recommendations (R) are proposed for TC Oil's consideration based on the contributing factors (CTF) identified for the MP 14 Incident.

- R9. Update welding specifications for bend assemblies to include scenario-based considerations when minimum code requirements may not be enough to ensure a weld will be appropriate for the service conditions. For example, define assembly designs that may have inherently higher stress girth welds and the additional provisions (e.g. tighter NDE requirements, detailed FEA to determine acceptable flaw sizes; redesign to reduce stresses) that are needed to ensure that weld workmanship aligns with the expected stresses (CTF1, CTF2).**

Lessons Learned: The selected welding process and NDE methods used at the fabrication shop did not consider the higher stress girth welds associated with the TAG 98 elbow assembly design. Therefore, additional precautions beyond API 1104 requirements were not instituted to ensure that the weld workmanship was acceptable for the service in which it was placed.

- R10. For elbows identified as potentially high stress locations when operating the Cushing Extension at increased capacity, reanalyze them to also consider fatigue from combined thermal and pressure cycles. For elbows that do not meet defined stress or strain criteria, consider performing girth weld NDE to verify that welds are defect free and/or limiting operating conditions (as had been done previously) so that stresses remain at acceptable levels (CTF3, CTF4).**

- R11. For future stress analyses and engineering assessments of Cushing Extension 3D elbows with taper transitions, perform sensitivity studies to understand the stress implications of hypothetical girth weld flaws that could have been missed by the MFL4 tool, by NDE in the shop, or by assuming a flaw that would still be acceptable per code requirements (i.e., girth weld misalignment of 3 mm (1/8-inch)) (CTF5, CTF6).**

Lessons Learned (R10 and R11): Though stress analysis and EAs were performed to understand and mitigate any potential increases in pipeline stress from the capacity increase projects, shortcomings were identified in the methodologies used. Specifically, hypothetical girth weld imperfections were not included in the analyses. For the elbow that failed, it experienced temperature and pressure cycles that alone may not have been a concern. However, in combination with a shallow, surface breaking LOF at the toe of the girth weld, the design of the 3D elbow and taper transition, and a large bending stress, the cyclic stresses were enough to grow a crack to failure. In absence of reliable girth weld crack detection ILI in the near term, TC Oil should consider revisiting the parameters used in stress analyses and EAs to define factors to include at 3D elbows with transition welds (e.g., girth weld imperfection, high-low, dynamic loads) or the need for targeted girth weld inspections.

6.3.3 Potential Improvement Opportunities

Several potential improvement opportunities were identified for the items of note that did not directly cause or contribute to the MP 14 Incident.

- PIO1. Update the DBM so that it reflects the changes that have been made to key design parameters (design factor, flow capacity, use of drag reducing agents, etc.) so that it can be used as a tool for future PHA, risk analysis, and management of change (MOC) activities (ION1).
- PIO2. Develop guidelines for pipeline stress analyses that include details on what factors must be considered in the analysis and when it is important to consider these factors (e.g., girth weld imperfections, dynamic operational loads, geometry features like ovalities) to reduce the potential for analysis gaps (ION2).
- PIO3. Schedule any future ramp up testing projects when no other activities are occurring along the pipeline, such as ILI, to limit overlapping concerns and the potential for errors (ION5).

7 References

1. 36-inch PROFILE™ Tool, Tool Data Sheet, 2016.
2. ABS Consulting, Root Cause Analysis Handbook (3rd ed. 2008).
3. Amended Corrective Action Order (ACAO) CPF No. 3-2022-074-CAO, March 7, 2023.
4. American Lifelines Alliance, Guidelines for the Design of Buried Steel Pipe, July 2001 (with Addenda through 2005).
5. American Society for Testing and Materials, “Standard Practices for Cycle Counting in Fatigue Analysis”, ASTM E1049-85.
6. Anderson & Associates, 220439 TC Energy – Metallurgical Analysis of NPS-36 KS10 MP-14 Pipeline, February 7, 2023.
7. API 579-1/ASME FFS-1, “Fitness for Service”, 2016.
8. API 5L, 44th Edition, Specification for Line Pipe, October 1, 2008.
9. API Standard 1104, 20th Edition, Welding of Pipelines and Related Facilities, April 2010.
10. Baker Hughes Geometry Inspection Report for TransCanada Pipelines Ltd, 36” GEMINITM Geometry Inspection NPS 36 KS10 Steele City to Burns, September 6, 2013.
11. Baker Hughes, Girth Weld Assessment and Defect Discrimination, 2019.
12. Baker Hughes, New MagneScan™ Inspection Report for 36 inch Crude Oil Pipeline, KS10 Steele City to Burns, NPS 36 November 9-11, 2018.
13. Barsom, J.M. and Rolfe, S.T., Fracture and Fatigue Control in Structures, 3rd Edition, 1999.
14. Boccard USA Corporation, Radiographic Testing RT-1, Revision 1, March 29, 2010.
15. [REDACTED], Material Test Report for Heat NOP-C, Piece Number 174469, Certificate Number 6235, November 15, 2010.
16. [REDACTED], Quality Manual According to ISO-9001-2000, January 15, 2002.
17. CAT 345GC Hydraulic Excavator found at <https://s7d2.scene7.com/is/content/Caterpillar/CM20181214-35962-39643> on March 20, 2023.
18. CAT 583T Pipelayer brochure found at <https://crosscountryis.com/pdf/CAT583TPipelayer.pdf> on March 20, 2023.
19. CAT 594 Pipelayer brochure found at <https://www.maats.com/wp-content/uploads/2020/09/Brochure-CAT-594H-coloured.pdf> on March 20, 2023.
20. CAT D8T Track-Type Tractor brochure found at <https://s7d2.scene7.com/is/content/Caterpillar/C658733> on March 20, 2023.
21. Corrective Action Order, CPF No. 3-2022-074-CAO, December 8, 2022.

22. Critical Workspace Solutions, Keystone Pipeline 4750 m3/hr Flow Rate What-If Report, July 18-19, 2022.
23. D. J. Warman and D. J. Hart, "Development of a pipeline surface loading screening process & assessment of surface load dispersing methods," Kiefner and Associates, Inc. for Canadian Energy Pipeline Association (CEPA), June 17, 2005.
24. D. J. Warman, J. Chorney, M. Reed and J. Hart, "Development of a pipeline surface loading screening process (IPC2006-10464)," in 6th International Pipeline Conference, Calgary, Alberta, Canada, September 25-29, 2006.
25. Daily Inspection Check List for Fitting # 108, MP 13.6, Spread 9C, December 17, 2010, and Daily Inspection Report, Form C37, Utility Inspector, December 4, 2010.
26. Daily Inspection Checklist, Fitting 108/109, MP 13.6, December 10, 2010.
27. DGIR-0001, General Procedure for Radiographic Examination, Diamond G Inspection, Rev 1, August 30, 2010
28. DNV, Phase 2 Final Report, Guidance for Field Segmentation and Welding of Induction Bends and Elbows for JIP on Welding of Field Segmented Induction Bends and Elbows for Pipeline Construction, December 6, 2011.
29. Dong, Y., Ji, G., Fang, L., and Liu, X., Fatigue Strength Assessment of Single-Sided Girth Welds in Offshore Pipelines Subjected to Start-Up and Shut-Down Cycles, Journal of Marine Science and Engineering, 2022.
30. Drawing No. 1862-03-ML-02-605, 36" OD Crude Oil Pipeline Typical Details Pipeline Construction, Rev 0, April 1, 2010.
31. Engineering Assessment of the Combined Stresses from Steele City B PS to Cushing South PS in Consideration of 4,500 m3/hr Capacity Increase, Rev 0, March 31, 2021.
32. ENV-6-1 Report RP-218-104509, "Field validation of surface loading stress calculations for buried pipelines - Milestone 2," Pipeline Research Council International, Inc (PRCI), Authored by Zand, B., Branam, N. and Webster, W., April 2018.
33. Exhibit F – Pipeline Construction Specifications, Rev 9, May 1, 2009.
34. Federal Register, Volume 49, No. 212, Notice of Proposed Rulemaking, Transportation of Natural and Other Gas by Pipeline; Ovality of Field Bends in Steel Pipe, October 31, 1984.
35. Final Auditing Report: Auditing Production of Large Diameter High Grade Fittings at [REDACTED] Becancour Quebec Facility, KXL Pipeline Project (PO 25472), October 11, 2012.
36. Form SQ-221, Quality Surveillance Report for Keystone Pipeline Replacement Fittings, QSR Number 25472-100-YQA-PV04-1D005, Rev 1, November 12 and 15, 2010.
37. Fox, R. W., and McDonald, A. T., "Introduction to Fluid Mechanics", John Wiley and Sons, Inc., New York, 1998.
38. Golder Associates (2012). Phase I Geologic and Hydrotechnical Hazards Assessment – Keystone Mainline and Cushing Extension Pipelines. Golder Associates.

39. Golder Associates, Phase I Geologic Hazards Assessment Update, Keystone Mainline and Cushing Extension Pipelines, Midwestern United States, January 18, 2022.
40. Golder Associates, Preliminary Desktop Mapping and Geotechnical Parameters for Terrain Analyses, TransCanada Keystone Pipeline Project (MP 0 to MP 62.7), December 2016.
41. <https://websoilsurvey.sc.egov.usda.gov/App/HomePage.htm> accessed on February 16, 2023.
42. https://www.phmsa.dot.gov/sites/phmsa.dot.gov/files/docs/TC_Keystone_2007-04-30_508compliant.pdf accessed January 13, 2023.
43. <https://www.tcenergy.com/announcements/2011/2011-02-08keystones-cushing-extension-begins-deliveries-to-oklahoma/> accessed February 10, 2023.
44. <https://www.tcenergy.com/incident/milepost-14-incident/> accessed on February 10, 2023.
45. <https://www.tcenergy.com/siteassets/incident/milepost-14/tc-energy-milepost-14-keystone-pipeline-system-map-12-14-2022-hi-res.png> accessed January 13, 2023.
46. <https://www.twi-global.com/technical-knowledge/published-papers/comparison-of-fatigue-of-girth-welds-in-full-scale-pipes-and-small-scale-strip-specimens> accessed on March 1, 2023.
47. <https://www.wunderground.com/history/weekly/us/ne/lincoln/KLNK/date/2010-12-12> accessed on February 15, 2023.
48. Integrity Verification Plan, Corrective Action Order CFP No. 3-2016-5003H, Liquids Pipeline Systems Engineering, May 4, 2016.
49. Internal Memo, Geotechnical Assessment of NPS 36 Keystone Mainline Leak at MP 14, January 16, 2023.
50. JIP final Summary Report, Enhanced Girth Weld Performance for Newly Constructed Grade X70 Pipelines, May 29, 2020.
51. Kiefner and Associates, Inc, Root Cause Failure Analysis of Transition Girth Weld 4B-CTT-1 Leak at Freeman +4, September 6, 2016.
52. Memo, Keystone MP 14 Leak Site – Historical Pipeline Stress Analyses, January 16, 2023.
53. Memo, KeyUS Cushing Extension – MP 13.9 – Mill Creek Crossing (64029), November 2, 2022.
54. MSS SP-75-2008, Specification for High-Test, Wrought, Butt-Welding Fittings, 2008.
55. NDT Global, DS Customer Response Report, 36" x 233.03 km Steel City – Burns, December 12, 2022.
56. NDT Global, Inspection Report Ultrasonic Crack Survey, TransCanada Keystone Pipeline, LP, 144.78 mi. x 36" KS10 Steele City – Burns, September 15-18, 2020.
57. PipeNav Consulting Ltd., Bending Strain and Pipeline Movement Analysis of TC Energy's 800 ft Section of NPS KS10 Steele City to Burns, January 6, 2023.

58. [REDACTED], Procedure Qualification Record (PQR), RCT-280, Groove weld, Single V-Groove, November 14, 2010.
59. [REDACTED] Welding Procedure Specifications (WPS), RCT-280, Groove and fillet welds, November 14, 2010.
60. [REDACTED], Repair Procedure, Job No. 12117.
61. [REDACTED], Hydrostatic Leak Test Procedure, Canadoil (RCT-12117), 36" SCH XS Pipe Spools, Undated.
62. Reed, R.P., et al, Fitness-For-Service Criteria for Pipeline Girth Weld Quality, National Bureau of Standards, NBSIR 83-1695, November 1983.
63. Rosenfeld, M.J., Hart, J.D., and Zulfiqar, N., "Acceptance Criteria for Mild Ripples in Pipeline Field Bends", Pipeline Research Council International, Inc., PR-218-9925, Catalog No. L51994, August 2008.
64. TC Energy Form, Excerpt from Heavy Equipment Crossing Information Form, 2023.
65. TC Energy Memo, Geotechnical Assessment of NPS 36 Keystone Mainline Leak at MP 14, January 16, 2023.
66. Technical Memorandum, Maximum Allowable Discharge Temperature Limits in Consideration of 4750 m3/hr Flow Rate Ramp Test, November 4, 2022.
67. TEP-MECH-TRAN-US, Selection of Transition Pieces and Joining Methods, Rev 0, October 15, 2009.
68. TES-CT-COMPC-GL Compaction Control Measures for Pipeline Excavations Specification (CAN-US-MEX), Rev 02, February 1, 2018.
69. TES-FITG-LD-US, Specification for High Yield Carbon Steel Buttwelding Fittings, February 9, 2007.
70. TES-NDT-RT-US, Rev 0, Radiographic Examination of Welds, June 15, 2007.
71. TES-PIPE-SAW-US, Specification for SAW Pipe, Rev 1, June 24, 2009.
72. TES-PROJ-COM, Compaction Control Measures for Pipeline Excavations (CDN-US-MEX), Rev 01, April 8, 2011.
73. TES-WELD-AS-US, Welding of Assemblies and Station Piping, Rev 01, November 25, 2009.
74. TransCanada Keystone Pipeline LP, Design Basis Memorandum, Rev 6, 017250-1000-40EM-0001, February 23, 2007.
75. TransCanada Keystone Pipeline, LP, Root Cause Analysis Report: Low Yield Strength 3D Pipeline Fittings Supplied by Canadoil Asia to the Keystone Cushing Extension Project, December 3, 2010.

8 Appendix A – Event Timeline

Date	Time (MST)	Description	Source
February 23, 2007		<ul style="list-style-type: none"> Revision 6 of the DBM issued for the Keystone Pipeline Project. 	<ul style="list-style-type: none"> Keystone DBM Rev 6 2-23-07.pdf
April 30, 2007		<ul style="list-style-type: none"> Special Permit issued by PHMSA for construction and operation of Keystone at a 0.80 design factor. Outlines 51 conditions that require Keystone to more closely inspect and monitor the pipeline over its operational life than would occur on pipelines installed under existing regulations. 	<ul style="list-style-type: none"> TC_Keystone_2007-04-300_508compliant.pdf
April 2010		<ul style="list-style-type: none"> Began construction of Keystone Phase 2, Cushing Extension from Steele City, NE to Cushing, OK. 	<ul style="list-style-type: none"> Construction notes
April 22, 2010		<ul style="list-style-type: none"> 36-inch diameter, 0.515-inch wall thickness, grade X70M PSL2, SAWL, cold expanded pipe (pipe number 0031378) manufactured by ILVA using a thermo-mechanical control process. Pipe 0031378 used for the [REDACTED] pups on the U/S and D/S end of elbow 174469 to create the fabricated bend assembly TAG 98. Tested to 1,890 psig (94% SMYS) at the mill. Chemistry, tensile test, impact test, and hardness test results met product specifications API 5L, 44th Edition and TES-PIPE-SAW-US, Rev 1 (under pipe purchase agreement 6308). Visual, marking, and dimensional inspections noted as 'OK'. NDE with ultrasonic inspection calibrated with N5 notch and hole 1, 6. 	<ul style="list-style-type: none"> Pup_ILVA_MRT991579.pdf
May 12, 2010		<ul style="list-style-type: none"> Stress analysis of Spread 9C, 10C, and 11C completed. Evaluated stresses during construction, commissioning, and operating phases. Highest stresses identified for lowering of concrete coated piping. Operating stresses assumed upper bound temperature differential of [REDACTED] ([REDACTED] in summer and [REDACTED] minimum product temperature). 	<ul style="list-style-type: none"> Cushing Extension Stress Analysis.pdf
September 22, 2010		<ul style="list-style-type: none"> Hydrostatic test for construction spread 9C-2 between MP 4.661 and MP 34.966. Minimum strength (4 hours) and leak (8 hours) test pressure of 1,847 psig at the high point (102% SMYS). Yield plot max deviation of [REDACTED]. 	<ul style="list-style-type: none"> 9C-2 Hydrotest Record.pdf

REDACTIONS MADE BY TC OIL - Pending PHMSA Review

TC Oil

**CONFIDENTIAL – Protected from release under
FOIA Exemptions 4 and 7(F), 5 USC 552(b)(4)
and (b)(7)(F).**



Date	Time (MST)	Description	Source
October 2010		<ul style="list-style-type: none"> Post construction caliper ILI tool run (TDW) 	<ul style="list-style-type: none"> PHMSA Request - ILI and Repair History.xlsx
October 25, 2010		<ul style="list-style-type: none"> Fitting in Spread 10 noted to have experienced coating failure during post-construction hydrostatic testing removed and sent for mechanical testing. 	<ul style="list-style-type: none"> question 6 privledged and confidential.pdf
November 2, 2010		<ul style="list-style-type: none"> Mechanical testing on fitting with coating failure completed and demonstrated that the fitting had a yield strength of [REDACTED]. TC Oil took immediate action to replace the [REDACTED] fittings supplied under the same purchase order (PO). 	<ul style="list-style-type: none"> question 6 privledged and confidential.pdf
November 11, 2010		<ul style="list-style-type: none"> Piece Number 174469, Heat Code NOP-C manufactured at [REDACTED]. In [REDACTED]. Met product specifications (MSS SP-75-2008; TES-FITG-LD-US) for chemistry, strength, toughness, and hardness requirements. Starting plate thickness for elbow was [REDACTED]-inch. Quenched and tempered at [REDACTED] for [REDACTED] minutes and cooled in ambient air. 	<ul style="list-style-type: none"> MTR Elbow_Tag 98.pdf
November 14, 2010		<ul style="list-style-type: none"> WPS RCT-280 was qualified using a single-V groove weld without backing, 30° groove angle, 3/16-inch root opening, and 1/16-inch root face. The base metal materials were API 5L, Grade X70, 36-inch OD, 0.500-inch wall thickness. 	<ul style="list-style-type: none"> 4650135 FINAL MANUFACTURERS DATA BOOK - CANADAOIL FORGE FITTINGS.pdf
November 15, 2010		<ul style="list-style-type: none"> 36-inch, 3D, 30°, 0.515-inch wall thickness elbow (piece number 174469; TAG 98) with heat code NOP-C manufactured at [REDACTED] in [REDACTED]. WPS/PQRs for the fitting is CF 1080-2007, Rev 0. Radiographed and acceptable to UW-51 of ASME, Section VIII, Division 1. Third party surveillance at [REDACTED] verified welding, hardness testing, dimensions, and radiographs complied with specification requirements. 	<ul style="list-style-type: none"> MTR Elbow_Tag 98.pdf Tag 98 138F – Pkg.pdf 25472-100-YQA-PV04-1D005 Revision-1.pdf
November 16-24, 2010		<ul style="list-style-type: none"> [REDACTED] began fabrication of [REDACTED] bend assemblies <ul style="list-style-type: none"> Tuesday 16th: [REDACTED] welds; [REDACTED] fittings; no defects. Wednesday 17th: [REDACTED] welds; [REDACTED] fittings; no defects. Thursday 18th: [REDACTED] welds; [REDACTED] fittings; no defects. Friday 19th: [REDACTED] welds; [REDACTED] fittings; [REDACTED] defects ([REDACTED]) on TAG 	<ul style="list-style-type: none"> 4650135 FINAL MANUFACTURERS DATA BOOK - [REDACTED] FITTINGS.pdf

REDACTIONS MADE BY TC OIL - Pending PHMSA Review

TC Oil

**CONFIDENTIAL – Protected from release under
FOIA Exemptions 4 and 7(F), 5 USC 552(b)(4)
and (b)(7)(F).**



Date	Time (MST)	Description	Source
		<ul style="list-style-type: none"> repair welds () on TAG 126; radiographed at positions and . o Saturday 20th: welds; fittings; no defects; welds re-radiographed at the request of TC Oil for noted offset () on TAG 138F). o Sunday 21st: welds; fittings; no defects; TAG 114C inspected. o Monday 22nd: welds; fittings; defect; repair weld radiographed at position . o Tuesday 23rd: welds; fittings; defect; repair weld radiographed at position . o Wednesday 24th: welds; fittings; defect; repair weld radiographed at position . 	
November 19, 2010		<ul style="list-style-type: none"> Fabricated weld assembly TAG 98 radiographed by a Level II Technician (certified September 13, 2010) from Diamond Inspection. No defects noted in girth weld G59A or G59B (the weld that failed). Technique A, 56 curies, Ir 192 source, AGFA D5 film, SWE/SWV per procedure DGRT0001, Rev 1 and acceptance standard ASME, Section VIII. A total of welds and fittings radiographed. Four defects were noted (on TAG 138F, on TAG 126A, on TAG 126); repair welds () radiographed at positions and . Crews were mobilized to the TAG 108 fitting replacement location. 	<ul style="list-style-type: none"> Tag 98 138F – Pkg.pdf 7532446 KCE40-42779-02-09-4-11-11-07-0 Inspector Reports-004 SPR9C 101119.pdf 4650135 FINAL MANUFACTURERS DATA BOOK - .pdf
November 20, 2010		<ul style="list-style-type: none"> TC Oil requested that welds G59A and G59B of the TAG 98 assembly be radiographed again at positions and because of “offsets for customer”. No defects reported in TAG 98. Hydrostatic test of TAG 98 assembly at . Minimum strength (4 hours) test pressure of 1,870 psig (94% SMYS). 	<ul style="list-style-type: none"> 4650135 FINAL MANUFACTURERS DATA BOOK - .pdf Tag 98 138F – Pkg.pdf
November 22, 2010		<ul style="list-style-type: none"> TAG 98 elbow assembly shipped via truck from in to in for coating application. 	<ul style="list-style-type: none"> Tag 98 138F – Pkg.pdf
November 23, 2010		<ul style="list-style-type: none"> Crews began installing truck mats on the access road at the TAG 108 location. 	<ul style="list-style-type: none"> 7467245 KCE40-42814-02-09-4-11-11-07-0 Inspector Reports-008 SPR9C 101123.pdf

REDACTIONS MADE BY TC OIL - Pending PHMSA Review

TC Oil

**CONFIDENTIAL – Protected from release under
FOIA Exemptions 4 and 7(F), 5 USC 552(b)(4)
and (b)(7)(F).**



Date	Time (MST)	Description	Source
November 24, 2010		<ul style="list-style-type: none"> Installing truck mats and began topsoiling at TAG 108 location. 	<ul style="list-style-type: none"> 7424345 KCE40-42836-02-09-4-11-11-07-0 Inspector Reports-009 SPR9C 101124.pdf
November 29, 2010		<ul style="list-style-type: none"> Continued installing truck mats on the access road. Built ROW along the creek bank. 	<ul style="list-style-type: none"> 8069136 KCE40-42903-02-09-4-11-11-07-0 Inspector Reports-013 SPR9C 101129.pdf
November 30, 2010		<ul style="list-style-type: none"> Began fabrication of 'box section' at Mill Creek 3 – three joints and sag bend were welded (9GT-020). 	<ul style="list-style-type: none"> 7554797 KCE40-42946-02-09-4-11-11-07-0 Inspector Reports-014 SPR9C 101130.pdf
December 1, 2010		<ul style="list-style-type: none"> Finished ROW for TAG 108. Continued welding creek section. Topsoil and rip rap removal on south side of Mill Creek to prepare for excavation. Excavated 150 ft of pipe on south side of Mill Creek to cut out overbend and prepare to dig creek. Made one cut and four welds. 	<ul style="list-style-type: none"> 7356782 KCE40-43038-02-09-4-11-11-07-0 Inspector Reports-015 SPR9C 101201.pdf
December 2, 2010		<ul style="list-style-type: none"> Hydrostatic test 9-S-003 for Mill Creek 3 fitting replacements at MP 13.76 (430.9 linear feet). Minimum strength (4 hours) test pressure of 1,822 psig (100% SMYS). 	<ul style="list-style-type: none"> 9-S-003 Hydrotest Record.pdf 7471005 KCE40-43039-02-09-4-11-11-07-0 Inspector Reports-016 SPR9C 101202.pdf
December 3, 2010		<ul style="list-style-type: none"> Cut creek bank down to excavate south side of Mill Creek 3 (TAG 108). Curlex and straw added to cuts for erosion control. Welds were inspected with AUT and four welds were coated. Began dewatering test section. 	<ul style="list-style-type: none"> 7430950 KCE40-43139-02-09-4-11-11-07-0 Inspector Reports-017 SPR9C 101203.pdf
December 4, 2010		<ul style="list-style-type: none"> Removed a three joint section from the ditch on the south side of Mill Creek (included overbend section). Welds 9GT-027 and 9GT-030 were completed. Coated two more welds (9GT-021 and 9GT-018). Began installing wire mesh around the creek section. 	<ul style="list-style-type: none"> 7622958 KCE40-43140-02-09-4-11-11-07-0 Inspector Reports-018 SPR9C 101204.pdf
December 5, 2010		<ul style="list-style-type: none"> Installed forms on creek section to prepare for concrete coating installation (TAG 108). 	<ul style="list-style-type: none"> 7534779 KCE40-43141-02-09-4-11-11-07-0 Inspector Reports-019 SPR9C 101205.pdf
December 6, 2010		<ul style="list-style-type: none"> Installed concrete coating and waiting for it to cure before installing the new creek section (TAG 108). Weld 9GT-030 x-rayed. 	<ul style="list-style-type: none"> 7610623 KCE40-43162-02-09-4-11-11-07-0 Inspector Reports-020 SPR9C 101206.pdf

REDACTIONS MADE BY TC OIL - Pending PHMSA Review

TC Oil

**CONFIDENTIAL – Protected from release under
FOIA Exemptions 4 and 7(F), 5 USC 552(b)(4)
and (b)(7)(F).**



Date	Time (MST)	Description	Source
		<ul style="list-style-type: none"> Weld 9GTT-031 on south side of TAG 98 fitting completed and x-rayed. Excavated and pulled out old creek section to prepare for installation of new creek section. 	
December 7-9, 2010		<ul style="list-style-type: none"> Began excavating creek to prepare for new section; clamming ditch to keep it from filling in; relayed spoil away from creek section for bank restoration (TAG 108). Waiting for concrete to cure. 	<ul style="list-style-type: none"> 7658681 KCE40-43200-02-09-4-11-11-07-0 Inspector Reports-021 SPR9C 101207.pdf 7422365 KCE40-43231-02-09-4-11-11-07-0 Inspector Reports-022 SPR9C 101208.pdf
December 10, 2010		<ul style="list-style-type: none"> Installed creek section and backfilled. Began excavating south side of creek for overbend installation and cut fitting (presumed to be TAG 98) for proper fit. Two welds made at TAG 108 location, 9GTT-033 and tie-in weld 9GT-032 to creek section; both welds x-rayed and accepted. Survey shot the location. Filled section with water for hydrostatic test. Sunny and cool with temperatures between 25°F (-3.9°C) and 50°F (10°C). 	<ul style="list-style-type: none"> 7667265 KCE40-43358-02-09-4-11-11-07-0 Inspector Reports-024 SPR9C 101210.pdf
December 11-12, 2010		<ul style="list-style-type: none"> Hydrostatic test 9-S-004 for Mill Creek 3 fitting replacements at MP 13.76 (430.9 linear feet). Minimum strength (4 hours) test pressure of 1,816 psig (101% SMYS). Dewatering pig froze up in pipe; had to heat manifold to clear the pig (broke free on December 12, 2010). 	<ul style="list-style-type: none"> 9-S-004 Hydrotest Record.pdf 7352631 KCE40-43394-02-09-4-11-11-07-0 Inspector Reports-025 SPR9C 101211.pdf
December 12, 2010		<ul style="list-style-type: none"> Backfilling at TAG 108 location to prepare to install creek banks 	<ul style="list-style-type: none"> 7557960 KCE40-43395-02-09-4-11-11-07-0 Inspector Reports-026 SPR9C 101212.pdf
December 13-14, 2010		<ul style="list-style-type: none"> Completed final tie-in weld on south side of Mill Creek 3 9GT-035; passed UT inspection; coated. Completed final tie-in weld at the going away side of 20th Road, 9GT-034; passed UT inspection; coated. Restoring creek banks; installed French drains; wrapped in Geotech fabric; installed trench breakers on north side; and shaded south side. 	<ul style="list-style-type: none"> 7304031 KCE40-43465-02-09-4-11-11-07-0 Inspector Reports-027 SPR9C 101213.pdf 7482277 KCE40-43503-02-09-4-11-11-07-0 Inspector Reports-028 SPR9C 101214.pdf

REDACTIONS MADE BY TC OIL - Pending PHMSA Review

TC Oil

**CONFIDENTIAL – Protected from release under
FOIA Exemptions 4 and 7(F), 5 USC 552(b)(4)
and (b)(7)(F).**



Date	Time (MST)	Description	Source
December 15-17, 2010		<ul style="list-style-type: none"> Completed rip-rap on north and south sides of Mill Creek 3. Replaced topsoil and seeding completed on north and south sides. 	<ul style="list-style-type: none"> 7417201 KCE40-43505-02-09-4-11-11-07-0 Inspector Reports-030 SPR9C 101216.pdf
February 7, 2011		<ul style="list-style-type: none"> Cushing Extension (Keystone Phase II) placed into service. 	<ul style="list-style-type: none"> https://www.tcenergy.com/announcements/2011/2011-02-08keystones-cushing-extension-begins-deliveries-to-oklahoma/ BAP for Contributory Pipeline Segments
September 20-21, 2011		<ul style="list-style-type: none"> Audit of [REDACTED] in Becancour, Quebec by [REDACTED] for Keystone Phase 3 and 4. Two major findings: short tempering duration that did not meet MSS SP-75-2008 requirements and lack of annual surveys on the austenizing furnace. NCRs issued and corrective actions put in place to re-temper and re-test 24 fittings that did not meet MSS SP-75-2008 requirements and to increase tempering times to meet specs. The mechanical properties of the 24 fittings were acceptable even at the shorter tempering duration. [REDACTED] studied tempering time effect on mechanical properties for 4 different plate thicknesses (0.625-inch to 1.500-inch) and concluded that the mechanical properties of fittings tempered for 30-minutes did not differ significantly from those tempered for durations meeting MSS SP-75-2008 requirements. 	<ul style="list-style-type: none"> [REDACTED] Report for LD Fittings for KXL PO 25472.pdf
October 11, 2012		<ul style="list-style-type: none"> Final audit report for the production of large diameter, high grade fittings at [REDACTED] Becancour facility. 	<ul style="list-style-type: none"> [REDACTED] Auditing Report for LD Fittings for KXL PO 25472.pdf
December 2012		<ul style="list-style-type: none"> BHI Profile ILI tool run (caliper). A [REDACTED] ID restriction was reported just upstream of girth weld 1352000 (failed girth weld G59B, GWD 13530) between measure distance 73,355 and 73,371. 	<ul style="list-style-type: none"> PHMSA Request - ILI and Repair History.xlsx
March 2, 2013		<ul style="list-style-type: none"> Excavation performed to investigate the [REDACTED] ID restriction reported by the December 2012 caliper ILI. The restriction was measured in the field ([REDACTED] ovality) without removing the coating, the ovality was assessed as non-injurious, and the excavations was backfilled. The ovality was in the TAG 98 bend assembly. 	<ul style="list-style-type: none"> PHMSA Request - ILI and Repair History.xlsx Threat Matrix PHMSA Request Dec 9 2022.xlsx

REDACTIONS MADE BY TC OIL - Pending PHMSA Review

TC Oil

**CONFIDENTIAL – Protected from release under
FOIA Exemptions 4 and 7(F), 5 USC 552(b)(4)
and (b)(7)(F).**



Date	Time (MST)	Description	Source
September 2013		<ul style="list-style-type: none"> Baker Hughes GEMINI MFL/Caliper/IMU ILI tool run. Reported minimum OD at [REDACTED] ([REDACTED]) at absolute distance 732+77.1 feet – the location of TAG 98 (BND 350). Bending strain data collected. 	<ul style="list-style-type: none"> PHMSA Request - ILI and Repair History.xlsx 2013_BHI_GEOPIG_NPS_36_KS10_SteeleCity-Burns Issue B.pdf
2016		<ul style="list-style-type: none"> [REDACTED] capacity increase project opened. The capacity increase project triggered stress analyses and EA to determine the impact of the proposed changes in operating conditions (particularly increased temperature with increased flow rate) on pipeline bending stresses. 	<ul style="list-style-type: none"> PositionStatement_Historical Pipeline Stress Analyses_20230116.pdf
March 28, 2017		<ul style="list-style-type: none"> Water crossing survey completed for the Mill Creek crossing. 	<ul style="list-style-type: none"> 2022 – KeyUS – MP 13.9 - Mill Creek (64029) - Tech Memo.pdf
October 26, 2017		<ul style="list-style-type: none"> AutoPIPE Linear-Elastic 1D Beam Finite Element Model report on bending stresses induced by internal pressure, temperature, and soil restraint for the Cushing Extension. [REDACTED] elbow fittings (out of [REDACTED], [REDACTED] on KS10 and [REDACTED] on KS11) were identified along the Cushing Extension with combined equivalent von-Mises stress that exceeded SMYS; TAG 98 (BND 350) was not one of the [REDACTED] elbows. Recommended performing FEA for more accurate predictions of the stress response at elbows. 	<ul style="list-style-type: none"> PositionStatement_Historical Pipeline Stress Analyses_20230116.pdf
June 15, 2018		<ul style="list-style-type: none"> Desktop hydrotechnical analysis of the Mill Creek crossing completed. Determined that the Mill Creek crossing could potentially be exposed in a 1:100-year event (no pipe integrity impact). 	<ul style="list-style-type: none"> 2022 – KeyUS – MP 13.9 - Mill Creek (64029) - Tech Memo.pdf
November 2018		<ul style="list-style-type: none"> BHGE MFL4 MFL/Caliper/IMU ILI tool run. No anomalous conditions noted in GWD 13530 or GWD 13520. No ID restriction in TAG 98 (BND 350) reported. 	<ul style="list-style-type: none"> PHMSA Request - ILI and Repair History.xlsx
2020		<ul style="list-style-type: none"> [REDACTED] capacity increase project opened. The capacity increase project triggered additional stress analyses and EA to determine the impact of the proposed changes in operating conditions on pipeline bending stresses. Analysis conservatively assumed temperature increases associated with flows at [REDACTED] An in-house machine learning model identified BND 350 as one with relatively 	<ul style="list-style-type: none"> PositionStatement_Historical Pipeline Stress Analyses_20230116.pdf

REDACTIONS MADE BY TC OIL - Pending PHMSA Review

TC Oil

**CONFIDENTIAL – Protected from release under
FOIA Exemptions 4 and 7(F), 5 USC 552(b)(4)
and (b)(7)(F).**



Date	Time (MST)	Description	Source
		<p>high stress and therefore was modeled using FEA. The combined von-Mises stress was 86.8% SMYS.</p> <ul style="list-style-type: none"> A temperature limit of [REDACTED] was placed on Steele City to not exceed stress limits for [REDACTED] bends that exceeded target stress levels. 	
September 2020		<ul style="list-style-type: none"> NDT Eclipse ultrasonic crack detection ILI tool run. No axial cracks found in TAG 98. 	<ul style="list-style-type: none"> PHMSA Request - ILI and Repair History.xlsx
March 31, 2021		<ul style="list-style-type: none"> Engineering assessment of the [REDACTED] elbow fittings along the Cushing Extension completed. The assessment reviewed each elbow for possible interaction with the nine integrity threats; girth weld flaw interaction was determined to not degrade the maximum permissible stress criterion. For the ovality at BND 350, the EA recommended that the elbow be reassessed with a high-resolution caliper tool during the increased flows and peak ground temperatures to determine if the ovality was stable or had increased. Did not identify any pipe integrity constraint that would preclude safe operation at [REDACTED] 	<ul style="list-style-type: none"> PositionStatement_Historical Pipeline Stress Analyses_20230116.pdf
February 17, 2022		<ul style="list-style-type: none"> Hydrotechnical analysis by Golder completed – considered site visit findings, flood frequency analysis, velocity calculations, and vertical scour depths. Concluded that the pipeline would not be negatively impacted during a 1:100-year return period event. 	<ul style="list-style-type: none"> 2022 – KeyUS – MP 13.9 - Mill Creek (64029) - Tech Memo.pdf
December 5, 2022	20:01	<ul style="list-style-type: none"> Leak detection tool launched at Steele City PS. 	<ul style="list-style-type: none"> KEYML ELOG Report 48Before 12After.pdf
December 7, 2022	19:34	<ul style="list-style-type: none"> Decreasing rate of change alarm for passage of ILI tool at Hope PS. Rate on the Cushing Extension reduced to ~3,500 m³/hr. 	<ul style="list-style-type: none"> KEYML ELOG Report 48Before 12After.pdf
December 7, 2022	19:59	<ul style="list-style-type: none"> Bypassed Hope PS for passage of ILI tool. 	<ul style="list-style-type: none"> KEYML ELOG Report 48Before 12After.pdf
December 7, 2022	20:01	<ul style="list-style-type: none"> LDS leak alarm STLCT-HOPEP. Secondary pressure leak trigger. 	<ul style="list-style-type: none"> KEYML ELOG Report 48Before 12After.pdf LDS ELOG Report 48Before 12After.pdf
December 7, 2022	20:07	<ul style="list-style-type: none"> LPCC made decision to perform an emergency shutdown due to suspected leak between Steele City PS and Hope PS per procedure. First responder notified. 	<ul style="list-style-type: none"> KEYML ELOG Report 48Before 12After.pdf LDS ELOG Report 48Before 12After.pdf

REDACTIONS MADE BY TC OIL - Pending PHMSA Review

TC Oil

**CONFIDENTIAL – Protected from release under
FOIA Exemptions 4 and 7(F), 5 USC 552(b)(4)
and (b)(7)(F).**



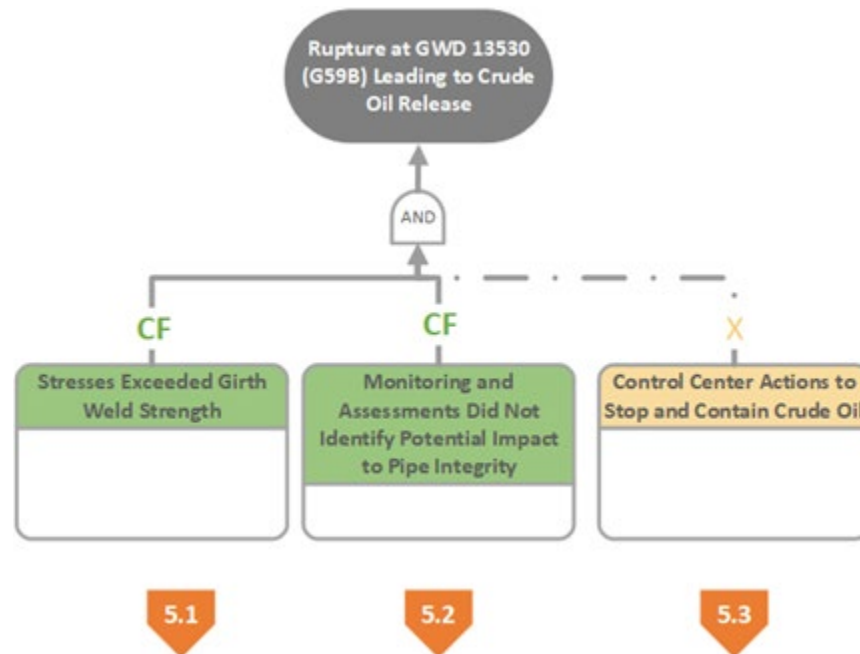
Date	Time (MST)	Description	Source
December 7, 2022	20:12	<ul style="list-style-type: none"> Oil Scheduling notified. 	<ul style="list-style-type: none"> KEYML ELOG Report 48Before 12After.pdf
December 7, 2022	20:28	<ul style="list-style-type: none"> Regional EOC notified. Oil Control Center (OCC) notified. 	<ul style="list-style-type: none"> KEYML ELOG Report 48Before 12After.pdf
December 7, 2022	20:31	<ul style="list-style-type: none"> Corporate EOC notified. 	<ul style="list-style-type: none"> KEYML ELOG Report 48Before 12After.pdf
December 7, 2022	23:15	<ul style="list-style-type: none"> Oil confirmed on the ground. 	<ul style="list-style-type: none"> KEYML ELOG Report 48Before 12After.pdf
December 7, 2022	23:28	<ul style="list-style-type: none"> The National Response Center (NRC) was notified (NRC Report #1354442) of the release. 	<ul style="list-style-type: none"> Original 7000-1 Accident Report MP14 20230106.pdf

9 Appendix B – Cause & Effect Trees

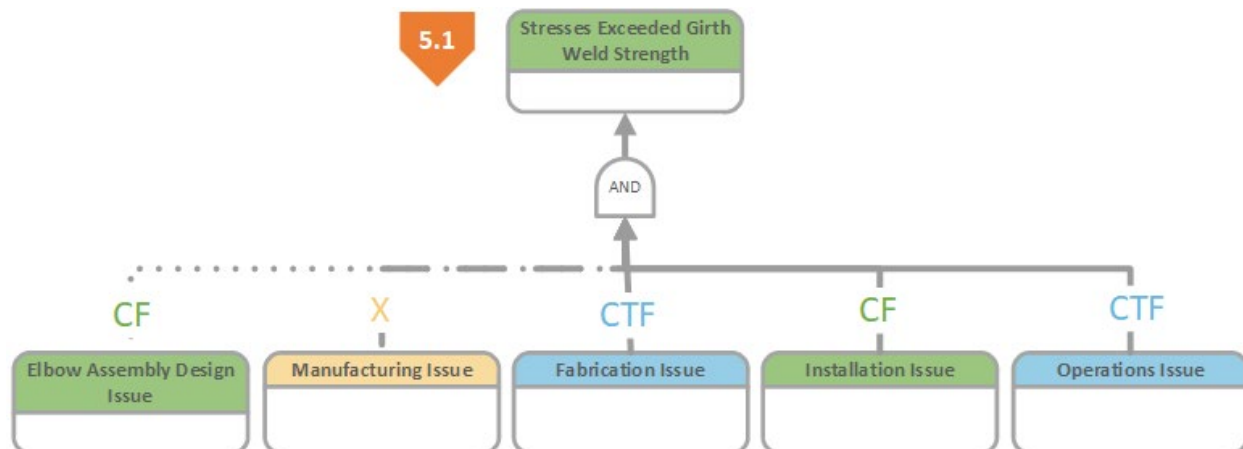
The Cause and Effect Trees used to determine the causal factors and root causes are presented in this Appendix. The events are color coded to aid interpretation as follows:

- Gray = Events or steps in event sequence;
- Orange = Inconclusive: causes or causal factors that are neither confirmed nor eliminated by available data or evidence;
- Yellow = Eliminated: causes or causal factors that are eliminated by available data or evidence;
- Purple = Confirmed but not a factor: causes or causal factors that are confirmed as factual but determined to not be causal;
- Light blue = Contributing factor: underlying reasons why a causal factor occurred, but not sufficiently fundamental to be causal.
- Light green = Confirmed: causes or causal factors that are confirmed by available data or evidence;
- Dark green = Root cause: conditions that are confirmed as root causes or near-root causes.

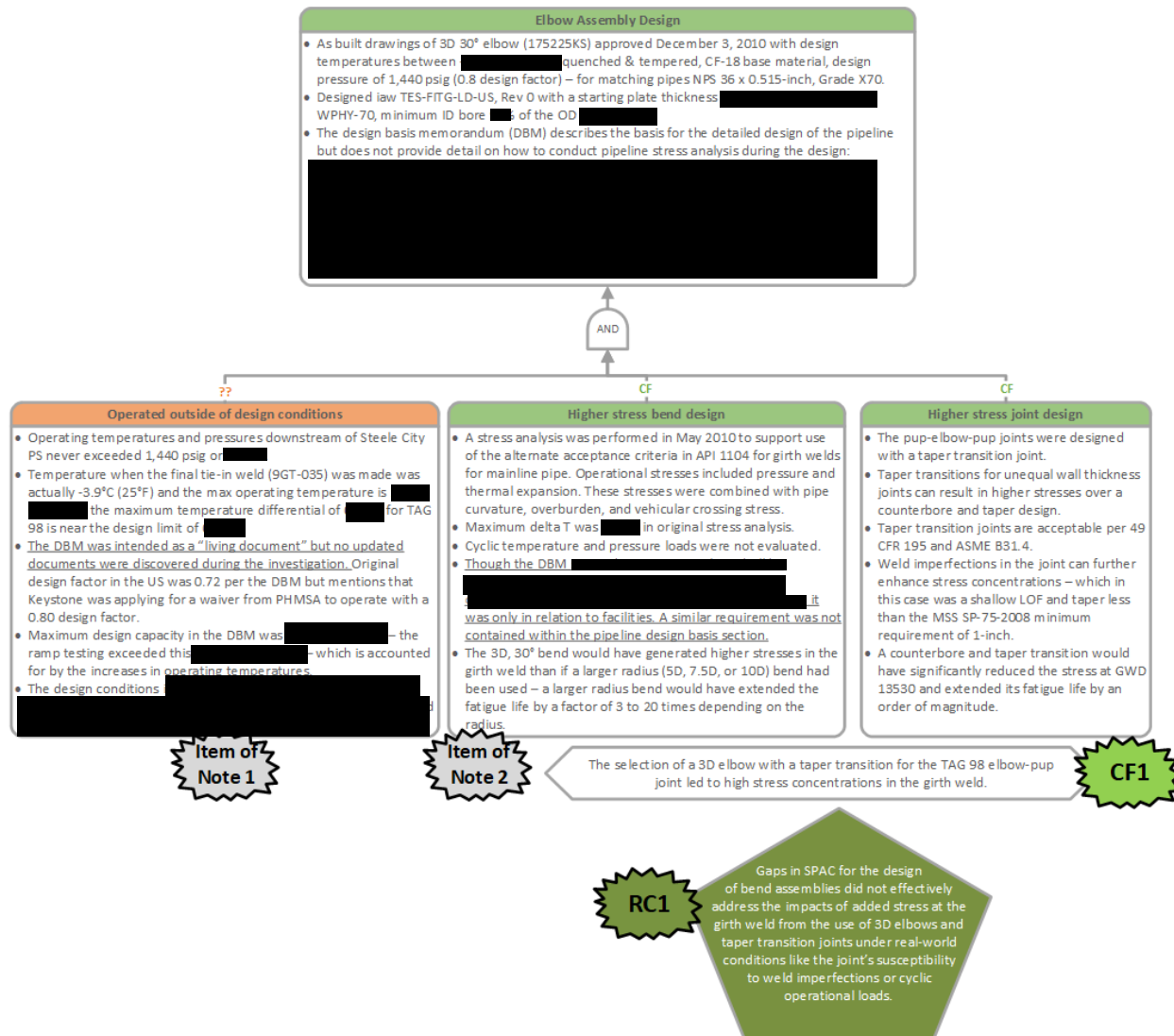
B.0 Rupture at GWD 13530 Leading to Crude Oil Release



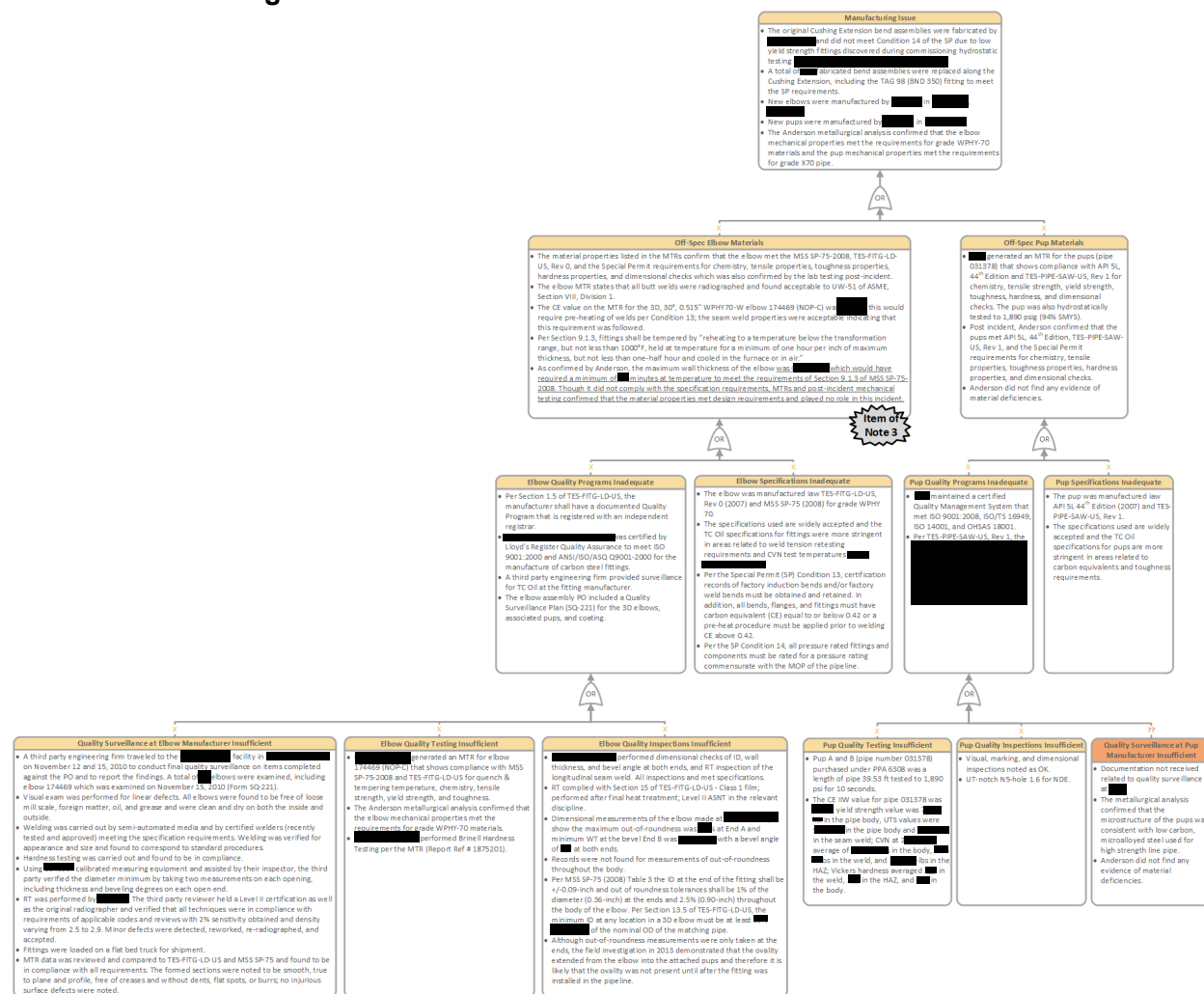
B.1 Stresses Exceeded Girth Weld Strength



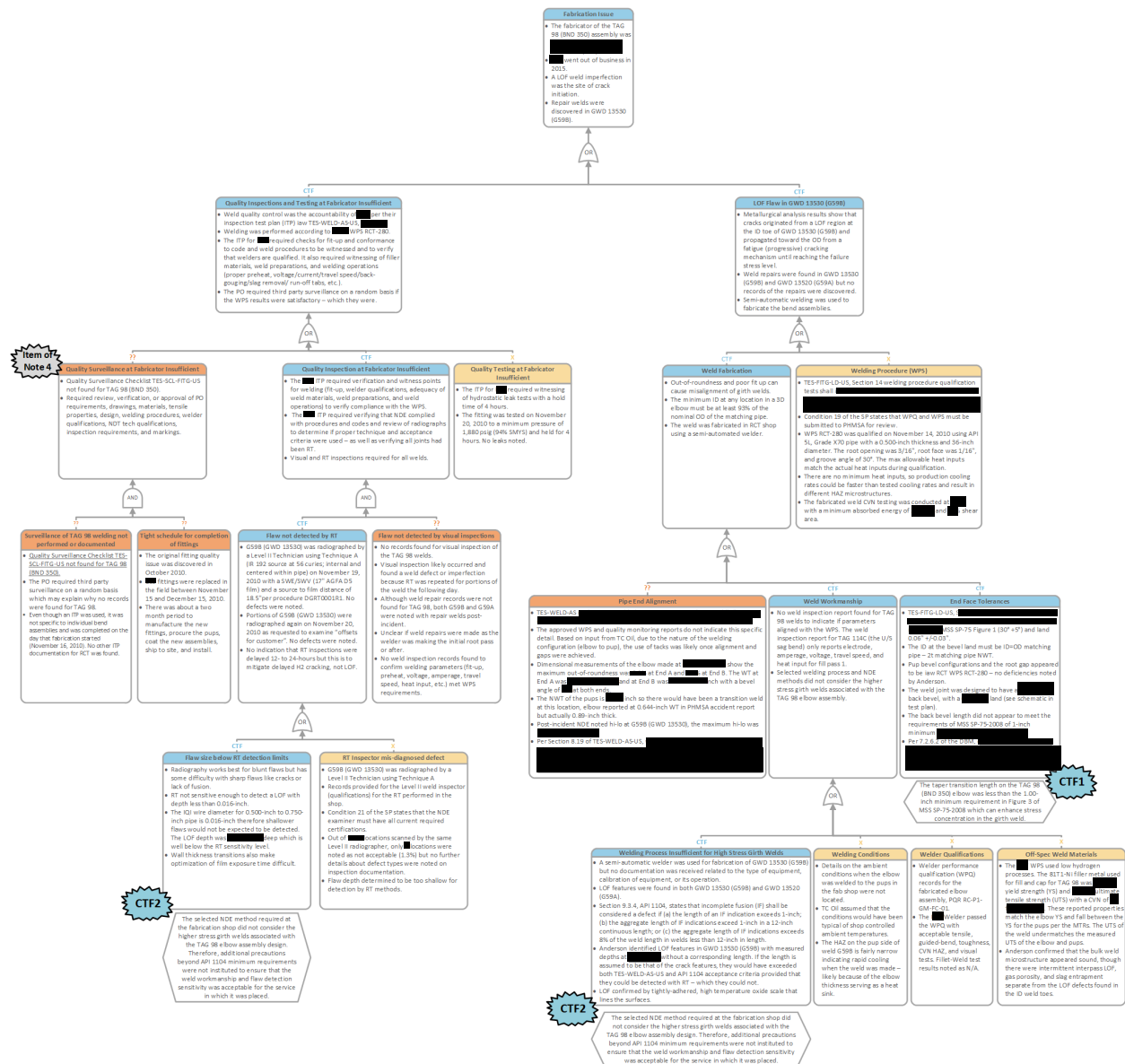
B.1.1 Elbow Assembly Design



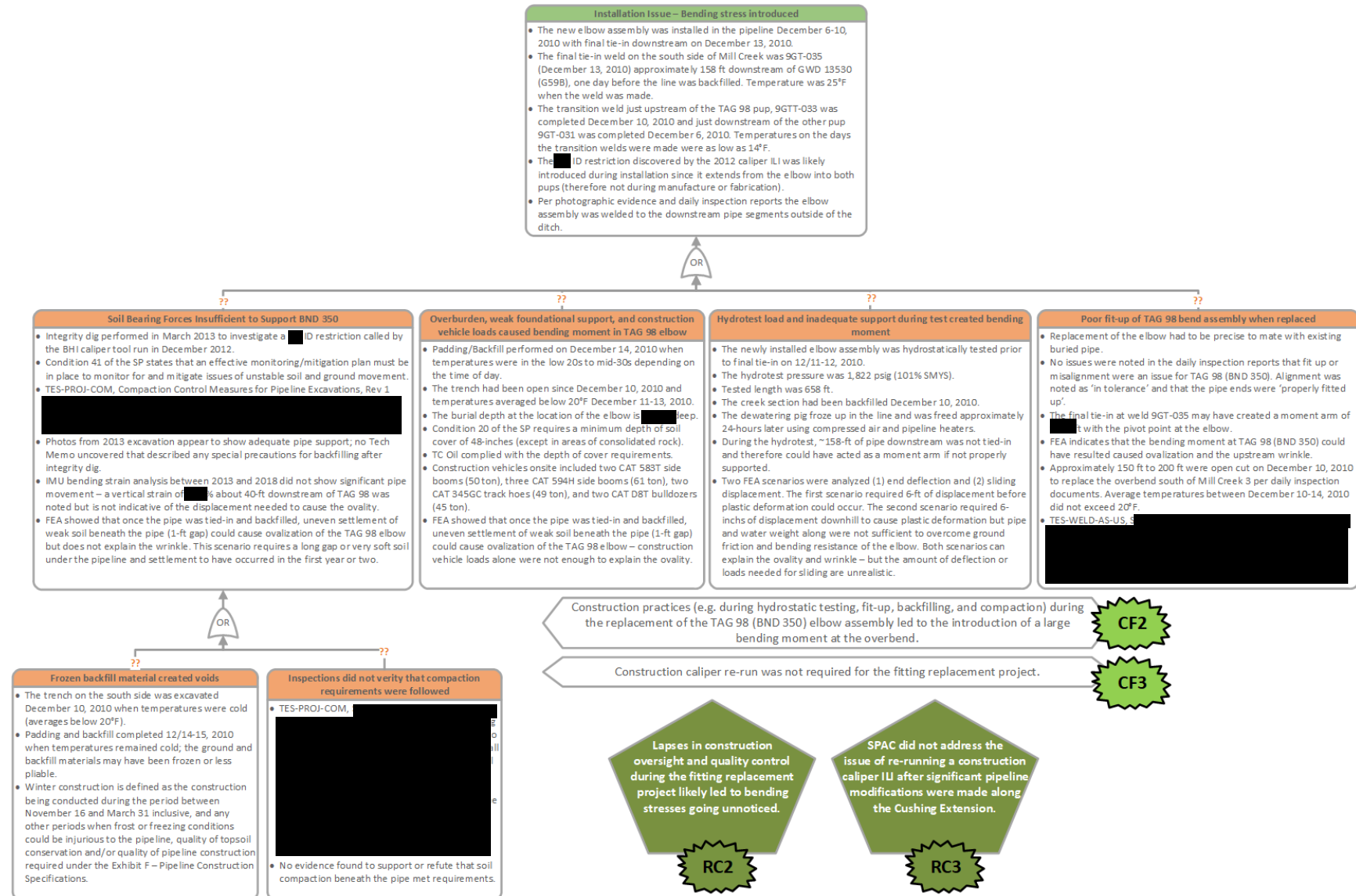
B.1.2 Manufacturing



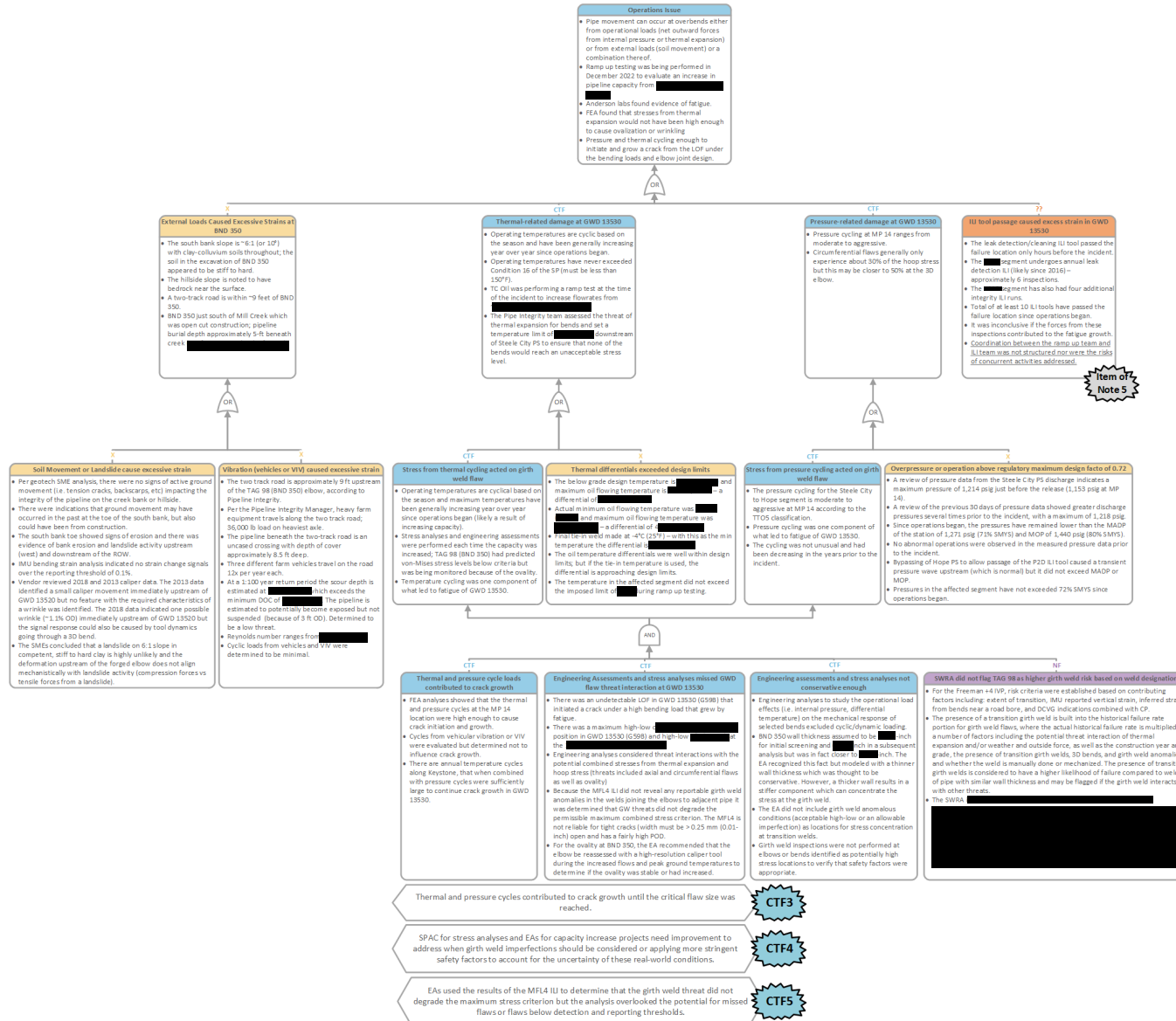
B.1.3 Fabrication



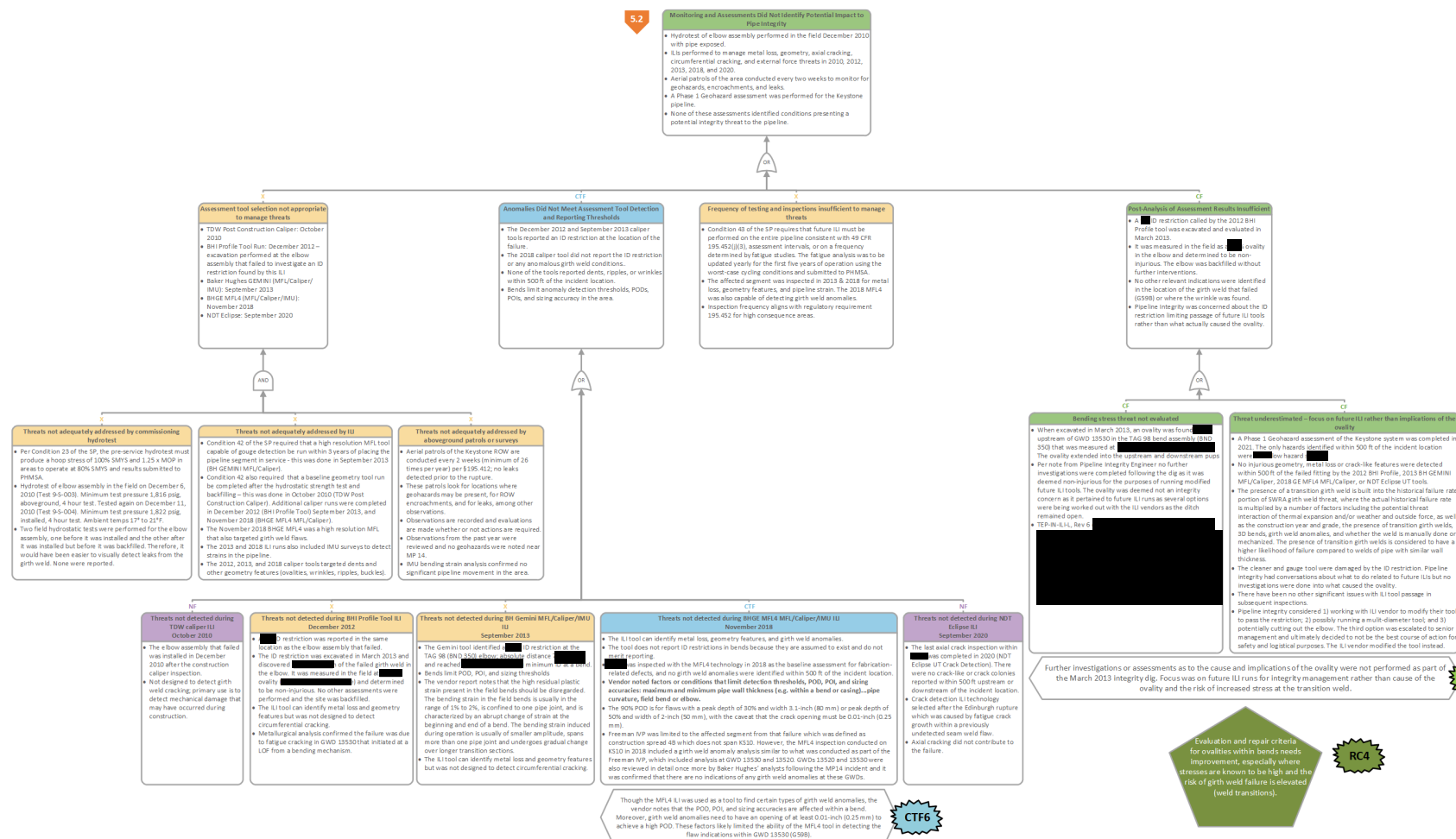
B.1.4 Installation

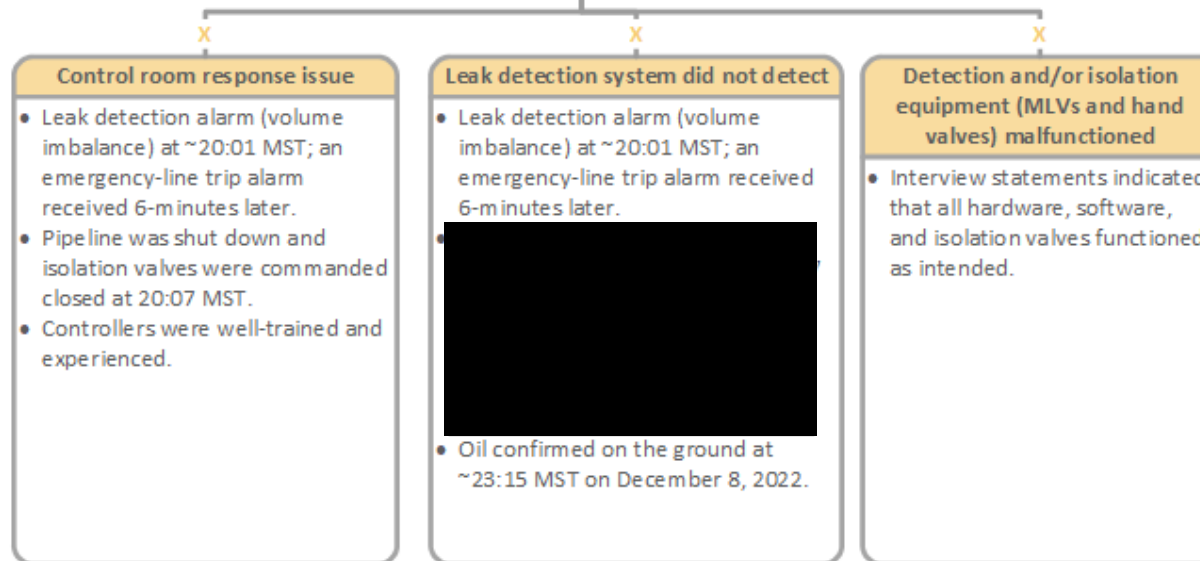
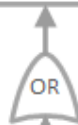
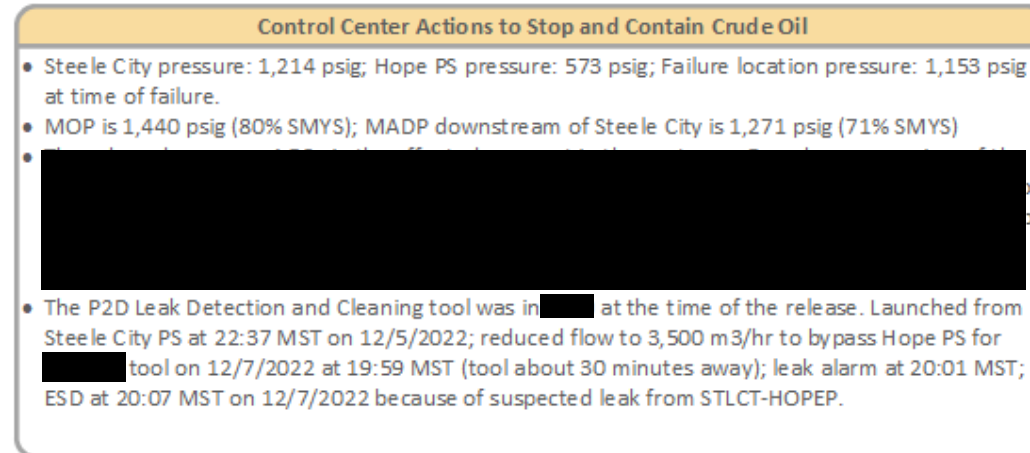


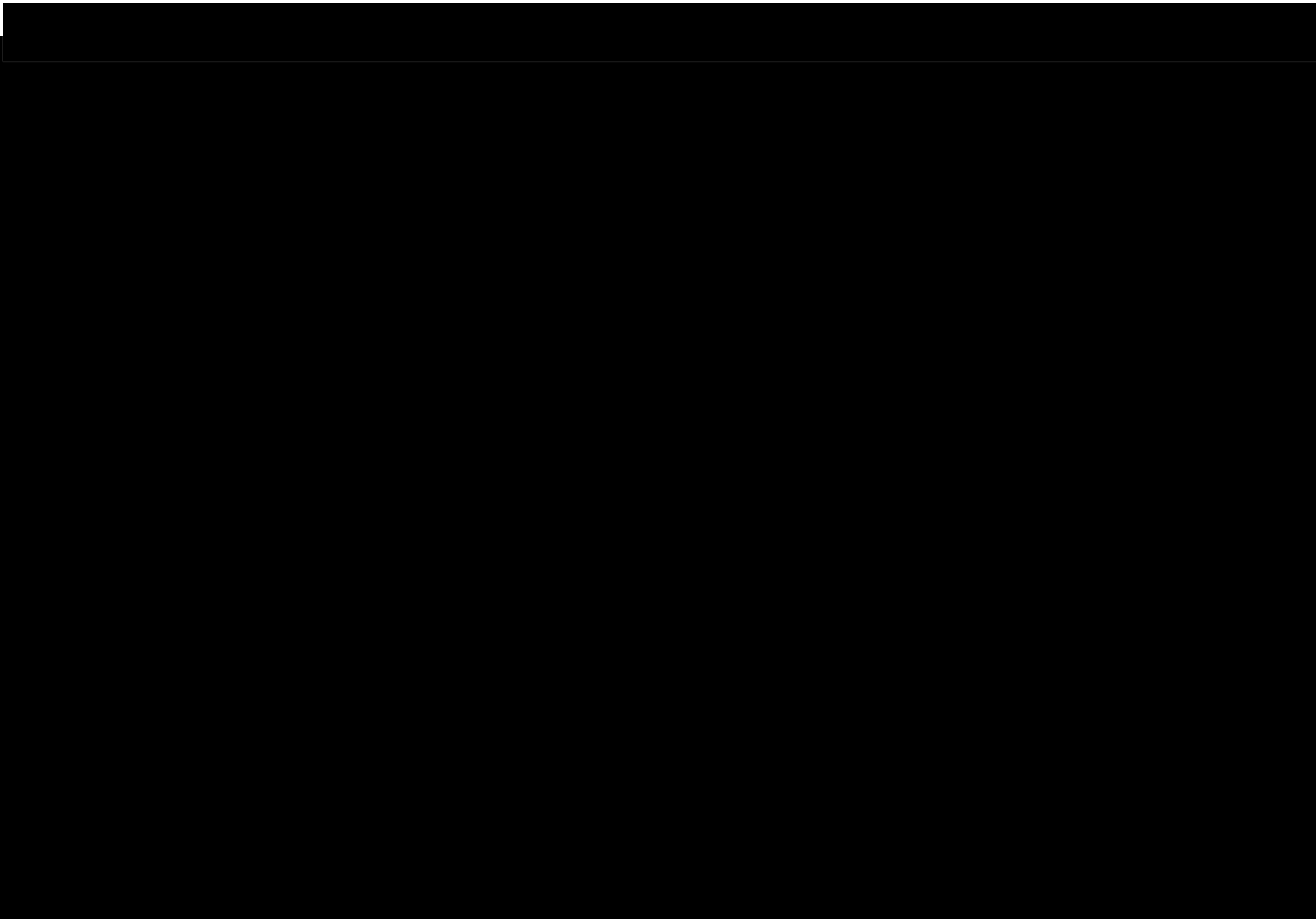
B.1.5 Operation

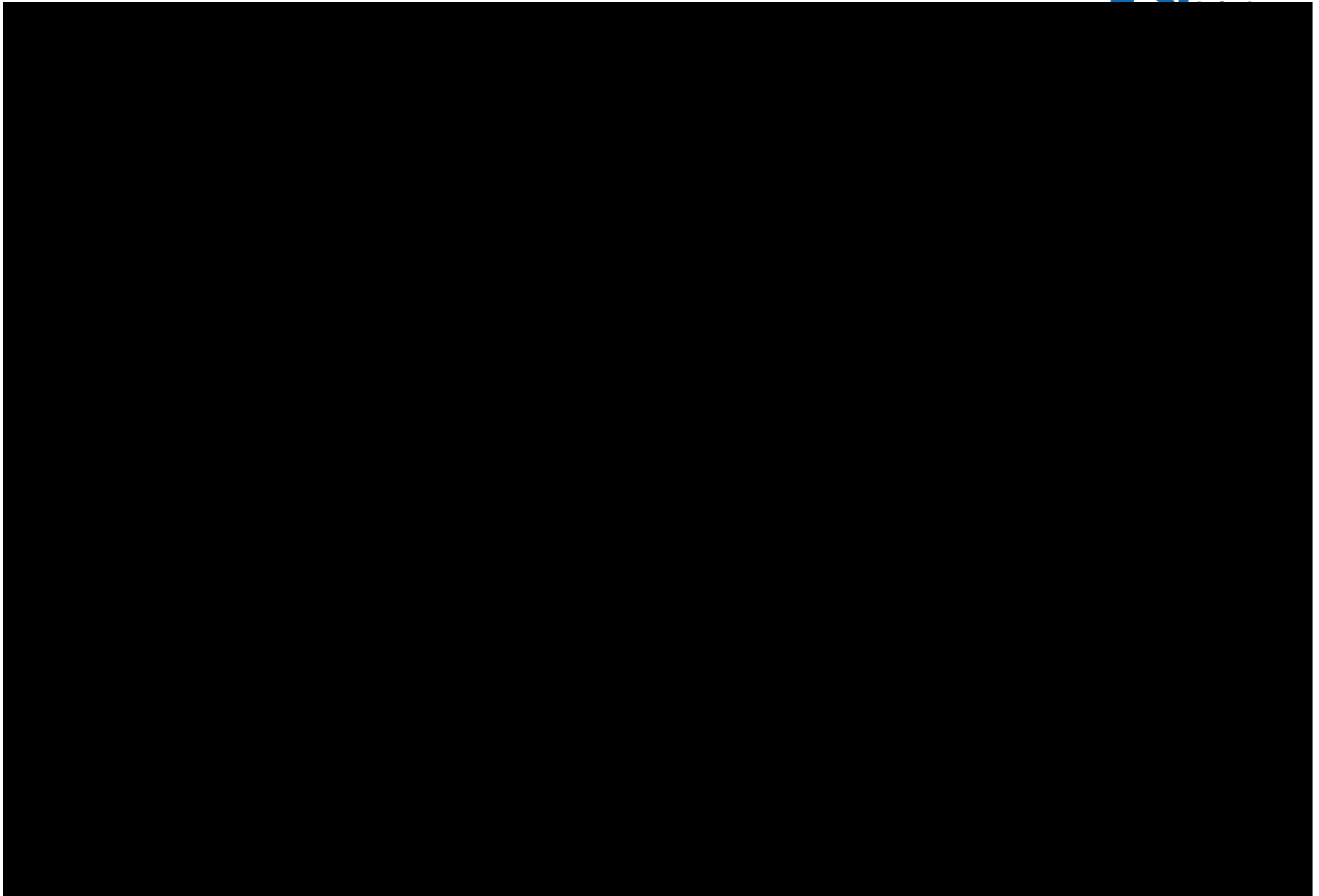


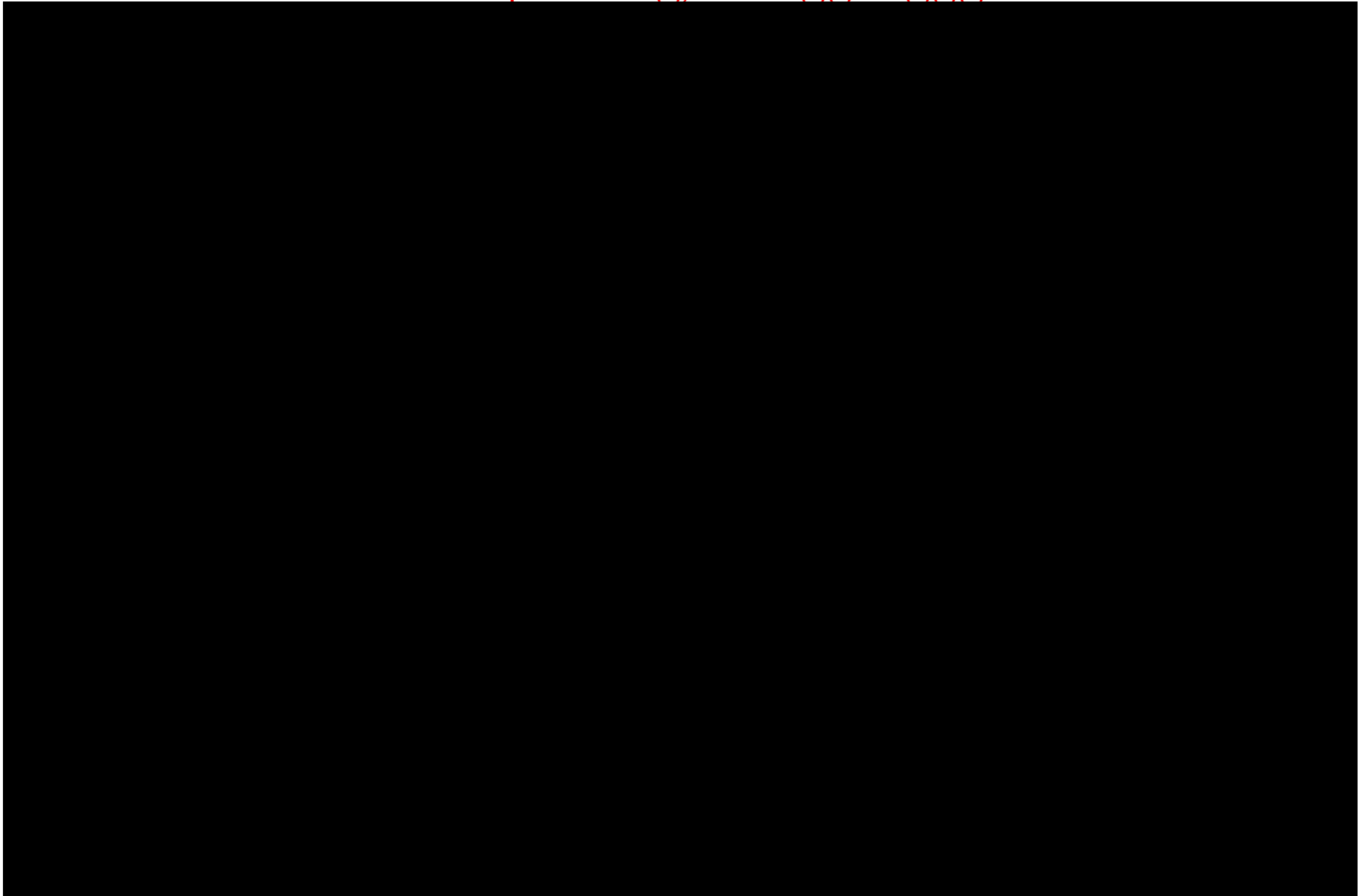
B.2 Integrity Assessments



B.3 Control Center Response**5.3**







11 Appendix D – Stress Analysis

The objectives of the pipeline and elbow stress analysis included the following:

- 1) Potential causes of the ovality and wrinkle, including:
 - a) Accidental loads being applied during the 2010 fitting replacement, such as during hydrostatic testing, fit-up, backfill, and compaction activities.
 - b) Operating loads, such as internal pressure and temperature differentials.
- 2) Stress cycles resulting from temperature differential and pressure fluctuations.
- 3) Stress concentration factors due to imperfect elbow geometry (i.e., out-of-roundness, wall thickness transition, and LOF).

Several different analytical models were used to determine the most likely sequence of events. These analyses are summarized in Table D-1.

Table D.1. Summary of FE Analyses

Analysis	Type	Objective	Model Size	Model Details
Beam Bending	Analytical using fixed and cantilever beam equations	Estimate span lengths and load levels as well as corresponding beam deflections required to yield the elbow during construction	Pipe lengths from 1 to 150 ft	Analytical, linear elastic, small strain, and deformations
Operating Loads	Soil-pipe interaction FEA	Calculate stresses in the elbow under operating loads (P=0 and 1,250 psig; ΔT=45°F; 25°C and 110°F; 61.1°C)	Pipe length ~4,900 ft from each side of the elbow	Numerical, nonlinear, finite strain, pipe elements and Elbow290 elements, upper- and lower-bound soil properties
Post-construction outside force (lack of support, settlement, and vehicle loads)	Soil-pipe interaction FEA	Calculate stresses in the elbow when there is a gap or weak soil under the pipe leading to settlement along the south slope coupled with construction vehicle loads		
Cantilever bending – End deflection during hydro or fit-up	Soil-pipe interaction FEA	Calculate stresses in the elbow from end deflection during the hydrostatic test or fit-up of the replacement segment	Pipe length from 695 ft upstream to 165 ft downstream of the elbow	
Cantilever bending – Sliding displacement during hydro or fit-up	Soil-pipe interaction FEA	Calculate stresses in the elbow from sliding displacement during the hydrostatic test or fit-up of the replacement segment		
Operating Load Cycles	Soil-pipe interaction FEA	Calculate stress ranges in the elbow from ΔP = 500 and 1,000 psig and ΔT = ±40°F (22.2°C) and ±80°F (44.4°C)	Pipe length ~4,900 ft from each side of the elbow	
SCF	Elastic FEA	Calculate SCF values due to wall thickness transition and elbow out-of-roundness	TAG 98 (BND 350) and pups	Numerical, elastic, shell elements, small strain, and deformation
Surface Loading	Elastic-plastic FEA	Calculate effects from surface loading from a high concentrated load on the elbow (e.g., plate compactor)	TAG 98 (BND 350) and pups	Numerical, elastic-plastic, shell elements, finite strain

D.1 Beam Bending

The beam bending model used analytical beam deflection and bending moment equations. Deflection and bending moment for a beam fixed at both ends are defined by the following equations:

$$\Delta(x) = \frac{wx^2}{24EI} (l - x)^2 \quad \text{Equation 1}$$

$$M(x) = \frac{w}{12} (6lx - l^2 - 6x^2) \quad \text{Equation 2}$$

$$\Delta_{max} = \frac{wl^4}{384EI} \quad \{\text{at center}\} \quad \text{Equation 3}$$

$$M_{max} = \frac{wl^2}{12} \quad \{\text{at ends}\} \quad \text{Equation 4}$$

Where x is distance along the beam, w is a uniformly distributed load on the beam, l is the beam length, and EI is bending stiffness. Deflection and bending moment for a cantilever beam are defined by the following equations:

$$\Delta_{max} = \frac{wl^4}{8EI} \quad \{\text{at fixed end}\} \quad \text{Equation 5}$$

$$M_{max} = \frac{wl^2}{2} \quad \{\text{at fixed end}\} \quad \text{Equation 6}$$

$$\Delta_{max} = \frac{Fa^2}{6EI} (3l - a) \quad \{\text{at fixed end}\} \quad \text{Equation 7}$$

$$M_{max} = Fa \quad \{\text{at ends}\} \quad \text{Equation 8}$$

Where F is a concentrated load at distance a from the fixed end and all other parameters are as defined previously.

D.2 Soil-Pipe Interaction Model

Pipe-soil interaction analysis is generally used to calculate the behavior of a long pipe segment under operating loads and outside forces. A pipe-soil interaction model uses one-dimensional beam elements for a pipeline and soil springs to simulate interaction of the pipeline with surrounding soil. This type of model is computationally efficient because it uses a relatively low number of nodes per unit length of the pipe, making it possible to model and analyze a long stretch of the pipeline relatively quickly.

Although the rupture only affected a short portion of the pipeline, to account for the pipe anchor length and the effect of soil-pipe friction in the longitudinal direction of the pipe it was necessary to model several thousand feet of the pipeline on each side of the rupture. The FEA model was built in ANSYS commercial software. Depending on the analysis, two different element types were used for the pipeline (see Table D.1). ANSYS quadratic pipe elements (PIPE289) or elbow elements (ELBOW290) were employed for modeling the pipeline and nonlinear springs (COMBIN39) were defined to represent soil pipe interaction. PIPE289 is capable of accounting for the effect of the internal pressure on pipe curvature (Bourdon's effect). Furthermore, it is well suited for large deformation finite strain analysis and includes the effect of shear deformation. ELBOW290 has all the capabilities of the PIPE289 element, and it uses terms of Fourier

expansion to simulate pipe ovalization and circumferential warping under bending moment. The quadratic pipe elements used in the model possessed a middle node which helped create a realistic representation of pipe curvature along the bends.

The soil-spring elements were defined in accordance with the guidelines of American Lifelines Alliance (AmericanLifelinesAlliance, July 2001 with addenda through February 2005). This idealized model is shown schematically in Figure D.1. In this model the soil spring elements are present in the axial, the transverse vertical, and the transverse horizontal directions. One end of each spring is connected to a pipe element while the other end represents the soil surrounding the pipe. The load displacement responses of the springs are bi-linear elastic-perfectly-plastic models which are shown schematically in Figure D.2.

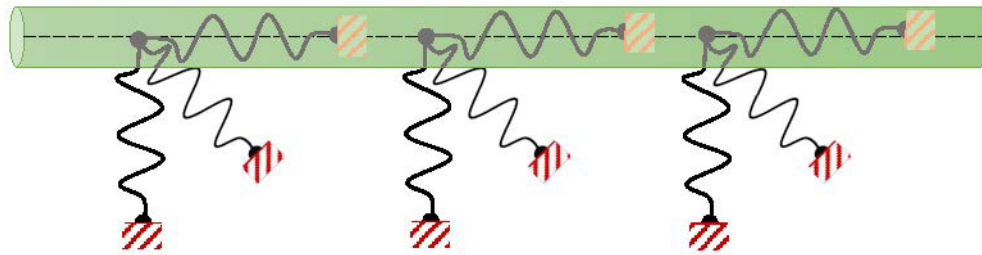


Figure D.1. Soil-Spring Model

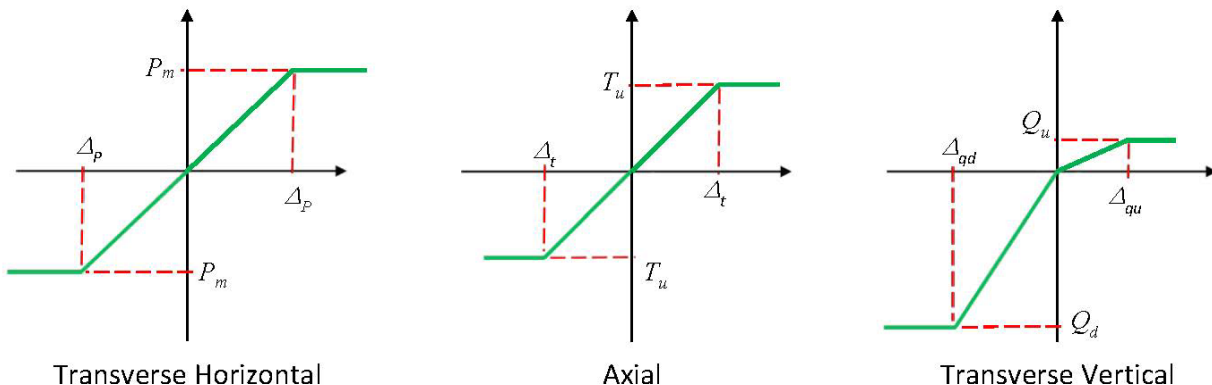


Figure D.2. Bi-linear Soil-Spring Constitutive Model for Transverse Horizontal, Axial, and Transverse Vertical Springs

The soil springs limit the maximum reaction force to the estimated bearing capacity of the soil in the respective direction. The maximum uplift soil capacity (Q_u) is usually significantly lower than the penetration bearing capacity (Q_d). As seen in Figure D.2, this fact is reflected in the definition of the vertical spring. Stiffness and maximum bearing of each spring is a function of soil shear strength, unit weight, depth of cover, and friction between the pipe coating and the soil. The parameters used in this analysis are listed in Table D.1. The spring parameters were calculated using an average cover depth of 5-ft as stated in the alignment sheets.

Lower-bound and upper-bound soil properties were determined based on the information provided in the Wood Group and AP Dynamics stress analysis reports¹⁴⁹ for colluvium and fluvial deposits. These properties are listed in Table D.2 and Table D.3.

Table D.2. Lower-Bound Soil Properties

Landform	Soil Classification	Unit Weight [pcf]	Effective Unit Weight [pcf]	Friction Angle [deg]	Undrained Cohesion [psi]	Elastic Modulus [psi]	Poisson's Ratio
Colluvium	Sandy and Silty Clay	108	108	0	1.45	1800	0.45
Saturated Fluvial	Loose Sand	108	45.6	26	0	4400	0.25

Table D.3. Upper-Bound Soil Properties

Landform	Soil Classification	Unit Weight [pcf]	Effective Unit Weight [pcf]	Friction Angle [deg]	Undrained Cohesion [psi]	Elastic Modulus [psi]	Poisson's Ratio
Colluvium	Sandy and Silty Clay	114	114	0	6.5	8700	0.45
Saturated Fluvial	Loose Sand	121	58.6	29	0	11600	0.25

The soil-spring model described above is suitable for a buried pipeline. In some of the soil-pipe interaction analyses portions of the pipeline were modeled as an exposed pipe. Using a contact element is a more appropriate way to model an exposed portion of a pipeline. In this analysis node-to-node contact elements (CONTACT178) were used for the exposed pipeline lengths. Each contact element was defined using two nodes, the first node was on the respective pipe element while the second represented the ground under the pipe. When the relative movement between the pipe and the ground is such that the pipe presses against the ground the contact element becomes activated and limits the penetration of the pipe into the ground. When a contact element is active, sliding (movement in the plane perpendicular to the element) is allowed but a resistance force is applied against the sliding to account for friction between the pipe and the ground. If the relative movement of the pipe and the ground is such that a gap is formed between the pipe and the ground, then the contact element becomes inactive.

To create the FEA models, the pipeline alignment sheets were digitized to obtain the three-dimensional pipeline (x,y,z) coordinates. Then cubic-spline interpolation was used to convert the discrete coordinates to a mathematical function. The cubic-spline function was then used to generate finite element nodes at equal distances (i.e., 6-inches) along the pipeline alignment. The nodal coordinates were reviewed for overshoots between the scanned data points, (cubic-spline interpolation sometimes overshoots a curve between the points), and when necessary minor adjustments were made. For comparison to the spline interpolation, some of the FEA

¹⁴⁹ See Table 4 of the Wood Group Report Number KCEC1399-WOOD-A-RP-0003, Rev A, February 4, 2021, and Table 1 of AP Dynamics Report Number APD-16-1774-005, Rev 2017-Oct-26.

nodes were also generated by creating a circular arc with a defined radius between the straight pipe segments, using a bend radius of 9 ft for the elbow and the sag, and 60 ft for all the other bends. The comparison between the two methods did not show a significant difference between the calculated stresses.

D.3 Shell Model

A shell model of the subject elbow was created based on the 3D laser scan data. The laser scan results were provided to RSI in STL format (i.e., 3D surfaces of the inner and outer pipe shell in the form of a fine triangular mesh). This model is shown in Figure D.3. RSI imported the STL files into SpaceClaim and inspected the model for any errors or anomalies. The portion of the elbow where the rupture occurred appeared to be deformed and discontinuous (see Figure D.4). The deformed elements were deleted from the model and replaced with a patch. The inspection further revealed several holes on the inner and outer surfaces of the elbow (see Figure D.4) which were patched to create continuous inner and outer surfaces. Furthermore, some local areas of the STL model contained sharp edges or similar geometrical imperfections which were removed and replaced with smooth surfaces (see Figure D.5). The overall quality of the laser scanned data was remarkable but minor imperfections in small areas are very common. Then, a middle surface was generated between the inner and outer surfaces by averaging the two surfaces to serve as the middle surface of the shell model. Some portions of the model that were unrealistic (such as irregularities at the girth welds) were replaced with smooth surfaces. Finally, since the scanned model was shorter on one side than the other side, a cylindrical length was created and blended with the shell model to create a relatively symmetrical elbow. The shell model was imported into the ANSYS mechanical model and representative wall thickness values were assigned to various portions of the shell model (see Figure D.6). Wall thickness values of 0.870-inch and 0.514-inch were assigned to the elbow and the pups, respectively. Between the elbow and the pups, regions with tapered wall thickness transition were defined (see Figure D.7). The elbow, transition regions, and parts of the pups were meshed using relatively fine quadratic shell elements with an average size of 0.5-inch. A larger element size of 2-inches was used for the remainder of the pups (see Figure D.8).



Figure D.3. STL Model of the Elbow from Laser Scanner

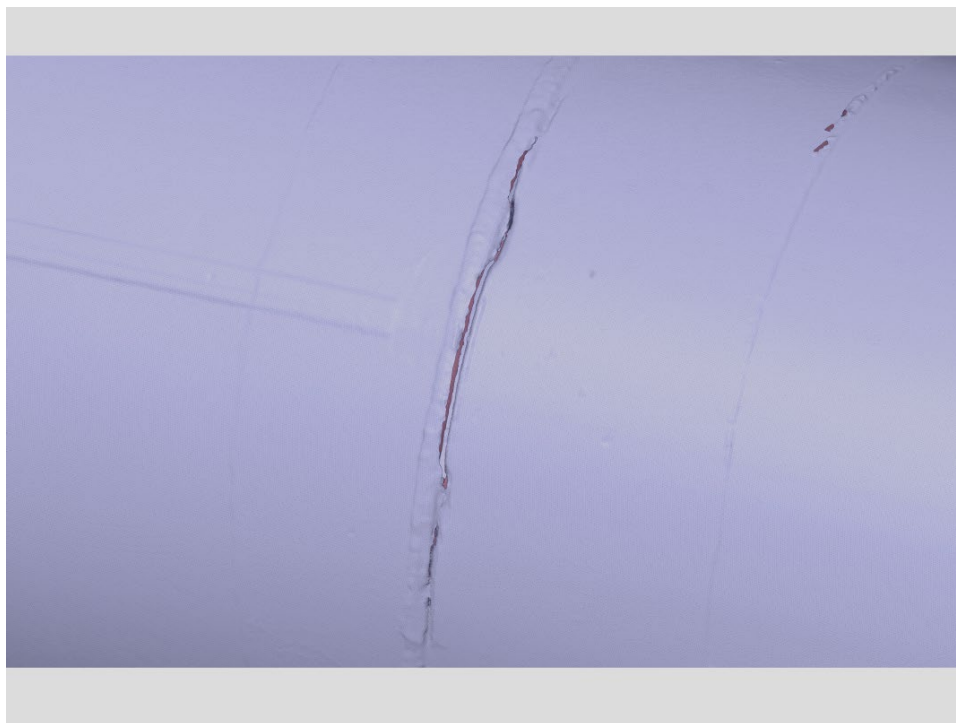


Figure D.4. A View of the Pipe Rupture Area in the STL Model. This Portion of the Model Was Removed and Replaced with a Patch. The Upper Right Portion of the Model Shows Another Example of Several Holes in the Data Which Needed to be Patched.

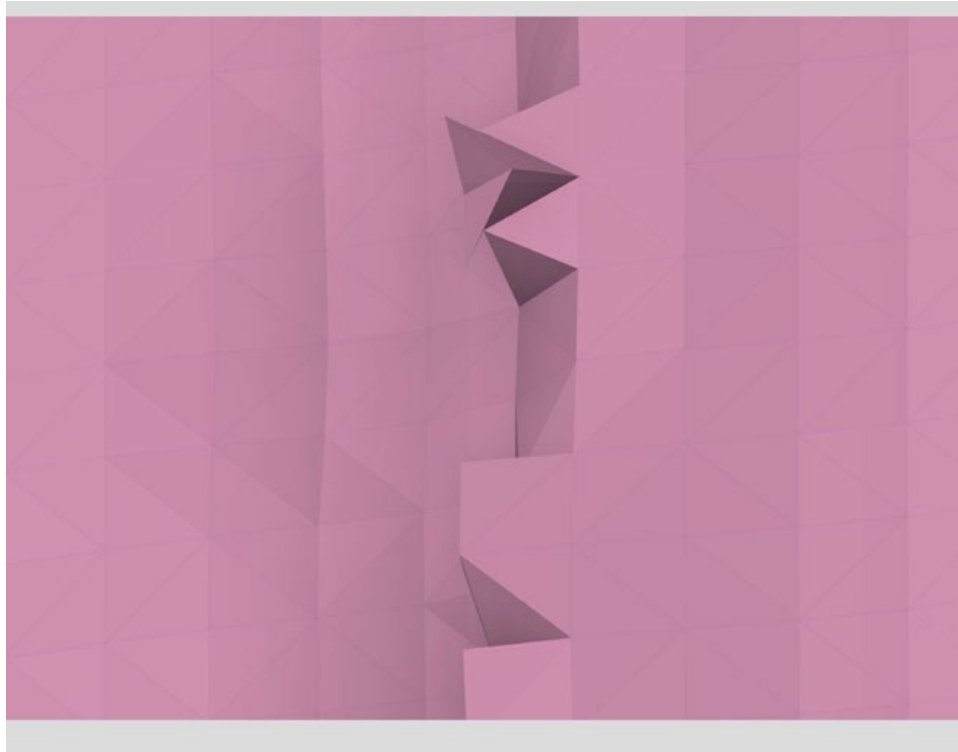


Figure D.5. An Example of Sharp Edges in the STL Laser Scanner Model which Needed Smoothing.

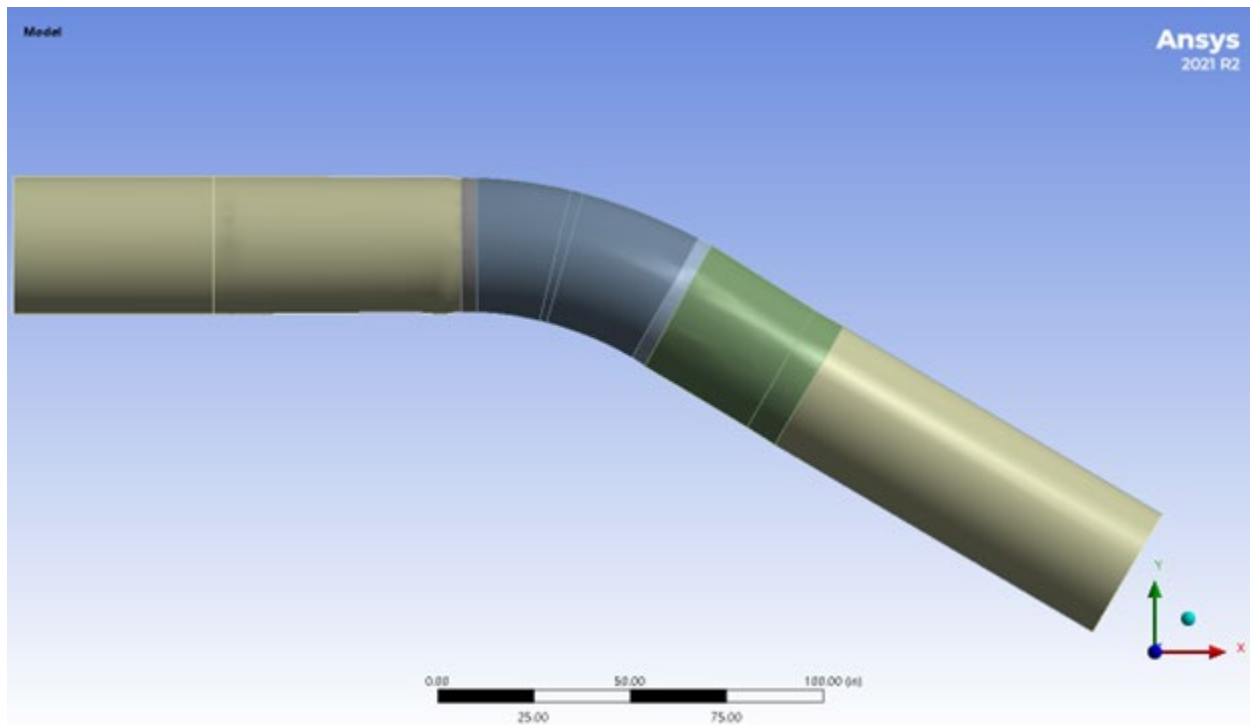


Figure D.6. FEA Geometry

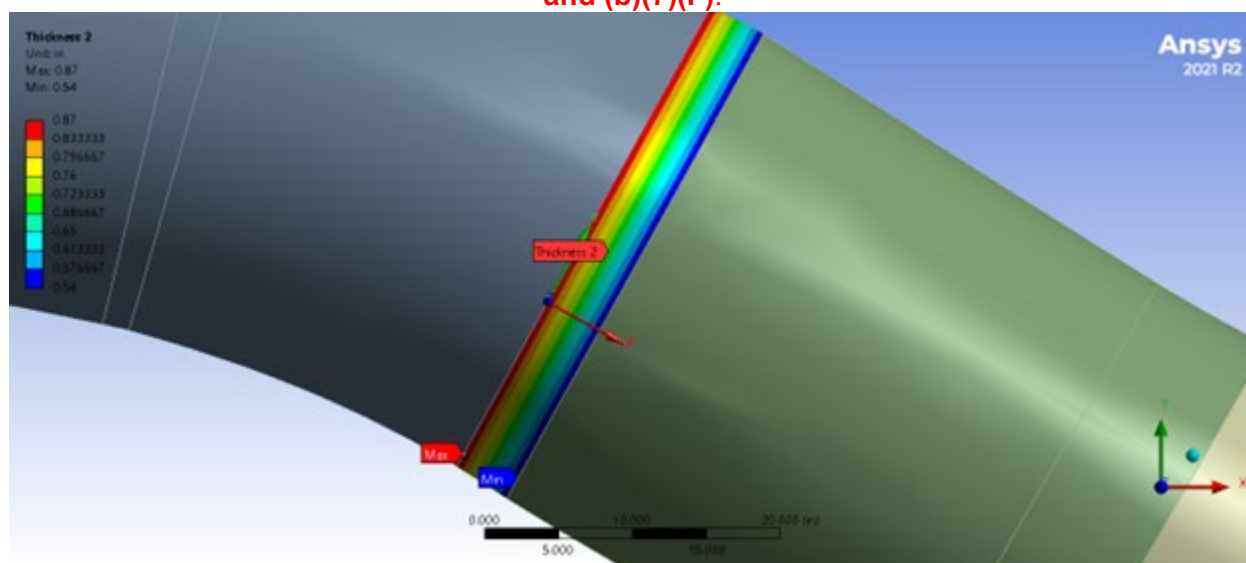


Figure D.7. Wall Thickness Transition

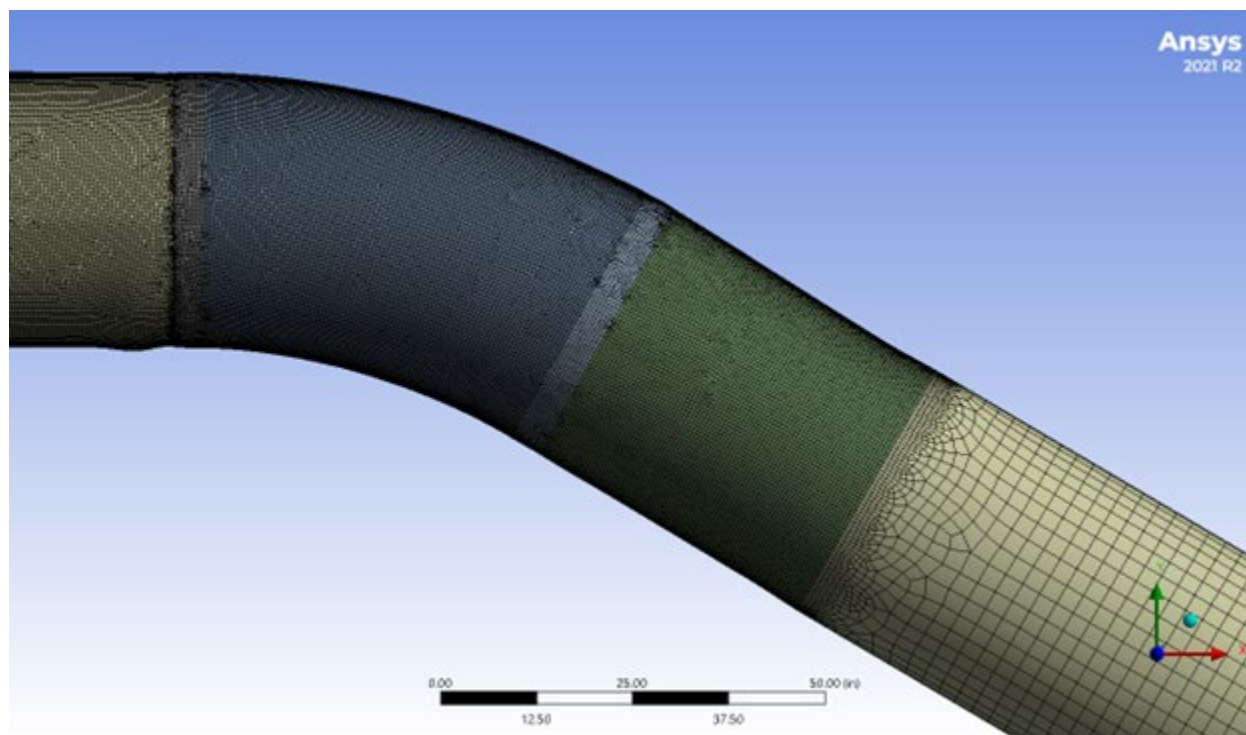


Figure D.8. Elbow Mesh

D.4 Pipeline Stress Analysis under Operating Loads

The purpose of this analysis was to calculate the pipeline stresses under operating loads, which included differential temperature and operating pressure, to determine if the operating loads could have caused the observed wrinkle and ovality in the TAG 98 (BND 350) elbow. The model that was developed for this analysis was described under Section D.2 'Soil-Pipe Interaction Model'. The loading combinations that were applied to the model are listed in Table D.4. The first scenario considers the pipeline under an internal pressure of 1,250 psig only to show the

effect of pressure. The second loading combination shows the effect of positive differential temperatures (operating temperature higher than installation temperature). For this scenario a differential temperature of [REDACTED] was applied to the model along most of the pipeline, however a higher differential temperature of [REDACTED] was applied to the segment that was replaced in December 2010 to reflect the fact that the replacement took place at lower winter temperatures. The third loading combination represents normal high operating pressure combined with low differential temperatures, and the last loading combination represents normal high operating pressure combined with high differential temperatures. These four loading combinations cover various aspects of operating conditions along the affected segment.

Table D.4. Loading Combinations – Operational Loads

Loading Case No.	Internal Pressure [psig]	Differential Temperature [°F]	Differential Temperature Applied to Replacement Length, [°F]
1	1,250	0	0
2	0	[REDACTED]	[REDACTED])
3	1,250	0	45 (25°C)
4	1,250	[REDACTED]	[REDACTED]

In the first analysis we used pipe elements (PIPE289) and the lower bound soil properties (see Table D.2). The results of this analysis are shown in Figure D.9 and Figure D.10. The x-axis in these figures is the 3D slope station of the pipeline and the y-axis shows the stresses in ksi for the four loading combinations listed in Table D.4. The analysis was conducted for approximately 10,000 feet of the pipeline length but in this report, we are only showing the results at and near the TAG 98 (BND 350) elbow (including the sagbend TAG 114C; BND 349). The purple boxes in these figures show the locations of the elbows along the segment, and the dashed dotted red line shows the 90% SMYS limit. Figure D.9 shows the maximum and minimum longitudinal stresses for the four loading scenarios and Figure D.10 shows the von Mises stresses. The longitudinal stress results indicate compressive stresses up to 30.6 ksi at the elbow. The amount of compression is well within the typical allowable stress of 90% SMYS and is not enough to cause the observed wrinkle. Although the von Mises stress is relatively high (64.7 ksi or 92% SMYS) at the wall thickness transition zone, these stress levels are not sufficient to cause permanent ovalization of the TAG 98 elbow.

The FEA results for the upper-bound soil properties (see Table D.3) with PIPE289 elements are shown in Figure D.11 and Figure D.12. The overall stresses are lower than those calculated with the lower-bound soil properties (see Table D.2) because a stiffer soil provides stronger support and a lower anchor length for the pipeline along bends and elbows. The normal pipe elements that were used in these analyses did not account for pipe cross-sectional warping and ovalization at the elbow. The following analyses address these effects by replacing the pipe elements with elbow elements.

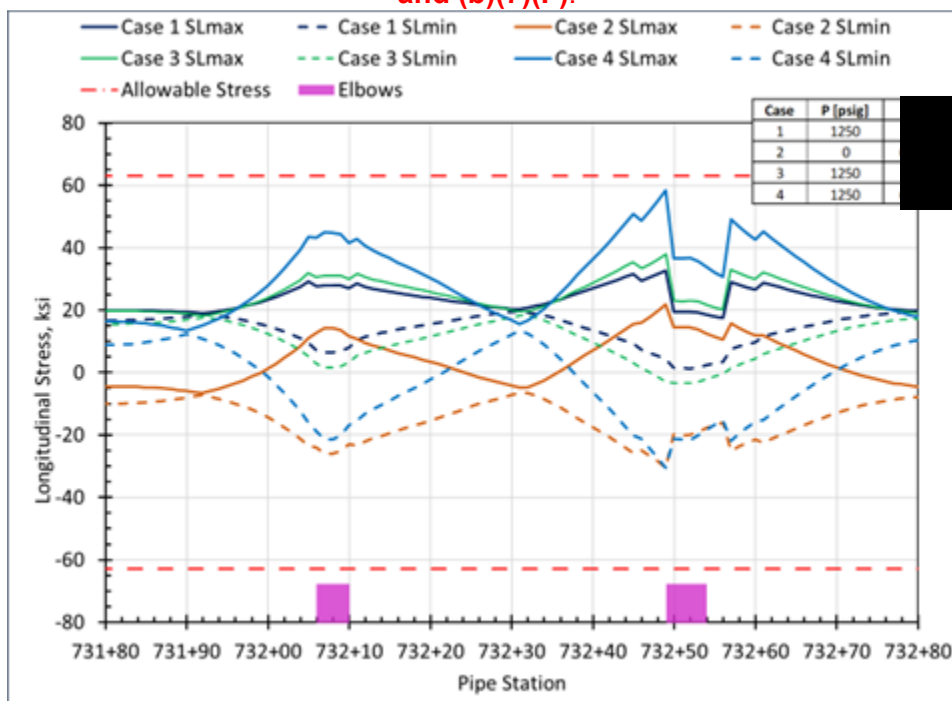


Figure D.9. FEA Longitudinal Stresses with Three-Node Pipe Elements and Lower-Bound Soil Properties

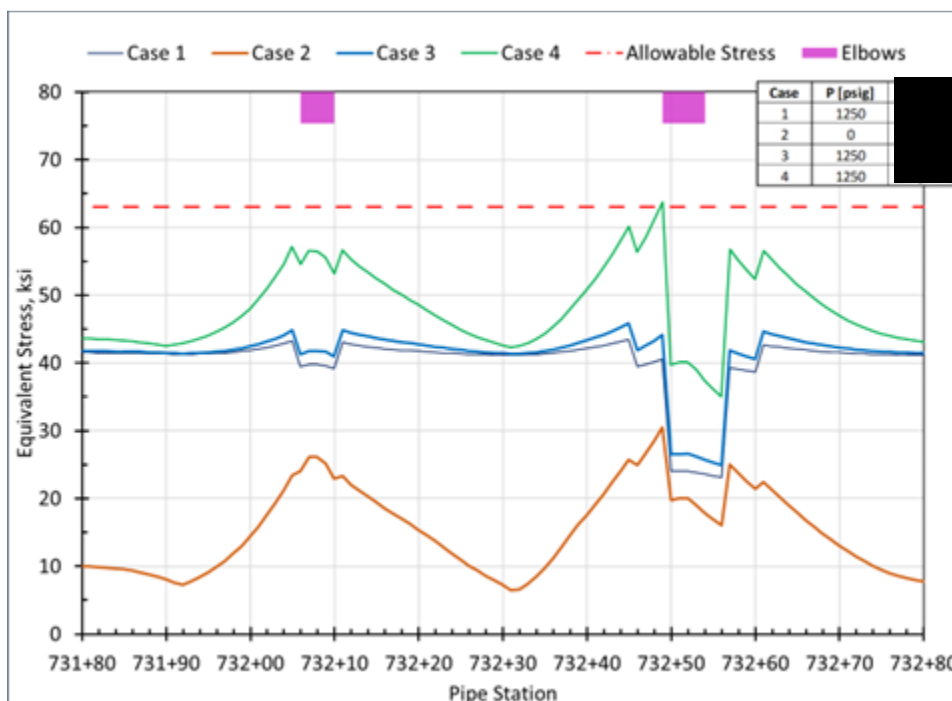


Figure D.10. FEA von Mises Stresses with Three-Node Pipe Elements and Lower-Bound Soil Properties

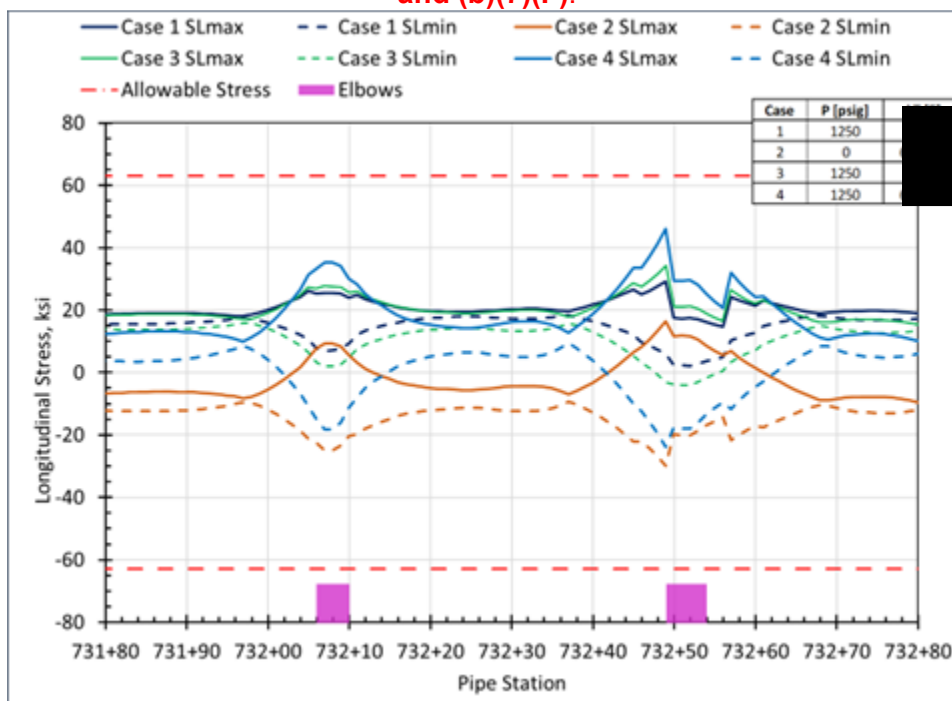


Figure D.11. FEA Longitudinal Stresses with Three-Node Pipe Elements and Upper-Bound Soil Properties

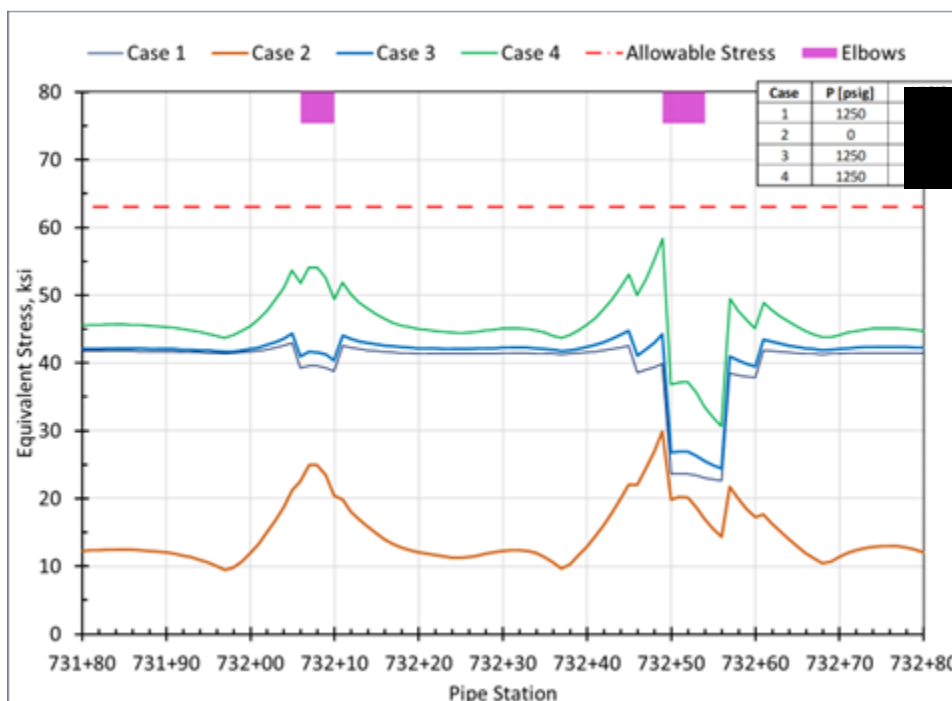


Figure D.12. FEA von Mises Stresses with Three-Node Pipe Elements and Upper-Bound Soil Properties

An elbow element (ELBOW290) accounts for elastic ovalization of the pipe bend under a bending moment, resulting from the internal pressure and differential temperature. The formulation of this element uses terms of Fourier expansion to model ovalization of the initially circular elbow cross-section, which enables the model to calculate out-of-roundness of the elbow. In the analysis we included four Fourier terms with an initially circular pipe cross-section (the residual ovality of the elbow is addressed later). The results of the elbow analysis with lower bound soil properties are shown in Figure D.13 and Figure D.14. Compared to the previous result (Figure D.9 and Figure D.10) the new result using ELBOW290 shows a higher compressive stress of 38.1 ksi. This amount of compression is still not sufficient to cause a wrinkle. To demonstrate this, the allowable compressive strain is calculated using the following ASME B31.8 equations:

$$\epsilon_{cf}^{crit} = 0.4 \frac{t}{D} - 0.002 + 2400 \left(\frac{PD}{2tE} \right)^2 \quad \text{when } \frac{PD}{2tS} < 0.4 \quad \text{Equation 9}$$

$$\epsilon_{cf}^{crit} = 0.4 \frac{t}{D} - 0.002 + 2400 \left(\frac{0.4S}{E} \right)^2 \quad \text{when } \frac{PD}{2tS} \geq 0.4 \quad \text{Equation 10}$$

In the above equations, D is pipe outer diameter (inch), P is the pipe operating pressure (psig), S is the yield strength (psi), and t is pipe wall thickness (inch). The above equations result in allowable compressive strains ranging from 0.4% to 0.6%. The calculated compressive strains in the longitudinal direction of the elbow and the pups were all less than 0.14%. The maximum equivalent stress from the ELBOW290 analysis (see Figure D.14) was 69.6 ksi (99.4% SMYS). Figure D.15 and Figure D.16 show the results for upper-bound soil properties. The stresses are lower compared to those associated with the lower-bound soil properties.

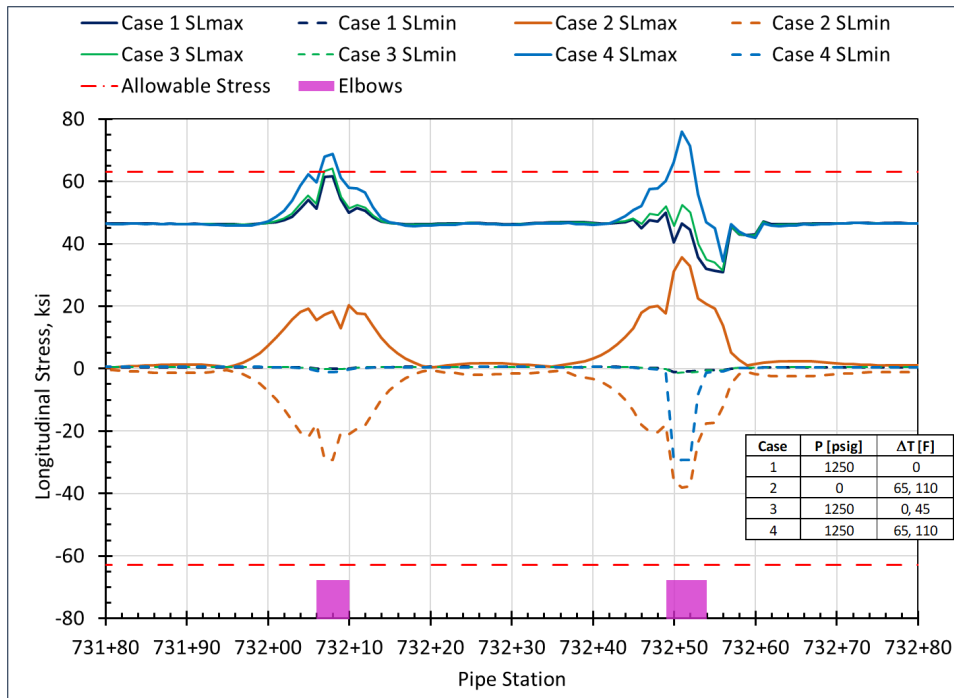


Figure D.13. FEA Longitudinal Stresses with Elbow Elements and Lower-Bound Soil Properties

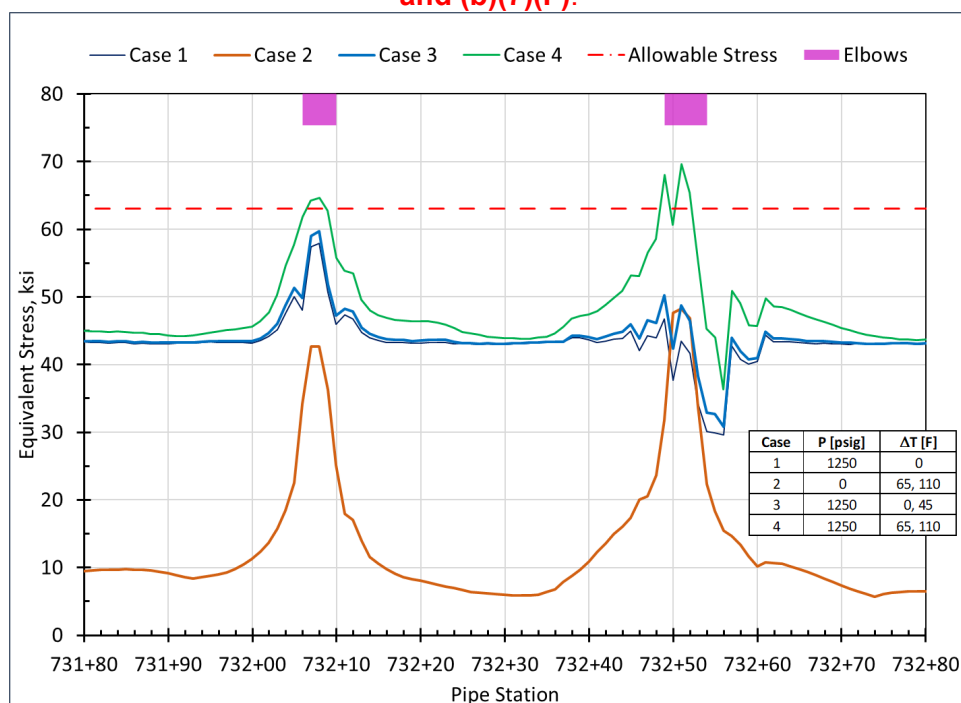


Figure D.14. FEA von Mises Stresses with Elbow Elements and Lower-Bound Soil Properties

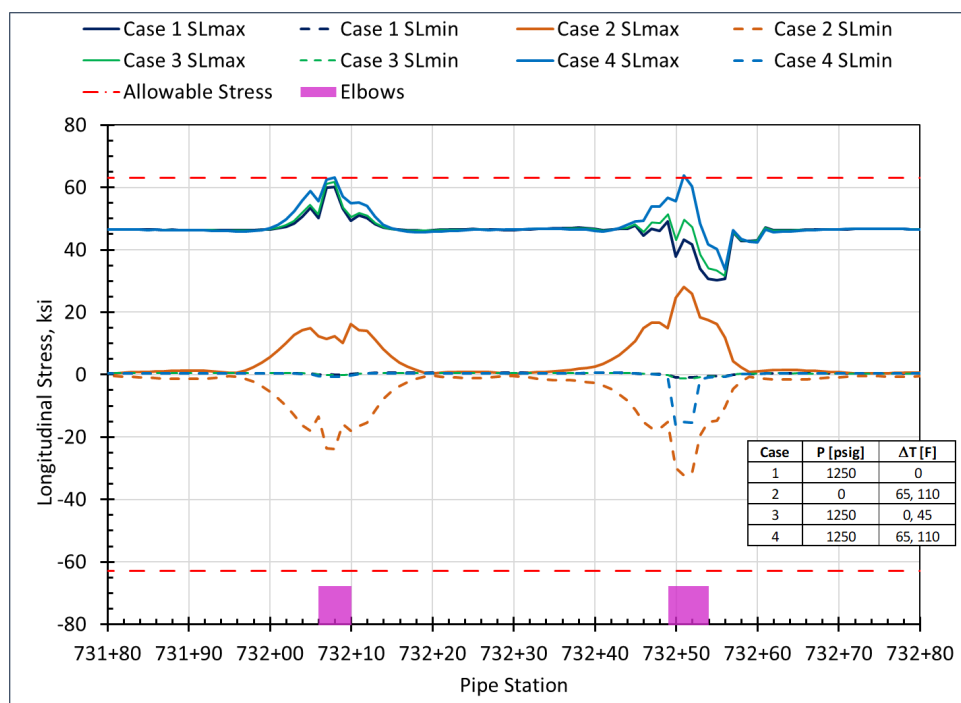


Figure D.15. FEA Longitudinal Stresses with Elbow Elements and Upper-Bound Soil Properties

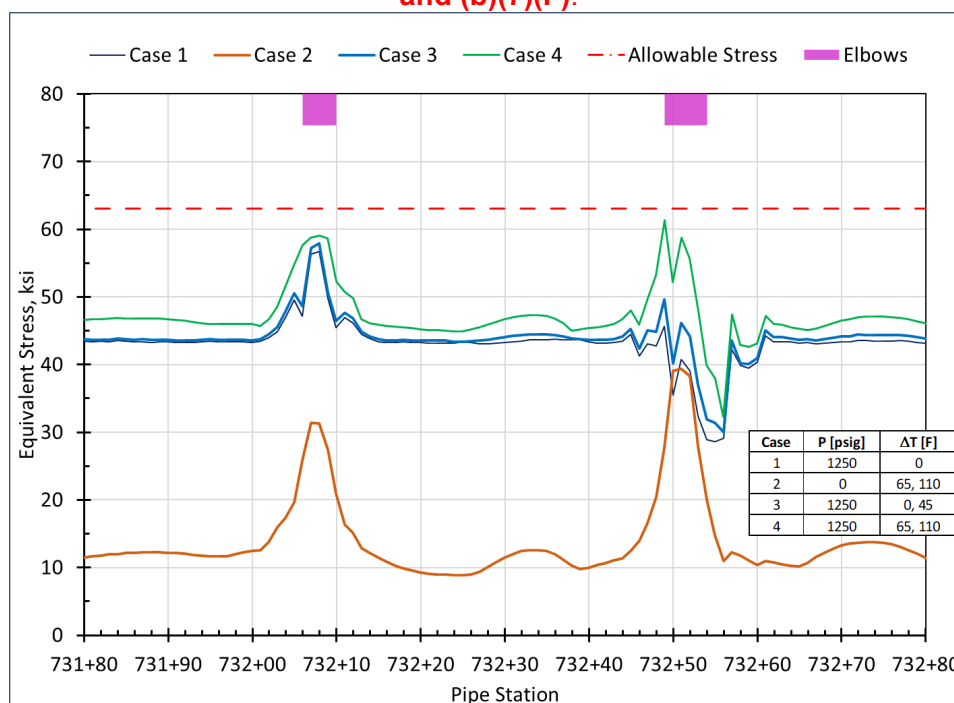


Figure D.16. FEA von Mises Stresses with Elbow Elements and Upper-Bound Soil Properties

The above results (i.e., the stress graphs in Figure D.9 through Figure D.16 and the compressive strain limit from Equations 9 and 10) shows that although the equivalent stress exceeds the allowable stress of the pipe material, it is insufficient to cause pipe ovality or a wrinkle. Based on the FEA results, RSI concluded that the TAG 98 wrinkle and ovality most likely did not occur because of pipeline operational loads.

D.5 Pipeline Stress Analysis under Construction and Hydrostatic Loads During December 2010 Replacement of TAG 98 (BND 350)

The FEA results discussed in the previous section showed that formation of the observed wrinkle and the ovality under normal operating loads is highly unlikely. Having ruled out operational loads, RSI next considered construction and hydrostatic loads during the December 2010 replacement work that may have caused the deformations seen in TAG 98.

D.5.1 Parametric Beam Bending Assessments

Scenario 1: Lack of Support

RSI first performed an analytical parametric study of the replacement segment using the beam equations (Equation 1 through Equation 8). The first possibility considered was that a gap was left underneath the replacement pipe segment, which allowed the pipeline to sag under soil overburden pressure, causing excessive bending. For this assessment the fixed-fixed beam equations and a soil overburden of 8-ft with a mass density of 130 lbm/ft³ were used. The weight of the pipe and product was also considered in this assessment. Figure D.17 shows the maximum bending stresses in ksi which is located at the fixed ends as a function of the span length in feet (not the length value along the beam). Figure D.18 shows beam deflections in

inches as a function of the span length (not the length value along the beam). The results show that it is possible to have high levels of bending stress that exceed the material yield strength. However, in order to generate bending stresses high enough to cause significant plastic deformation, the span length must be around 100-ft or longer, and beam deflections must be several inches. Although, in theory this scenario is possible, in practice it is very unlikely that such a long and wide gap under the pipeline would have gone unnoticed before placement of the overburden soil.

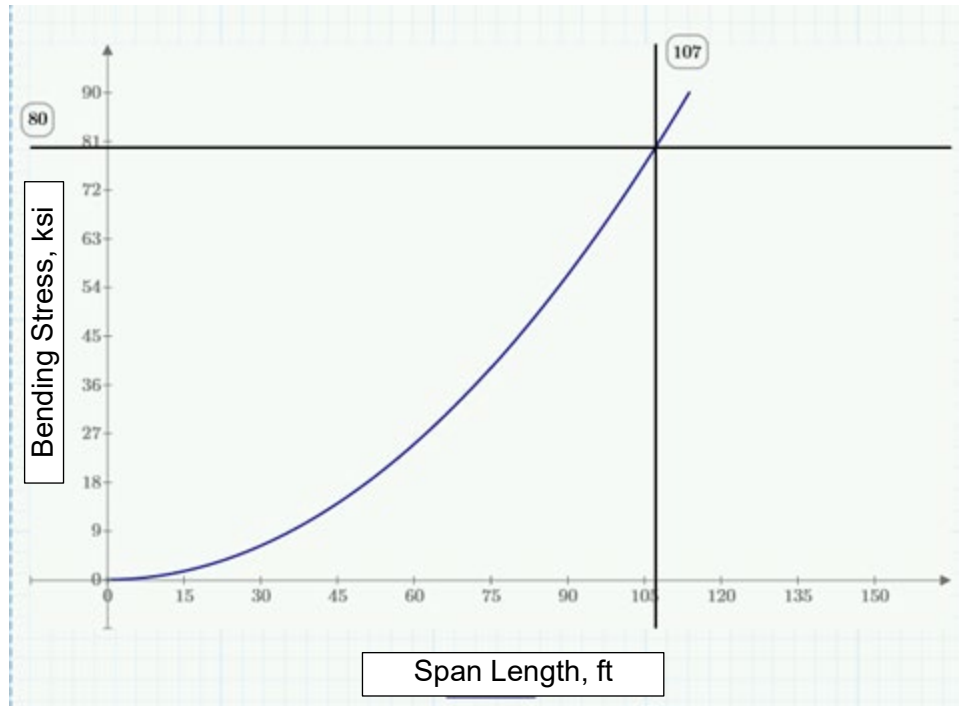


Figure D.17. Beam Bending Stress with both Ends Fixed as a Function of Span Length

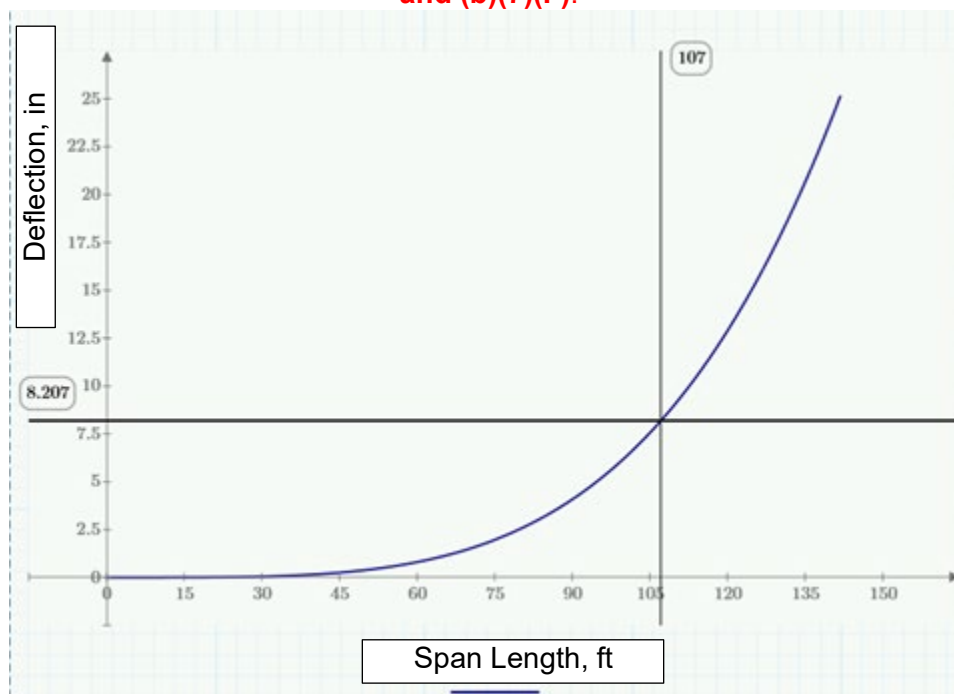


Figure D.18. Beam Deflection with Both Ends Fixed as a Function of Span Length

Scenario 2: Cantilever Bending

The second scenario considered is cantilever bending of the replacement segment after the upstream tie-in weld was complete but before the final tie-in weld was made downstream. A review of photographs during the December 2010 replacement of TAG 98 show that two side booms were used to hold the pipe segment above the ground over the south-slope (Figure D.19). It is also known that the creek portion of the replacement segment was buried with 5-ft of soil but the downstream overbend section was likely exposed during the hydrostatic test on December 11, 2010. Furthermore, the downstream tie-in weld (GWD 13590; 9GT-035) was completed after the hydrostatic test on December 13, 2010. A note in the daily inspection report from December 11th suggests that the side booms may have been demobilized (prior to the hydrostatic test), however, these records are unclear as to how the pipeline was placed in the ditch or how it was supported during the hydrostatic test. Improper operation of side booms can sometimes create high levels of bending stress. To assess this hypothesis, RSI first performed several analytical cantilever beam-bending analyses. Figure D.20 shows a schematic of the assumed model. The cantilever assessment model included (1) an accidental load at some distance from the fixed end and (2) the weight of the pipeline and hydrostatic test water. It was assumed that the free end of the beam will, after some amount of deflection, touch the ground generating an end reaction force. The model was set-up in Mathcad Prime, allowing us to define the point load, weight per unit length of the pipe, and the end reaction as variables. The span length in all the cantilever analyses were set to 170-ft.



Figure D.19. Use of Sidebooms During Replacement of TAG 98 (December 10, 2010)

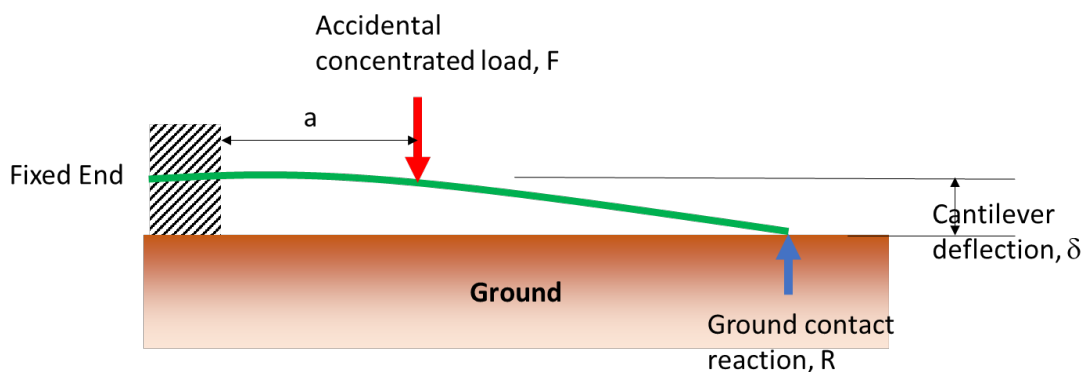


Figure D.20. Schematic Description of the Cantilever Beam Analysis

The side booms on site during the TAG 98 replacement project included two Caterpillar 583T and three Caterpillar 594H side booms. The lifting capacity for each side boom model are shown in Figure D.21 and summarized in Table D.5. Assuming that the two side booms holding the overbend section in Figure D.19 were the smaller capacity 583T models, a 170-ft long pipe segment filled with water would weigh approximately 101,200 lbs (50.6 tons)¹⁵⁰. Two of the 583T side booms might have been sufficient to support the pipe during the hydrostatic test without collapsing under the load. However, statements made by the Field Engineer onsite during the hydrostatic test and notes in the daily inspection reports indicate that it is probable

¹⁵⁰ From Section 5.1.4.2 of this report, a 158-ft pipe span filled with water weighs about 94,000 lbs or 595 lbs per linear foot. Hence, a 170-ft span would weigh about 101,200 lbs (50.6 tons).

that the side booms were removed during the hydrostatic test and the pipe was potentially supported by cribbing or soil supports in the ditch.

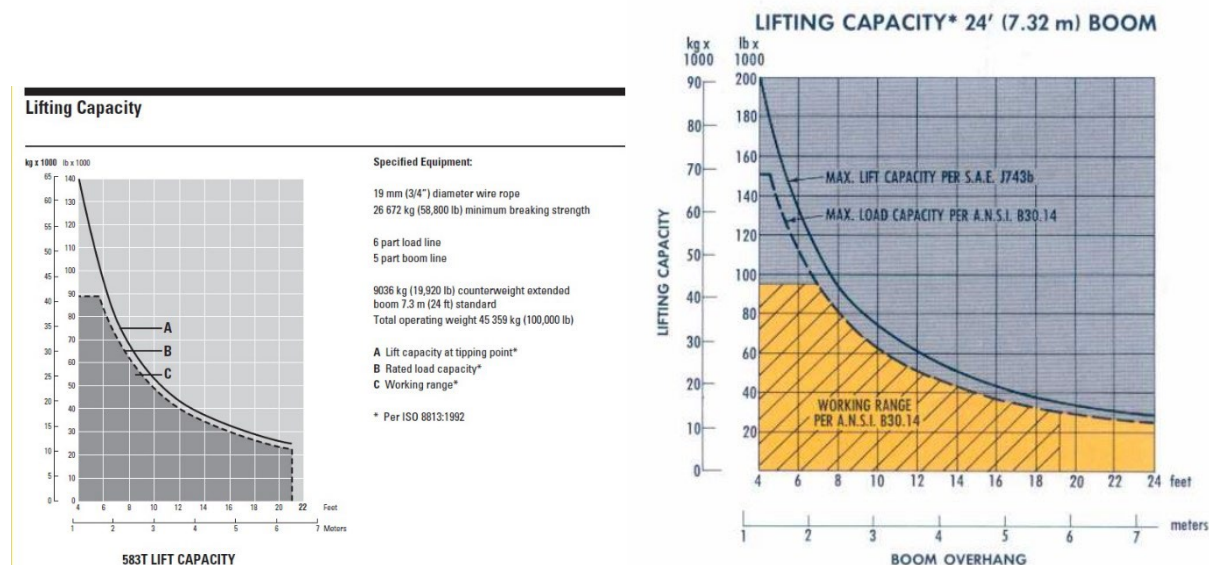


Figure D.21. CAT 583T (left) and CAT 594H (right) Lifting Capacity Charts^{151, 152}

Table D.5. Lifting Capacity of Side Booms On Site December 2010

Equipment Model	Maximum Lifting Capacity [lbs]	Operating Weight [lb]	Total On Site	Assumed Boom Overhang [ft]	Working Lifting Capacity [lb]	Total Working Lifting Capacity [lb]
CAT 583T ¹⁵¹ Side boom	140,000	100,000	2	8	60,000	120,000
CAT 594H ¹⁵² Side boom	200,000	121,475	3	8	80,000	240,000
CAT 345GC ¹⁵³ Track hoe		95,500	2			
CAT D8T ¹⁵⁴ Bulldozer		87,733	2			

Figure D.22 shows cantilever beam bending stresses for an empty pipe with concentrated loads of 10,000, 20,000, 40,000, and 80,000 lbf at a distance of 10-ft from the fixed end (assumed location of the point load). The x-axis in this graph is the amount of end reaction force in lbf. A

¹⁵¹ CAT 583T Pipelayer brochure found at <https://crosscountryis.com/pdf/CAT583TPipelayer.pdf> on March 20, 2023.

¹⁵² CAT 594 Pipelayer brochure found at <https://www.maats.com/wp-content/uploads/2020/09/Brochure-CAT-594H-coloured.pdf> on March 20, 2023.

¹⁵³ CAT 345GC Hydraulic Excavator found at <https://s7d2.scene7.com/is/content/Caterpillar/CM20181214-35962-39643> on March 20, 2023.

¹⁵⁴ CAT D8T Track-Type Tractor brochure found at <https://s7d2.scene7.com/is/content/Caterpillar/C658733> on March 20, 2023.

zero reaction represents a beam with a completely free end. A reaction force of about 14,500 lbf represents a beam with one fixed end and one pinned end (i.e. this is equivalent to the south end of the pipe segment sitting on the ground). The results suggest that high accidental loads can cause sufficient bending stress such that it exceeds the yield strength of the material. However, as seen in Figure D.23 the amount of deflection associated with high bending stress levels is relatively high (i.e. greater than 100-inches).

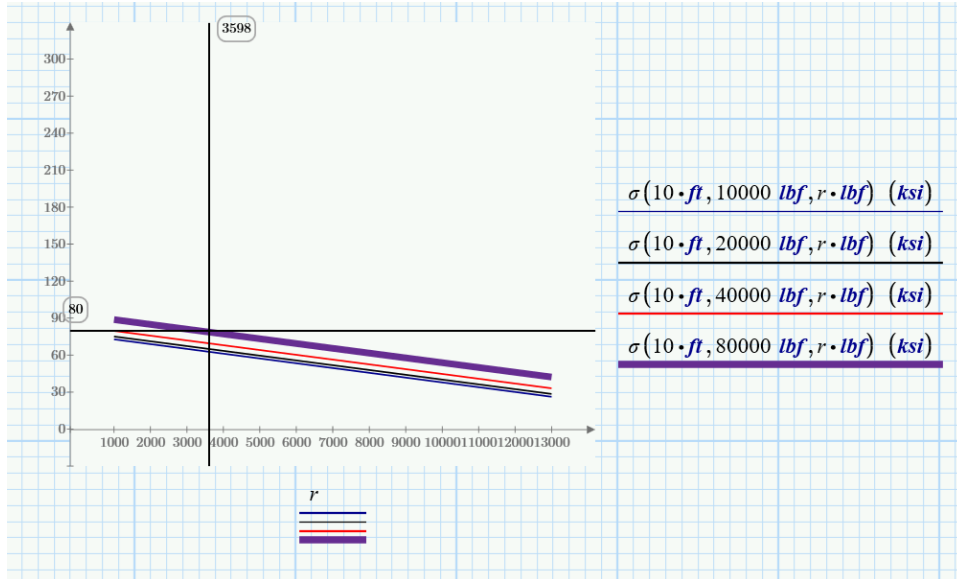


Figure D.22. Cantilever Beam Bending Stress for Empty Pipe with Various Concentrated Loads at a Distance of 10-ft from the Fixed End. The x-axis in this figure is end reaction force in lbf, and the y-axis is the bending stress in ksi.

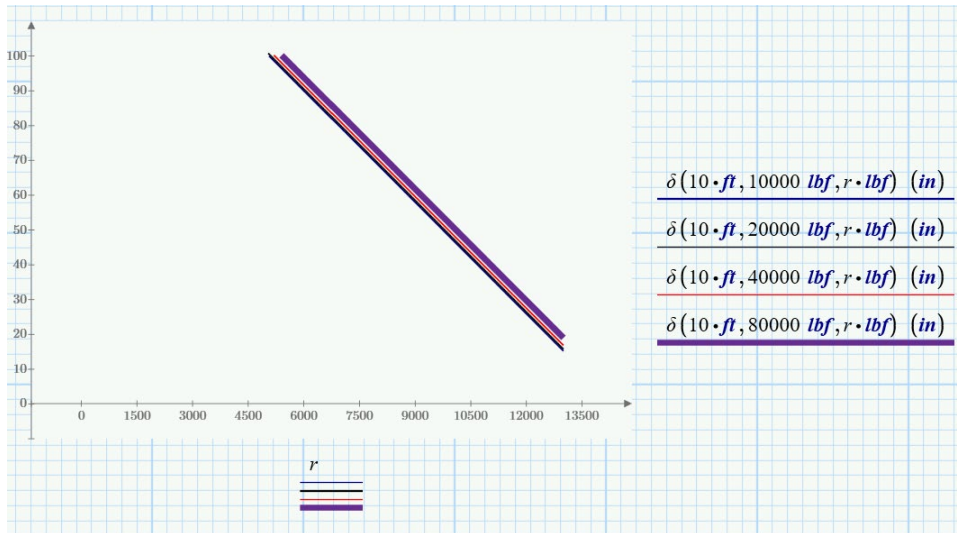


Figure D.23. Cantilever Beam Bending Deflections (inch) for Empty Pipe with Various Concentrated Loads at a Distance of 10-ft from the Fixed End. The x-axis in this figure is the end reaction force in lbf, and the y-axis is the end deflecting in inch.

Another potential scenario is the excessive bending stress during the hydrostatic test. The results of this scenario are shown in Figure D.24 and Figure D.25. The results indicate that high bending stresses (e.g. 80 ksi) would be possible when the pipe segment was filled with hydrostatic water if it lacked proper support.

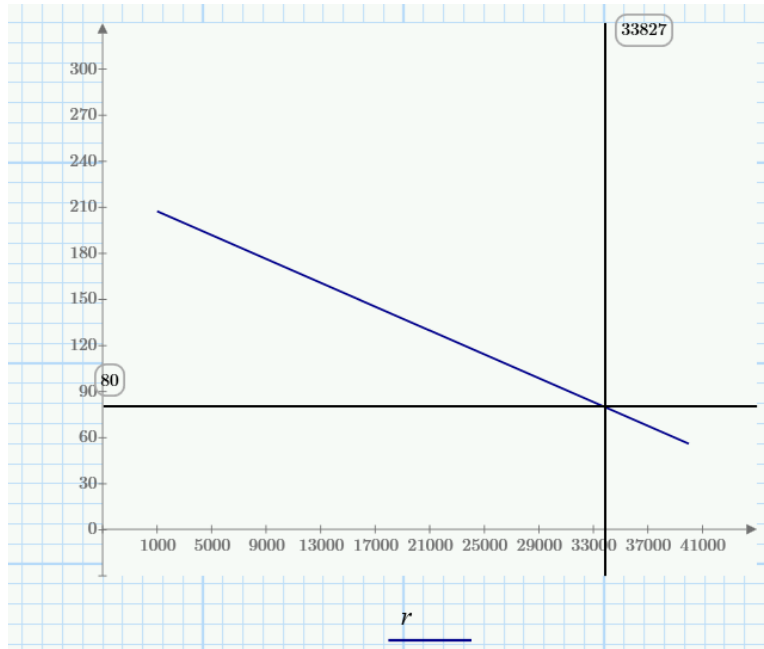


Figure D.24. Cantilever Beam Bending Stress for Pipe Filled with Hydrostatic Test Water. The x-axis in this figure is end reaction force in lbf, and the y-axis is the bending stress in ksi.

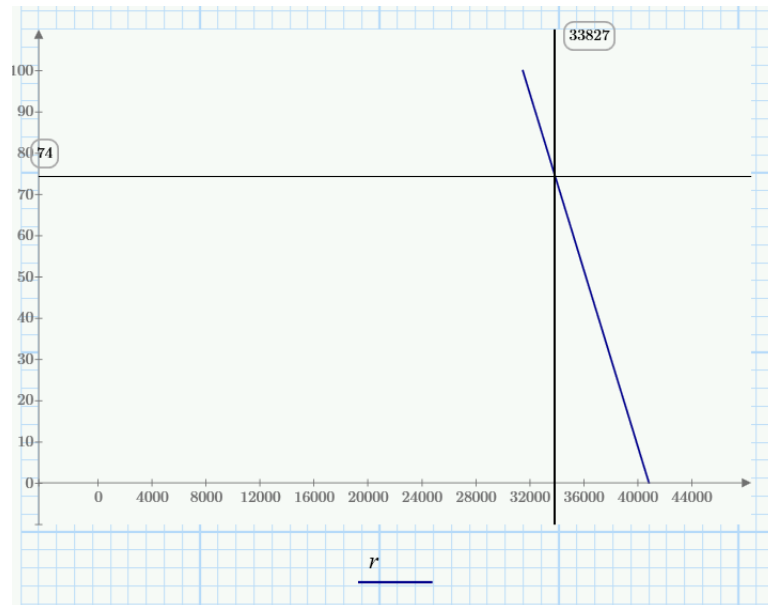


Figure D.25. Cantilever Beam Deflection for Pipe Filled with Hydrostatic Test Water. The x-axis in this figure is end reaction force in lbf, and the y-axis is the bending Deflection in inch.

D.5.2 Soil-Pipe Interaction FEA

The above parametric beam bending assessments used idealized assumptions about the end boundary conditions and the geometry of the replacement pipe segment. To determine potential effects of the boundary conditions and pipe segment bends and ground slope, supplemental soil-pipe interaction FEA were conducted. Unless mentioned otherwise, the soil-pipe interaction analyses in the remainder of Appendix D used ELBOW290 elements and lower-bound soil properties.

Scenario 1: Post-Construction Outside Force Analysis

The effect of a gap or extremely weak soil under a pipeline is similar to that of ground settlement as in both cases the pipeline will sag. To examine the gap scenario, ground settlement analysis was performed in which settlement displacements were applied to the end of the vertical soil spring that represents soil support. The settlement profile was assumed to span a 100-ft distance starting from the subject elbow (TAG 98) to the south slope. The soil pressure from a 122 kip side boom crossing the pipeline was also included in the analysis. A schematic of the soil-pipe interaction gap model is shown in Figure D.26. Figure D.27 shows the assumed settlement profile. Three sets of analyses were performed to examine the effects of the side boom and settlement, namely (1) load from the largest side boom with no settlement, (2) settlement only (no side boom load), and (3) settlement and side boom load. Each set of analyses used the three loading combinations listed in Table D.6. The analysis also used the ELBOW290 model (see Section D.2 'Soil-Pipe Interaction Model' and Section D.4 'Pipeline Stress Analysis under Operating Loads' for details). The FEA results are shown in Figure D.28 through Figure D.33.

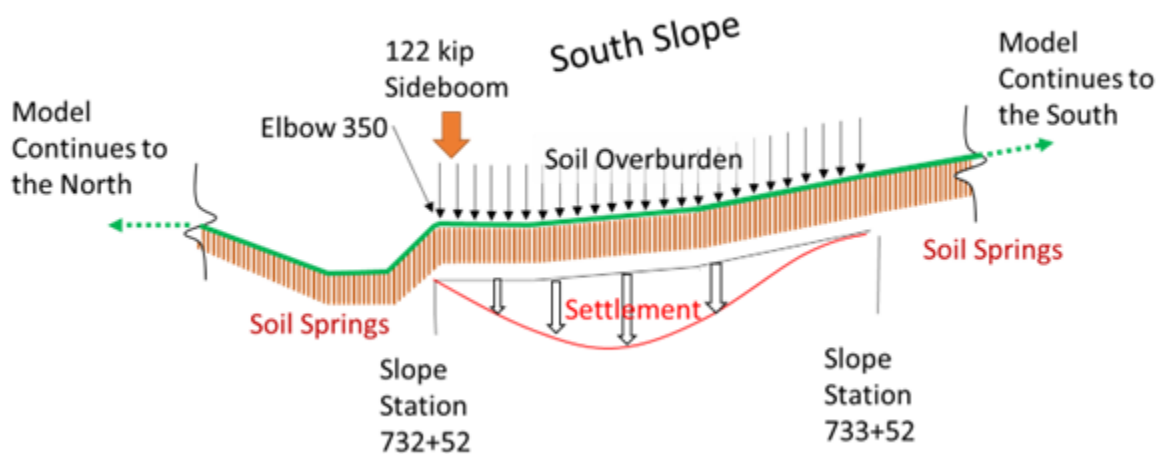


Figure D.26. Schematic of the Gap Scenario FEA Model (Scenario 1)

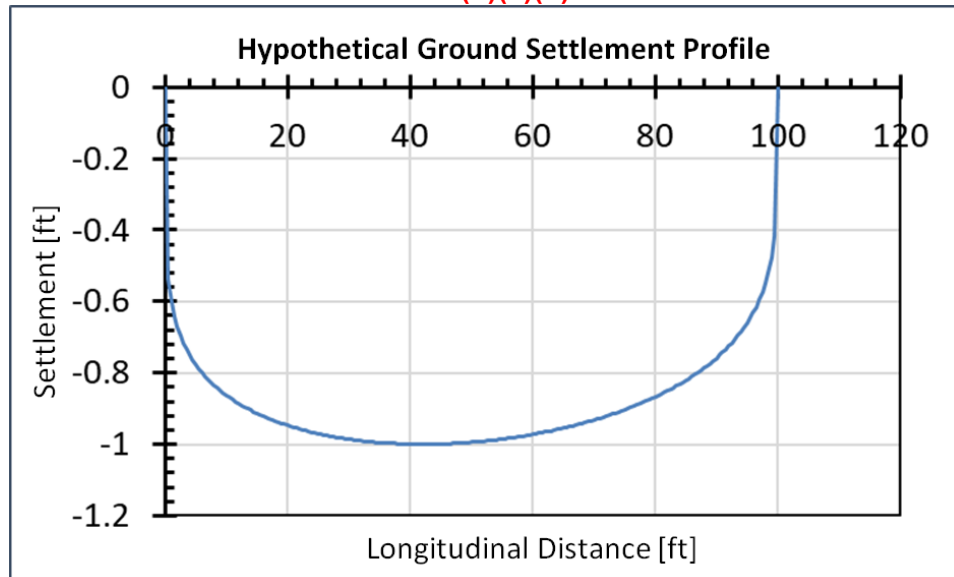


Figure D.27. Hypothetical Ground Settlement Profile

Table D.6. Loading Combinations for Gap Analysis

Loading Case No.	Internal Pressure [psig]	Differential Temperature [°F]	Differential Temperature Applied to Replacement Length [°F]	Overburden Soil Cover [ft]
1	0	0	0	8
2	1,200	65 (36.1°C)	110 (61.1°C)	8
3	1,200	0	45 (25°C)	8

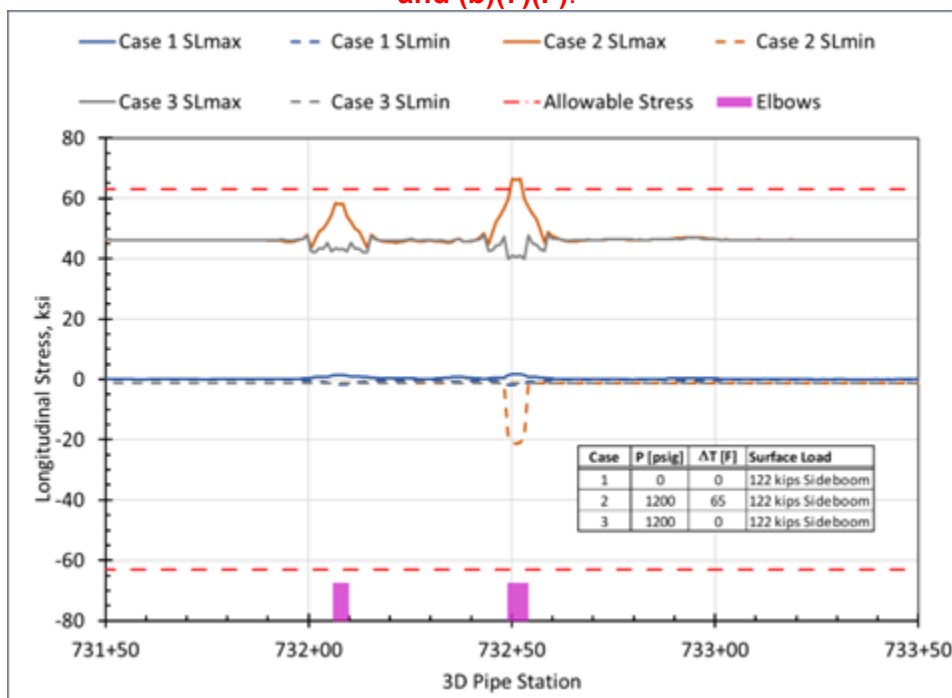


Figure D.28. FEA Longitudinal Stresses for Post-Construction Analysis with Side Boom Load Only

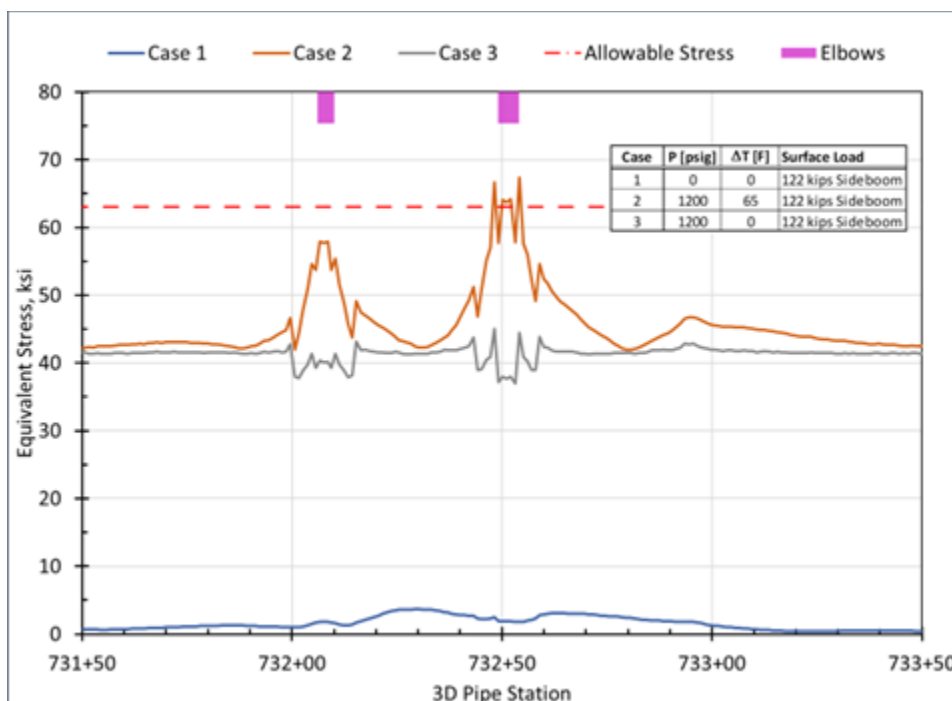


Figure D.29. FEA von Mises Stresses for Post-Construction Analysis with Side Boom Load Only

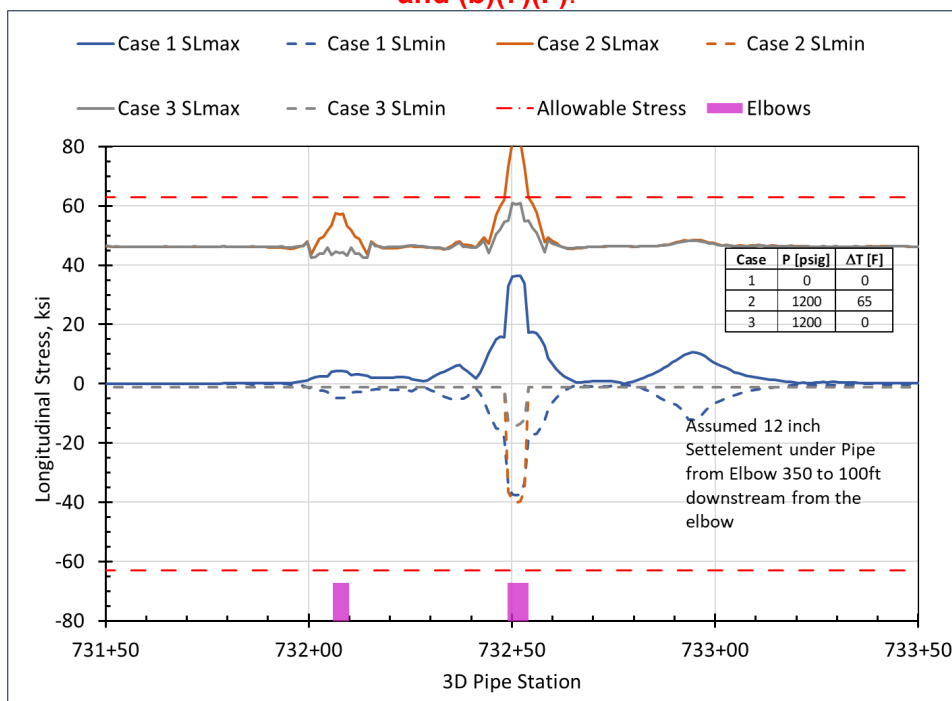


Figure D.30. FEA Longitudinal Stresses for Post Construction Analysis with Ground Settlement Only

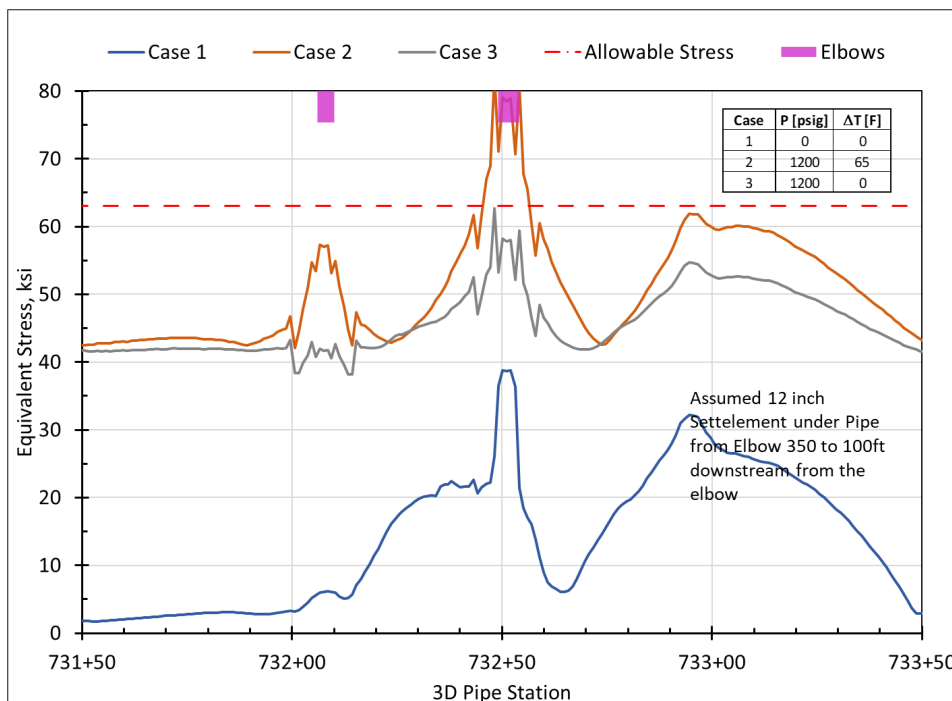


Figure D.31. FEA von Mises Stresses for Post Construction Analysis with Ground Settlement Only

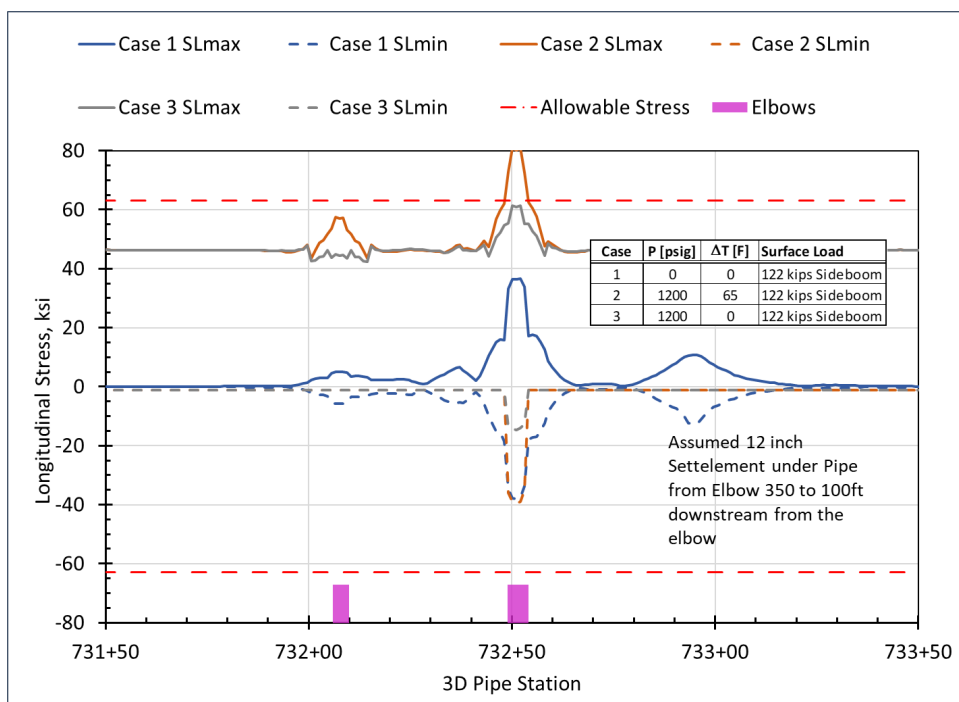


Figure D.32. FEA Longitudinal Stresses for Post Construction Analysis with Ground Settlement and Side Boom Load

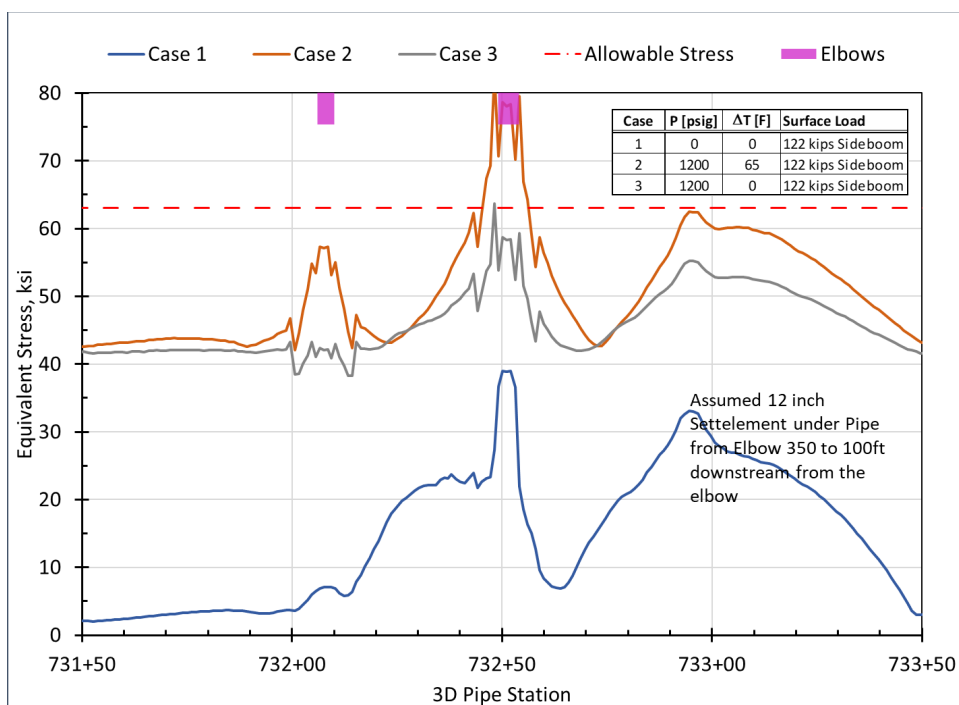


Figure D.33. FEA von Mises Stresses for Post Construction Analysis with Ground Settlement and Side Boom Load

The results show that the surface loading from the side boom alone would not induce high stress levels (Loading Case 1 in Figure D.28 and Figure D.29). In contrast, post-construction ground settlement could have produced enough bending and axial stresses to bring the elbow to yielding (Figure D.30 and Figure D.31). The longitudinal stress plot for Load Case 1 in Figure D.30, shows that although the bending stresses are generated near the middle of the span (~ Sta 732+95), it is lower than the bending stress at the elbow. This is due to the shape of the assumed settlement profile which is skewed towards the elbow (see Figure D.27) and the stress concentration at the elbow. The peak settlement that was assumed in this analysis was 12-inches which may appear excessive, however, since a gap under the pipeline would have a similar effect 12-inches of settlement could have been the result of a small gap under the pipeline plus some post-construction consolidation settlement.

The post-construction settlement or gap under the pipeline can explain the out-of-roundness of the elbow. However, this scenario does not explain the wrinkle as the amount of compressive stress at the elbow is not excessive (Figure D.28, Figure D.30 and Figure D.32). In order for ground settlement to cause a wrinkle, the amount of movement should be around 24-inches or more. It is also possible that the wrinkle was formed at a later time due to thermal cycles or ground movement, but that would require two independent coincidences both affecting the same location of the pipeline at different times, which although is possible it decreases the overall likelihood of the scenario. In addition, the bending strain analysis from the IMU data and assessments by Geotech SMEs did not find evidence of significant ground movement near the TAG 98 elbow.

Scenario 2: Cantilever Bending Scenarios

The first cantilever scenario (Scenario 2a) used a soil-pipe model in which the portion of the pipeline from the elbow to the tie-in location on the south slope did not have soil support or any soil overburden. The remainder of the replaced length, from the elbow to the northern tie-in was assumed to be buried. Contact elements with a gap were defined along the cantilever portion of the pipeline to allow the pipeline to undergo cantilever bending until the end of the cantilever experienced enough deflection to close the gap¹⁵⁵. A schematic of the model is shown in Figure D.34. Table D.7 shows the loading combinations used in the analysis. Combination 1 represents the unpressurized pipe filled with hydrostatic test water. Combination 2 represents hydrostatic test pressure. A low differential temperature was applied to the model because the hydrostatic test was conducted in winter at low ambient temperatures. The construction notes indicate that the dewatering pig froze in the line, suggesting that the hydrostatic water was at or near freezing 32°F (0°C).

Various amounts of gap in the contact elements (cantilever end deflection) were examined to determine how much end deflection would be required to overstress the elbow. The results of the cantilever model with a 6-ft gap are shown in Figure D.35 for the longitudinal stresses and

¹⁵⁵ The gap allows the pipe end to deflect before it meets the ground. Although the model has soil support at the southern end once the gap is closed, the relatively low stiffness of the contact elements (compared to carbon steel) and the free rotation and displacement boundary condition allows for cantilever action to dominate the pipe response.

Figure D.36 for the equivalent stresses. The results show that cantilever action could have overstressed the TAG 98 (BND 350) elbow if the end deflection was at least 6-ft. This amount of end deflection is excessive and could only happen if the pipe length on the south slope was supported above ground before the hydrostatic test and then lost the support after it was filled with water. This type of movement would have been noticeable by construction crews and most likely would have resulted in a safety standdown (which there is no evidence of in the daily inspection reports).

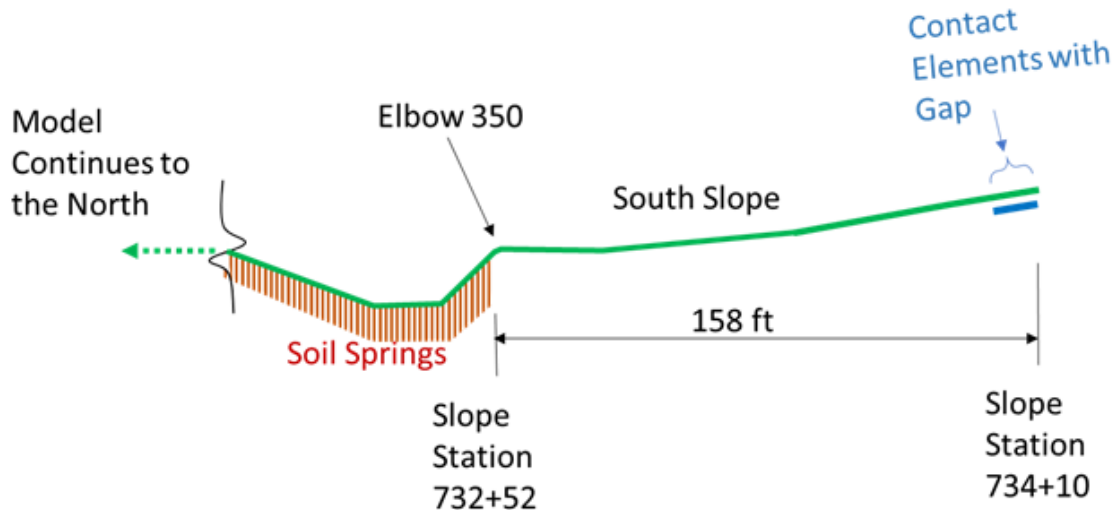


Figure D.34. Schematic of the Cantilever Model (Scenario 2a)

Table D.7. Loading Combinations for Cantilever Soil-Pipe Interaction Analysis

Loading Case No.	Internal Pressure [psig]	Differential Temperature [°F]	Differential Temperature Applied to Replacement Length [°F]	Overburden Soil Cover [ft]
1	0	0	0	0
2	1,850	10 (5.6°C)	10 (5.6°C)	0

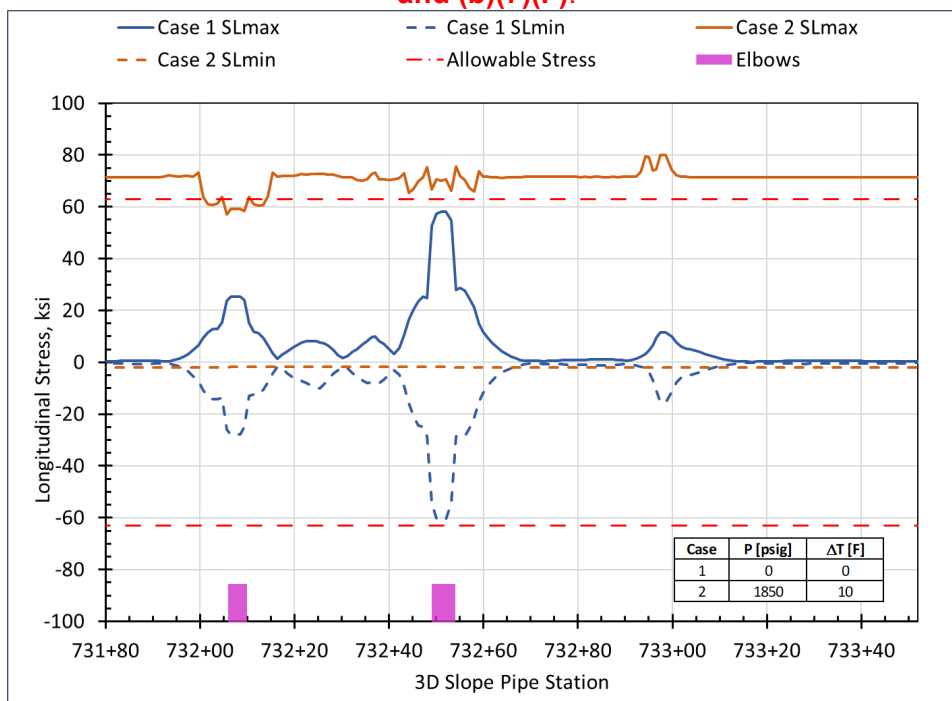


Figure D.35. FEA Longitudinal Stresses with 6-ft End Deflection

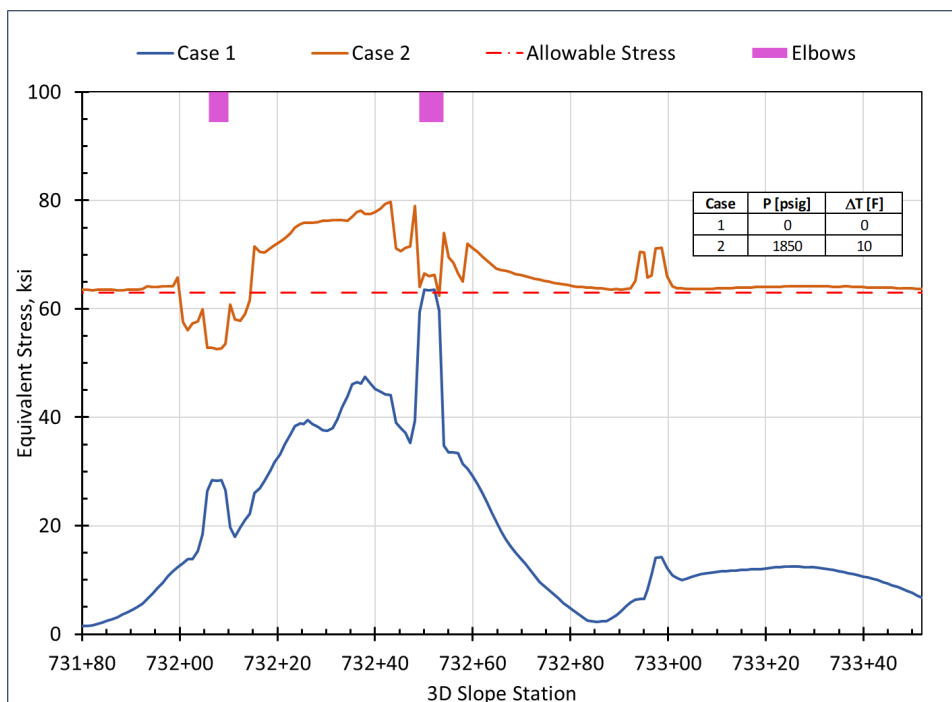


Figure D.36. FEA von Mises Stresses with 6-ft End Deflection

Another scenario that was examined with this model was downhill sliding of the pipeline on the south slope, as shown schematically in Figure D.37 (Scenario 2b).

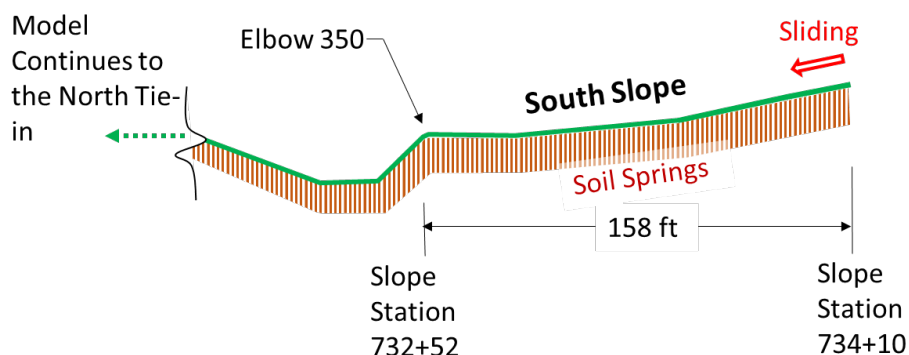


Figure D.37. Schematic of the Cantilever Model with Sliding (Scenario 2b)

A sliding displacement of 6-inches in the downhill direction was applied to the end of the cantilever length and the model was run to calculate stresses. The results of this analysis are shown in Figure D.38 and Figure D.39. The results show that sliding of the pipeline down the slope can also create excessive bending stress at the elbow, however, the weight of the pipe filled with hydrostatic water is insufficient to cause the sliding. In other words, some outside loading had to act on the pipeline to force it to slide.

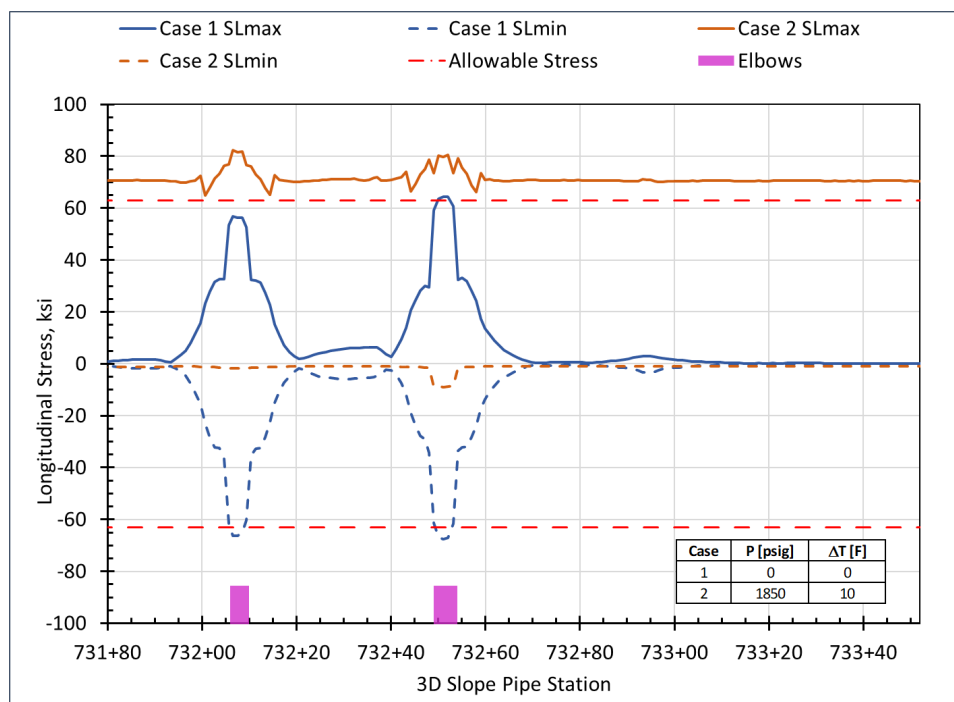


Figure D.38. FEA Longitudinal Stresses with 6-inches of Sliding

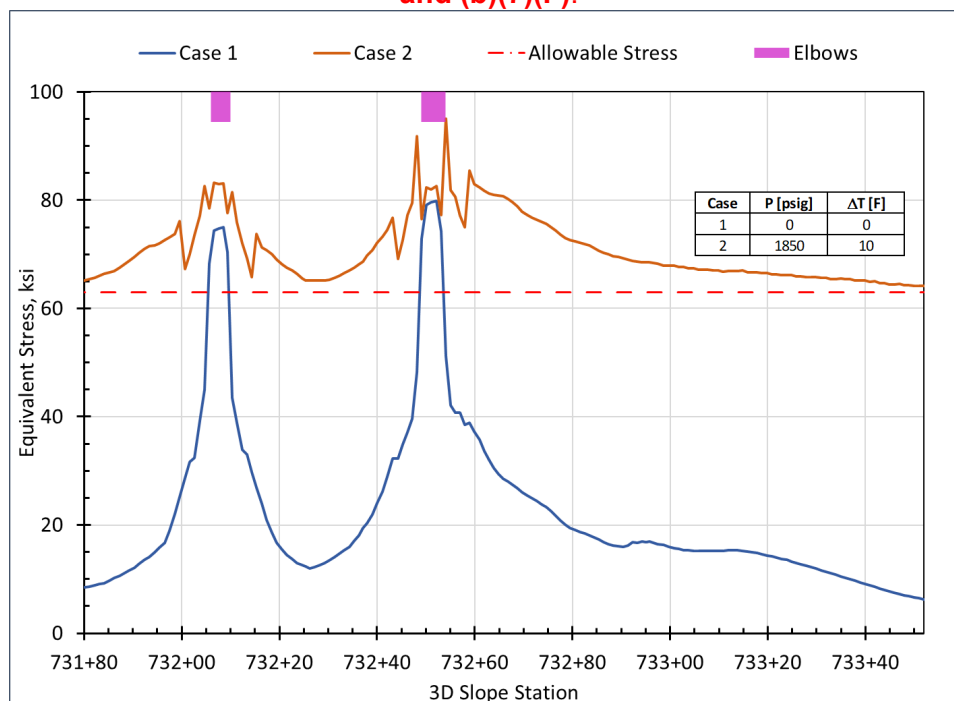


Figure D.39. FEA von Mises Stresses with 6-inches of Sliding

RSI analyzed two cantilever-type scenarios in this section to determine the potential for high bending stresses during hydrostatic testing (Scenario 2a and 2b). Under Scenario 2a it was assumed that the pipeline was supported (e.g., with side booms or cribbing) at some distance above the ground. The pipeline then experienced cantilever bending due to loss of this support. Under Scenario 2b, the pipeline was assumed to slide down the hill. Compared to the post-construction scenario (Scenario 1) considered in the previous section, the cantilever action (Scenario 2a) required a large amount of end deflection, but it explained the ovality as well as the wrinkle (the compressive stress in Figure D.35 is at 90% SMYS at the elbow). The sliding action (Scenario 2b) also explained the ovality and wrinkle but required some sort of outside force to overcome ground friction and bending resistance of the elbow. Scenario 1, on the other hand, does not require excessive pipe deflection or outside force, but requires the presence of a long gap or soft layer under the pipeline or post construction settlement (or a combination thereof).

D.6 Stress Ranges Under Pressure and Temperature Changes (P&T)

The subject elbow has endured stress ranges due to pressure¹⁵⁶ and temperature fluctuations (Figure D.40 and Figure D.41). The stress ranges from pressure and temperature fluctuations were calculated in a soil-pipe interaction FEA with the lower-bound soil properties and ELBOW290 elements (see Section D.2 'Soil-Pipe Interaction Model' and Section D.4 'Pipeline Stress Analysis under Operating Loads' for details). The analysis used two different pressure changes of 500 and 1,000 psi, and two different temperature changes of 40°F (22.2°C) and 80°F (44.4°C). Listed in Table D.8 is a summary of the loading scenarios and the results of the

¹⁵⁶ The pressure spectrum from 2013 was used to represent worst-case pressure cycling conditions since the equivalent full MOP cycles per year were highest in 2013.

analysis. The last column of this table ($\Delta\sigma_L$) contains the calculated longitudinal stress ranges at the subject girth-weld (GWD 13530).

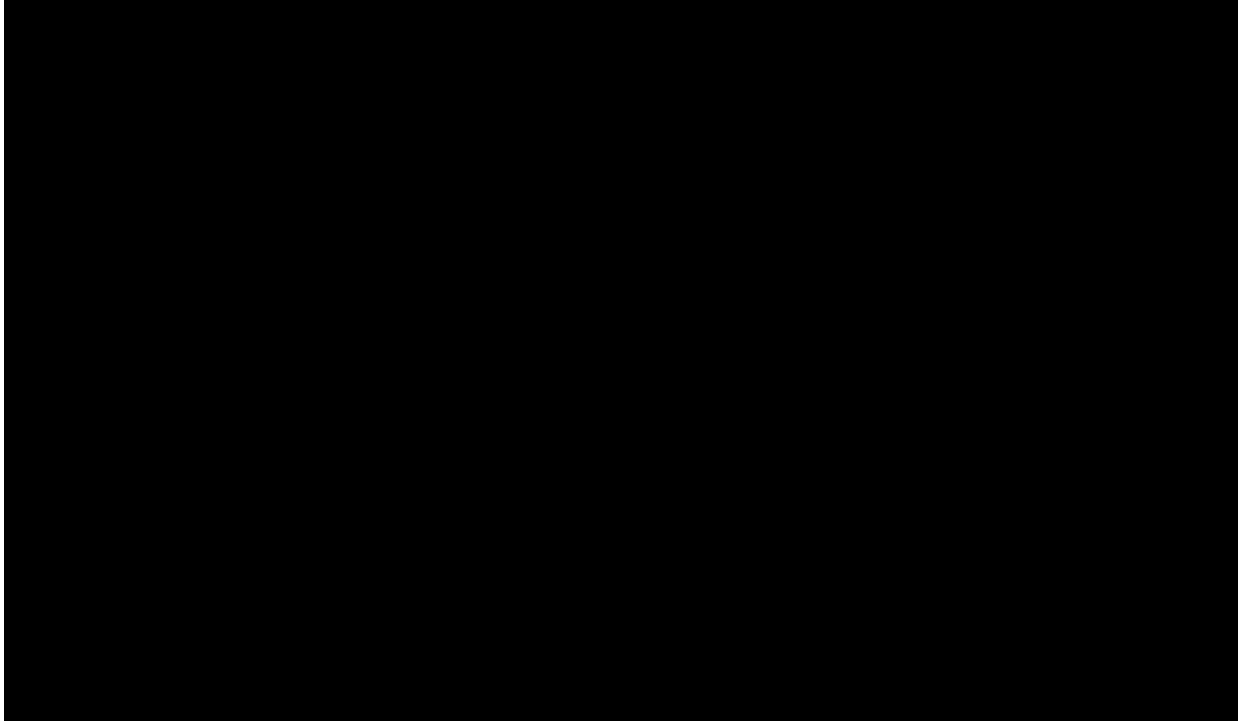


Figure D.40. Temperature Fluctuations Since 2011

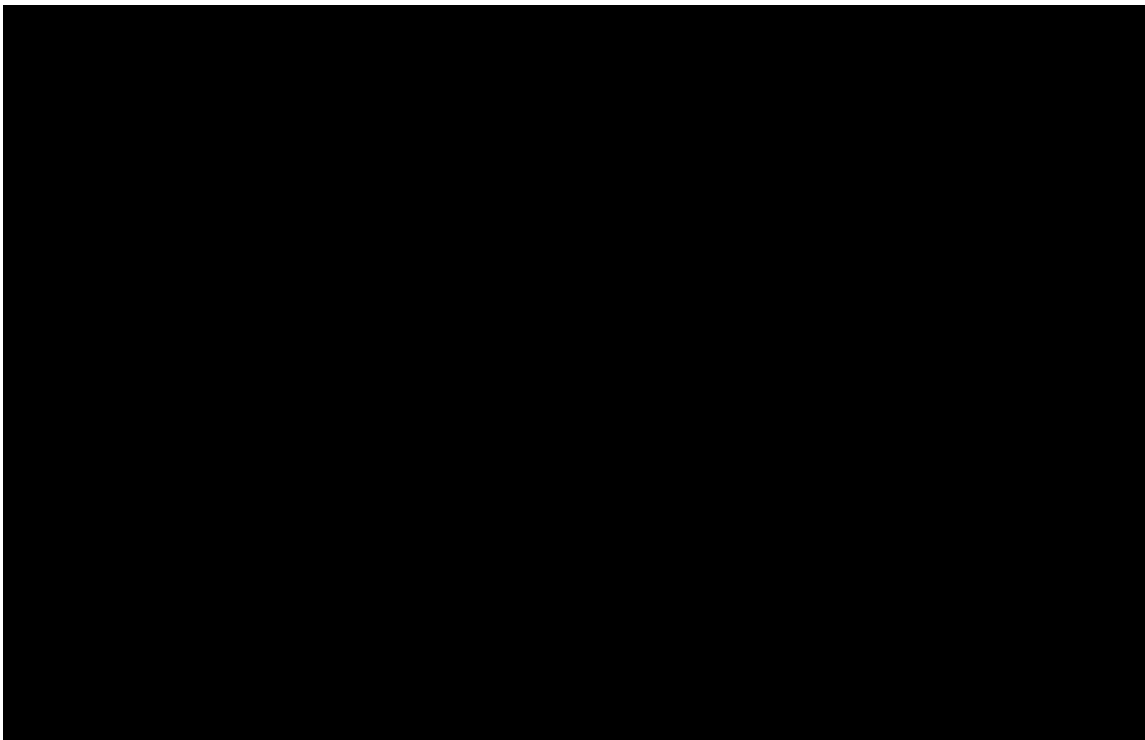


Figure D.41. 2013 Pressure Spectra

Table D.8. Loading Scenarios of P&T Analysis

Loading Type	ΔP [psig]	ΔT [°F]	$\Delta\sigma_L$ [ksi]
Pressure	500	0	16.54
Pressure	1,000	0	30.43
Thermal	0	40 (22.2°C)	12.64
Thermal	0	80 (44.4°C)	26.22

The above results were used to make correlations between the pressure and temperature changes and the resulting stress range at the subject girth-weld (GWD 13530). These correlations are shown in Figure D.42 for pipe internal pressure and Figure D.43 for differential temperature. These correlations were employed in fatigue crack growth analyses.

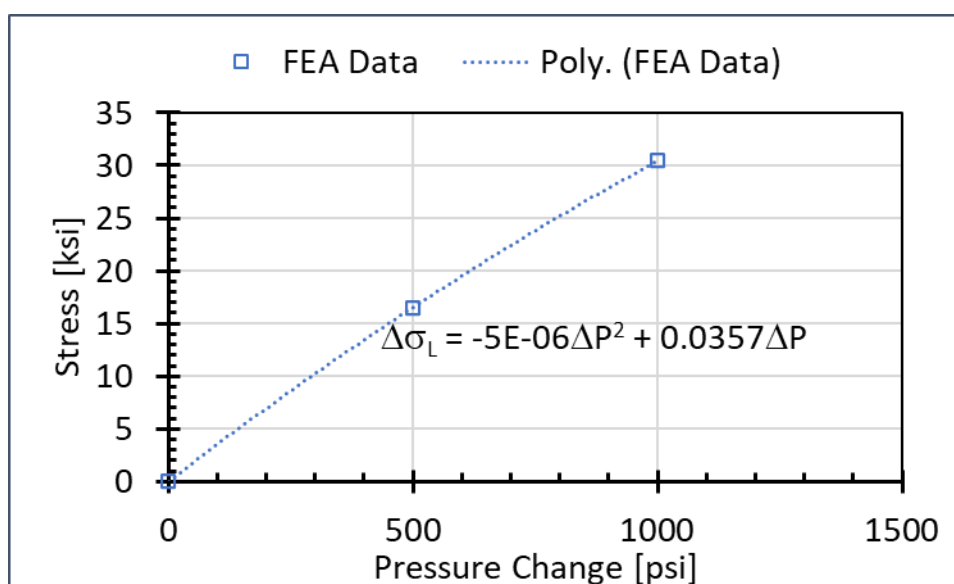


Figure D.42. Correlation between Stress Range and Pressure Change

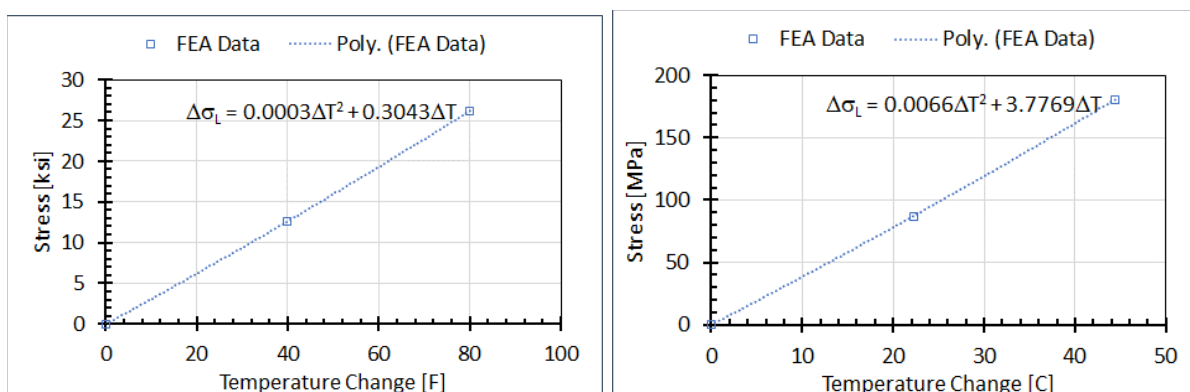


Figure D.43. Correlation between Stress Range and Temperature Change

D.7 Stress Concentration Factor (SCF)

D.7.1 SCF for Out-of-Roundness

The wall thickness transition and geometrical features of the subject elbow, including the wrinkle and ovality, are expected to have caused stress concentration at the girth-weld, intensifying the stress ranges calculated in the previous section. Three sources for the SCF were identified after reviewing Anderson's metallurgical report, the laser scanner STL files, and other information including elbow out-of-roundness, wall thickness transition, and weld hi-lo. The three-dimensional (3D) shell model described under Section D.3 'Shell Model' was used to calculate the SCF associated with elbow out-of-roundness. This was achieved by applying a uniform bending moment to the end of the model (the end closer to the subject girth-weld), fixing the other end, and solving the model to calculate longitudinal stresses around the girth-weld. The highest tensile stress from this analysis was calculated as 2,399 psi (Figure D.44)¹⁵⁷. Then another shell model was built with similar dimensions and wall thickness values to the actual elbow model but with ideal geometry (i.e., a perfectly circular cross-section). The ideal elbow model was analyzed under the same boundary conditions to calculate the longitudinal stresses at the girth weld. The highest tensile stress from this model was calculated as 2,199 psi (Figure D.45). The ratio of these two stresses is the SCF due to out-of-roundness¹⁵⁸:

$$SCF_o = \frac{2399}{2199} = 1.091$$

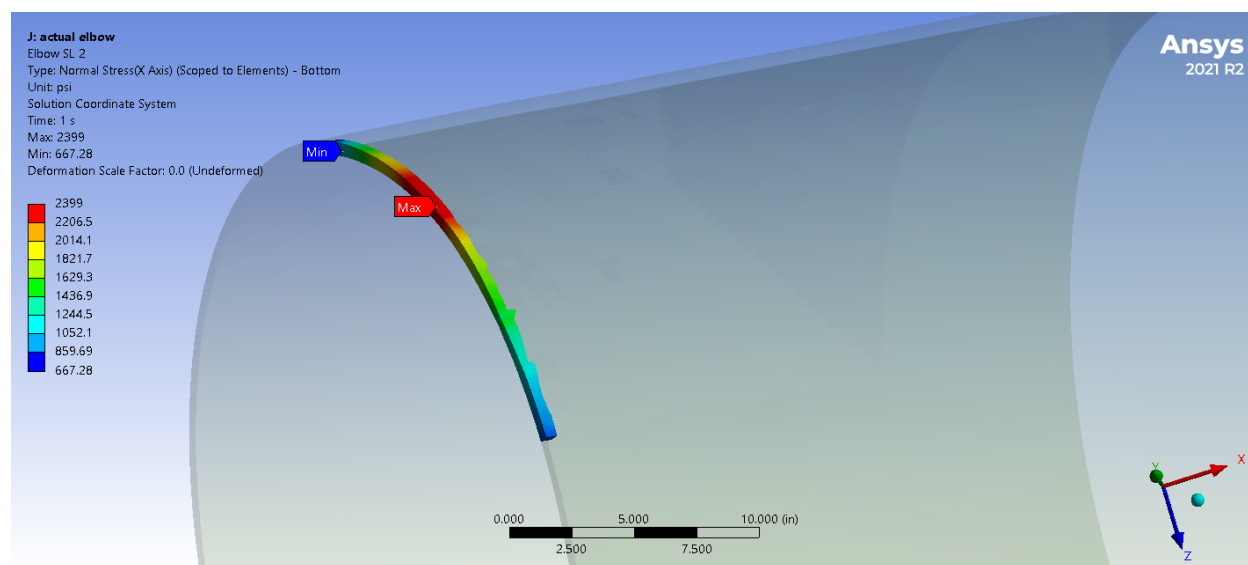


Figure D.44. FEA Longitudinal Stresses at the Hot-Spot of the Subject Girth-Weld Under a Uniform Bending Moment of 1×10^6 ft-lb – Actual Elbow with Out-of-Roundness

¹⁵⁷ The orientation of the coordinate system in the two models are not the same as seen in the figures. The circumferential locations of the maximum tensile stresses in both models were about 10 deg off the 12 o'clock position.

¹⁵⁸ The SCF for out-of-roundness was calculated using the actual elbow geometry from the 3D laser scan data measured at Anderson post-incident. The ovality was larger when measured in the field in 2013 and likely relaxed when the failure occurred as well as when the pipe was cut-out for metallurgical analyses. Therefore, the SCF for out-of-roundness prior to failure was likely higher than the SCF calculated by the FEA.

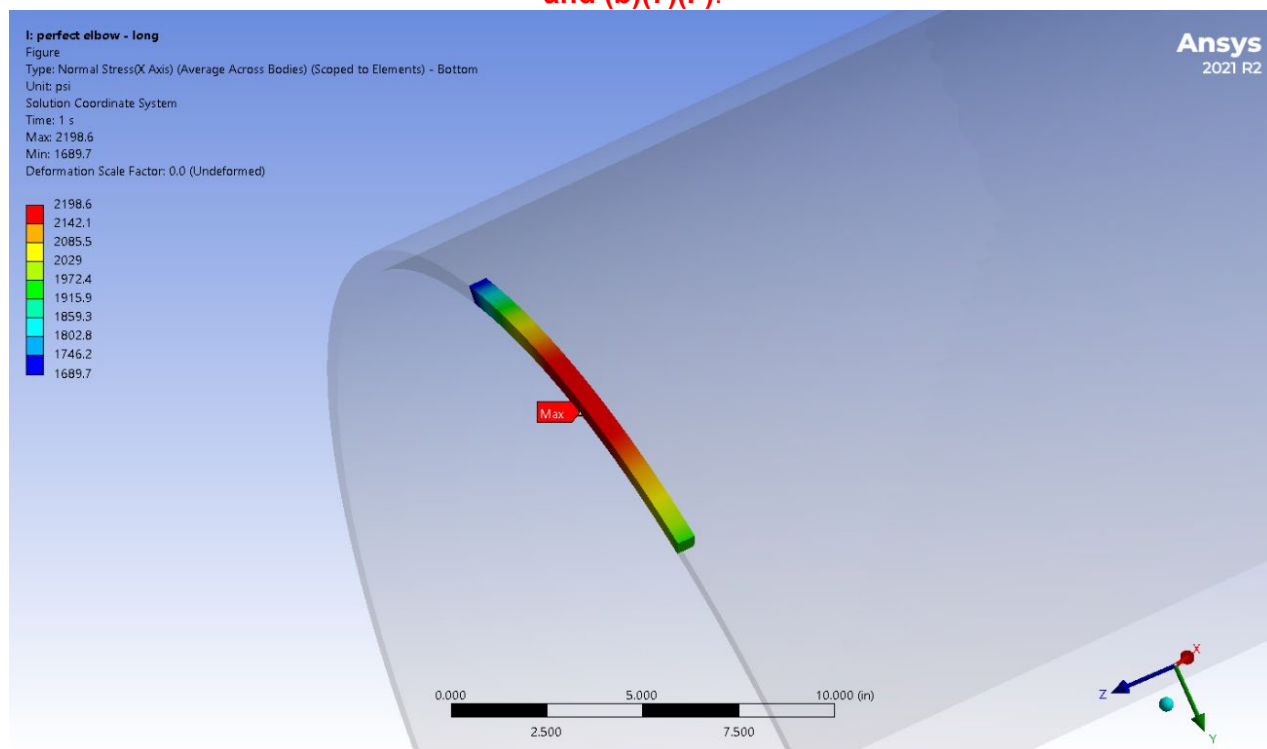


Figure D.45. FEA Longitudinal Stresses at the Hot-Spot of the Subject Girth-Weld Under a Uniform Bending Moment of 1×10^6 ft-lb – Idealized Elbow Geometry

The SCF value calculated from the above analysis accounts for the residual ovality (ovality after the elbow is detached from the rest of the pipe) and wrinkle. The bending moment that was used in the analysis was relatively small, generating a bending stress of about 2,199 psi. Consequently, elastic ovality caused by the application of the bending moment was negligible. The difference between the measured ILI and laser scanner ovality measurements suggests that the elbow was under a residual bending moment. In other words, the amount of ovality was greater when the elbow was buried and connected to the rest of the pipeline, which would have generated a higher SCF. To explore the SCF value under a potentially high residual bending moment, RSI ran a second analysis in which an initial bending moment was applied to the elbow to increase the ovality to 10% (the highest measured ovality from the 2013 caliper ILI). The bending moment required to create this amount of ovality was 1.8×10^7 ft.lbf. Then an additional bending moment of 2×10^6 ft.lbf was applied to the elbow to calculate the increment in the longitudinal stress. A similar analysis was performed on the idealized elbow. The increment in the stress from the actual elbow was calculated as 8,869 psi, and that from the idealized elbow was calculated as 4,642 psi. These results show that the SCF value for an elbow with 10% ovality could be as high as 1.91.

The measured values of ovality since the 2011 replacement are as follows:

- [REDACTED] % from 2012 PROFILE caliper ILI December 2012
- [REDACTED] ovality measured during 2013 excavation in March 2013
- [REDACTED] ovality from 2013 GEMINI caliper ILI September 2013
- [REDACTED] ovality¹⁵⁹ from 2018 MFL4 caliper ILI November 2018

The above data does not show any increasing trend in the elbow ovality since 2012, but it suggests that the ovality measured in the 2013 dig was somewhat lower than those measured through ILI, which could be related to ILI accuracy or a lower overburden pressure after the elbow was excavated. RSI performed crack growth analyses using both SCF values of 1.091 and 1.91.

D.7.2 SCF for Girth Weld Geometry

The wall transition SCF was calculated from a formula given in Section 3.3.7.3 of DNVGL-RP-C203 (DNVGL-RP-C203 - 2016, April 2016) for weld root and defined by the following equations:

$$SCF_t = 1 + \frac{6(\delta_t + \delta_m)}{t_1} \cdot \frac{1}{1 + \left(\frac{t_2}{t_1}\right)^\beta} \cdot e^{-\alpha} \quad \text{Equation 11}$$

$$\alpha = \frac{1.82L}{\sqrt{Dt_1}} \cdot \frac{1}{1 + \left(\frac{t_2}{t_1}\right)^\beta} \quad \text{Equation 12}$$

$$\beta = 1.5 - \frac{1}{\log \frac{D}{t_1}} + \frac{3}{\left(\log \frac{D}{t_1}\right)^2} \quad \text{Equation 13}$$

Figure D.46 shows the geometrical parameters in the above equations. An SCF value of 2.102 was calculated from the above equations using an eccentricity of 10%, the wall thickness values of 0.54-inch and 0.87-inch, and a transition length of 0.8-inch (see Figure D.47). RSI also used the idealized FEA shell model to confirm the above SCF value. A uniform axial stress was applied to one end of the model, while the other end was fixed. The membrane and bending stresses were calculated at the girth weld. The SCF was calculated as one plus the ratio of the through-thickness bending stress to the membrane stress as shown in Equation 14.

$$SCF_{FEA} = 1 + \frac{\sigma_{bending}}{\sigma_{membrane}} \quad \text{Equation 14}$$

¹⁵⁹ The 2018 caliper tool center appeared to not be aligned with the pipe centerline (tool center sagged in the line) which erroneously exaggerated the ovality measurement from this tool run. Baker Hughes communicated that ovality measurement within an elbow fitting will be erroneously exaggerated due to the dynamics of the tool traversing the elbow.

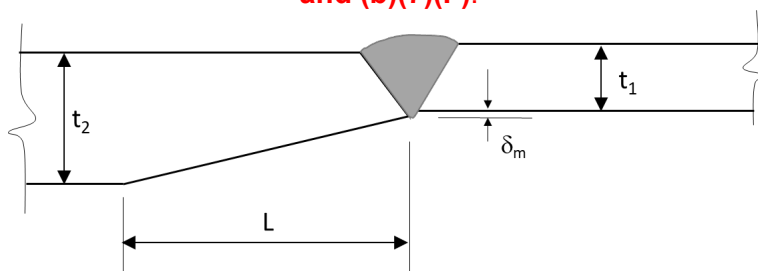


Figure D.46. Girth-Weld with Wall Thickness Transition

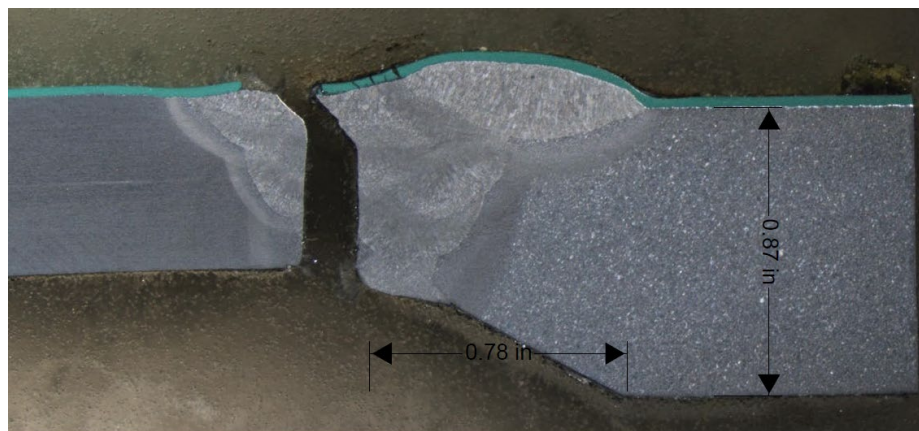


Figure D.47. Weld Details

The overall SCFs were calculated by multiplying the out-of-roundness and wall thickness transition SCF values:

$$SCF = SCF_o \times SCF_t = \text{[REDACTED]}^2 \quad (\text{laser scan ovality})$$

$$SCF = SCF_o \times SCF_t = \text{[REDACTED]} \quad (\text{ILI measured ovality})$$

D.8 Surface Loading Analysis

The objective of the surface loading analysis was to determine if the weight of the construction equipment crossing the unpressurized pipeline could have caused excessive stress in the elbow.

RSI performed a surface loading analysis using the Canadian Energy Pipeline Association (CEPA) model¹⁶⁰ to calculate surface loading induced stresses in the pipe. The CEPA model assumes that the pipe is straight and therefore does not account for stress concentration at the elbow. As such, the results are approximate. Table D.9 shows the vehicles that were used in the surface loading analysis. Table D.10 shows the resulting stresses in the unpressurized straight

¹⁶⁰ D. J. Warman and D. J. Hart, "Development of a pipeline surface loading screening process & assessment of surface load dispersing methods," Kiefner and Associates, Inc. for Canadian Energy Pipeline Association (CEPA), June 17, 2005.

D. J. Warman, J. Chorney, M. Reed and J. Hart, "Development of a pipeline surface loading screening process (IPC2006-10464)," in 6th International Pipeline Conference, Calgary, Alberta, Canada, September 25-29, 2006. ENV-6-1 Report RP-218-104509, "Field validation of surface loading stress calculations for buried pipelines - Milestone 2," Pipeline Research Council International, Inc (PRCI), Authored by Zand, B., Branam, N. and Webster, W., April 2018.

pipe under surface loading from three different construction vehicles for cover depth ranging from 2-ft to 8-ft. It is clear from the results that the surface loading induced stresses are not high enough to cause excessive deformation of the pipe.

Table D.9. Construction Vehicles Considered in the CEPA Analysis

Vehicle Model	Footprint	Gross Weight [lbf]	Footprint Dimensions [inch]	Impact Factor
345 GC Excavator	Track	96,000	155x130	2
CAT 594H Side boom	Track	122,500	200x130	2
CAT 583 Side boom	Track	45,500	200x92	2

Table D.10. Maximum Equivalent Stress in Empty Pipe [psi]

Vehicle Model	Cover Depth = 2 ft	Cover Depth = 3 ft	Cover Depth = 4 ft	Cover Depth = 6 ft	Cover Depth = 8 ft
345 GC Excavator	34,859.15	25,352.82	19,794.76	14,953.60	14,953.60
CAT 594H Side boom	36,445.69	26,707.77	21,025.31	16,149.53	16,149.53
CAT 583 Side boom	14,938.72	11,481.65	9,716.11	8,752.04	8,752.04

To explore the effect of a potentially high concentrated load on the elbow (e.g. from a plate compactor) we conducted another FEA. The model used for this analysis was the same shell model that was described in Appendix D.3, with elastic-plastic constitutive models for the pipe and the elbow. The Ramberg-Osgood (Ramberg & Osgood, 1943) elastic-plastic stress-strain curves were used in this analysis. The Ramberg-Osgood (R-O) parameters were determined through curve fitting to the digitized experimental data from Anderson's metallurgical analysis report. The R-O curves and experimental data for the base metal (the pups) and the elbow material are shown in Figure D.40 and Figure D.41. The data points for each tensile test were obtained by digitizing the respective graphs provided in Appendices D through F of Anderson's report. Then the engineering stress-strain data were converted to true stress and strain data as described in (API 579-1/ASME FFS-1, June 2016) using the following equations.

$$\sigma_{Tr} = (1 + \varepsilon_{En})\sigma_{En} \quad \text{Equation 15}$$

$$\varepsilon_{Tr} = \ln(1 + \varepsilon_{En}) \quad \text{Equation 16}$$

The R-O parameters on each figure were determined by the Least Square method. These stress-strain curves are shown in Figure D.48 and Figure D.49. Figure D.50 shows the shell model used for this analysis and the annotations on the figure show the boundary conditions. A vertical concentrated load of 100,000 lbf was applied to the pipeline right next to the elbow in

five-time steps. The concentrated load was applied to a 10-inch by 20-inch area of the pipe surface (Figure D.51).

The results show a maximum von Mises stress of 28.6 ksi in the elbow (Figure D.52), which is insufficient to cause plastic deformations. In conclusion, typical construction equipment would not be able to exert pressures and forces high enough to cause permanent deformation of the elbow.

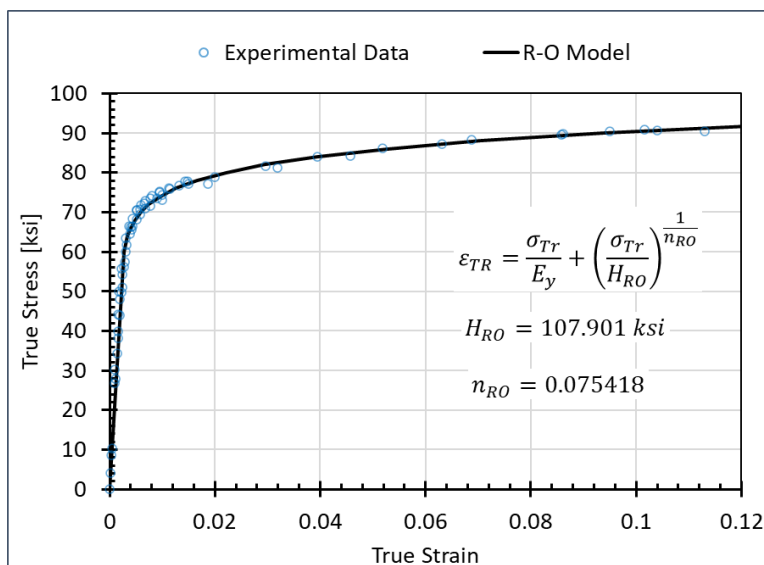


Figure D.48. Ramberg-Osgood Stress-Strain Curve Fitting Through Tensile Test Data from Longitudinal Base Metal Specimens

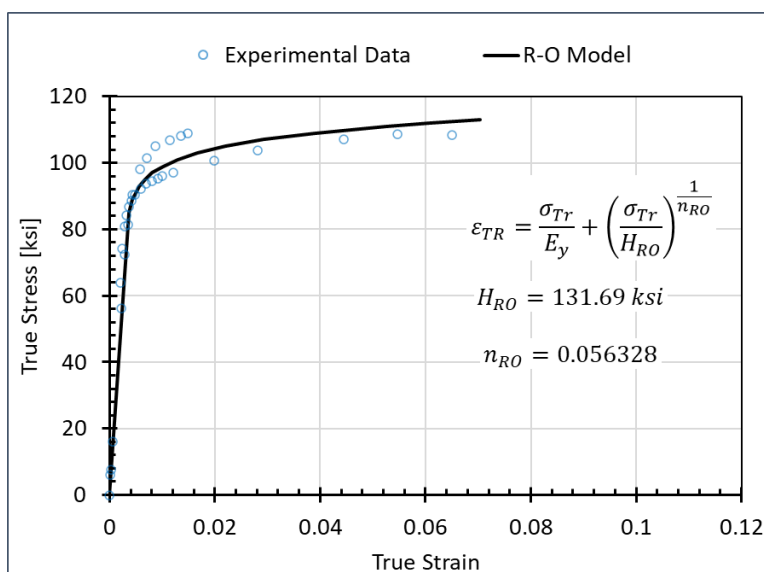
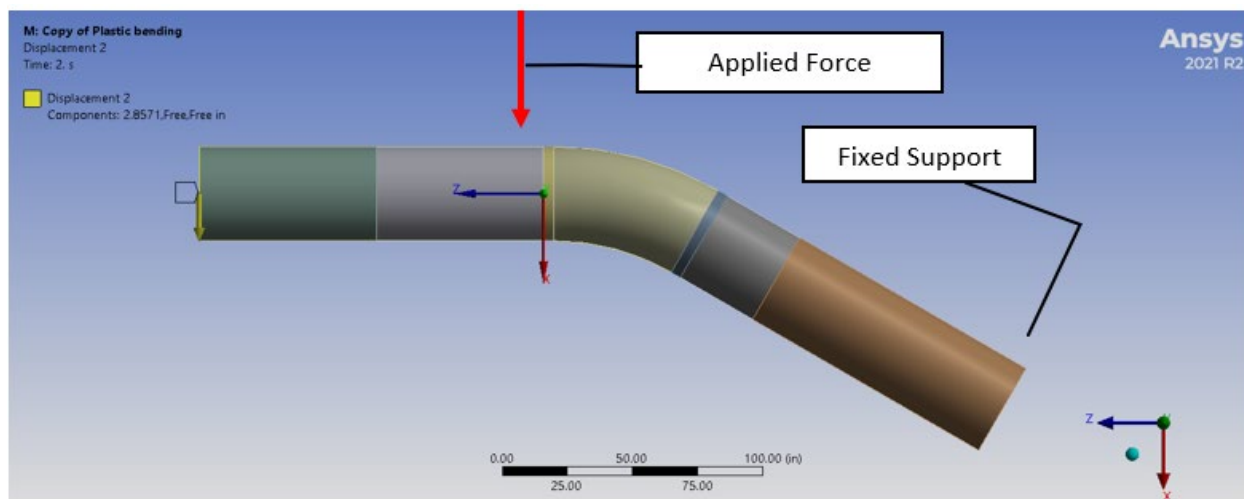
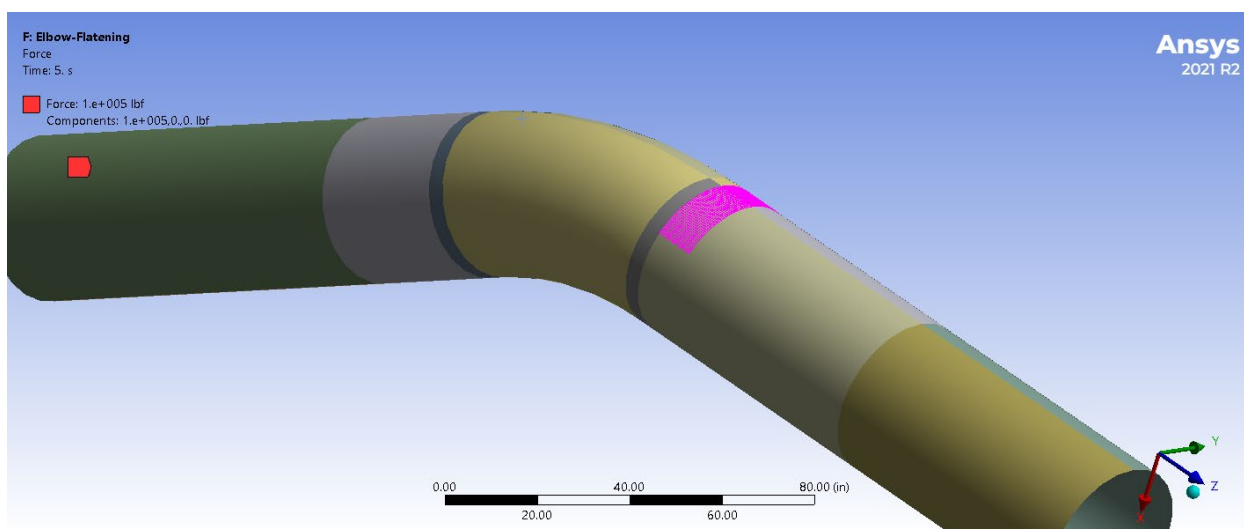


Figure D.49. Ramberg-Osgood Stress-Strain Curve Fitting Through Tensile Test Data from Longitudinal Elbow Specimens

**Figure D.50. FEA Model for Concentrated Load Scenario****Figure D.51 The Pipe Area Where the Concentrated Load was Applied**

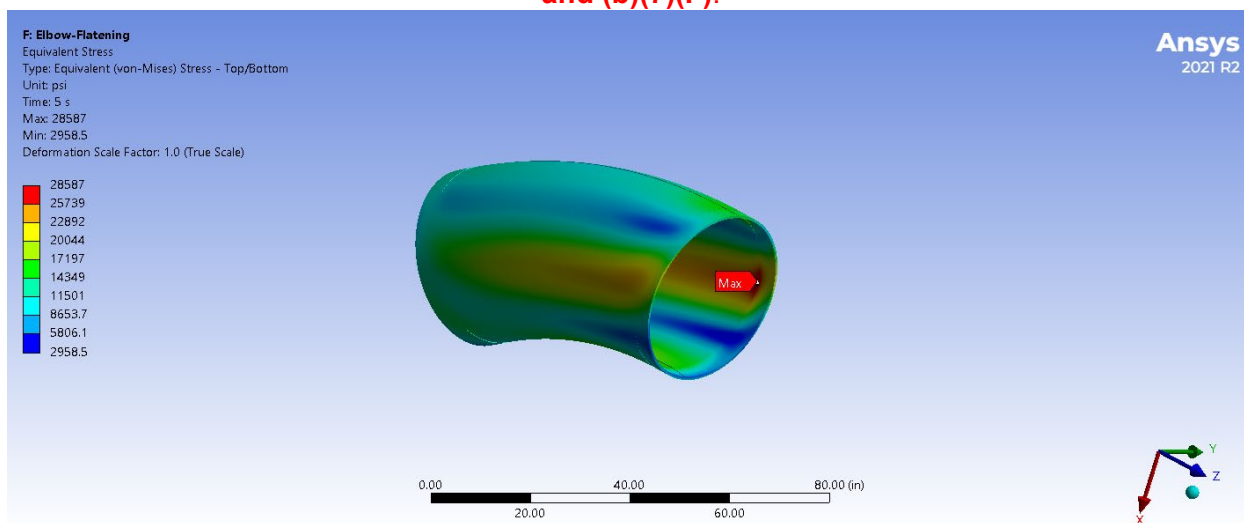


Figure D.52. Calculated von Mises Stress in the Elbow under a Concentrated Load of 100,000 lbf.

12 Appendix E – Temperature and Pressure Cycle Histograms

